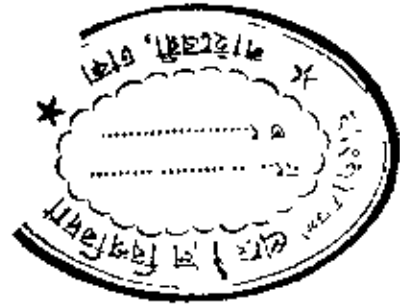


Department of Metallurgical Engineering,
Bangladesh University of Engineering and Technology,
Dhaka-1000, Bangladesh.



STUDIES ON MECHANICAL ALLOYING

A Thesis submitted to the Department of Metallurgical Engineering, Bangladesh University of Engineering and Technology, Dhaka-1000, Bangladesh, in partial fulfilment of the requirements for the Degree of Master of Science in Engineering (Metallurgical).



by
Md. Ismail Hossain.
Dhaka, August 27, 1996.



Declaration

This is to certify that the work has been carried out by the author under the supervision of Professor A. S. W. Kurny, Department of Metallurgical Engineering, Bangladesh University of Engineering and Technology, Dhaka, Bangladesh and it has not been submitted elsewhere for the award of any other degree or diploma.

Countersigned.




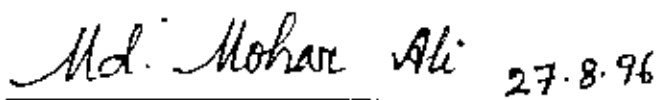
Professor A. S. W. Kurny.
(Supervisor)

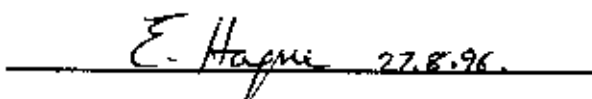


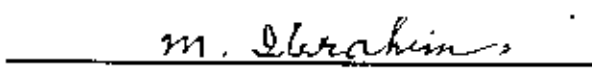
Md. Ismail Hossain.
(The Author)

The undersigned examiners appointed by the Committee of Advanced Studies and Research (CASR) hereby recommend to the Department of Metallurgical Engineering of Bangladesh University of Engineering and Technology, Dhaka, the acceptance of the thesis entitled, "**Studies on Mechanical Alloying**" submitted by Md. Ismail Hossain, B.Sc. Engineering (Metallurgical), in partial fulfilment of the requirements for the Degree of Master of Science in Engineering (Metallurgical).

1. 
Professor A. S. W. Kurny 29/7/96
Dept. of Metallurgical Engineering.,
BUET., Dhaka-1000. **Chairman**
(Supervisor)

2. 
Head,
Dept. of Metallurgical Engineering.,
BUET., Dhaka-1000. **Member**
(Ex-officio)

3. 
Professor Ehsanul Haque
Dept of Metallurgical Engineering.,
BUET., Dhaka-1000. **Member**

4. 
Professor Md. Ibrahim
House No. 31, Road No. 4,
Dhanmondi Residential Area,
Dhaka, Bangladesh. **Member**
(External)

Acknowledgements

I express my deepest sense of gratitude and profound respect to my supervisor Professor A. S. W. Kurny for his inspiring guidance, invaluable suggestions, stimulating discussions and continued encouragement throughout the period of this work. I consider it a great opportunity to have a share of some of his knowledge and expertise and find myself proud to work with him. His deep sense of understanding has seen me through many difficult and frustrating moments. I am particularly indebted to Dr. Kurny for his painstaking effort to in creating confidence in me and also for his help in the preparation of this thesis.

I wish to express my gratitude to Dr. Maglub Al Nur, Associate Professor, Department of Mechanical Engineering for providing necessary equipment's and also for his kind help in the design of the attritor.

I am also grateful to Mr. Yusuf Khan for his help in the X-ray diffraction work. I am highly indebted to Mr. Fazlul Hauque Bhuyan and Mr. Ahmed Ali Mollah for their help in the various stages of this work.

The workshop and laboratory staff in the Department as well as those of the Department of Mechanical Engineering have readily co-operated with me in the fabrication work and to carryout the experiment for which I wish to record my deep appreciation.

I wish to thank the authority of Bangladesh University of Engineering and Technology, Dhaka, for the facilities provided.

Md. Ismail Hossain

Md. Ismail Hossain.

Dhaka, Bangladesh.
Aug 27, 1996.

Mechanical alloying is a powder processing technique in which solid state reactions are caused to occur when materials are processed in an attritor under an inert atmosphere. By mechanical alloying a wide variety of starting materials, including elemental powders can be converted into fully homogeneous alloys with novel composition and microstructure.

In an attempt to acquire the knowhow of the technology locally, an attritor and a hot pressing die have been designed and fabricated and the related process variables have been set. In order to produce metal powder locally, a powder production cell has also been designed and fabricated. In this respect copper powder has been successfully produced from commercial grade solid copper and chemicals.

The progress of mechanical alloying of 70 wt. % copper-30 wt. % zinc has been investigated by means of X-ray diffraction (XRD), optical metallography and sieve analysis. Results obtained show that the mechanical alloying proceeds such that the zinc atoms preferentially inter into the copper lattice. X-ray patterns indicates that the progress of alloying, the crystallinity decreases gradually leading the alloy to amorphous state. Investigation of the effect of particle size on the progress of mechanical alloying revealed that the milling time is particle size dependent and finer particles result in more optically homogeneous alloy at a much less time of milling. In order to study the mechanical property microhardness of consolidated body, from mechanically alloyed powder particle and that of from the powder metallurgy technique, has been determined. Mechanically alloyed body showed homogeneous micro-hardness while that from the conventional powder metallurgy technique body showed non-homogeneous micro-hardness hardness throughout. Study of the shape characterisation of the particles showed that with the progress of milling particle of a particular size become more regular in shape and most of them become more or less spherical. These particles are of characteristics fine lamellar composites at the early stage of milling, after the structural and grain refinements during mechanical alloying , finally reaches to optically homogeneous alloy.

Declaration.

Acknowledgements.

Synopsis.

Chapter - 1 : Introduction

Introduction	1
Advantages of mechanical alloying over other methods of alloying.	1
Objective and scope of present work.	4

Chapter - 2 : Mechanical alloying - a survey.

Introduction.	5
Powder processing	5
Mechanism and mechanics of mechanical Alloying	11
Introduction	11
Collision geometry and collision duration	12
Processing time	14
Deformation during collision	14
Powder hardness	16
Coalescence mechanisms	18
Fragmentation mechanisms	20
Welding and fracturing probabilities	23
Shape factor	23
Friction in a powder mass	24
Effect of friction on compacting and sintering	25
Consolidation	25
Introduction	25
Cold Process	26
Die compaction	26
Explosive forming	39
Powder rolling	31
Hot Process	33
Hot die pressing	33

Hot extrusion	34
Hot isostatic compaction	35
Processing control of mechanical alloying	35
Process modification	35
Powder size and size distribution	36
Processing time	36
The Equipment	36
Introduction	36
Conventional ball mill	37
Attritor (high energy ball mill)	37
Centrifugal planetary ball mill	38
Vibratory ball mill	39
Chemical kinetics of mechanical alloying and energy consideration	41
Chemical kinetics of mechanical alloying	41
Energy consideration and structural refining	42
Grain size refinement and mixing of atoms	43
Structural refinements	44
Application of mechanical alloying	44
Introduction	44
Alloy synthesis	44
Nickel base oxide dispersion super alloys	48
Aluminium-alumina oxide dispersion strengthened alloys	50
Iron base oxide dispersion alloys	51
Coating applications	51
Supercorrodng alloys	51
Other alloy systems	53
Amorphous and nanocrystalline materials	55
Chapter - 3 : Production of metals powder.	
Introduction	56
Mechanical Processes	56
Machining	56
Crushing	57
Milling	57

Shotting	57
Graining	57
Atomisation	57
Cold stream process	62
Physic chemicals and chemical process	62
Condensation method	62
Thermal decomposition	63
Reduction method	64
Electrodeposition	66
Precipitation from aqueous solution	69
Precipitation from fused salt	70
Gaseous reduction process	70
Intergranular corrosion	72
Oxidation and decarburisation	72
Ultrafine powder	72
Alloy powders	72
Characterisation of powder	72
Introduction	73
Characterisation of powder particle shape	73
Chapter - 4 : Design and fabrication	
Introduction	80
Preliminary considerations	80
Theoretical considerations	81
Design and fabrication	83
Design of an attritor	84
The main parts	84
The hot pressing die	85
The powder production cell	85
The accessory system	86
The power supply system	86
The gas supply system	87
The cooling system	87

Chapter - 5 : Experimental methodology	
Introduction	110
Production of powders	111
Characterisation of powder particles	111
X-ray diffraction	112
Hot pressing (Consolidation) of milled powder	112
Optical metallography	112
Powder Milling	113
Measurements of microhardness	113
Chapter - 6 : Results and Discussions	114
Chapter - 7 : Conclusion	132
Recommendation for future work	133
Appendix :	135
Appendix - A : Expressions and equations	i
Appendix - B :	v
Article one- Collision mechanisms	v
Article two- Deformation of particle as a function of position	viii
Article three- Welding and fracturing probabilities	x
Appendix - C :	
References	xii



Introduction

Introduction:

Mechanical alloying is a powder processing technique in which solid state reactions among the powder particles are caused to occur for generating powders manifesting novel composition and extremely fine microstructures. The crucial point of mechanical alloying is the interparticle cold welding. Cold welding is a function of melting points of the powder particles to be processed and is essentially a process of solid state bonding under external pressure. The fundamental process in mechanical alloying is the balanced repetitive welding, fracturing and rewelding of a mixture of powder particles entrapped in the collision sites of the grinding media in a dry highly energetic ball mill known as attritor. The central feature of the process is the formation of uniform dispersions of stable particles in super alloys. A wide variety of starting materials can be employed, including elemental powders, which can be converted into fully homogeneous alloys. This ability to process different starting materials with various characteristics gives the process great flexibility. State of the art is, dispersion-strengthened materials are produced commercially through this process and novel uses of mechanically alloyed materials are currently being developed¹⁻⁴.

Advantages of mechanical alloying over other methods of alloying :

Alloying results in superior engineering properties and are widely used. Large majority of alloys are made by heating different metals together to temperatures above melting points so that they form a solution with each other. This conventional

method of making alloys i.e. melting the mixture of required constituents and subsequent casting is susceptible to some serious limitations.

One of the serious limitations of conventional alloying technology is the reluctance of some metals to alloy. For example, it is quite difficult to alloy, by conventional techniques, a metal with a high melting point and one with a low melting point. Even though two such metals may form a solution in the liquid state, the metal with the lower melting point tends to separate out in the course of cooling and solidification that leads to segregation and other inhomogeneties. Alloying of refractory metals by conventional techniques implies use of high temperature furnaces which makes the whole process uneconomical.

The powder metallurgy technique offers a viable alternative to the above limitations. Powder metallurgy, for example provides a break through (a) in segregation elimination, (b) in the manufacture of high purity and precise composition controlled parts and (c) in application of super plasticity. Powder metallurgy process can combine metals of different melting points and densities and also metal and non-metals into engineering materials with 'tailored properties'. Aside from the above, powder metallurgy is the most competitive process for making parts from reactive metals like titanium and molybdenum and refractory metals like tungsten, tantalum, zirconium and the like. In conventional powder metallurgy technique, alloys are made by blending the elemental powders followed by subsequent compaction and sintering. The mixed powders are formed into solid metal by the application of high pressures and heat. These two operations can be performed in sequence.

When solid articles are made from blends of different metal powders the degree of homogeneity attained in the final product depends upon the extent of intermixing and on the sintering time. Also the degree of homogeneity attained in the final product is limited by the size of the particles in the powders. If the particles are too coarse, the different ingredients will not interdiffuse during solidification or prolonged heating. This problem can be overcome to some extent by starting with very fine powders. One way to make a fine powder is to grind a coarse powder in a ball mill. There is however, a practical limit to the fineness of the powder that can be produced in this way; the particles begin to weld together as the milling continues. Sometimes lubricants such as kerosene or fatty acids are added to prevent the particles from coming in contact. Although lubricants make finer grinding possible, they may severely contaminate the powders and degrade the alloy made from them. Another serious limitation is the hazards due to their large surface area, when brought into



contact with air, they burn spontaneously. This necessitates very careful handling of the fine powders produced. An alternative method of making alloys by powder metallurgy technique is by making use of alloy-powders produced by atomisation technique which will have different phases depending on the cooling rate. Generally a multiphase material is stronger than single phase material. Hence higher compaction pressure is necessary for pressing. In addition, the density of dislocation present in a particle after quenching is so high that the particle gets hardened. This too necessitate the use of higher compaction pressures.

Mechanical alloying was developed as a means of overcoming the disadvantages of blending of ultrafine powders. The process consist of simultaneous milling of different powdered constituents to produce metal powders with controlled microstructures by repeated welding, fracturing and rewelding in a dry, highly energetic ball mill. This occurs under conditions in which the rates of welding and fracturing are in balance and the average powder particle size remains relatively coarse⁵.

The driving force behind development of mechanical alloying was the long search for a means of combining, in a nickel base super alloy, the high temperature strength of an oxide dispersion with the intermediate temperature strength of a gamma prime precipitate including the required corrosion and oxidation resistance. But the mechanical alloying process is not restricted to produce complex oxide dispersion strengthened alloys, it is a means for producing composite metal powders with controlled, extremely fine microstructures. Most mechanical alloying development have been directed towards producing alloys that derive high temperature strength from a fine homogeneous distribution of oxide particles. The alloys have also contained elements such as chromium, aluminium and titanium for corrosion resistance; in some alloys the latter two elements also provide intermediate temperature strength by precipitation of gamma-prime $\text{Ni}_3(\text{Al,Ti})$ intermetallic compound.⁶⁻⁷

By mechanical alloying mixture of ultrafine alloy powders can be blended with fine refractory oxides to form an oxide dispersion strengthened alloy⁸; however, the dispersoid interparticle spacing is limited by matrix powder particle size and the fine powders, required to give sufficiently small interparticle spacing, present handling problems and are often pyrophoric. The problem of pyrophoricity is more severe if reactive alloying elements are present. Not only that mechanical alloying is a only

powder process which can be applied to a variety of systems like amorphous powders, intermetallic materials, solid solution alloys and metal-matrix composites, ceramic-metal composites etc.

Objective and scope of present work :

Even though mechanical alloying is already a commercially viable process for producing materials with enhanced behaviour no work in this field has so far been reported in Bangladesh. So the main objectives of the present work were

- to develop the knowhow and facilities for mechanical alloying locally at BUET.
- to produce mechanical alloy of some common metals like copper, zinc etc. and
- to study the structural homogeneity and microhardness of the alloys produced.

The program of work involved the design and fabrication of a laboratory model mechanical alloying unit (attritor), metal-powder production unit and the hot-pressing unit. The combination of the aforesaid units constitute the required facilities for mechanical alloying. The units were subsequently used to study and identify the effects of the process variables e.g. speed of attrition (rpm), the time of attrition; the current density, applied voltage, temperature and bath composition of the powder production unit and the pressure, temperature and time for hot-pressing unit.

In order to gain a clear understanding of the process, not complicated by the presence of a variety of alloying elements, it was considered to include a simple alloy system in these studies. As a result 30 wt.% Zn and 70 wt. % Cu system was chosen as the candidate materials for investigation. The processing time is known to affect the progress of mechanical alloying. In order to gain some information on the progress of alloying, samples milled for different ranges of time were investigated by X-ray diffraction techniques, sieve analysis and optical metallography. Finally, the mechanically alloyed powder mass was hot-pressed to have a solid component and micro hardness of the structure was measured.

Mechanical Alloying-A Survey

Introduction:

The underlying phenomenon⁵ in mechanical alloying is the repetitive welding, fracturing and rewelding that take place among the comminuting particles entrapped in the collision sites of the grinding balls. With times, a balance is reached between the two competing processes of welding and comminution. To facilitate interparticle cold welding, which is essentially a process of solid state bonding under external pressure without the aid of external heat, adequate energy is imparted to the grinding medium during milling. Here the presence of a malleable constituent act as a binder for the other harder constituents, the latter also readily bond with the grinding balls. This makes it necessary that milling is done in a dry atmosphere, especially for metals of high melting point, to promote cold welding. On the other hand, for milling metal powders of low melting point, it is necessary to introduce suitable surface deactivates to control excessive cold welding.

Powder processing:

Mechanical alloying begins by blending individual powder constituents, having diameters ranging from 1 to 500 μ m. The powder blend, depending on the desired alloy to be processed, contains one or more ductile metal components, as represented in Fig. 2.1. The starting metal powders can be of almost any form including powder made during metal refining (e.g. carbonyl nickel), electro-deposited powder, gas or

made during metal refining (e.g. carbonyl nickel), electro-deposited powder, gas or water atomised elemental or prealloyed powders, or powder prepared from crushed stock (e.g. titanium sponge powder). Additional constituents may include powdered intermetallic compounds. The powder of intermetallic compound is formed by pulverising a cast master alloy. Adding reactive elements such as aluminium or titanium in this way reduces their activity compared to that of elemental additions. A fine interdispersoid can also be added for dispersion strengthening.

The effects of a single collision on each type of constituent are also shown in Fig. 2.1. The initial ball -powder-ball collision causes the ductile metal powders to flatten and work harden¹. The severe plastic deformation increases the particle's surface-to-volume ratio and ruptures the surface films of adsorbed contaminants. The intermetallic powder fractures and is refined in size. The oxide dispersoid pseudomorphs are comminuted more severely.

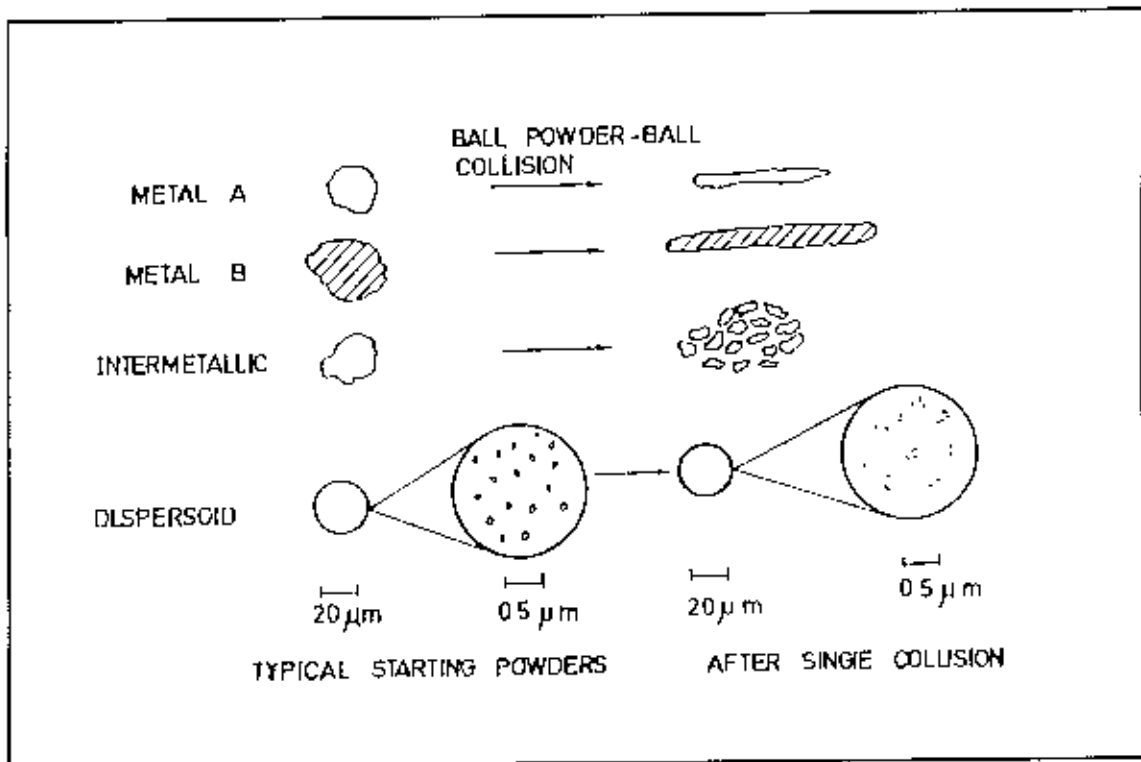


Figure 2.1 : Representative constituents of starting powders used in mechanical alloying showing their deformation characteristics.

A single **ball-powder-ball collision** early in the mechanical alloying processing sequence can modify the powder morphology in two ways as represented in Fig. 2.2. When the metal particles being flattened overlap, automatically clear metal interfaces are brought into intimate contact, forming cold welds and building up layered

composite powder particles consisting of various combinations of the starting ingredients. The more brittle constituents tend to become occluded by the ductile constituents and trapped in the composites. Concurrently, work-hardened elements or composite particles may fracture. The competing events of cold welding and

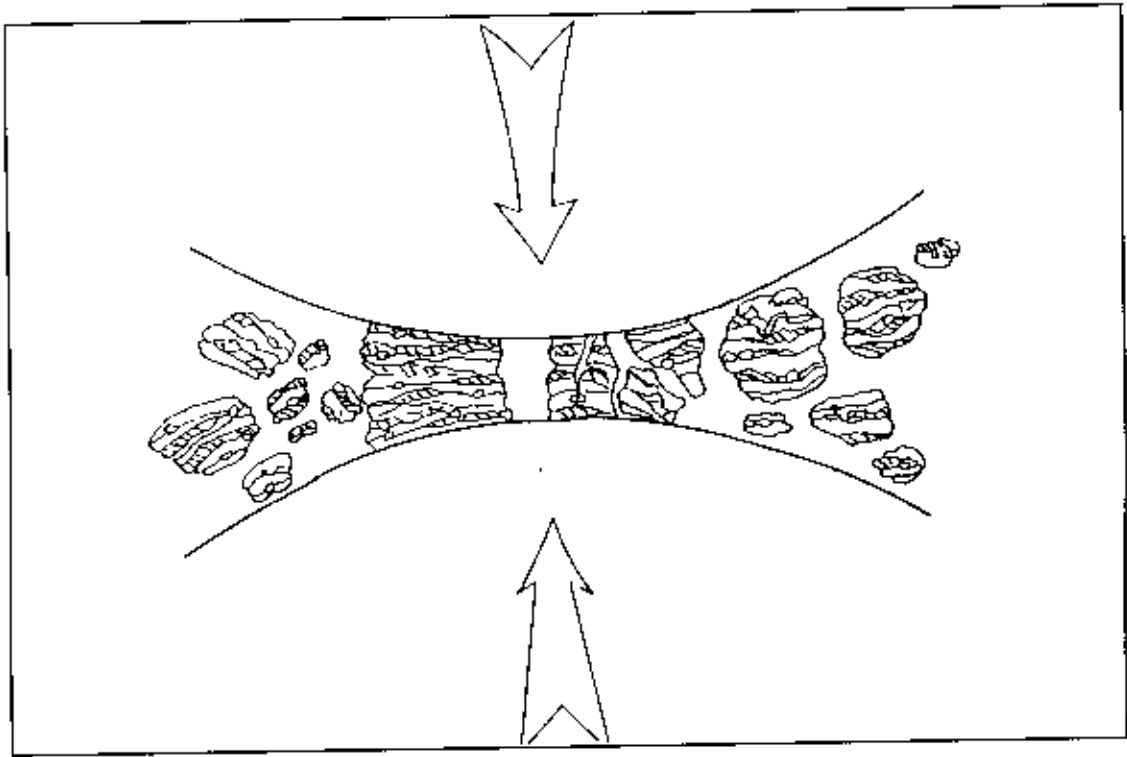


Figure 2.2 : Ball-powder-ball collision of powder mixture during mechanical alloying.

fracturing continue throughout the processing. The interplay of welding (with plastic deformation and agglomeration) and fracturing (size reduction) kneads the internal structure of the composites so that the particles are continually refined and homogenised. At the same time that powders cold weld to each other, they may also coat the ball charge or the interior surfaces of the mill. The presence or absence of a ball coating and the thickness of the layer encasing the mill walls depends on the particular alloy system and the processing control agents used. Typically 3-4 wt. % of the powder charge is tied up as ball coating. A slight ball coating is beneficial in that it acts to prevent wear of the steel ball charge. The milling conditions must be properly adjusted so that the ball coating remains relatively slight during processing and is continuously exchanged back and forth with the powder charge. If this is not done, an excessive layer of poorly processed material may form and spall off at the end of the run. This will lead to inhomogenities in the mechanically alloyed powder.

At an **early stage of processing** the particles are layered composites of the starting constituents as represented in Fig. 2.3. The composite particles may vary in size from a few micrometers to a few hundred micrometers. At this stage, fragmented starting powders that have not been cold welded may also exist. The original starting constituents are identifiable within the composites. The dispersoid is closely spaced along the welds while the spacing between the welds, equal to the lamellar thickness, is rather large. The chemical composition of the composite particles varies significantly within the particles and from particle to particle.

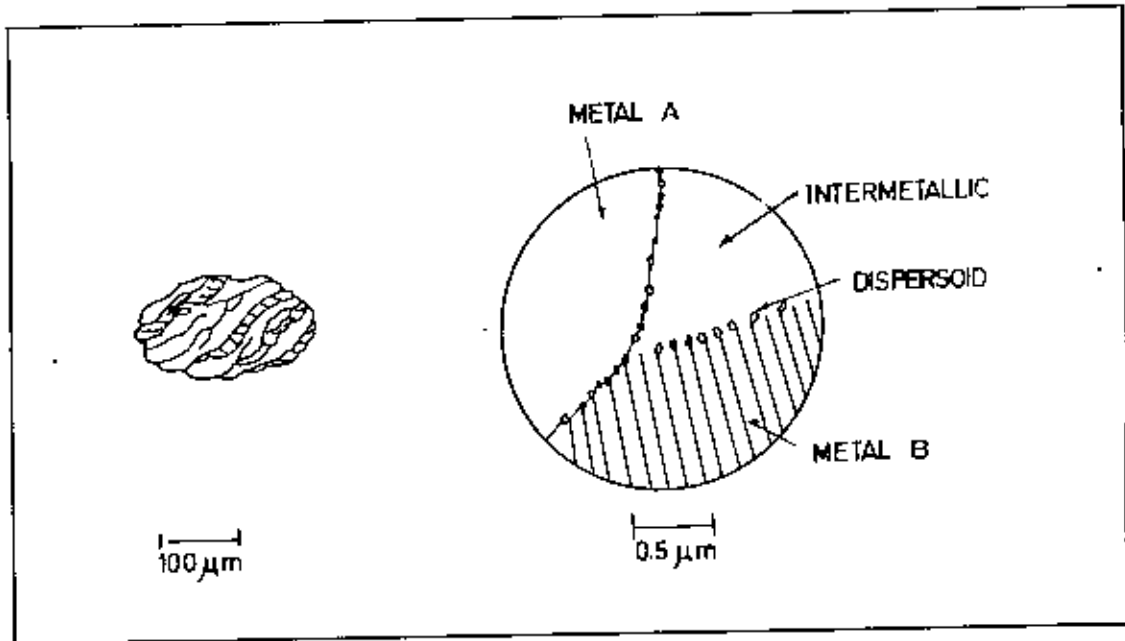


Figure 2.3 : Early stage of processing. Particles are layered composites of starting constituents.

The composite powder particles are further refined as fracturing and cold welding continues. At an **intermediate stage of processing** the particles consist of convoluted lamellae as represented in Fig. 2.4. Beginning with this stage of the process, dissolution of solute elements and the formation of areas of solid solution throughout the powder particle matrix are facilitated by slight heating, lattice defects, and short diffusion distances. Heating occurs during processing as the kinetic energy of the balls is absorbed by the powder being processed. The severe cold work resulting from mechanical alloying also aids diffusion by providing many sites for low activation energy pipe diffusion. In addition, the intimate mixture of the powder constituents decreases the diffusion distances to the micrometer range. Precipitation may occur, or metastable phases may now form throughout the powder particles. As the composite particles are fractured and kneaded together, the oxide dispersoid distribution becomes further refined. The dispersoid spacing along the welds

increases, while the distances between the welds decrease; gradually the oxide distribution becomes more uniform. The oxide dispersion may combine with reactive elements and excess oxygen to form complex refractory oxides such as yttrium aluminium garnet¹⁰⁻¹². Other stable compounds such as alumina and titanium carbonitride may form in situ during processing¹³.

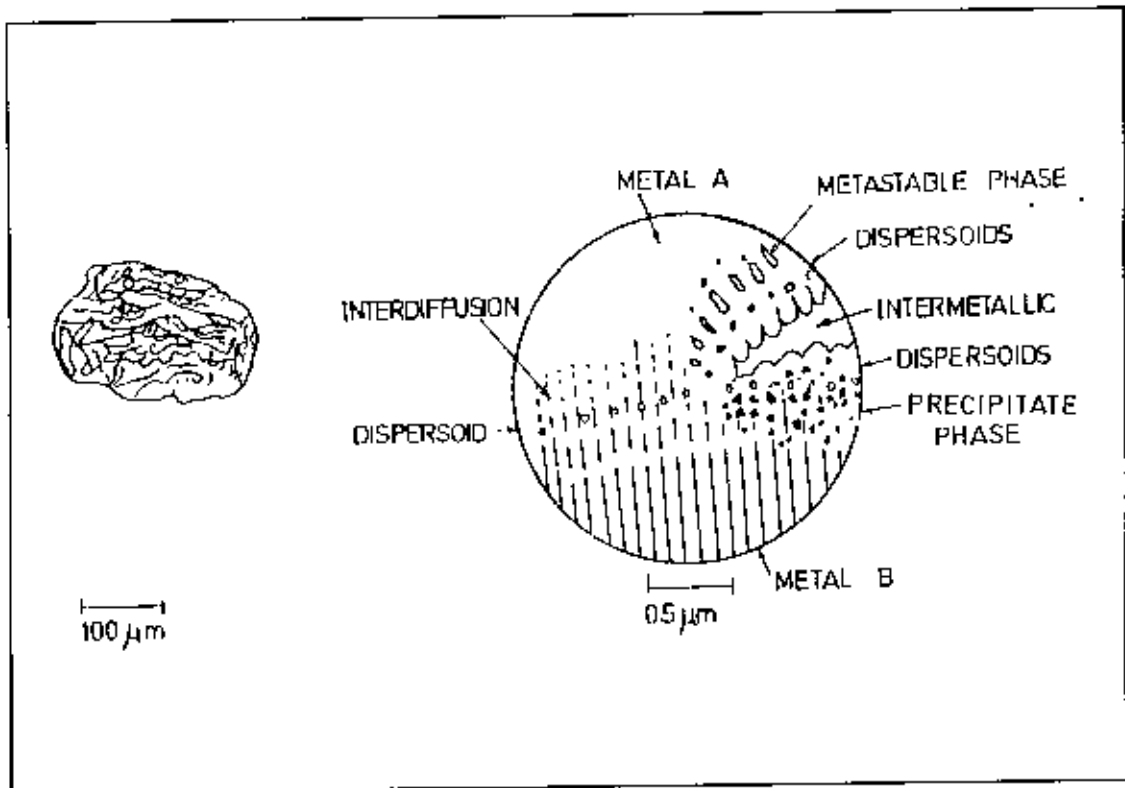


Figure 2.4 : Intermediate stage of processing. Particles consist of convoluted lamellae. It is possible to get some short-range interdiffusion of constituents and new phase formation.

The lamellae become finer and more convoluted as processing approaches completion, **the final stage of processing**, as represented in Fig. 2.5. The composition of individual particles converges toward the overall composition of the starting powder blend. The lamellae spacing decreases to one micrometer or less and approaches the optimum dispersoid spacing. Powder particles still contain minute areas that are higher in concentration of one particular metal constituent or contain an embedded remnant of the intermetallic. The precipitation of equilibrium phases is now possible because of the nearly complete mixing of the components. At this time the micro hardness of the individual powder particles attains a saturation level. The severe plastic deformation that occurs during mechanical alloying causes the powders to have very high hardness. Hardness increases roughly linearly during the initial stages

of the mechanical alloying process, reaching a saturation value after which time it is presumed that work softening balances further work hardening.

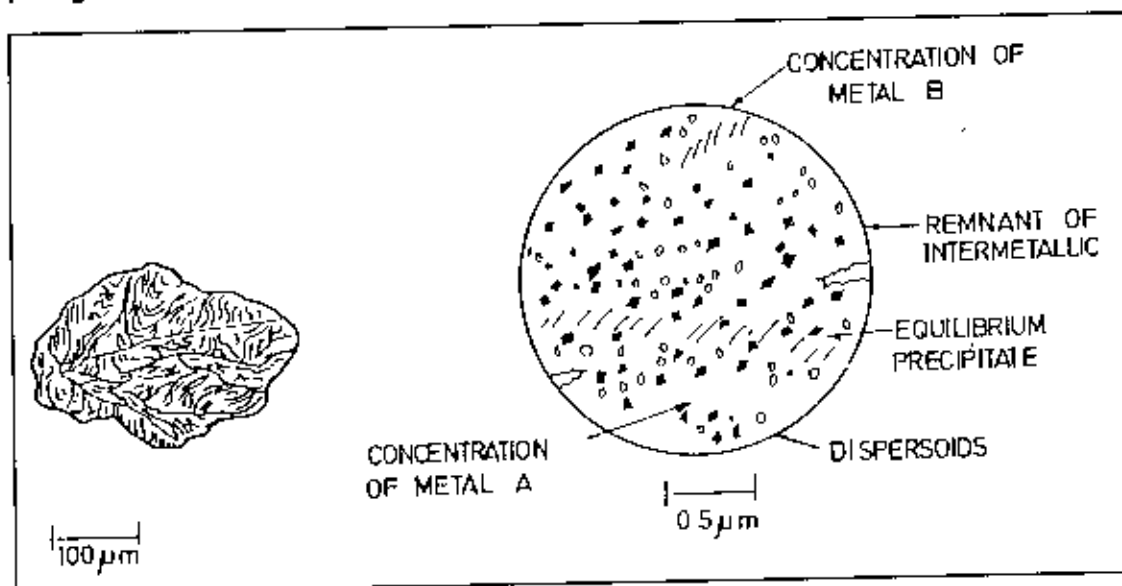


Figure 2.5 : Final stage of processing. All regions of powder particle approach composition of starting powder blend, and lamellae approaches dispersoid spacing.

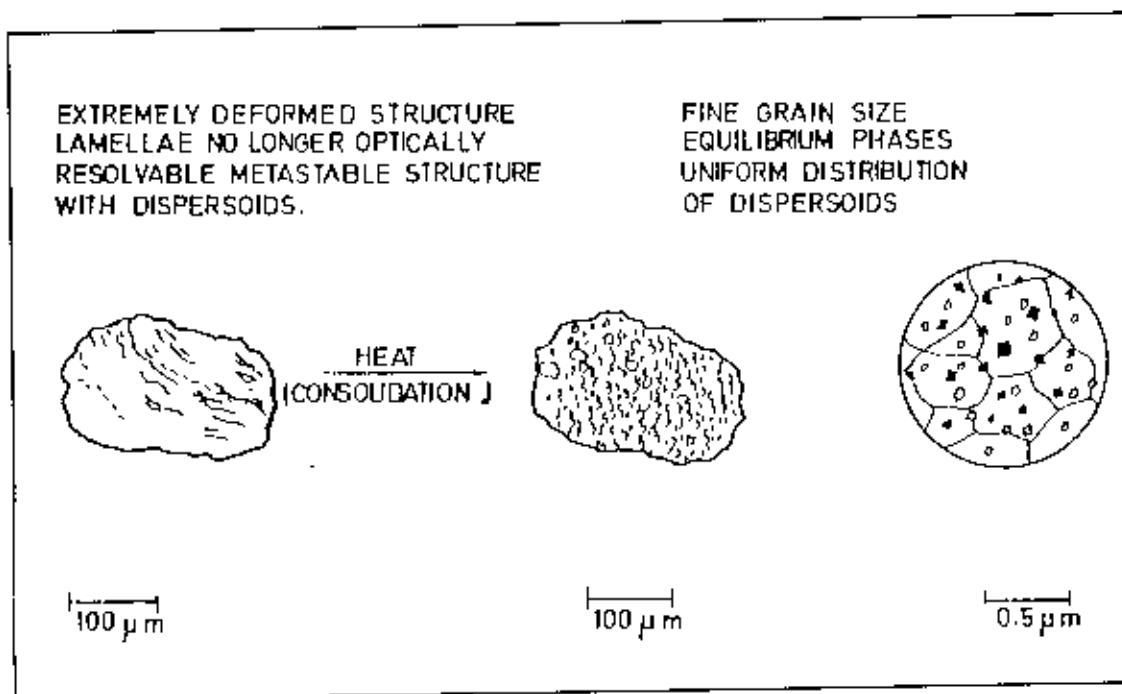


Figure 2.6 : Completion of processing. Each powder particle composition is equivalent to starting powder blend and contains a uniform distribution of dispersoids.

At this step in the process the lamellae are no longer resolvable by optical microscopy. The distance between the oxide particles along the weld interfaces is approximately equal to the spacing between the welds. The maximum weld spacing is about $0.7 \mu m$

while the average value is considerably finer¹⁴. This spacing also coincides with the random interparticle spacing of oxide dispersoids calculated on the basis of the average oxide particle size and volume fraction added to the original powder mix¹⁵. Further mechanical alloying beyond this point could not physically improve the dispersoid distribution. The compositions of the individual powder particles are now equivalent to the starting powder blend.

The powders are heated to temperatures greater than half of the homologous temperature (temperature in degrees Kelvin divided by the melting temperature in degrees Kelvin), in order to consolidate them. This homogenises the powder structure even further on an atomic scale¹⁶. Any impurities introduced into the system inadvertently, as for example iron or carbon contaminants from degraded mill balls or interior mill surfaces, are refined and uniformly distributed. Consequently, impurities are not in the form of large inclusions that may be present in powder fabricated from processes such as atomisation. The extremely deformed microstructure of the powder particles is transformed to one containing a submicrometer grain size¹⁷.

Mechanism and mechanics of mechanical alloying:

Introduction :

Mechanical Alloying is a complex materials process. If the parameters controlling of such a complex process can be identified, are few in number, and do not interact significantly, analytical expressions can easily describe parametric effects.

In mechanical alloying, a powder charge is placed in a high-energy mill, along with a suitable grinding medium. Powder particles trapped between colliding balls are subjected to deformation, as well as to potential coalescence and/or fragmentation. These are the sources of the evolution of powder morphology and size; the relative rates with which the events take place control microstructural development. The powder coalesce and fracture events also alter powder particle shape. Finally, the repetitive particle kneading associated with deformation, coalescence, and fracture processes produces significant microstructural refinement. The product powder influences the properties of subsequently consolidated products.

Collision geometry and collision duration:

Regardless of the mill used, mechanical alloying is characterised by collisions between grinding media and powder particles. There are several possible geometry for such collisions. For example, powder may be trapped between two colliding balls or caught between a ball and the container wall. In the case of an attritor, powder may be impacted between the grinding media and the rotating impellers. From a geometrical standpoint, the greatest number of collisions take place, are of the ball-powder-ball type. Rolling (sliding) of balls is commonplace in attritors and horizontal ball mills. However, Rydin et al¹⁸. have presented evidence suggesting that such events do not contribute significantly to powder plastic deformation, and hence to coalescence and fragmentation, in attritors. The extent of deformation of powder depends on the amount of powder involved in a collision¹⁹. Balls are coated with a thin layer of powder as they move between collisions by sweeping mechanism. A second potential influence on the outcome of a collision is the shape of the powder particles involved in it. Initial powder shape can vary from spherical to flake, and particle shape also varies during processing. The shape of a particle is an oblate spheroid. The shape can be characterised by a ratio: that of the minor to the major axis of the spheroid as represented in Fig.²⁰ 2.7. Deformation necessarily changes particle shape. The nature and extent of such changes depend on both the extent of deformation and the deformation direction. This direction in turn depends on the orientation of the particle with respect to the direction of impact a colliding ball makes with it. Usually particles rest on a grinding ball with their major axes parallel to the ball's surface as represented in Fig.²⁰ 2.8. which is consistent with the sweeping mechanism, satisfies the requirement of lowest potential energy, and recognises the effects of adhesive forces. Potentially hundreds to thousands of particles may be present on a ball at the time of impact; in reality their orientations may vary. (Fig.²⁰ 2.9). The geometry of a Hertzian collision between colliding balls is characterised by a maximum contact radius (r_h , the Hertz radius). This radius is attained at a time τ following collision initiation (the collision duration is 2τ). The Hertz radius and collision duration can be expressed as a function of media collision velocity, media radius, density, and tensile modulus (Appendix A Eqn. A-1). Hertz radius r_h ranges from tens to hundreds of μms , depending on v which is itself estimated to range between 0.5 m/s (e.g., for an attritor) to 5 m/s (e.g., for a SPEX mill). Collision duration are believed to be on the order of 10^{-6} s.

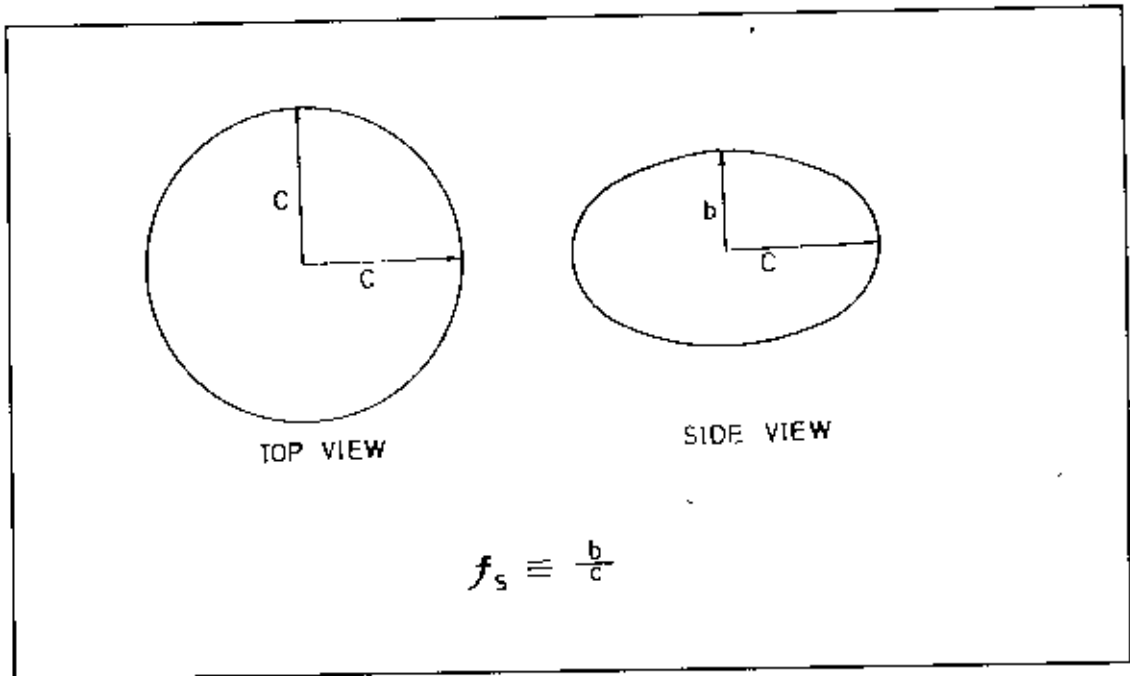


Figure 2.7 : Powder particles with oblate spheroids shapes. The shape is characterised by the factor f_s , which is equal to b/c , where b is the minor axis and c is the major axis of the particle.

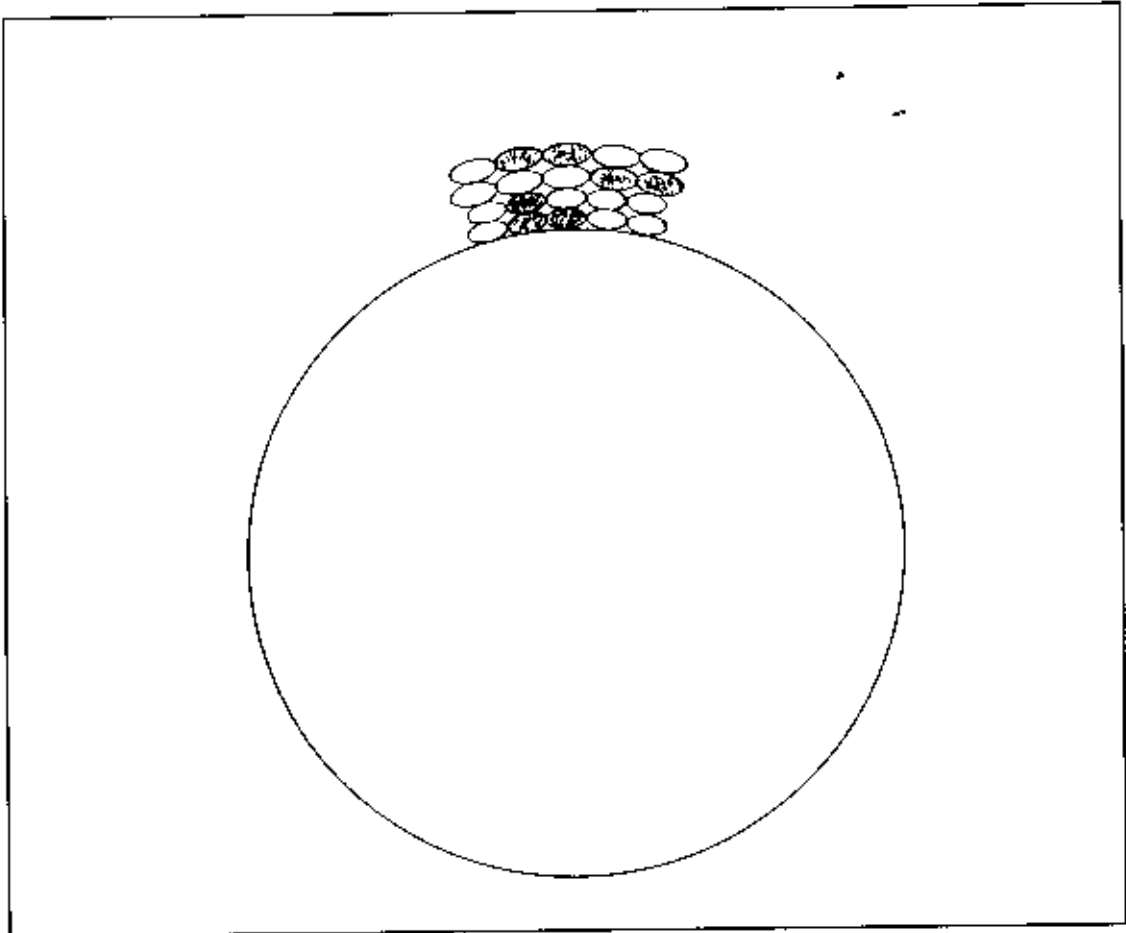


Figure 2.8 : Individual powder particles are oriented so that the major axis of the particle lies parallel to the ball's surface. The differently shaded particles represent different species.

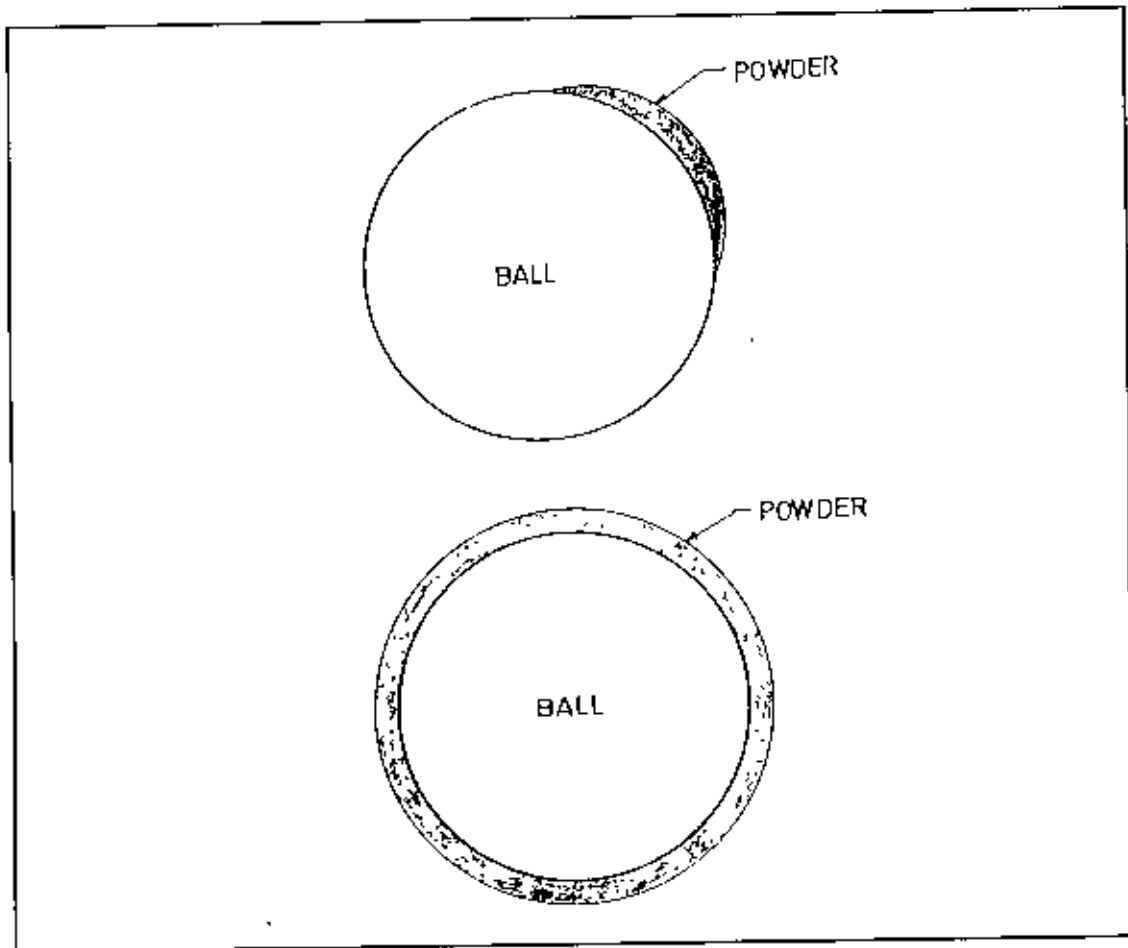


Figure 2.9 : Grinding balls are typically not uniformly coated with powder, as indicated on the top. A ball and its associated coating constitute a composite ball, as shown on the bottom,

Processing time:

Courtney and Maurice²¹ estimated processing times by assuming that a critical amount of powder deformation (Σ) is needed to accomplish alloying. The number of

impacts therefore needed to alloy scales with Σ/c , where $\epsilon = -\ln\left(1 - \frac{v\tau}{2h_0}\right)$. The time

between collisions varies as v^{-1} . That only a small fraction of the powder associated with a given media ball is involved in each collision must also be taken into account

when estimating processing times. The greater the powder affected volume ($=\pi r^2 h_0$) the less the required alloying time, other factors being equal²⁰. For $v\tau/2h_0 \ll 1$,

$\epsilon = v\tau/2h_0$. The alloying time, t_p , varies which can be expressed as in appendix A, Eqn A-3. Thus from the velocity dependencies of the collision time and radius, the alloying time depends on pre-collision velocity as $t_p \sim v^{-2.6}$.

Deformation during the collision :

Powder particles entrapped between balls undergo deformation. The degree of this deformation largely determines coalescence and fragmentation proclivities during impact, and the degree may be determined by modelling a collision in stages that allow apportionment of deformation between the balls and the powder on their surfaces.

The kinetic energy of the balls is converted to deformation energy during the approach of their centres as represented in Fig. 2.10. The stress homologous to this energy conversion is the materials' resistance to elastic and plastic deformation. For the powder (much of which plastically deforms), this resistance is taken as that of the softer material present when milling of two-phase materials is considered.

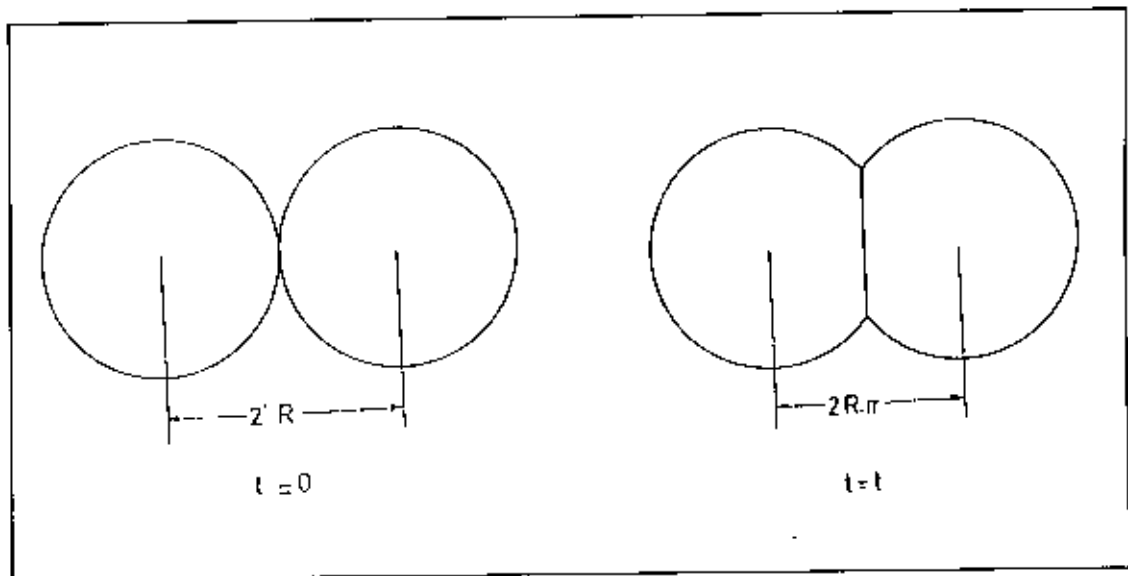


Figure 2.10 : When composite balls collide, their kinetic energies are converted into deformation energy. This is manifested by a decrease in their centre-to-centre spacing.

To plastically deform harder material requires that the softer species be work-hardened to a flow stress equivalent to that of the harder one. This delays, and certain instances may limit, the occurrence of welding and fracture of some particles. Generally grinding media used are harder than all the powder to be processed. So the grinding media experience only elastic deformation during impact. In practice, however, some powders may well attain the hardness of the media. The average strain theorem, states that the average state of strain in a given volume element is determined from the deformations applied to its boundaries. So in mechanical alloying all particles of a given species at a given distance from the centre of contact as

undergoing the same deformation. In a similar vein the average stress theorem, which equivalently states that the average stress in a volume element is equal to the tractions applied to its boundaries. What these theorems imply is that essentially all particles of a species that are located on a line between homologous points on colliding balls (for example, their centres) experience the same average stress and strain. Thus, for example, the average state of stress between powder particles (at a given position in the contacting region of the balls) is the same as that between the colliding balls.

A ball and adhering powder constitute a composite ball. A magnified view as represented in Fig.²⁰ 2.8, schematically shows how powders of different species might aggregate. Although the arrangement is idealized, it is statistically correct in that some fraction of each powder species resides in each column. It is assumed that each species to be that of an individual (fully dense) particle, rather than that of a porous body based on that the true plastic strains the powder experiences during an impact are much greater than the strain associated with densification during uniaxial compression²².

The presence of species of different hardnesses results in collisions in stages, with the softer species deforming first. In the initial stages of impaction, both powder and balls deform elastically. The distribution of stress over the contact area is shown schematically in Fig.²⁰ 2.11. On further approach of the ball centres, the stress at the contact centre attains the powder hardness. With further deformation, this stress is reached over a finite radius, the radius increasing with time of contact. Outside this radius, the stress distribution is the same as it would be in an elastic collision. As mentioned, balls are assumed sufficiently hard so as to not plastically deform during impacts. It should be noted that for a different collision geometry (e.g., ball-container wall), the stages of the collision do not change. One important result is that, for most collisions, the first stage (during which both the ball and the powder deform elastically) is very short in comparison with the total time of collision. Most of the approach between two balls are associated with plastic deformation of the powder. The approach (Fig. 2.10.), and hence deformation, may be expressed as a function of radius within the contact area²³. Expression has been represented in Appendix A Eqn. A-4. Mechanics of collision and deformation have described in detailed in Appendix B Article One.

Powder hardness :

Powder hardness is an important process parameter in that it affects the degree of powder deformation during impact and determines the normal elastic force acting to

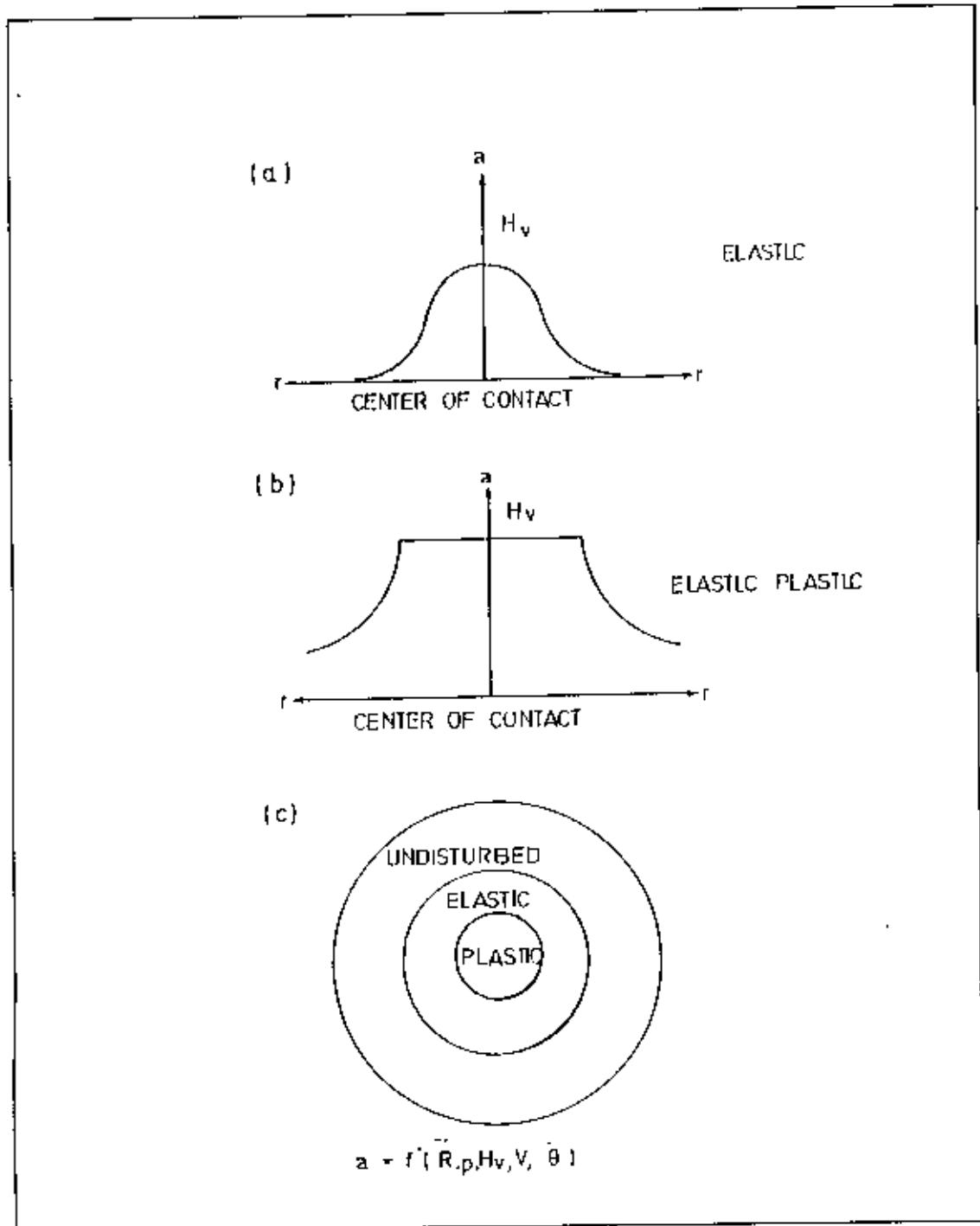


Figure 2.11 : Schematic of the distribution of stress over the contact area during a collision between composite balls. (a) Early in the collision, the balls deform elastically. (b) The powder begins to deform plastically when the stress attains the powder hardness. (c) During this stage, the centre of the contact area is characterised by plastic deformation of the powder, the annulus around it by elastic deformation of both powder and ball, and outside this annulus there is no deformation of either.

separate particles during welding. Hardness also affects the time interval between successive impacts of a particle. There is a dearth of constitutive relations for metals valid over the wide range of strains to which they are typically subjected during mechanical alloying. As a consequence, a simple plastic constitutive relation commonly applied over lesser strain ranges. Expressions have been represented in Appendix A Eqn.A-5 to 7 from which it is straightforward to determine strain as a function of radial position within the contact zone. With the aid of computational techniques, the strain (and the hardness) resulting from a series of impacts can also be monitored. However, one difficulty arises from the paucity of work-hardening exponent and strength coefficient data over the wide range of strains, strain rates, etc., to which powder particles are subjected during mechanical alloying. Additional errors could arise from temperature and strain-rate effects (although the two factors tend to cancel) on material hardness and of the changes in hardening rate²⁴ at the very large strains endemic to mechanical alloying.

Coalescence mechanisms :

Cold pressure welding has been the subject of considerable quantitative study²⁵⁻²⁶ as well as the qualitative study. As colliding balls plastically deform powder particles, their contaminant films (typically oxides) rupture, exposing underlying metal. When the free metal surfaces of the particles come into contact, a bond is formed. The oxide layer on the particles is usually brittle and fracture at the onset of plastic deformation of the underlying metal. A consequence of assuming such brittle behaviour is that the area of the contaminant film remains constant. However, as the particles flatten in compression, their surface area increases and underlying metal is progressively exposed. Two such particles in contact generally do not have complete overlapping of their exposed metal surfaces. The statistically averaged fractional matching area on two particles varies with the square of the exposed fractional area²⁷. Welding is assumed to take place only in the region over which intimate metal-metal contact is established via plastic deformation. The expression of metal-metal contact area and the force required to separate the weld that forms are represented in Appendix A. Eqn. A-8 to 9, respectively.

In a system of two species having disparate starting hardnesses, welding is delayed until the hardnesses of both are equal. As a corollary, there are thus two ways in which a composite particle can be formed. If particles of the two species are of equal hardness, they may weld directly according to the description just presented; this is termed as an "A-A" weld as represented in Fig.²⁰ 2.12(a). If they are of different

hardness and the harder particle is considerably smaller than the softer one, hard particles may be encapsulated in the softer species; this is "A-B-A" welding as represented in Fig. 2.12(b). Here should be noted that deformation constraints

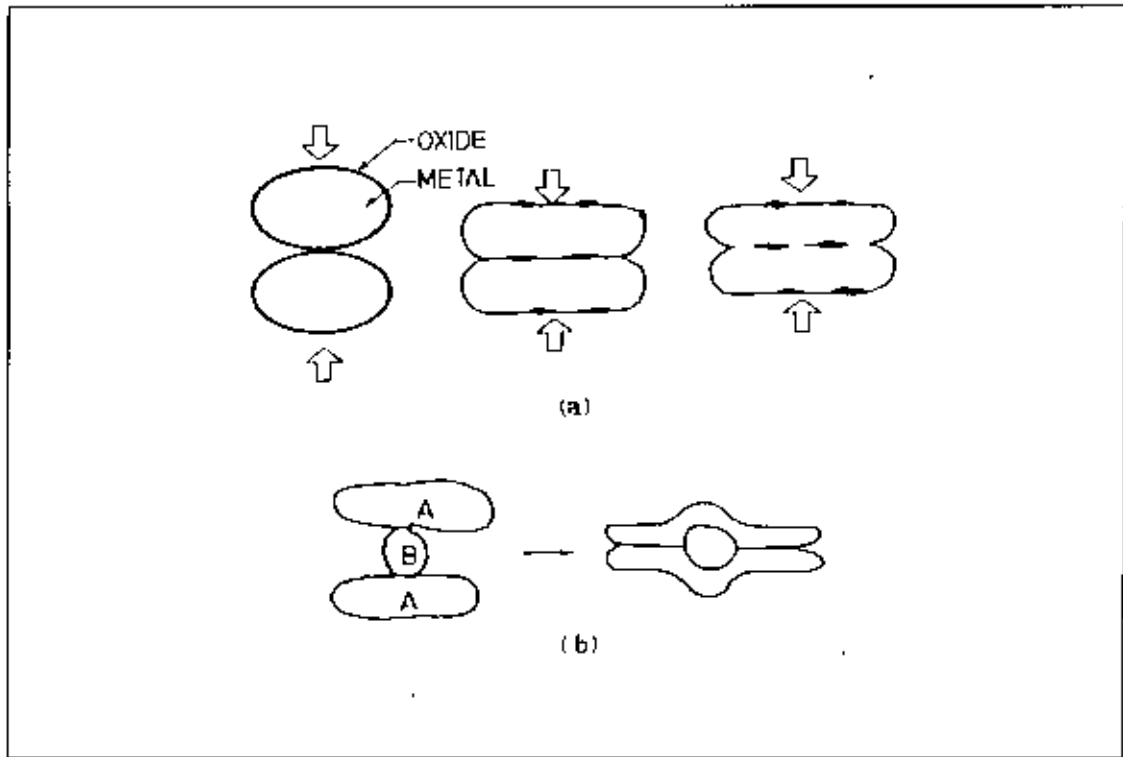


Figure 2.12 : Two different forms of coalescence during mechanical alloying. (a) Coalescence effected by cold welding, termed as A-A weld. (b) Coalescence effected by particle encapsulation (A-B-A welding).

might lead to deformation of the harder particle once it is incorporated into the softer one²³;

Elastic recovery forces (arising from particle deformation) and shear forces (resulting from any relative tangential motion of the colliding balls, (Fig. 2.13) act to separate welded particles and sever the juncture between them. The elastic recovery forces act in an annulus about the plastic deformation zone. If dispersoids are trapped between powder particles, an elastic recovery force acts through them as well. Expression of this elastic recovery force and average shear force are represented in Appendix A Eqn.A-10 to 11

An effective stress argument is applied as a success/failure criterion for the weld. If the following condition is met, the particles remain welded; if not, they separate: If particles separate, the possibility remains that they may exchange metal through adhesion. $F_w^2 \geq N_e^2 + 3T_b^2$. Where F_w is the force required to separate the weld, N_e is the total elastic recovery force. T_b is the average shear force acting over the weld surface.

The effect of surface reoxidation. Powder particles typically have an oxide coating of 2 to 10 nm²⁸⁻²⁹.

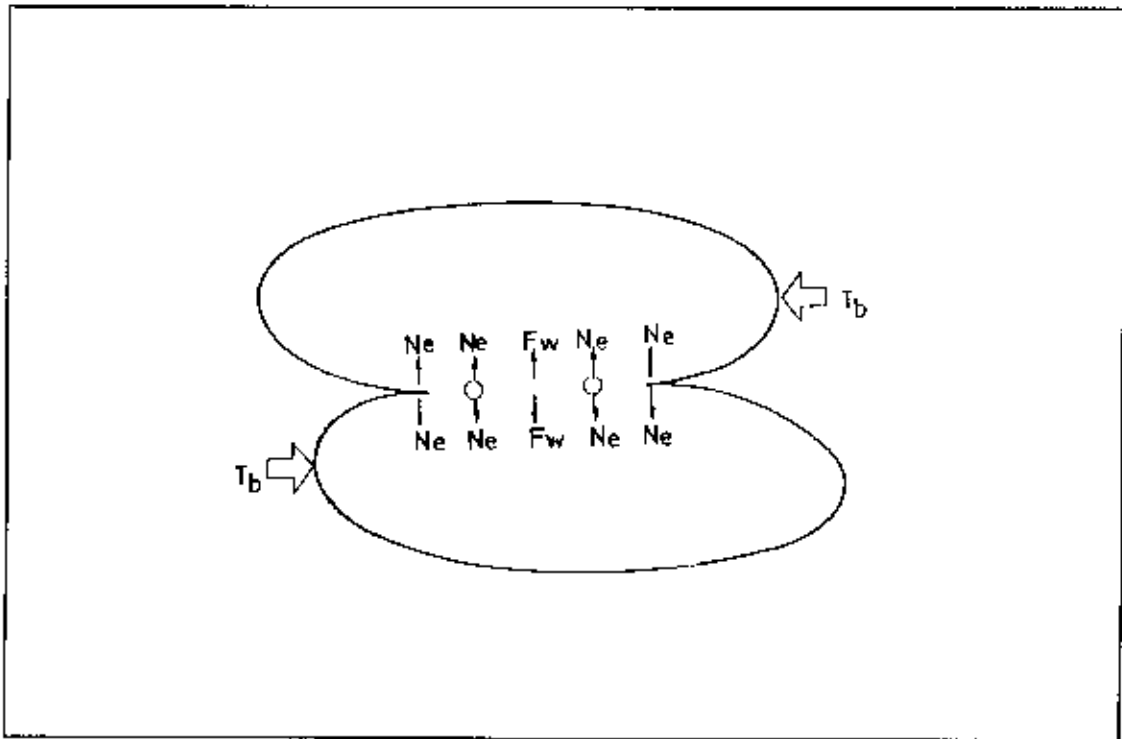


Figure 2.13 : The newly formed bond between welded particles is subjected to forces acting to sever the weld as the grinding media balls separate.

As this is just several atomic layers thick, Dr. Maurice et al¹⁹ stated that oxide reforms as islands, rather than coating the entire particle. That is, the oxide is treated in terms of surface coverage rather than thickness. This allows to determine the amount of exposed metal surface prone to reoxidation during processing. The fractional metal surface exposed is reduced by reoxidation; This reduction of metal of surface exposed is represented in Appendix A Eqn. A-12.

Fragmentation mechanisms :

There are three possible mechanisms of particle fragmentation during mechanical alloying. The first, forging fracture as represented in Fig.²⁰ 2.14(a), may develop over several impacts. Cracks formed in this way grow radially along the major axes of the particles. The second type of fracture considered is termed shear fracture as represented in Fig.²⁰ 2.14(b). This fragmentation mode is characterised by cracks running perpendicular to the particle's minor axis. As a result of crack closure forces, this mechanism is likely not operational in mechanical alloying³⁰. A third type of fragmentation is dynamic fracture as represented in Fig.²⁰ 2.14(c). This requires strain

rates higher than those characteristic of common mechanical alloying devices, but may occur in some of the higher-energy mills during impacts characterised by

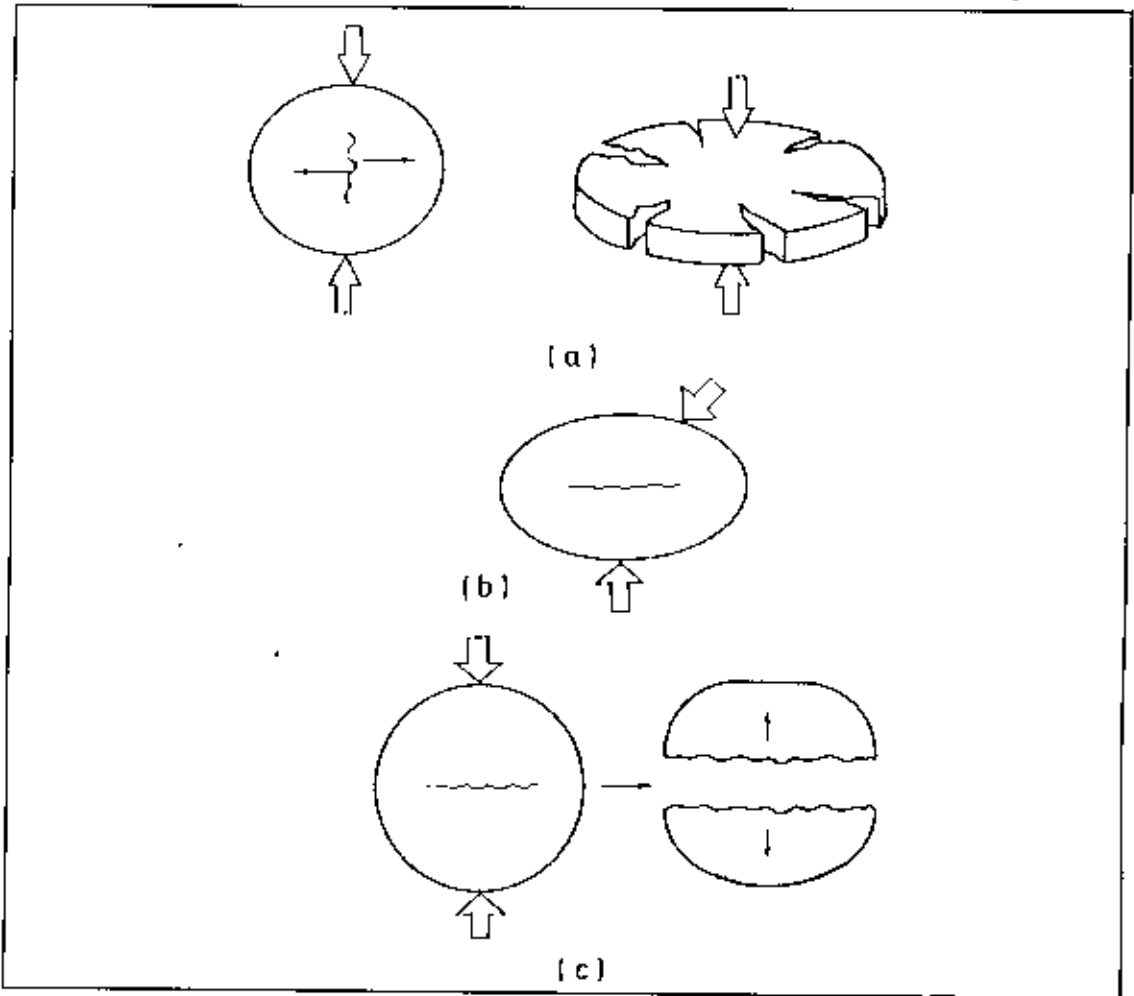


Figure 2.14 : Three possible fracture modes taking place during MA. (a) forging fracture is the fragmentation mechanism most likely to occur. Edge cracks are formed (perhaps over several impacts) along the particle circumference and grow along the particles axis. This is a microscope version of fractures that take place in macroscopic forging; (b) Shear fracture, in which cracks run perpendicular to the particle's minor axis, is not as likely to occur due to crack closure forces. (c) Dynamic fracture, in which separation is effected by a reflected tensile wave, requires high strain rates.

high collision velocities and/or minimal powder coatings. Crack initiation is a precursor to forging fracture. A crack initiates when a critical tensile strain is attained and that the initial crack length is equal to the distance over which that threshold strain is exceeded. Subsequent crack propagation occurs when the plastic energy release rate exceeds a value characteristic of the material. This requires that the crack exceed a certain length. If the particle is sufficiently small so that this length is greater than the particle size, the particle is considered below its comminution limit and will not fracture. It necessitates to determine the location and directions of tensile strains in a compressed body. Hereby considered two methods of determination. The first, based

on work of Avitzur,³¹ incorporates the concepts of sticking friction at the tool-work piece interface and of barrelling. Strain is greatest at the outer circumference, and there is a dead metal zone at the contact centre. This method predicts crack initiation at the outer circumference of the particle; based on studies of forging failure of ductile materials,³⁰⁻³¹ this seems most reasonable. In the second method, the presence of a dead metal zone has disregarded and strain has been computed as a function of position based on theoretical considerations (For detail please see Appendix B, Article Two). Strain is greatest at the contact centre and decreases with radial distance from this point. This predicts crack initiation in the particle centre, as would be expected for a brittle material. While the first method is more plausible with respect to the conditions and materials of mechanical alloying, there is little difference in the criteria for crack initiation or final fracture between the two approaches. The prediction of fracture is based on the determination of strain distribution. This is done by considering powder particles as oblate spheroids. An individual spheroid, in turn, can be imagined as constituting a series of nested, concentric cylinders of differential thickness. The innermost cylinder has a height equal to the particle's minor axis and a radius approaching zero; the outermost cylinder has a height tending to zero and a radius equal to the spheroid major semi-axis. Those differential cylinders are sequentially compressed as powder is deformed. A cylinder under axial compression experiences equal tensile strains in the radial and circumferential directions. It is most convenient to work with axial strain, since that is immediately determined from the approach at impact. For a cylinder under axial compression (and no barrelling), we have $\epsilon_0 = 0.5\epsilon_z$, where ϵ_0 and ϵ_z are the circumferential and axial strains, respectively. In Appendix B, Article Two determination of the plastic deformation of a powder particle as a function of radial position within the particle, has been described so that the axial (and hence circumferential) strain can be determined. Crack initiation (and growth) is assumed to occur for the condition $\epsilon_0 = \epsilon_f$, where ϵ_f is the tensile true fracture strain. For ductile materials, the requirement for initiation/growth at some distance r from the centre of contact between two particles becomes $\epsilon_z(r) = -2\epsilon_f$. A similar analysis can be carried out for brittle materials. In this case, the requirement for initiation/growth is $\epsilon_z(r) = -\frac{1}{\nu} \epsilon_f$. This can be applied to predict fracture strain of a powder particle. Due to the small size of powder particles, linear elastic fracture mechanics cannot be applied; rather, an elastic-plastic analysis is necessary. Crack length is assumed equal to the distance over which a critical strain, discussed earlier, is exceeded. When the crack reaches a critical length, determined by the critical value of

the J integral, it propagates catastrophically. The value of the J integral is approximated by³⁴ the expression is represented in Appendix A, Eqn. A-13. Using the expression for strain as a function of radial position within the powder particle permits determination of the total approach between balls needed in order to exceed some critical strain over a given length and to exceed the critical strain over a_c requires that the strain be exceeded over a radial distance one-half of a_c . Expression of critical crack length is expressed in Appendix A, Eqn. A-14. And the condition for forging fracture is expressed in Appendix A Eqn. 15.

Welding and fracturing probabilities :

Welding and fracturing probabilities during mechanical alloying depend on the charge ratio and on the type of powder milled³⁵ not on particle size or on milling time³⁶. Welding probabilities increases with charge ratio giving rise to shorter milling times. This is likely due to a smaller number of particles and a larger amount of energy absorbed per particle during collision. Probabilities in this respect are described in detail in Appendix B (Article Three).

Shape factor :

Particle shape may affect coalescence and fragmentation events. Moreover, particle shapes are altered by these occurrences as well as by plastic deformation. Most particle shapes, with the exception of needles, may be reasonably described as oblate spheroids as represented in Fig. 2.7. The expression related to shape factor of powder particle have been represented in Appendix A Eqn. A-16 to 17. Particles on ball surfaces are assumed to have their major axes parallel to the surfaces and the minor axes perpendicular to them. The minor axis is reduced, and the major axis increased, as a particle is compressed. This change in, the shape factor after deformation are expressed in Appendix A, Eqn. A-18 to 19.

In the case of a weld event between two particles, the minor axis of the new particle is taken as the sum of the minor axes of the original two. If the two powders are of different species, the minor axis of the composite particle formed is equal to the sum of the minor axes of the particles of the different species, and the major axis is set equal to the greater of their major axes. Similarly, in the case of forging fracture, the major axis is halved, again doubling the shape factor. As both weld and fracture events take place after some deformation, the final shape factor is a multiple of the shape factor after deformation, determined on the basis of the events the particle

experiences. The surface area of a particle is also altered by deformation, fracture, and coalescence. Surface area affects the proclivity for welding,

Friction in a powder mass :

Friction between the particles in powder is a valuable characteristics of a powder. The effect of the particle characteristics such as shape; size and surface configuration and conditions on the friction in a mass of powder is prominent. The friction in a powder mass is not only affected by the particle characteristics, but by the type of powder material, e.g. soft metal usually have higher friction than hard metal. The friction conditions in a mass of powder include static as well as kinetic friction. Static friction is a function of the load between surfaces and in the rearrangement of particles in the loose powder. The load (gravity) is low and the sliding forces (kinetic friction) during packing of the particles are less.

Oxide Films on powder particles affects the friction in a powder mass. Powders seldom have a clean surface and are more less oxidised; this surface oxide film decreases the coefficient of friction to approximately 50 per cent of that of the material with clean, i.e.; non-oxidised surfaces³⁷. The powder behaviour is strongly affected also by the medium surrounding the powder, inasmuch as this gaseous or liquid medium changes substantially the friction condition and the friction coefficient. Particle size affects the friction in a powder mass in several ways: it determines the number of contact points where friction occurs, the specific surface of the powder, and it determines also the surface energy of the particle. The shape of the particle affects the friction in the powder independent from the size in several different ways. The more the deviation of the particle shape from the sphere, the larger is the specific surface, the number of contact points and the surface energy. The shape of the particle affects greatly the friction conditions and therefor the loose powder density. It has been found that the friction in a powder mass increases the more the shape of the particle deviates from the spherical shape. The humidity in the air also affect the friction conditions between particles. A higher relative humidity however lowered the flow and also the apparent density.

Effects of friction on compacting and sintering :

Friction between powder particles as well as the particles and the surface of the compacting device plays an important role in compacting. The compression ration of a plastically deformable metal powder actually consists of two subsequently and

somewhat overlapping parts. The initial part of the compaction (low pressure) results in a rearrangement of the particles and the applied pressure has to overcome the frictional forces between the particles. The second part of compaction (higher pressure) result in plastic deformation of the particles. There are also indications that the sinterability of a powder i.e. the rate of strengthening at the early state of sintering and the rate of densification at the later stages are strongly affected by the friction between the particles, i.e., by all the many factors such as size, shape and surface conditions of the powder which affects friction.

Consolidation :

Introduction : At present most mechanically alloyed powders are consolidated by hot compaction followed by hot extrusion or by direct hot extrusion at temperatures greater than half of their melting point. The extruded bars can then be thermo-mechanically processed to desired grain structures, such as coarse elongated grains for high temperature creep resistance or cold rolled to sheet, such as for the ferritic alloy. Mechanically alloyed powder is also amenable to the consolidation techniques used for high performance powder metallurgy alloys such as hot isostatic pressing.³⁷ As yet, simple pressing and sintering has not been a successful consolidation technique for high temperature alloys. The characteristically high hardness of the mechanically alloyed powder prevents cold pressing, and oxide dispersion strengthened alloys have been found not to density during simple sintering. However, other mechanically alloyed systems without oxide dispersions may find applications in the pressed and sintered form. Novel consolidation techniques such as consolidation by atmospheric pressure³⁸, powder rolling, Conforming³⁹, or explosive forming may also be applicable. Finally, mechanically alloyed powders can be consolidated by plasma spraying for use as oxidation-resistant, or thermal barrier coatings.

Cold process:

Die compaction: Compaction in metal dies is one of the most important methods for shaping metal powders and this still accounts for the bulk of commercial production. Both experimental and theoretical work have been carried out by numerous workers.⁴⁰⁻⁴³ in attempts to explain exactly the behaviour of metal powder when subjected to external pressure in a metal die.

When the die cavity is uniformly filled with metal powder it gives rise to a certain packing density, but a certain amount of bridges are formed as represented in Fig. 2.15a. When the powder is slightly pressed by the application of one punch or more punches as represented in Fig. 2.15b the first identification occurs by particle movement and rearrangement causing improved packing density (here all bridges are collapsed).

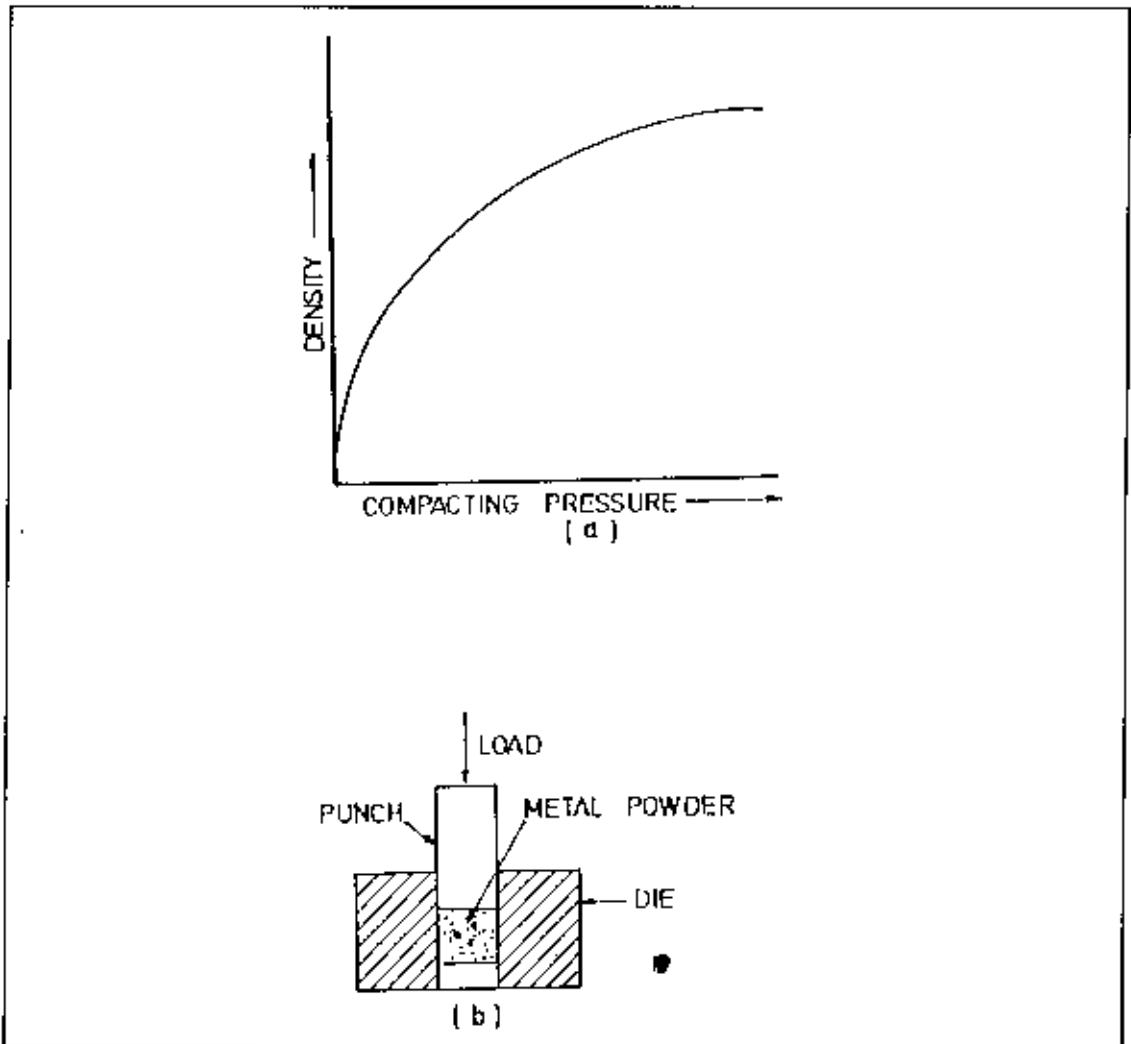


Figure 2.15 : Die compacting : (a) Typical pressure-density curve, (b) Tools for die compacting

The degree to which this occurs is dependent on particle size distribution, particle shape, preliminary treatment of powders, amount of lubricants, etc. The interparticle movement produces superficial abrasion of surface film comprising oxides, absorbed atmospheric gases which are usually present or wedged between the metallic surfaces. These films obstruct the occurrence of direct metal contact and thus the formation of appreciable interparticle bonding. Because of the interparticle movement the films surrounding the particles are ruptured which are usually more brittle with

respect to the metal underneath. The initial contact areas between the particles are so small that even a slight punch load causes very high pressure on these areas thereby breaking up the surface films at the areas of contact. At this stage compacting produces only dense packing of powder particles; neither deformation nor adhesion between the individual particles has as yet occurred.

If the pressure is further increased, clean particles are brought close enough together and they adhere to each other with some strength. This metal-to-metal contact has been described by Jones⁴⁴ as "cold welding" or adhesion. Further increase in pressure causes deformation of the particles and large areas of contact and mechanical interlocking of neighbouring grains will take place as well as filling of voids by the squeezing of small particles. Strength and density are thus increased. Deformation is the major mechanism of densification with regard to production of high density parts. Both types of deformation, elastic and plastic may take place. Most of the elastic deformation will be recovered on removal of stress from the compact. This may occur before, during and after ejection from the die cavity. In general, the compacts have dimensions slightly greater than the die dimension due to this reason. The magnitude of elastic deformation will depend on elastic modulus values and particle stress values relative to the yield stress of the material. In the case of very hard and brittle powders such as Cr, refractory metals and carbides, density may increase after initial packing stage without plastic deformation. The elastic recovery is much greater for hard metal powders and thus it decreases the size of contact areas and consequently the strength. Hence micron sizes are usually employed to produce a maximum number of contact points and relatively large pressure is required.

With the exception of porous parts, plastic deformation of powder particles usually represents the most important mechanism of densification during compacting. Soft metal powders such as Pb, Sn, and Ag possess the greatest capacity for plastic deformation under moderate pressures with extended areas of contact. Application of higher and rapid rate of pressures will give rise to larger degree of plastic deformation of the particles.

Most materials work harden to an appreciable extent, so that it becomes increasingly more difficult to improve densification of the compact by increasing the compacting pressure. In these cases low pressure will be more effective since plastic deformation will occur at ease and the external pressure will become less effective with increasing pressure. Thus powders of pure metals, single phase and well annealed materials are

most suitable for this process. The increase in hardness of individual particles after varying amounts of compaction is a direct result of work hardening due to plastic deformation.

Materials having a limited plasticity or ductility compacted at relatively high pressures have the tendency to exhibit higher stress than the fracture stress of the individual particles which would finally lead to fragmentation of the particles during compacting. Thus method of fracturing also results in densification of the compact, since smaller fractured places easily move to the adjacent pores.

Numerous investigators⁴⁴ have identified three stages of compaction of metal powders. In the first stage particles are brought close together without undergoing deformation as a result of particle movement and rearrangement. The second stage attributes to plastic deformation and cold working. Since pressure is greater than the bulk yield stress of the material, plastic flow becomes homogeneous instead of local. The third stage corresponds to bulk compression and involves fracture or fragmentation of brittle powders.

Hewitt et. al⁴⁵ have inferred that plastic deformation always occurs throughout powder compaction, though it does not always produce consolidation or densification. Consolidation occurs as a result of the combined effect of mechanical interlocking and associated friction welding due to surface shear deformation caused by asymmetrical loading. Following compaction, ejection of the pressed part is effected by the movement of the die or punch. The density and strength of the unsintered compact are called green density and green strength respectively.

Many studies on the effect of applied pressure on the density and its distribution within the compact have been made in detail by many workers⁴⁶. Of the numerous formulae put forward one, which has got wide acclaim, is that of Shapiro and Kolthoff and Konopicky⁴⁶, $\ln\{1/(1-D)\}=KP + \text{constant}$, where D is the relative density, P the applied pressure, and K a compaction constant. The plot of density as a function of the applied compacting pressure would be as the graph as represented in Fig. 2.15a.

There are several different types of die compaction techniques as follows. (a) Single action compaction, (b) Double action compaction, (c) Double action floating die compaction, (d) Double action withdrawal compaction.

Explosive forming : The explosive compacting of metal powders is a comparatively recent development which offers some advantages. Here, the pressure generated by an explosive is employed to compact powdered material into a desired shape. Thus very high and uniform density green compacts of the order of 94-98% of the theoretical value together with superior mechanical properties are obtained⁴⁷ with a wide variety of materials, e.g., metals, refractory materials, ceramics, and cermets. Die costs are lessened and expensive (hydraulic) equipment now required for preparing metal powder parts are eliminated.⁴⁸ In conventional die pressing, rapid speed produces poor compacts and speeds up to 5 ft/sec. are utilised while in explosive compacting speeds of the order of tens of thousands of ft/sec. are employed with superior result. This process is so rapid that it is very difficult to know the various stages of powder compaction. However, it is anticipated that a greater amount of cold welding and plastic deformation takes place when compared with conventional die compaction.⁴⁸

Explosive charges have been employed for the movement of punch or piston into the dies containing the powdered metal which are well protected from the products of the explosive charge. Single acting explosive press is the simplest one which is shown in Fig. 2.16a. Double acting explosive presses have been employed by many workers (Fig.⁴⁹.2.16b.) and they have compacted sponge cobalt and ductile titanium powders to a density of 95% of the rolled bar stock density. Montgomery and Thomas⁵⁰ have used the transmission of shock waves through water on to Al powder confined in a thin-walled Al tube which produced a compact with variation in density depending upon the distance from the charge. But compacts of cylindrical shapes of uniform density were produced by wrapping the detonating fuse in a continuous spiral around the thin walled metal container holding the powder, placing them in a suitable water bath and finally detonating the explosive charge.

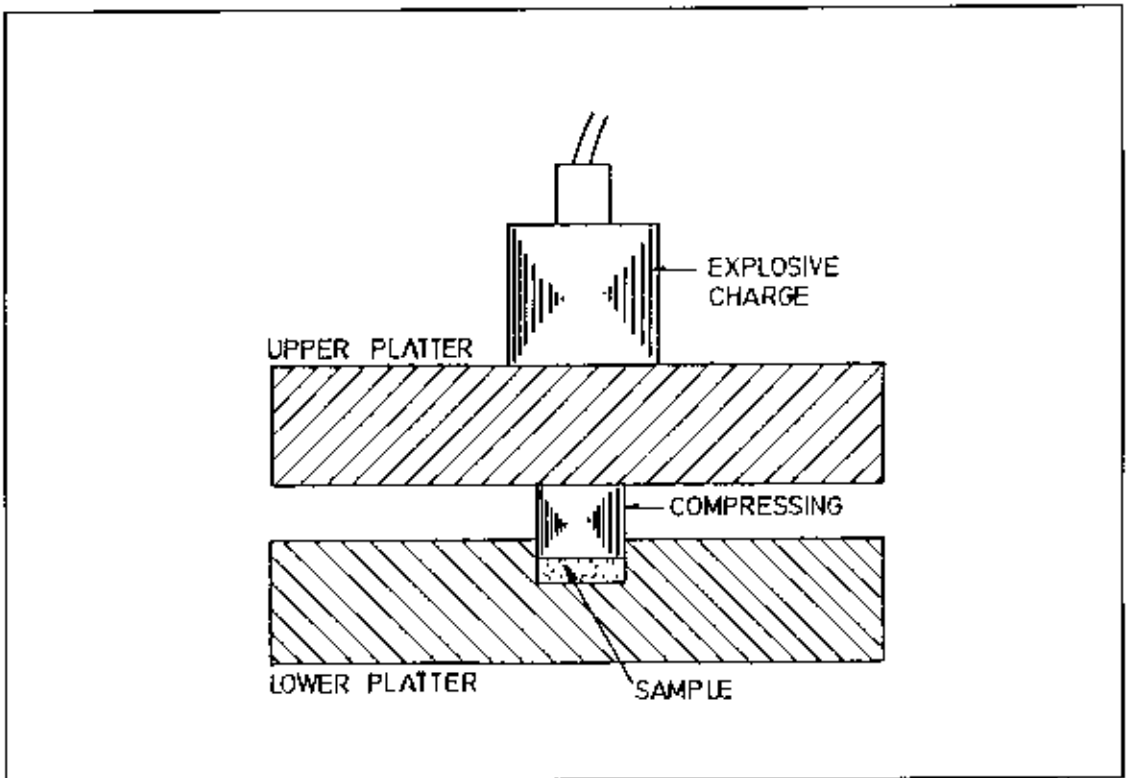


Figure 2.16 : (a) Single acting explosive press.

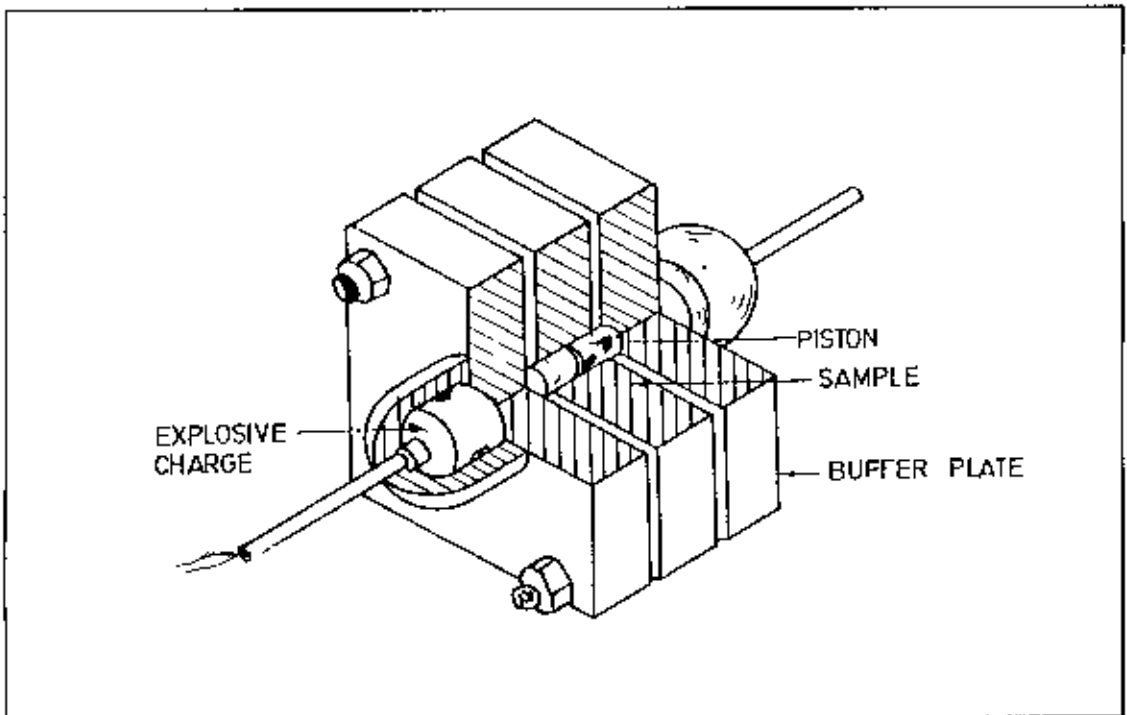


Figure 2.16 : (b) Design of double acting explosive press for compressing powder.

In general, the detonation of low explosives such as smokeless powder and black powder causes reaction zone travel velocities of hundreds of feet per second and

pressures up to about 300,000 psi., while high explosives such as dynamite, TNT and RDX, etc. are characterised by a burning rate of several thousand feet per second and pressures of several millions psi.

Powder rolling: The continuous compaction of metal powders by rolling has been first reported by Naeser and Zirm in Germany in 1950. From then on, much work has been done on this method⁵⁰.

In powder rolling, the rolls are set directly above each other so that the strip emerges horizontally as shown in Fig. 2.17, or they are set side by side so that the strip emerges vertically downward, as shown in Fig. 2.18 and Fig. 2.17. is a schematic representation of horizontal arrangement in which powder is being poured on to a carrier; its amount being regulated by an adjustable tip, and finally wound on reels on the opposite side of the mill. This method is more convenient from the view point of strip handling. In Fig. 2.18 showing vertical arrangement, hopper may be avoided and the powder is directly dumped in the channel between the rotating rolls up to the required height on the roll surface. When the rolls turn the powder is drawn into the gap between the rolls and is pressed into a strip. This method has the advantage of gravity feeding and, therefore, the powder feeding becomes easier.

It has been shown⁵²⁻⁵³ that during roll compaction the powder particles are densified in the several stages such as restacking and reorientation, local deformation (deformation of individual powder particles), and plastic deformation. However, these three stages overlap each other. Hoar⁵⁴ has pointed out that pressure increases are much more effective in causing densification during rolling, since frictional effect is negligible in this case as compared with wall-friction effect in the conventional compaction.

The characteristics of the finished strip are dependent on many factors, the most important of which are:

- (1) Roll compaction: of between 100 and 300 times the strip thickness are required to obtain optimum powder compaction^{49,50}. Maximum strip thickness that can be produced, therefore, increases with increasing roll diameter.
- (2) Surface finish of the rolls: Roll roughness has a pronounced effect resulting in an increase in strip thickness. Further increase in thickness is obtained by the use of wet roughened rolls.
- (3) Size of roll gap: Evans⁵⁷ has pointed out that a given powder can not be

compacted into a coherent strip if there is a very large roll gap. (4) Roll speed : For a given powder flow, higher rolling speed reduces the time during which the

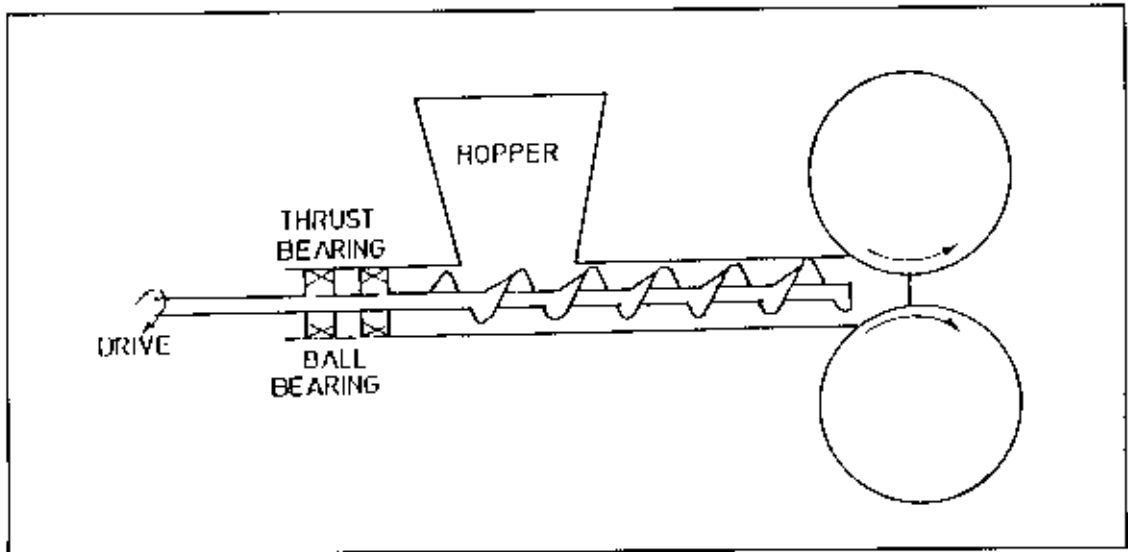


Figure 2.17 : Schematic representation of horizontal arrangement of powder rolling.

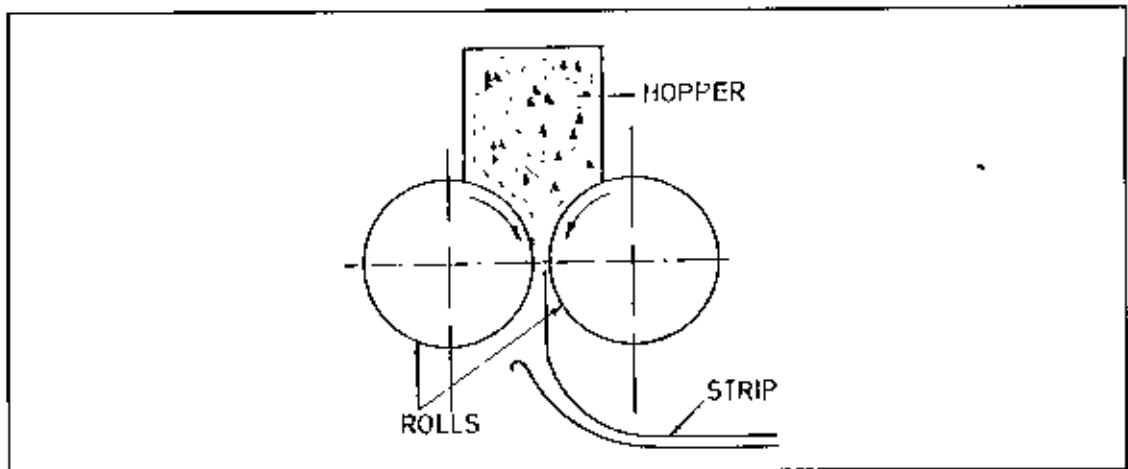


Figure 2.18 : Schematic diagram of powder rolling showing vertical arrangement.

rolls. (3) Size of roll gap: Evans⁵⁷ has pointed out that a given powder can not be compacted into a coherent strip if there is a very large roll gap. (4) Roll speed : For a given powder flow, higher rolling speed reduces the time during which the compressive load is applied to the powder, thus resulting in a decrease in density and strip thickness. A higher output is possible by using a greater powder head which causes an increase in thickness and density of strip produced at a given roll gap. Maximum rolling speed is governed by the powder flow to the compaction zone. Faster rolling speed is achieved with better flow properties of the powder⁵⁷. (5) Rate of powder feed to the rolls: This has already been mentioned in (4). (6) Particle shape, size and size distribution: Other characteristics of the powder which have a definite

influence on the thickness of the strip produced are particle size, its distribution, and shape. Thin strip requires fine powders while the heavy sheet is produced from coarse powders having a normal particle size distribution. The strength of strip produced is largely a function of the particle shape. (7) Sintering temperature: A rise in sintering temperature has a great influence on the strip thickness and sintered strength. Thus, Evans⁵¹ has reported that a rise in temperature of 300°C results in an increase thickness of Cu strip by 25%. Usually higher sintering temperatures are employed for shorter dwell time in a sintering furnace of reasonable size to obtain the requisite strength. Thus, the strength of the Cu and Fe strip becomes doubled by raising the temperature from 750 to 1000°C and from 950 to 1200°C respectively.

Hot Process :

Hot die pressing: In hot pressing the powder is placed into a die and pressure is applied simultaneously with heat. In other words, the two basic steps such as compacting and sintering are combined in one process. In pressure-sintering green compacts are sintered instead of the powder and comparatively low pressure is applied much more slowly during sintering than in hot pressing. Usually compacts of about 90% theoretical density can be obtained from the metal powders by employing a pressure of about 100 kg/cm² and a temperature of $\sim 2/3$ rds. of the absolute melting point of the material. According to Tsukerman⁵⁸ usually compacts of specified density at high temperatures are produced by the application of 10-20% of the cold compacting pressure. It can, therefore, be concluded that the amount of pressure required for compacting the powder decreases with the increase of pressing temperature.

The mechanisms of hot pressing have been described by Williams⁵⁹ (for metals) and by Murray⁶⁰ (for ceramics). There are two mechanisms of densification in hot pressing.⁵⁹ The first is termed "transient state" and the latter "steady state diffusion" mechanisms. Though these two mechanisms occur simultaneously, normal deformation mechanism dependent on the existence of yield point has been found to occur at the earlier stage. An approximate second power relationship between the rate of strain and stress is found to exist. This mode of densification results mainly from the plastic flow which can be regarded as the distinguishing feature of hot pressing only. The second mode of densification is considered of greater importance during the later stages of hot pressing. Murray⁶⁰ has also concluded that plastic flow is the main mechanism of densification.

Hot pressing, generally, does not eliminate the subsequent normal sintering operation which makes the composition and structure of the parts homogeneous thereby securing the advantages derived from hot pressing. A protective atmosphere is frequently needed to prevent oxidation during filling, heating, and cooling on ejection. The use of inert and reducing atmospheres such as argon and hydrogen respectively have been found helpful for hot pressing. Now-a-days hot pressing is often carried out in vacuum.

The most generally applicable methods of heating the dies and the materials being pressed are convection heating using external heaters, passing high current source through the die or powder and induction heating. Hot processing furnaces employed are usually vertical. In case of metallic dies, since the temperature of the powder does not exceed 1000°C , simple wire wound resistance furnace is adequate.⁶¹ In hot pressing, the temperature employed varies from 100 to 500°C for non-ferrous materials.

Hardened high speed steel (14-4-1, W-Cr-V steel) dies are satisfactorily employed at temperatures up to about 600°C and at pressures up to 30 tsi. The temperature limit for cemented carbide dies is $950\text{-}1000^{\circ}\text{C}$. For temperatures above 1000°C , graphite, oxides, nitrides, silicides, borides and uncemented carbides may be employed.

Hot Extrusion : This method is important particularly in the atomic energy field for producing cermets, fuel materials (e g, UO_2 in stainless steel matrix), dispersion strengthened materials (e g., S.A.P., T.D. Nickel and others with copper, zinc or lead base), refractory metals, Be and Cr into simpler shapes such as rods, tubing, flats, etc., by employing the canning process as shown in Fig. 2.19.

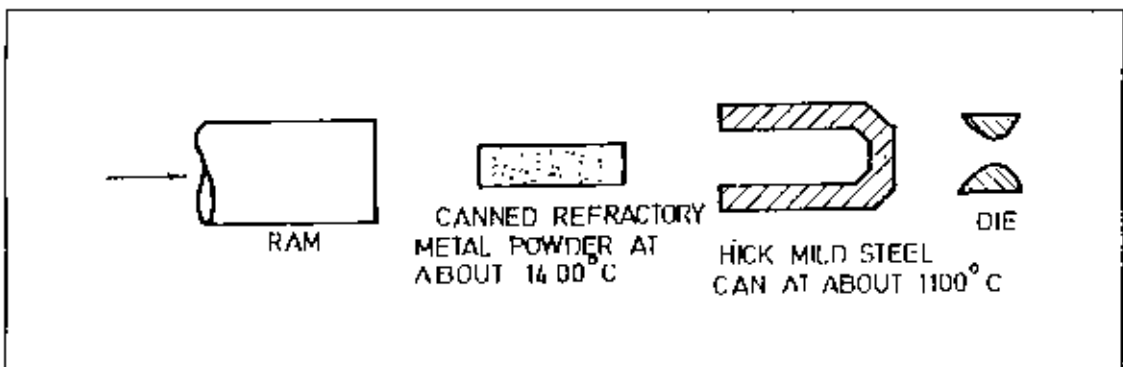


Figure 2.19 : Schematic diagram of hot extrusion employing the canning process.

The powders are cold compacted in a mild steel or stainless steel container and extruded at the appropriate temperature to yield a completely dense material with better mechanical properties and controlled grain size and grain orientation. Canning technique facilitates easy handling of pyrophoric, toxic and even radioactive materials (and controlled atmosphere can also be used without any problem).

Hot-Isostatic Compaction: The process consists in enclosing the powder contained in a pressure-tight metal container of appropriate geometry which is subjected to isostatic pressure (using either gases or liquid metals as the pressure transmitting media) with simultaneous application of heat. The desired densification is obtained by maintaining this condition for sufficient time. This method is well suited for the consolidation of refractory metals, high melting point compounds, super alloys, beryllium high speed steel, cement and ceramic materials. Usually dense parts with controlled grain size are produced by using low sintering temperature (for example, 0.5 to 0.6 times the melting point in case of refractory metals) and short sintering time⁶¹. Gas autoclaves are most widely used for hot isostatic compaction. There are two types of equipment - hot-wall and cold-wall, the choice of which depend on whether the heat source is external to the pressure vessel or is contained within it. But the latter equipment has proved more versatile. This technique avoids pressure, temperature, and size limitations of hot pressing because refractory tool materials are not involved here. The problems of contamination owing to tool material/powder reactions are also avoided. As in die compaction uniformly dense compact with large length-to-diameter ratios are produced and extremely high degree of accuracy and shape control are achieved by this technique. The other advantages include isotropic microstructure and possibility of producing complex shapes.

Processing control of mechanical alloying :

Process modification : It is critical to establish a balance between fracturing and cold welding in order to mechanically alloy successfully. Developing this balance may require different process modifications depending on the alloy systems. Two approaches have been used for the aforesaid purpose. The first technique is to modify the surface of the deforming particles by the addition of a suitable processing control agent that impedes the clean metal-to-metal contact necessary for cold welding. Processing of aluminium-alumina dispersion strengthened alloys requires the addition of an organic compound e.g. methanol (3% mass) to reduce excessive cold welding of aluminium powder particle by modifying the powder particles' exposed metallic

surfaces^{63,64}. Sometimes lubricants e.g. kerosene or fatty acids are added to prevent the particle from coming in contact, but their use may severely contaminate the powders and degrade the alloy made from them. The second approach is to modify the deformation mode of the powder particles so that they fracture before they are able to deform to the large compressive strains necessary for flattening and cold welding. This can be accomplished by cryogenic milling. For example, lead is very difficult to mechanically alloy because it is extremely soft and ductile at room temperature. Cooling the mill chamber to 77°K promotes fracturing and establishment of steady state processing⁶⁵.

Powder size and size distribution: The powder size distribution of mechanically alloyed powders may range from 10 to 500 μm in diameter with an average size of 50 to 200 μm ; it is a function of starting powder size distribution and composition. Powders that cold weld easily, such as aluminium, quickly grow in size; the average particle diameter at which the powder size distribution stabilises depends on the type and amount of processing control agent used and the time of processing. In many cases, after long processing times, the processing control agent will become alloyed into the powder particles and will no longer prevent excessive cold welding. For most applications, once well alloyed, homogeneous powder particles are made and a specific powder size distribution is not necessary. Also the flexibility of mechanical alloying is such that the powder size distribution can be altered by processing beyond the point of homogeneity with or without the addition of extra processing control agents⁶⁸.

Processing time : Processing times may vary from a few hours to over 24 hours, depending upon the alloy system, the necessity for end quantity of any added processing control agent, the energy input, and the type of equipment used. Because of the nature of the process, large starting powder particle sizes lengthen processing time only slightly.

The equipment's.

Introduction: A variety of ball milling equipment's have been used to carry out mechanical alloying. These include:

1. Conventional ball mill
2. High energy ball mills or attritor.
3. Centrifugal planetary ball mill

4. Vibratory ball mill

Conventional ball mills : Conventional ball mill is preferred by some workers^{71,72}, consist of a rotating horizontal drum half filled with small steel balls. The rate of grinding depends on the rpm of rotation below the critical speed that is above which speed the centrifugal force acting on steel balls exceed the force of gravity and the balls are pinned to the internal wall of the drum and at this point the action is stopped. The ball charge in mechanical alloying usually consist of 52100-bearing steel grinding balls, SUS 304 stainless steel⁶⁹, High carbon- high chromium steel ball. Balls of other materials like tungsten carbide or nickel have also been used⁷⁰. Balls fabricated from alloys similar to the material to be processed has also been used to avoid minor contaminator through ball wear. For mechanical alloying the vial should be as long as they are of sufficient size (>1 min. diameter of attritor) and the ball to charge weight ratio⁶⁸ of 100:1. Conventional ball milling in a lower energy environment gradually reduces the size of metal powder particles and the formation of composites in this way takes an exceptionally long time. The competing of cold welding also occurs but it can be inhibited by the use of milling liquids or serperents. The effects of the cold welding are minimised until the powder reaches sizes as small as one micrometer. A model of a conventional ball mill is schematically shown in Fig. 2.20 below.

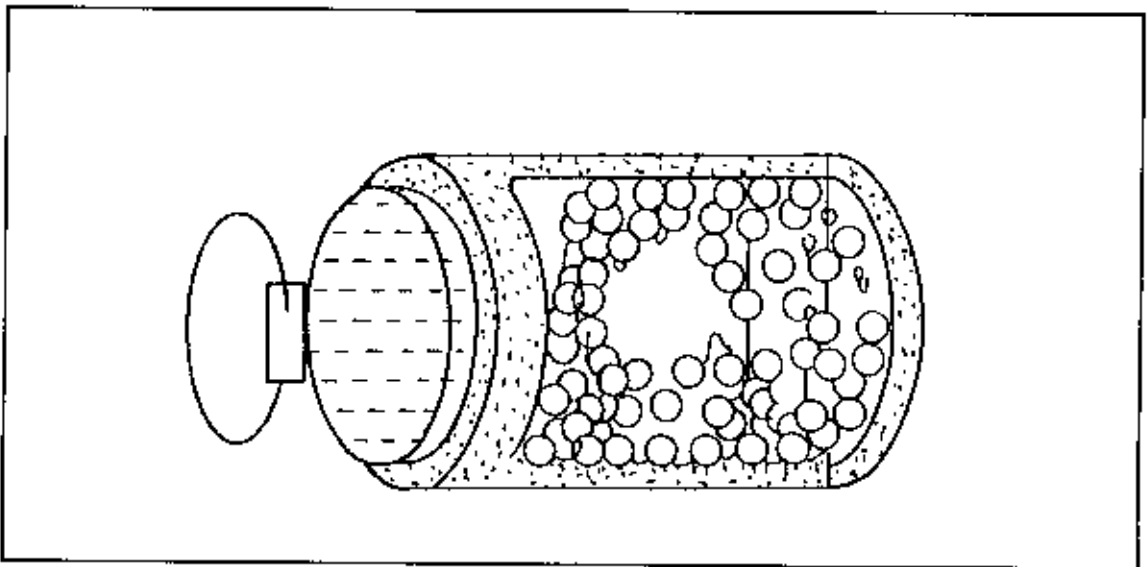


Figure 2.20 : Conventional ball mill.

High energy ball mills or attritor : In order to accelerate the formation of metal compositas, to eliminate the dependancy of final powder homogeneity on initial powders and to avoid the hazards of fine powders, it is reasonable to use vertical ball mill, the so called attritor, that would generate higher energies than convantional ball

mill. More than any other ball mill, the attritor is preferred by most workers^{71,72} because of its operational flexibility for mechanical alloying.

The attritor is originally a comminuting blending machine which consists of water cooled stationary vessel with a centrally mounted vertical shaft with impellers radiating from it. The shaft is connected to a high speed geared motor. The vessel is usually made gas-tight with rubber seals, especially when a controlled atmosphere such as argon is required to be maintained. As the shaft is rotated at high speed, the impellers impart kinetic energy to the grinding medium which welds and comminutes the powder particles.

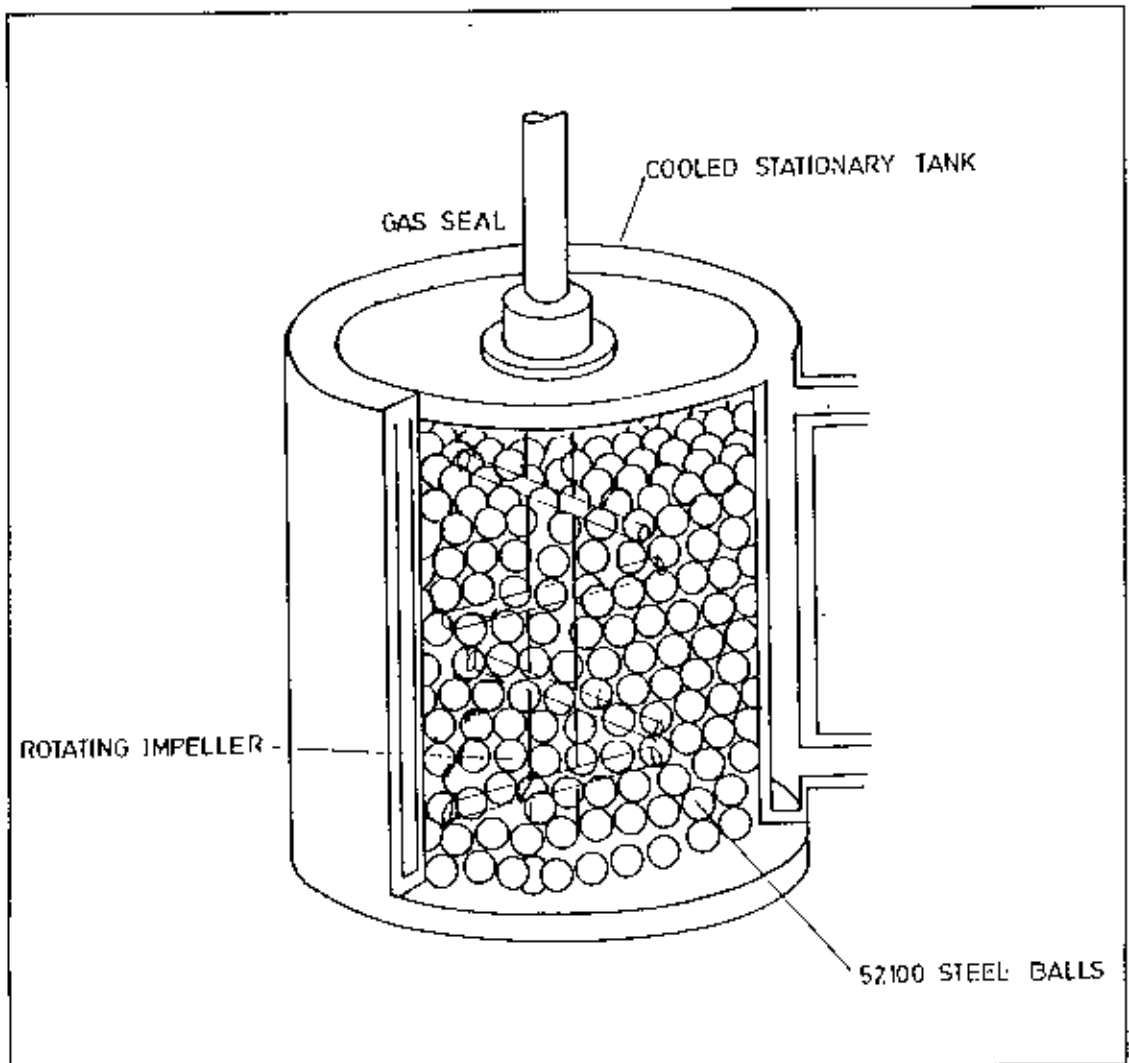


Figure 2.21 · High energy attritor-type ball mill used for mechanical alloying.

Such a machine can achieve grinding rates more than 10 times higher than those typical of a conventional mill. A model of a high energy ball or attritor is schematically shown in Fig.2.21. The capacity of attritor used for mechanical alloying ranges from

$3.8 \times 10^{-3} \text{ m}^3$ (1 gallon) to $3.8 \times 10^{-1} \text{ m}^3$ (100 gallon) and the central shaft rotated at speed up to (500 rpm).

Centrifugal Planetary Ball Mills: The centrifugal planetary ball milling has been promoted by S. Sumimoto et al⁷³ and Nabuo Ashahi et al⁷⁴. Planetary mills are of two types (a) planetary mill, "p-5" (b) planetary micro mill, "p-7", which of each is described below.

Planetary mill, 'P-5': The instrument has two or four bowl holders which are attached on a supporting disk, each of which accommodates one bigger size or two small size grinding bowls. The centrifugal forces of the grinding bowls rotating in opposite directions and the supporting disk act on the bowl content consisting of the sample and the grinding balls. Because of the grinding bowls and the supporting disk rotating in opposite directions, the centrifugal forces act on the bowl content in the same and in the opposite direction, alternatively. There by the grinding balls and sample particles turn from running half way along the wall of the grinding bowl (friction effect) to crossing the bowl space and hitting the opposite part of the wall (impact effect and homogenisation). This impact effect is even intensified considerably by the balls bouncing against one and other.

The versatility of this instrument lies in the possible combinations of bowl arrangement. Up to bowls of 250 or 500 ml each, or 80 ml each (one above the other in pairs) can be utilised in one batch: each bowl is available in 8 different materials. This means that the preparation of various, even different samples can be carried out simultaneously. Independently of the instrument that is used in sample preparation each grinding process develops a slight quantity of abrasion from the grinding elements, which pollutes the sample.

Planetary mill, 'P-7': The planetary micro-mill "pulverisette-7" is an absolutely comparable, down-sized version of the "pulverisette-5" for the fine grinding of small samples (dry or in suspension) up to 20 ml. The instrument has 2 bowl fasteners that take grinding bowls of either 12, 25, or 45 ml gross volume. The net capacity for one sample preparation varies between 5 and 20 ml accordingly.

Vibratory ball mill : Vibratory ball mill⁷¹⁻⁷⁹ combines the operating principles of the ball and mortar mills. A motor bowl, which is hermetically sealed at the top by means of a cover, is made to oscillate vertically by a magnet located underneath. The oscillations are transmitted via the grinding stock to a single large ball (50 mm or 70

mm diameter). First of all, the ball movement produces preliminary crushing of the grinding stock from a maximum edge length of 5 mm to about 1 mm. The impact movement of the ball becomes an attritional tumbling motion as the grinding process continues. Smaller particles rise up the mortar wall to the top, whilst larger particles are increasing by the reduction in size. This selective grinding produces a particularly homogeneous product with a rather narrow size distribution. An interval circuit interrupts oscillation and also causes improved mixing of the grinding stock. Milling in the vibratory ball mill can be carried out dry or wet, and can be supplied with grinding element of known different materials. Schematic diagram of such high speed vibratory ball mill is as shown in Fig. 2.22.

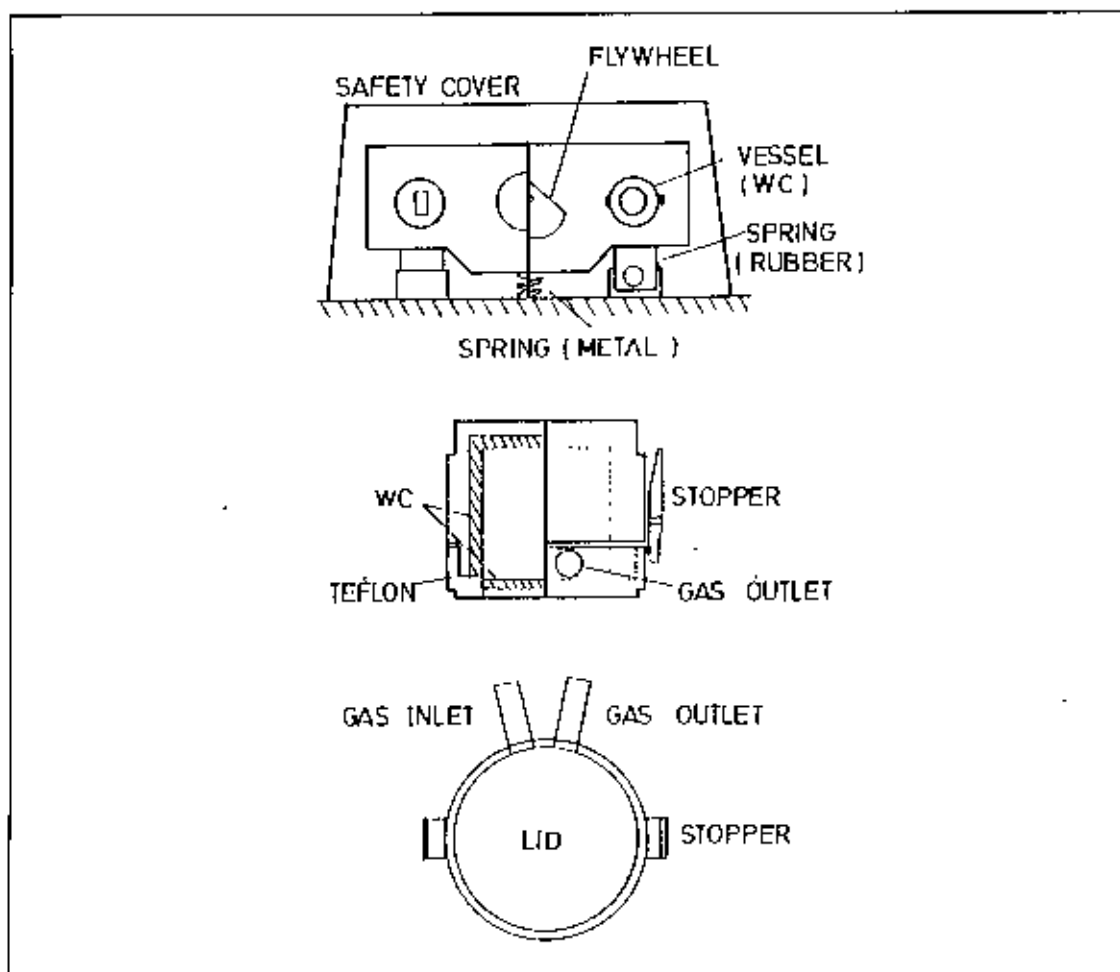


Figure 2.22 : Schematic diagram of high speed vibratory ball mill, milling vessel and its cross-sectional lateral views.

The chemical kinetics of mechanical alloying and energy consideration:

The chemical kinetics of mechanical alloying :Mechanical alloying may be considered as a means to mechanically induce solid-state chemical reactions that occur across welded interfaces, formed when powder particles are impacted in a

collision between the grinding media. The nature of these chemical reactions is, therefore, of equal importance as the mechanics in the development of knowledge of the mechanism of mechanical alloying as well as the mechanics of mechanical alloying, mathematical and empirical modelling to determine collision frequency, impact velocities, and collision energies, and the temperature rise associated with ball/powder collisions and the effect of these parameters on the rate at which alloying proceeds. A defining characteristic of all solid-state reactions is that the product phases physically displace the reactants. These products constitute a barrier layer opposing further reaction. The reaction interface, defined as the nominal boundary surface between the reactants, is continually diminished during the course of the reaction. Solid-state reactions are controlled⁸³⁻⁸⁵ by the initial reactant geometry and by the diffusion rates of the reactants through product barriers. Such reactions necessarily require elevated temperatures to proceed at reasonable rates. It has been suggested⁸⁶ that the efficacy of mechanical alloying is a consequence of the continual fracturing and welding of powder particles because this both increases and dynamically maintains the reaction interfacial volume during milling, thereby minimising the detrimental effects of product barriers. Chemical kinetics not only describe the rate of a chemical reaction but may also be used to determine the mechanism, i.e., kinetic measurements can be used to identify the rate controlling step in a reaction. Reaction kinetics are usually described as a function of temperature, collision frequency, activation energy and universal gas constant by the Arrhenius type of equation as represented in Appendix A Eqn.-21. The collision frequency has little significance in solid-state reactions⁸⁴, whereas the activation energy is the energy barrier that must be overcome during the rate-limiting step of the reaction. The quantitative determination of the activation energy may be used to identify this step. A change in activation energy during the course of a reaction also implies a change in the rate-controlling step. Chemical reactions in the solid state generally occur spontaneously⁸⁷ when the reactants are brought into atomic contact. The rate-limiting step may be either the transport of reactants to the reaction zone (diffusion): a chemical reaction at the reaction site, such as the dissociation of a reactant into its constituent parts; or the availability of a suitable nucleation site, so diffusion is rate controlling and that the reaction reaches a critical condition when short circuit diffusion paths are operative. The rate of diffusion has an exponential relationship with temperature, and the diffusivity has an Arrhenius form as represented in Appendix A Eqn A-22. Factors which influence diffusion rates, are defects structure and densities, local temperature and product morphology⁸³⁻⁸⁵.

It has been established that mechanical alloying significantly increases solid-state reaction rates by dynamically maintaining high reaction interface areas⁸⁸ and by simultaneously providing the conditions for rapid diffusion.⁸⁹ Mechanical alloying thereby minimises the effect of product barriers on reaction kinetics and hence provides the conditions required for the promulgation of solid-state reactions at low temperatures. While mechanical alloying is often defined as a high (collision) energy process, so the magnitude of this energy requirement is an important factor. During conventional ball milling, powder particles are simply mixed; particle size, shape, and chemistry are not altered. When ball milling is used as a comminution process, the particle size is reduced by fracture during collisions; the particle chemistry is not altered. What distinguishes mechanical alloying from other ball milling processes is that both fracture and welding occur in the former process. Fracture of particles creates automatically clean surfaces; hence, the requirement that mechanical alloying be performed in an inert environment. Particle welding can occur when such surfaces are impacted during subsequent collisions and reactions can proceed across these new, internal interfaces. Hence, the chemical composition of the powder particles can change during milling. It may be argued that the minimum collision energy is that required for these fracture and welding events to occur. Any additional energy will merely accelerate the events that occur as a consequence of increased plastic deformation and particle heating. Recent studies⁹⁰⁻⁹¹ have shown that the collision energy and the method of milling can significantly influence product structure.

Energy consideration and structural refining during mechanical alloying: During mechanical alloying the system uses part of the input energy and moves into higher energy state. The part of the input energy which the system uses for alloying, phase change, compound and metastable phase formation has chemical energy. The remaining part of the input energy which the system stores in the form of defects or distortions is termed as non-chemical energy. Recent calculations⁹² have shown that the system stores maximum energy in the form of grain boundaries. This results in grain refinement of the mechanically alloyed powders.

Quantitative estimation of the amount of energy which the system can store in the form of defects and distortions have been carried out for Al, Cu and δ -Fe⁹². It was found that the ability of the system to store energy increases in the following sequence, namely, surface, strain, dislocation and grain boundary. With the increase in the amount of input energy i.e., the milling time, the system can afford to have more

and more grain boundary area, which leads to the generation of grain boundary. In other words, grain size refinement takes place with milling time.

Grain size refinement and mixing of atoms by mechanical alloying : The grain size refinement⁹² is a combination of compression, folding and rotation (one cycle). Grain size reduces to half after the completion of six cycles. Gradually the reduction in grain size for successive cycles reduce because of the following reasons. The elastic limit of the powder particle increases by hardening and to deform them plastically requires more energy. Further deformation of these particles is possible by grain boundary sliding. However, this process deforms the particles but not the crystals. If both the crystal and particles are plastically deformed under the impact of the colliding balls, static recrystallization takes place at the expense of the grain boundary and dislocation energies, once the colliding balls move apart. The steady state crystal size is achieved when the dynamic recrystallization takes place. During the dynamic recrystallization both the plastic deformation and recrystallization occurs simultaneously and further grain refinement is not possible.

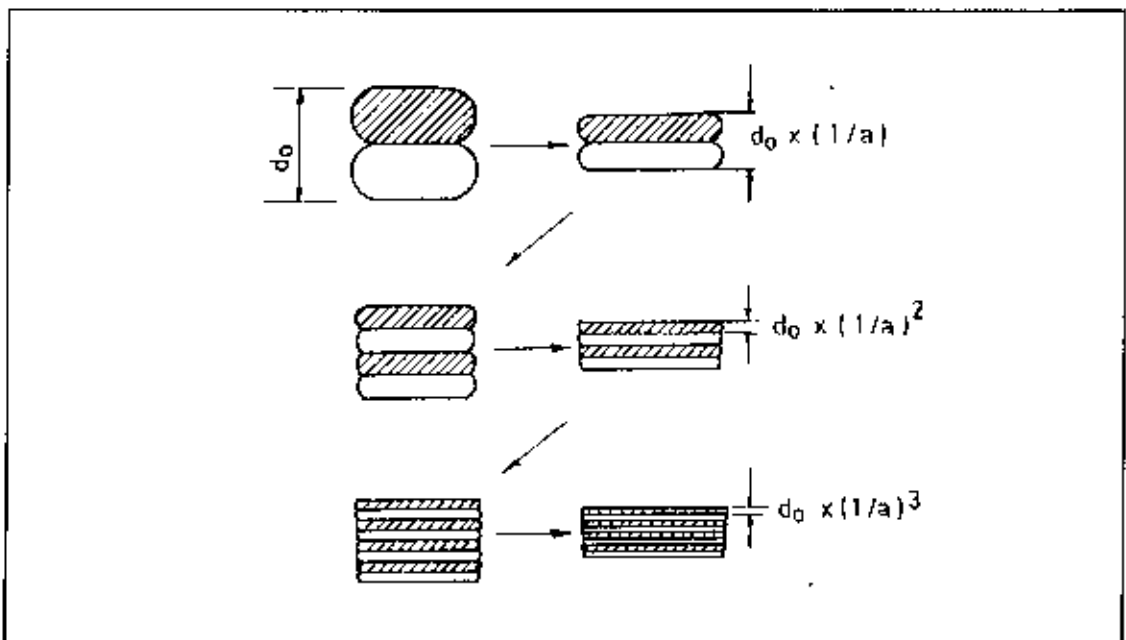


Figure 2.23 : Decrease in layer thickness with the successive number of compression and folding .

In Fig. 2.23, here considered a particle consisting of two different layers as layered structure is observed in mechanically alloyed samples. If the layer thickness to start with is d_0 , then the mixing of atoms depend on the initial layer thickness (d_0), the number of times the powder particle is compressed and folded and the reduction

produced by one cycle ($1/a$). The layer thickness after n cycles⁹³ is given by $d_0(1/a)^n$. Under these conditions, diffusions by an atomic distance can lead to mixing of atoms.

Dissimilar atoms mixing during mechanical alloying is brought out by slip deformation of a two layered structure consisting of various slip systems operating randomly along the close packed directions. Computer simulation of the mixing after the operation of 0,10,20 and 60 slips are as shown in Fig. 2.24.a-d respectively. The displacement produced by each slip deformation is taken as one atomic distance. The fraction of A-B bond is identical either starting from alternating dissimilar atoms or alternating layers of dissimilar atoms. Hence the resultant structure is similar to that of by the diffusion of both the species, even though the final structure has been arrived at without any diffusion. However, in a real system, diffusion takes place together with slip deformation to mix atoms.

Structural Refinement : During the initial period of processing a wide variety of structures exist in the mechanically alloyed powder, powder which have been trapped between colliding balls are severely deformed while a portion of the powder remains relatively unaffected. This makes determination of the average refinement rate at early times in the process very difficult. However the amount of deformation required to cold weld can be obtained for the powder at this stage. The average lamellar thickness in this coarse size fraction in the first few minutes of processing is reduced in thickness and with increased processing time, the structural differences between the size fractions are gradually eliminated as represented in Fig. 2.25 and in Fig. 2.26.

Application of mechanical alloying :

Introduction : Since its inception, mechanical alloying process has been applied mostly to the production of nickel, iron or aluminium based oxide dispersion strengthened alloys. However the utilisation of mechanical alloying in its truest sense as a technique for alloying different or normally incompatible system is increasing. The distinctly different direction for this process technology, is described below.

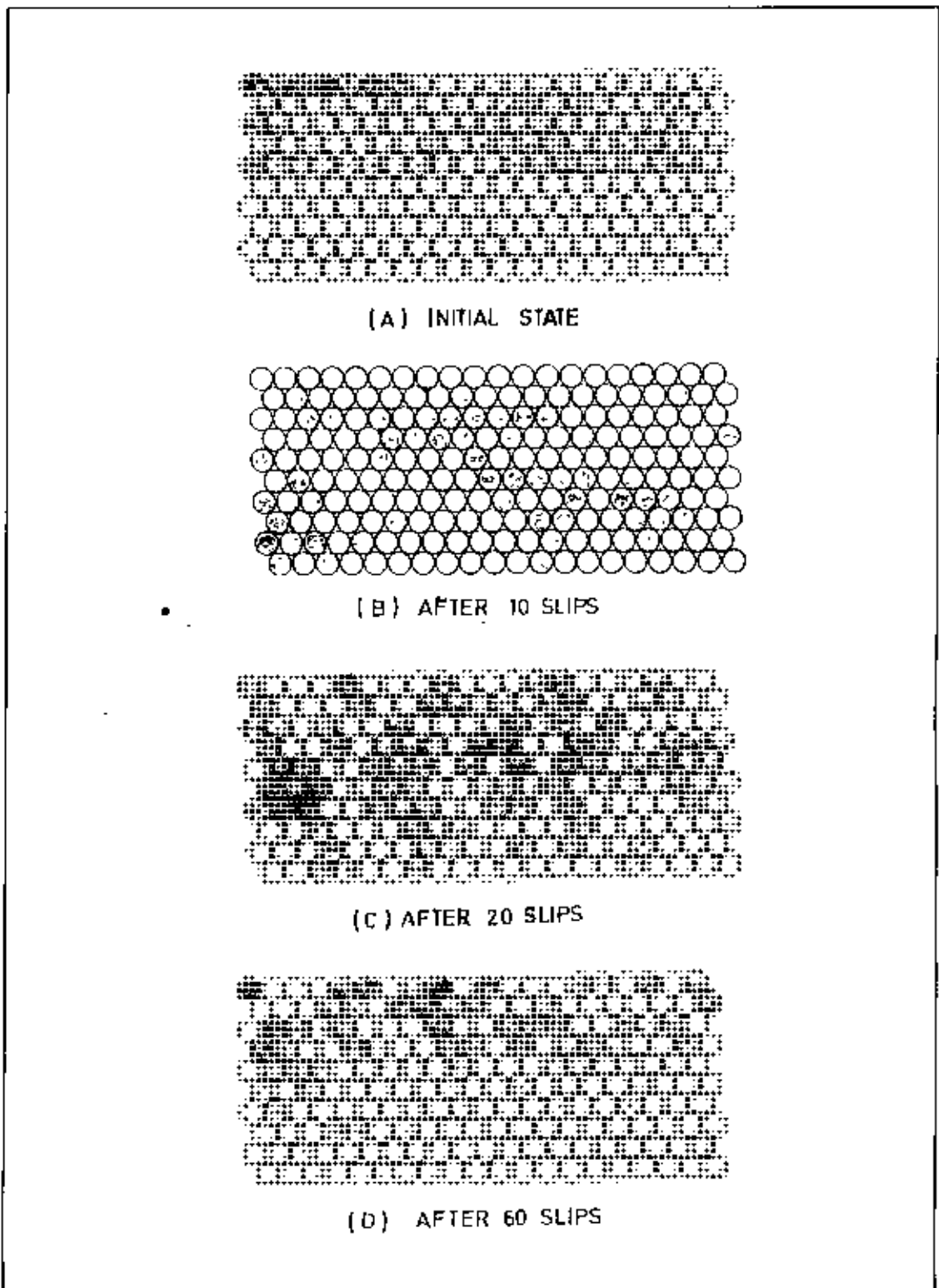


Figure 2.24 : Atomic configuration after 10, 20 and 60 slips starting from layered structure.

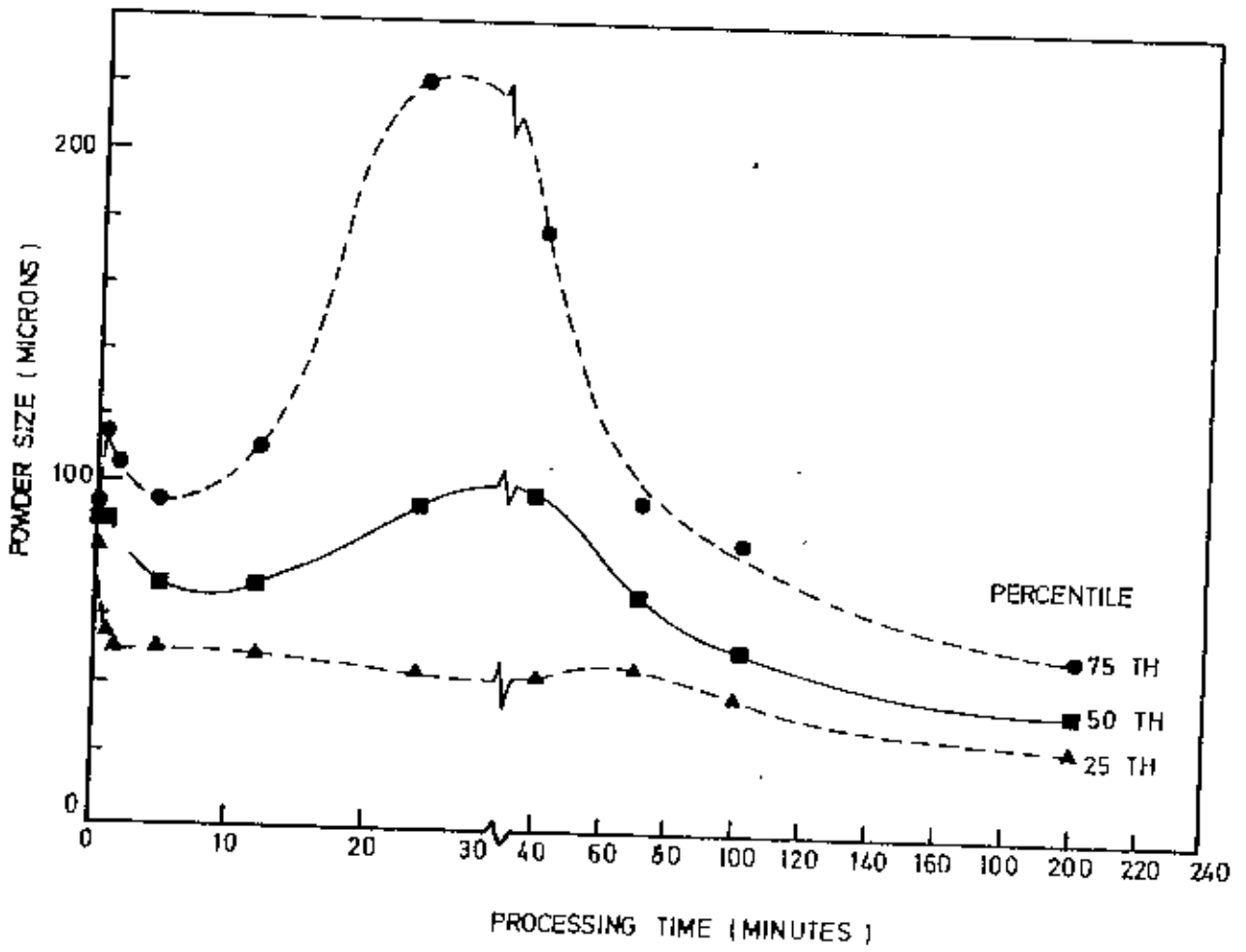


Figure 2.25 : Powder size distribution as a function of processing time.

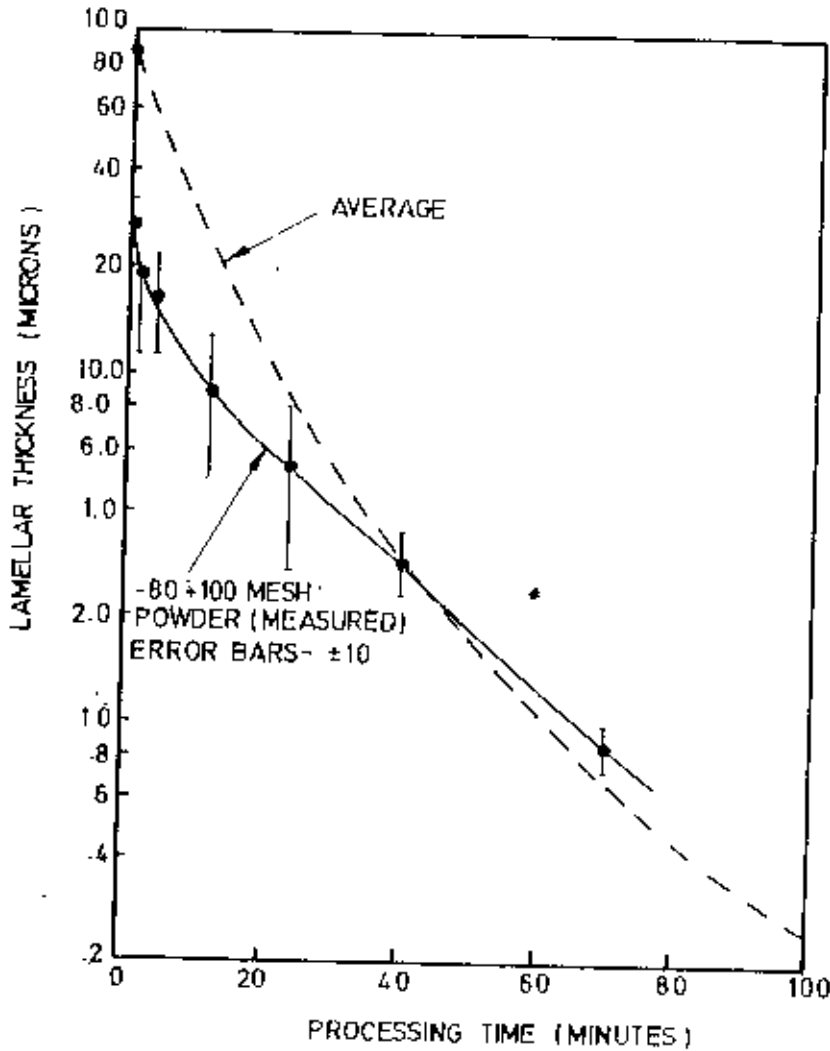


Figure 2.26 : Variation of lamella thickness with processing time.

Alloy Synthesis : Mechanical alloying is generally used to produce alloys from elemental precursors. Thus brass is formed when copper powder and zinc powder are milled. That a true alloy is indeed produced has been demonstrated using both X-ray diffraction⁹⁴ and magnetic measurements⁹⁵. The alloying reaction is not confined to metals but can also be used for oxides⁹⁶, nitrides^{97,98}, chalcogenides^{99,100} and semi-metals¹⁰¹. Potential applications for novel materials produced by mechanical alloying therefore include dental prostheses¹⁰², hydrogen storage materials¹⁰³, permanent

magnets¹⁰⁴⁻¹⁰⁷, superplastic alloys¹⁰⁸, intermetallic compounds¹⁰⁹, electrodes¹¹⁰ supercorroding alloys¹¹¹ and superconducting materials, both low¹¹² and high T_c ^{113,114}. However, not all metals form an alloy during milling. Nd and Fe, for example, remain a mixture of the elements¹¹⁵ and $Nd_2Fe_{14}B$ actually separates during milling into α -Fe and an indeterminate amorphous phase¹¹⁶. This de-alloying or phase separation also occurs with Sm_2Fe_{17} ,¹¹⁷ Ti_3Cu_4 ¹¹⁸ and $ZrCo$ ¹¹⁹ and Fe_2Zr .¹²⁰ The etiology is unknown but the factors determining whether a system will alloy or de-alloy appear to be controlled by the milling energy¹¹⁹ and/or the crystal structure¹¹⁷. Composite structures result when ceramics and metals are milled. The original oxide dispersion strengthened alloys are composite mixtures of rare earth oxides dispersed in a nickel-based metal matrix. The only current commercial applications for mechanical alloying are Fe-based, Ni-based, and Al-based oxide dispersion strengthened alloys, which are being used as a rotor-blade material in a helicopter engine, in a fighter engine and in a land-based turbine.

Nickel base oxide dispersion super alloys : The full flexibility of the mechanical alloying process to design simultaneously for a variety of critical material properties has been used to produce the oxide dispersion strengthened super alloy of which MA 6000 has attained much commercial maturity.

INCONEL alloy MA 6000 combines two types of strengthening: (a) gamma-prime hardening (from its aluminium, titanium, and tantalum content) for intermediate temperature strength; and (b) oxide dispersion strengthening (from the Y_2O_3 addition) for strength and stability at very high temperatures. The oxide particles directly increase high temperature strength by acting as obstacles to dislocation motion. The oxide dispersion, coupled with the high level of stored energy from processing, indirectly helps to attain maximum high temperature strength by aiding the formation of coarse elongated grains in the hot working direction. Tungsten and molybdenum act as solid-solution strengtheners in this alloy. Oxidation resistance comes from the aluminium and chromium content of the alloy, while titanium, chromium, and tantalum act collectively to provide sulfidation resistance.

A comparison as illustrated in Fig. 2.27. of the specific rupture strength (strength/density) for a 1000-hour life as a function of temperature for INCONEL alloy MA 6000 and several other turbine blade alloys-directionally solidified (DS) MAR-M200+ Hf, single-crystal alloy PWA 454, and thoriated nickel clarifies the benefits of the combined strengthening modes in the mechanically alloyed material¹²¹.

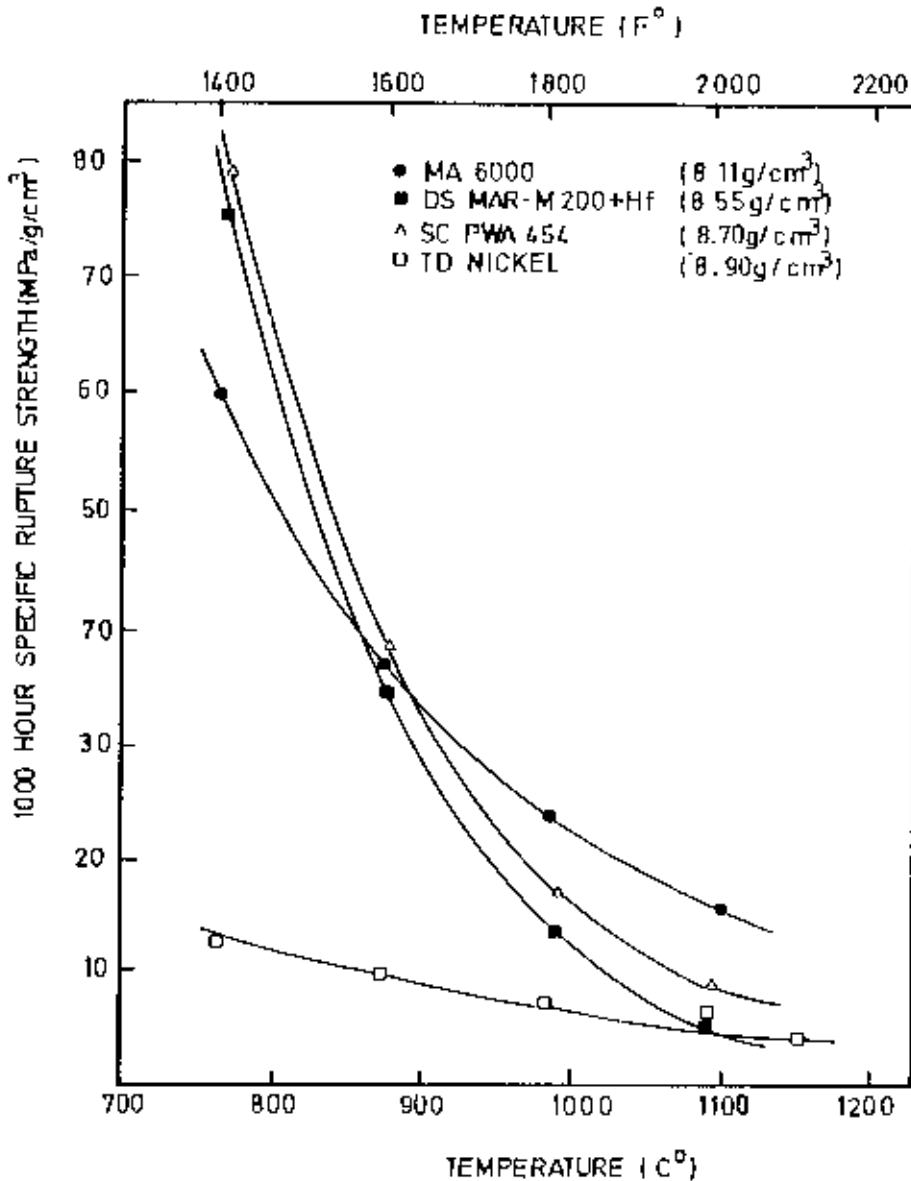


Figure 2.27 : Comparison of specific rupture strength of INCONEL alloy MA 6000 with DS MAR-M200+Hf, TD-Ni, and single-crystal PWA 454.

Aluminum-alumina oxide dispersion strengthened alloys : Sintered aluminium powder, aluminium containing a dispersion of aluminium oxide, was the first structural oxide dispersion strengthened metal¹²². Because, the production method for sintered aluminium powder relied on fragmenting the surface oxides on aluminium powder or

flake to provide the dispersoid, the dispersion was relatively coarse and unevenly distributed, requiring a very large volume fraction of Al_2O_3 to obtain high strength. Mechanical alloyed aluminium-alumina oxide dispersion strengthened alloys has achieved high strengths at far lower dispersoid contents by refining the oxide particle size homogenising its distribution. The mechanically alloyed aluminium alloys are characterised by a fine grain structure that is stabilised by a dispersion of oxide and carbide particles¹²³. This contributes to high tensile and fatigue strengths. The production of oxide dispersion strengthened aluminium alloys by mechanical alloying is not restricted to available pre-alloyed powders; consequently, a variety of aluminium alloy systems have been developed. IN-9052 (Al-4.0% Mg 0.8% O-1.1%C) and IN-9021 (Al-1.5% Mg-4.0% Cu-0.8% O-1.1%C) are two commercially matured mechanical alloyed aluminium alloys possessing attractive combinations of tensile strength, fatigue strength, toughness, and corrosion resistance¹²³. The significant improvement properties induced mechanical alloying in such alloys are shown in Fig. 2.28.

Iron based dispersion strengthened alloy : Various types of ferrous alloy have been made by mechanical alloying, of which the most highly developed material is the Fe-20Cr-4.5Al ferritic steel. Incoloy MA 956, dispersion strengthened with 0.5% Y_2O_3 ; MA 956 has been made in the form of bar, sheet, plate, wire, tubing, forging, rings, hot spinning and fabrications. The high-strength capability is combined with exceptional high-temperature oxidation and corrosion resistance, associated with formation of an alumina oxide scale.¹²⁴ In cyclic oxidation resistance, MA 956 is superior to Hastelloy. The alumina scale is an excellent barrier to carbon and no carburization occurs. Sulfidation resistance is also good. MA 956 is used in gas-turbine combustors, but with its combination of high strength up to 1300°C , corrosion resistance and formability, the alloy has found many other applications. Gas turbine applications under development include fabricated nozzles, inlet plenum and compressor nozzle parts of vehicle turbines, rings for aeroengine combustors, and a combustors baffle for industrial turbines. Use in power stations include oil and coal burners and swirlers, and fabricated tube assemblies for fluid-bed combustion.¹²⁵

Coating applications : Mechanical alloying is used to produce corrosion and wear-resistant cobalt-based, iron-based and nickel-based alloy powders for use as coatings, deposited by plasma spraying and other processes. High temperature oxidation-resistant coatings processed by mechanical alloying are generally based on the system MCrAl, where M is Ni, Fe, Co, or a combination of these elements.

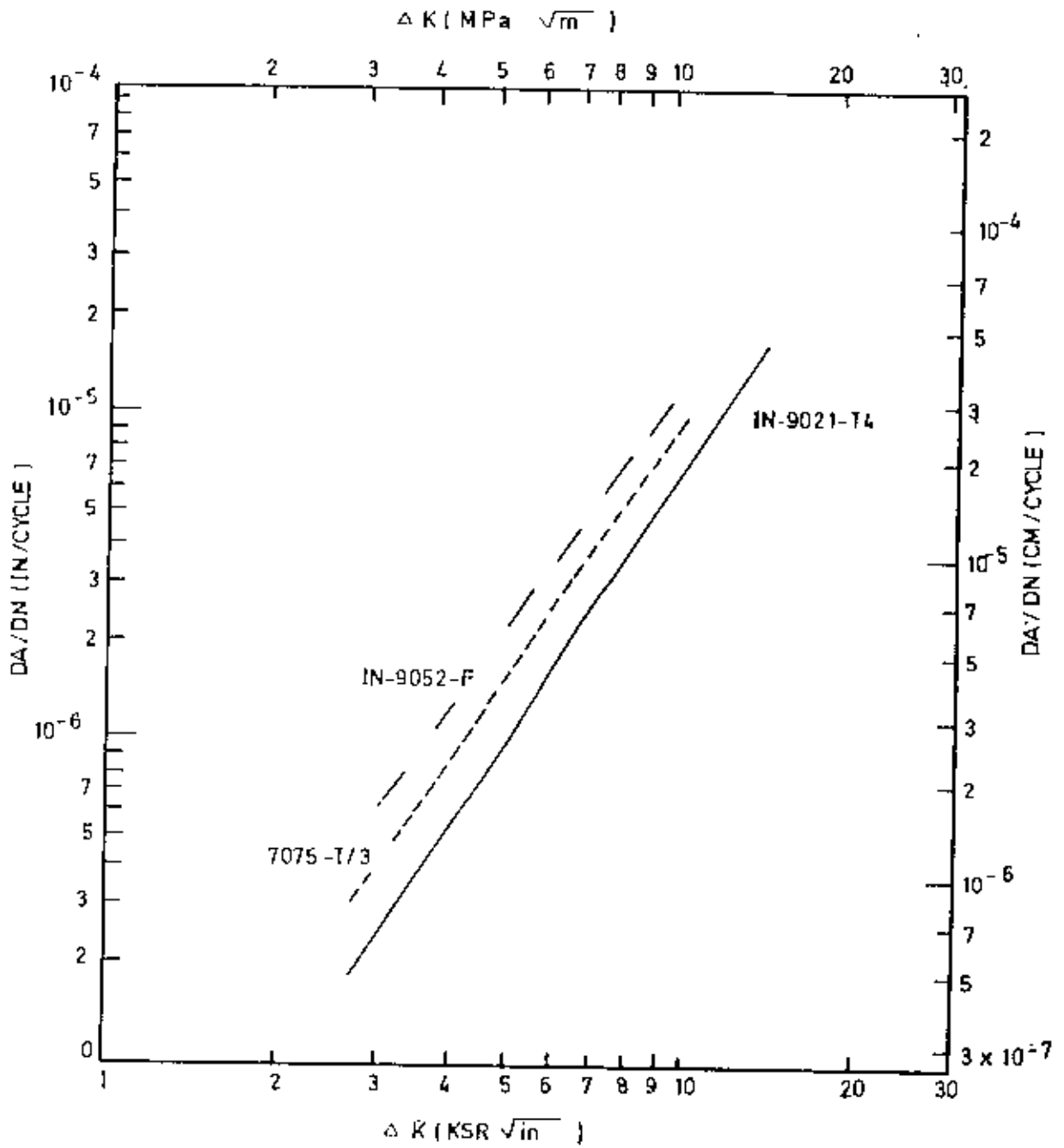


Figure 2.28 : Fatigue crack growth rate of aluminium alloy forging in dry air.

These coatings are characterised by having fine oxide and carbides dispersions formed in situ during mechanical alloying. These dispersoids can be beneficial for environmental protection¹²⁵. Carnet powders that include large volume Fractions of Y_2O_3 have also been made¹²⁶ and applied as diffusion inhibiting coatings. This type of coating acts as a barrier to reduce adverse effects of concentration gradients between the substrate and an over coating of widely differing composition from the substrate. Mechanical alloying can be used to produce coating feed stock because of the ease with which a fine admixture of constituents can be formed, including the homogeneous dispersion in the matrix of large volume fractions of refractory oxides. Mechanical alloying can be used to produce wear-resistant coatings that contain a fine, homogeneous distribution of a hard component such as tungsten carbide.

Supercorrodng alloys : A somewhat different utilisation of the mechanical alloying process is the production of supercorrodng magnesium alloys that operate as short-circuited galvanic cells to corrode (react) rapidly with an electrolyte such as sea water to produce heat and hydrogen gas¹²⁷⁻²⁸. To maximise corrosion rate and efficiency, it necessary to (a) provide a short electrolyte path between anode and cathode; (b) provide a large amount of exposed surface area between cathode and anode; (c) provide a strong bond (weld) between anode-cathode pairs; and (d) provide a very low resistance (less than 10^{-4} ohms) path for external currents to flow through the corroding pairs. Prior to mechanical alloying, the systems devised could not meet all of these requirements. For use as an underwater heater or hydrogen gas generator a mechanically alloyed Mg-5 to 20% Fe alloy is ideal because of its extremely fast reaction rate, high power output, and the high percentage of theoretical completion of the actual reaction. For corrodable release links an alloy with a slower reaction rate is desired, such as Mg -5% Ti. (Fig. 2.29).

Other systems : Liquid immiscible systems are difficult to pyrometallurgy. As an example, the monotectic copper-lead system tends to separate into two liquids upon cooling. Mechanical alloying can be used to form a homogeneous distribution of copper in a softer lead matrix. Solid immiscible systems such as copper-iron are also amenable to mechanical alloying. Solid pure copper dissolves only 4.5 wt. % iron while gamma iron dissolves only 8 wt. %. copper. For copper-rich alloys a maximum of 3 wt.% of fine iron particles can be obtained,. Attempts to make alloys with higher amounts of iron give large globs of primary solidified iron in addition to the fine precipitate.

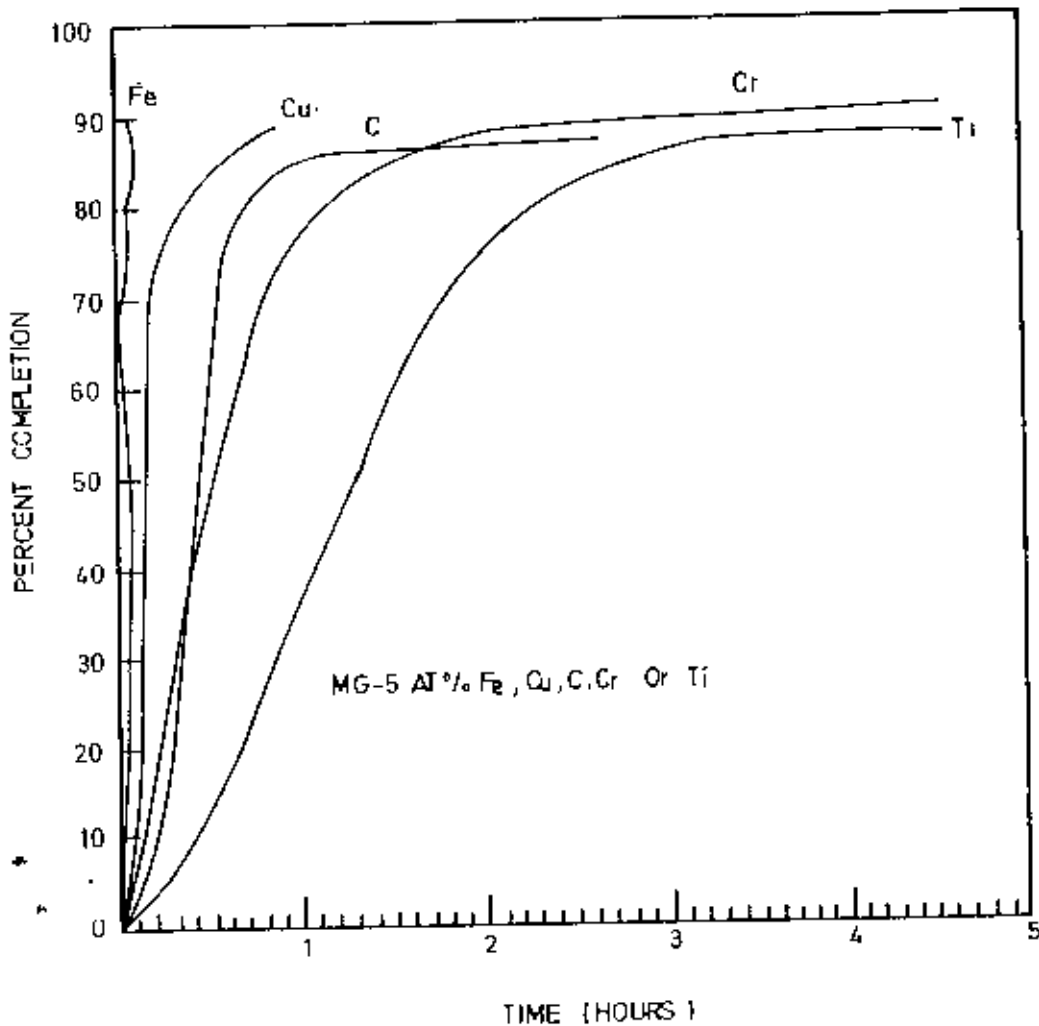


Figure 2.29 : Corrosion of supercorroding mechanically alloyed Mg-5% X alloys.

This limitation can be circumvented by mechanical alloying and a 50 wt. % iron can be finely dispersed in copper. Many useful intermetallic compounds have constituents with very different melting points and are difficult to fabricate by normal melting techniques. An example is the superconducting compound Nb_3Sn , which is formed by a peritectic reaction. During the casting of niobium-tin, the compound that solidifies first is niobium rich. The final liquid to solidify is very rich in tin. The resulting extreme coring, which remains even after prolonged homogenisation anneals, causes poor superconducting properties. Other methods used to produce these alloys include:

- (a) vapour codeposition of niobium and tin,
- (b) (b) splat cooling, and
- (c) a composite technique.

These processes are all tedious and do not always lead to a homogeneous product. Fabrication of Nb₃Sn with excellent superconducting properties by mechanical alloying¹²⁹ has been proved.

Amorphous and nanocrystalline materials : Mechanical alloying can successfully used for the production of amorphous structures. First reported by Koch et.al¹³⁰, mechanically-induced amorphisation has been extensively studied and was reviewed by Weeber and Bakker¹³¹ and by Koch.¹³² Amorphisation occurs either by a diffusion-controlled reaction, where the more stable crystalline state is constrained kinetically from forming¹³³⁻³⁴ or by the defect-induced decomposition of the crystalline state¹³⁵⁻³⁶ which is analogous to amorphisation by irradiation.

Those systems which can sustain the high defect densities produced by mechanical alloying without transforming to the amorphous state generally become nanocrystalline. This nanocrystallization is widely reported and occurs in both single phase¹³⁷⁻³⁸ and multiphase systems¹³⁹⁻⁴⁰. It has been suggested¹⁴¹ that at a critical level of strain, dislocations align to form small angle grain boundaries. The subgrains so formed are nanocrystalline and relatively strain free. On further milling, the orientation of these subgrains becomes completely random.

Production of Metals Powder

Introduction : The techniques of powder manufacture can be divided into two headings :

- Mechanical processes, and
- Physico-chemical processes.

Additionally, newer production techniques especially applicable to highly alloyed systems have been developed in recent years.

Mechanical processes :

Powder preparation by mechanical disintegration is widely employed. A drawback common to all methods of mechanical comminution of metals and alloys into powders is the extraordinarily low productivity thereby causing expensive powder production. Techniques included in this group are described below :

Machining is employed to produce filings, turning, scratching, chips, etc., which are subsequently pulverised by crushing and milling. Since relatively coarse and bulky powders entirely free from fine particles are obtained by this method, it is particularly suitable in a very few special cases; such as the production of magnesium powders (for pyrotechnic applications where the explosiveness and malleability of the powder would prohibit the use of other methods) beryllium powders, silver solders, and dental alloys. The powder particles produced are of irregular shape. This method is highly expensive and, therefore, has a limited application.

Crushing is mostly used for the disintegration of oxides and brittle materials. Any type of crushing equipment such as stamps, hammers, jaw crushers or gyratory crushers may be employed for crushing brittle materials. Various ferrous and non-ferrous alloys can be heat treated in order to obtain a sufficiently brittle material which can be easily crushed into powder form¹⁴². Some metals particularly titanium, zirconium, vanadium, and tantalum when heated to moderate temperature in hydrogen atmosphere are converted to brittle hydrides. The powders produced by this method are of angular shape which are subsequently comminuted by milling to attain the required fineness of the powder.

Milling is used for producing powders of brittle, friable, tough and hard materials and pulverisation of malleable and ductile metals. It involves the application of impact force on the material being comminuted. The milling action is carried out by the use of a wide variety of equipment such as ball mill, rod mill, impact mill, disk mill, eddy mill, Jet mill, vortex mill, etc. some of which are illustrated in Fig. 3.1.

Shotting consists essentially in pouring a fine stream of molten metal through a vibrating screen into air or neutral atmosphere. In this way, molten metal stream is disintegrated into a large number of droplets which solidify as spherical particles during its free fall. All metals and alloys can be shotted; the size and character of the resultant shot depending on the temperature of molten metal and gas, diameter of the holes and frequency of vibration in case of vibrating screen. One drawback of this process is the formation of high oxide content which can be minimised with the use of inert gas.

Graining involves the same procedure as the shotting, the only difference being that the solidification is allowed to take place in water. In similar manner, other pulverisation methods are used for the production of very fine powders. Frequently cadmium, zinc, tin, bismuth, antimony, and lead alloys are pulverised by this method.

Atomisation consists of mechanically disintegrating a stream of molten metal into the fine particles by means of a jet of compressed air, inert gases or water. This is the main process for preparing aluminium, zinc, lead, pure iron, and low alloy steel powders, noble metals and more recently, high temperature alloys and special alloy powders, (e.g., super alloys). Typical atomising process is represented schematically in Fig. 3.2(a).

This process, in its simplest form, were known as D.P.G. Spinning Disc method and the Mannesmann R. Z. process. Fig. 3.2.(b). and Fig. 3.2.(c). show the schematic representation of the principle of operation of these process. The molten metal is first decanted into a heated tundish and passes through a small hole in the centre of its base as a thin stream falling on a number of knives mounted on disc and rotating at high speed which varies between 1500 to 3500 revolutions per minute. The metal stream strikes the apex of a conical high velocity water jet fixed below the tundish. In this way the metal stream is disintegrated into metal powder particles and mixture of water and powder is collected on a filter bed situated at the base of the atomising chamber. The powder having a considerable residual moisture is sent from the filter bed to a drying oven. When dry it is finally sieved. Irregular powder particles are formed by this method. However, spherical particles may be produced by employing superheated molten metal. By proper control of temperature of the metal, the height from which the metal is allowed to fall on the knives, water pressure, the diameter of the tundish hole and the speed of rotation and the shape of the knives suitable powders can be produced. Numerous modifications have been-introduced in the atomisation technique e.g. the modified D.P.G. process for the manufacture of alloy steel powders particularly stainless steel powders and the centrifugal atomisation method for the production of various metal powders. This method is based on the disintegration of a stream of molten metal by centrifugal force. In the other modified technique, known as the rotary atomisation or the rotating electrode process, the front end of a rotating electrode is heated, by an electric arc or plasma¹⁴³, allowed to melt and the liquid droplets are thrown off by centrifugal action and finally collected in a helium (a quenchant) filled chamber Fig.3.2.(e). Generally, spherical, solid particles with a fine dendritic structure is produced which is also the characteristic of inert gas atomisation process.

A recent variation of this technique known as soluble gas atomisation or dissolved gas process consists of introducing the molten metal-saturated with a soluble gas such as hydrogen, under pressure into a vacuum chamber through an orifice where the pressurised liquid explodes (or breaks out) into fine particles¹⁴⁴ as illustrated in Fig. 3.2.(d). This method is used particularly to prepare special alloy powders (super alloys such as complex nickel and cobalt materials; titanium alloys; tool steels; etc.)¹⁴⁵. The size, shape, and structure of the powder produced is similar to the powders obtained by inert gas atomisation or rotary electrode process.

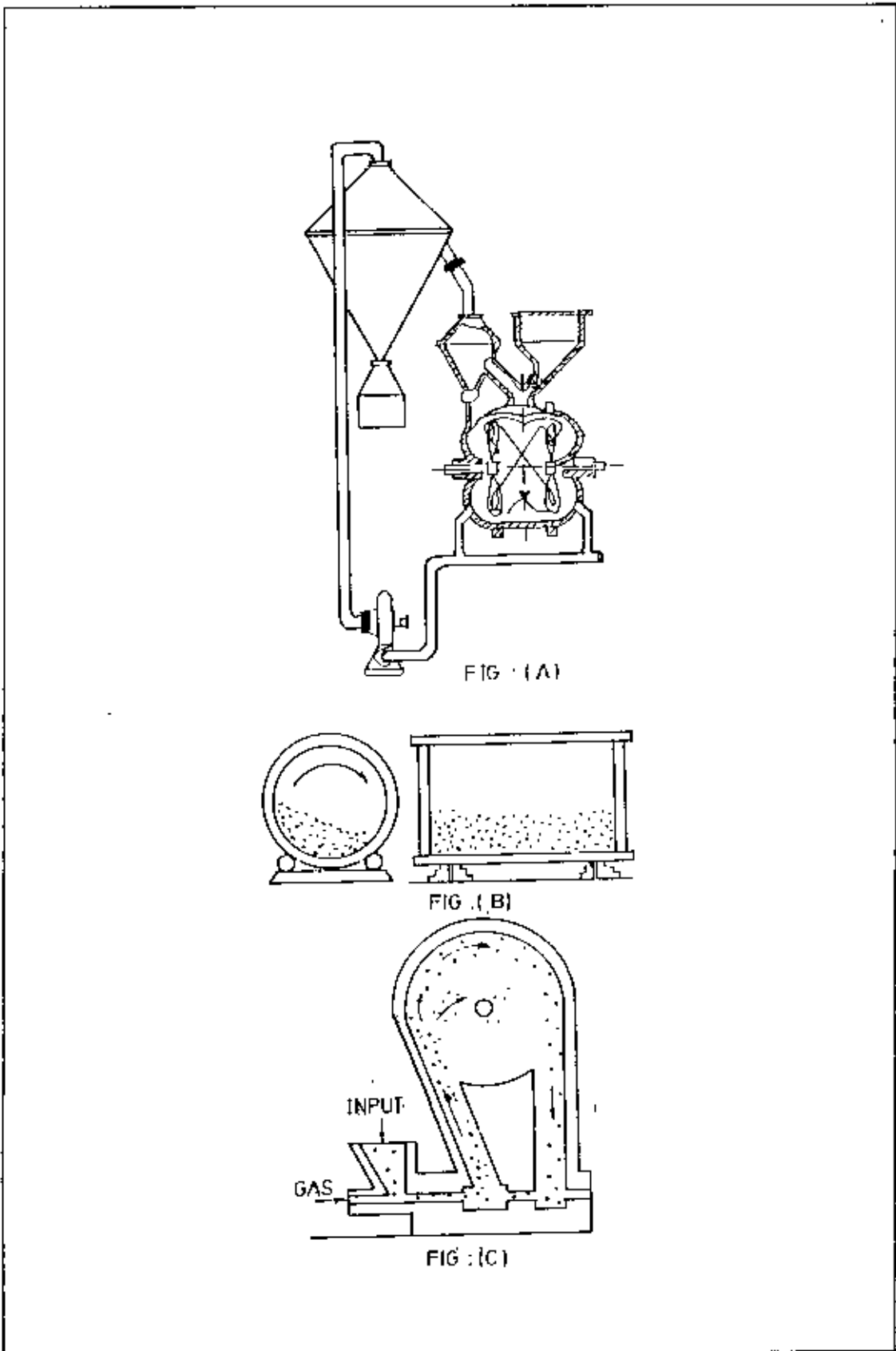


Figure 3.1 : Schematic representations of milling processes (a) Simple eddy mill (b) Ball milling. (c) Jet milling

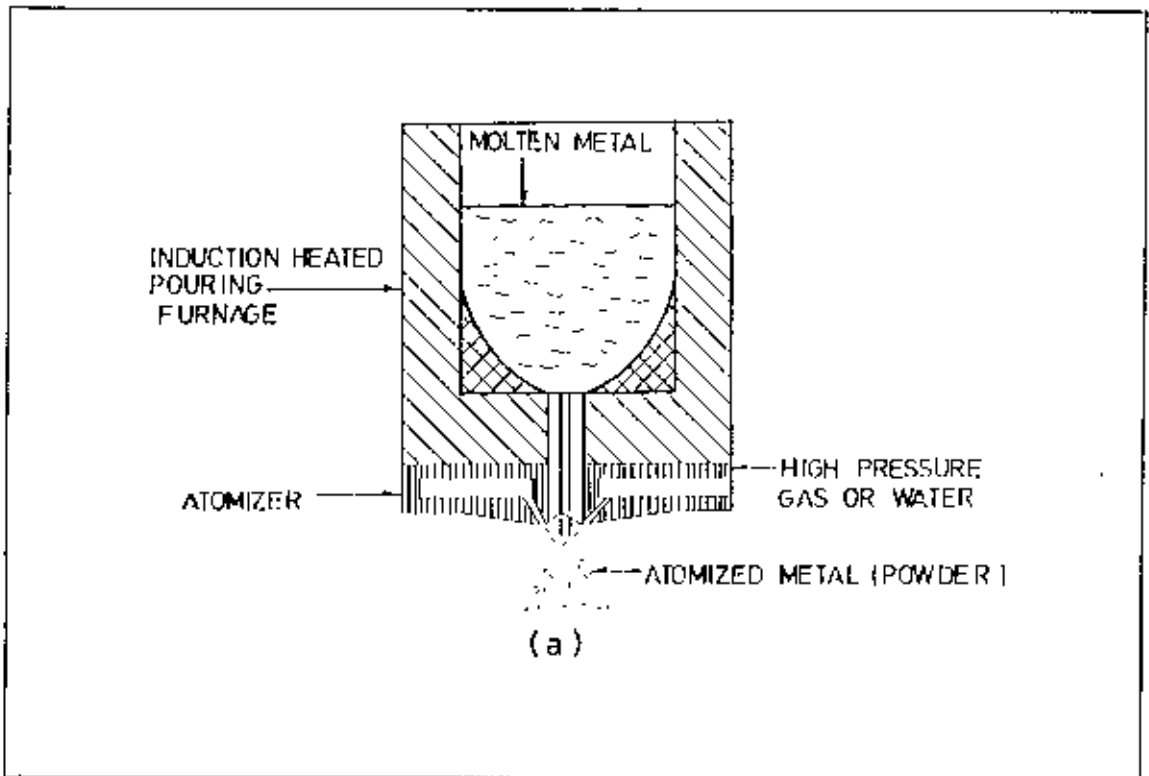


Figure 3.2 (a) : Schematic representations of typical atomising process

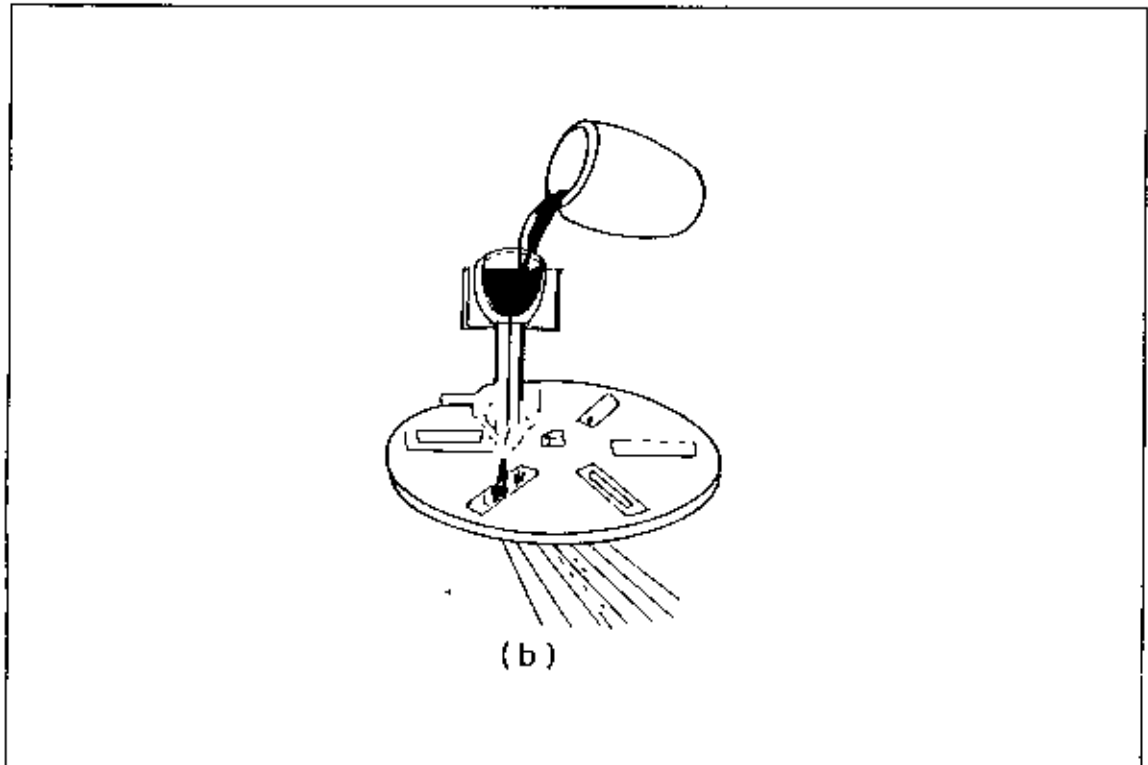


Figure (b) 3.2 : Schematic Representation of the principle of operation of D P G Process

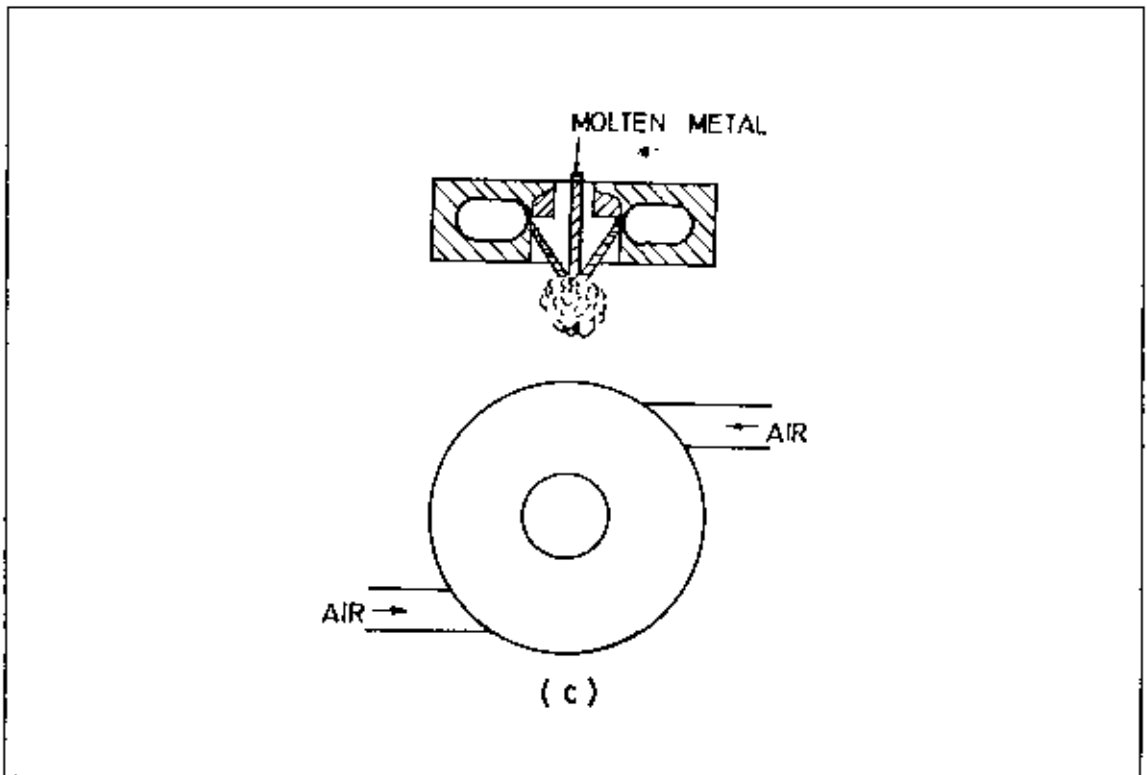


Figure 3.2 (c) : Schematic Representation of the principle of the Mannesmann process for atomising metals

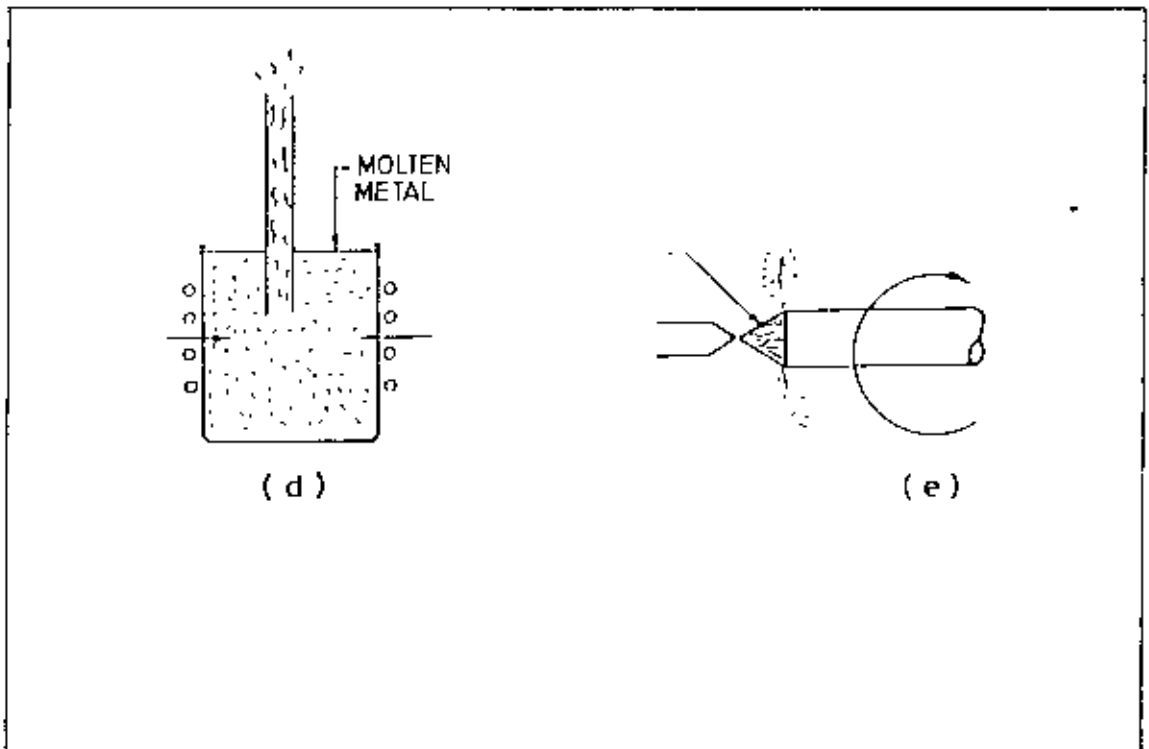


Figure 3.2 (d) and (e): Schematic representations of modification of atomising process.

Cold stream process relies upon the brittleness of certain metals and alloys at low temperatures. The starting material is coarse particles (often obtained by grinding or atomisation) of the required composition. This is conveyed in a high velocity, high-pressure air stream through a vertical nozzle and strikes on a target in an evacuated blast chamber. At the nozzle, the pressure drop occurs at once from about seven atmospheres to atmospheric and this results in a very quick temperature drop to subzero. The brittle raw material shatters against the target into an irregular shaped powder having very little surface contamination and excellent pressing characteristics. The resulting powder is separated into suitable size fractions using a classifier. This process has been used to produce tungsten, tantalum, tungsten carbide and tool steel powders as illustrated in Fig. 3.3.

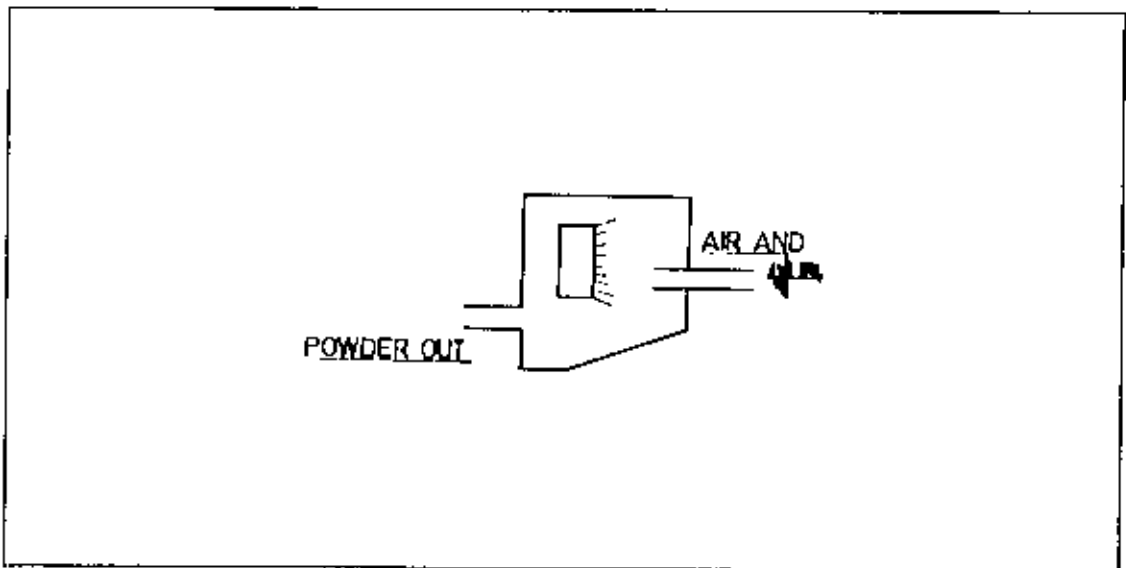


Figure 3.3 : Cold Stream Process.

Physico chemical and chemical processes :

Condensation method may be considered as a modification of the usual distillation process employed for refining zinc. First of all, zinc oxide is mixed with powdered charcoal and heated until zinc vapour is formed by the reaction of zinc oxide with carbon monoxide. The zinc vapour is condensed in a cooler extension of the retort. Reoxidation of the zinc vapour to zinc oxide also occurs during cooling due to the formation of carbon-di-oxide and the presence of this oxide will prevent its coalescence into liquid causing 'blue powder' as a normal by-product¹⁴⁶. Very fine powder of high purity can be obtained by joining a second condenser and carefully controlling the carbon dioxide content in the condenser. The powder thus obtained,

however, contains higher amount of oxygen than the atomised powder. Magnesium powder is produced by the same method such as reduction of MgO with CaC₂ followed by chilling the magnesium vapour in oil.

Thermal decomposition of vapour produces metal powders which has achieved industrial importance particularly in the manufacture of Fe and Ni powders by the decomposition of their respective carbonyls. Other metals such as Zn, Mg, Co, W, Mo, and Cr can also form their carbonyls which at certain temperature and pressure can decompose to give a gas and a metal. The decomposition reaction of various common carbonyls may be expressed as¹⁴⁷ $M(\text{CO})_x \rightarrow M + x \text{CO}$. Where M denotes Ni, Fe, Mo, W, Co etc. Carbonyls are volatile liquids. Iron pentacarbonyl, Fe(CO)₅, is an almost colourless liquid boiling at 102.7°C while the nickel tetracarbonyl, Ni(CO)₄, boils at 43°C.¹⁴⁸ They are produced by allowing carbon monoxide to pass over spongy or powdered metal at suitable temperature (200-270°C) and pressure (70-200) atmosphere. At reduced pressure (one atmosphere) and elevated temperature (150 - 400°C) both of these carbonyls decompose to reform both metal and the carbon monoxide; the latter being recycled and employed again to produce no more carbonyl liquid and continue the process.¹⁴⁹ Too low a decomposition temperature would result in slow and incomplete decomposition while higher temperature (above 400°C) would lead to oxidation of iron in carbon monoxide atmosphere. By varying the conditions of deposition the iron can be made available in various forms. Smooth layers, sponges or brittle nodules are produced by its decomposition on the hot surface. If a very fine powder with high purity is to be obtained, contact with a hot surface wall should be prevented, the walls are kept perfectly cool or carbonyl is mixed with a stream of hot inert gas such as nitrogen and introduced into a decomposition chamber. The carbonyl dissociates into a cloud of microscopic condensed metal particles which have been found to be about 0.01μ in size and serve as nuclei for building up of condensing metal into quite large shots. Thus nucleation phenomena often control the morphology and growth rate of carbonyl metal deposit in the size range between 1 and 10μ, as illustrated in Fig. 3.4. Fe powders produced by this technique are perfectly spherical and purest of all commercial metal powders (over 99.5%) containing only small amounts¹⁵⁰ of C, O₂ and N₂.

Reduction of compounds particularly oxides by the use of a reducing agent in the form of either solid or gas for producing metal powders is the most widely used

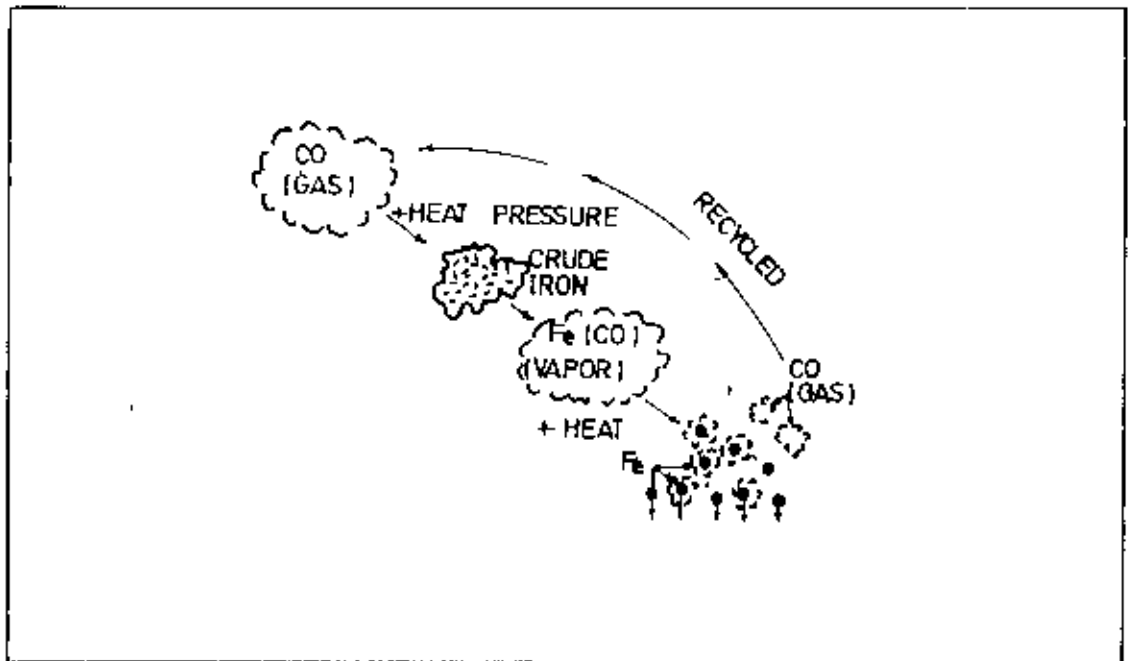


Figure 3.4 : Schematic drawing of decomposition using carbonyl process.

method. Other compounds such as formates, oxalates and halides may also be used as a starting material for reduction. This is a convenient, economical and extremely flexible method for controlling the properties of the product regarding size, shape and porosity over a wide range. It is extensively employed for the manufacture of Fe, Cu, Ni, W, Mo and Co, though Ta, Th, Zr, Ti and even Al and Cr are also being produced. This process yields extremely fine powders with irregularly shaped particles and considerable porosity.

Gases such as hydrogen, dissociated NH_3 , CO, coal gas, enriched blast furnace gas, natural gas, partially combusted hydrocarbons or alkali metal vapours, carbon and metals are used as reducing agents. Carbon is the cheapest reducing agent but with its use difficulties have been experienced in closely controlling the carbon content of the final powder. Hydrogen, dissociated ammonia and other atmospheres rich in hydrogen are used conveniently. Metallic reducing agents are also used for reduction of various metallic oxides involving exothermic thermit reactions as carbon as carbon and other reducing gases are unable to reduce them economically. Thus, Cr powders are produced by the reduction of Cr_2O_3 with Mg^{151} , Zr powder by reduction of zirconium oxide with Ca or Mg in inert gas atmosphere¹⁵², and Th metal by the calcium reduction of thorium under an inert atmosphere¹⁵²⁻⁵⁵.

Reduction by hydrides particularly calcium hydride is applied where very active nascent hydrogen is a necessity for the reduction. The chemical reduction for the hydride process may be expressed by the equation. $M_xO_y + yCaH_2 = xM + yCa + yH_2O$. Powdered eutectic alloy such as Cu-Ti alloy is made by mixing copper and titanium hydride powders in proper proportion, heating in hydrogen or vacuum slightly higher than the melting point of the eutectic alloy, holding the same for a sufficient time for complete diffusion between copper and titanium and cooling the molten eutectic alloy followed by pulvencation to powder.

Close control over the purity, particle size and shape, apparent density and related properties of the deposited metal powder and completeness of reduction can be obtained by varying the degree of purity, particle size and shape of the raw material, the temperature and time of reduction, the type of reducing agent, and in case of gaseous reduction, the pressure and flow rate of the gas. Since oxides are generally brittle and easily comminuted to the desired degree of fineness, it is possible to obtain very fine metal powders. Decreasing the reduction temperature also results in the production of very fine powders. Pyrophorical product is, thus, obtainable with some metals such as iron, nickel, etc. by grinding the oxide extremely fine followed by low temperature reduction. When the reduction processes are carried out at higher temperatures the final metal powder particles sinter together into a 'sponge' that is easily crushed and comminuted to powder. If H_2 is employed as the reducing agent, great precautions are need to be made it absolutely dry by removing all the water vapour content both in H_2 and that formed during the reducing reduction, otherwise complete reduction into metal powder (particularly Cr) is not possible.

Several reducing agents such as Li, Na, K, Mg, Ca, Mn, Al and Si may be employed to reduce the anhydrous chlorides of Ti, Zr, Hf or V. If a purer metal is desired, use of Mn, Al or Si is to be avoided. Li and K have to be abandoned due to their high cost and thus Na, Ca, and Mg only have to be employed¹⁵⁶. Thus, gaseous anhydrous chlorides of Zr, Ti and Hf are reduced by Na and Mg to spongy metals which are subsequently pulverised.

W and Mo powders are prepared from WO_3 and MoO_3 respectively by reduction with H_2 . The reduction is carried out a temperature of about $800^\circ C$ and $1050-1100^\circ C$ in the case of oxides of W and Mo respectively. The initial oxides in the form of pellets are kept in the tubular resistance furnace and they are moved into the furnace through heating zones, each indicating a different temperature. After complete reduction, they

are introduced into the cooler which is cooled by flowing water. H_2 is passed into the furnace through the cooler while the oxide is conveyed as a counter flow to the gas current. The resulting size of the metal particles is as small as 1μ . Extremely fine spherical W particles with very good properties have also been prepared by the reduction of tungsten hexafluorides. Iron powder has also been produced from oxide ore, pure oxides or a cheap initial product such as mill scale¹⁵⁷ by reducing with carbon, hydrogen, or natural gas. The ground scale is reduced with H_2 at a temperature of $650-800^\circ C$. The largest tonnage of iron powders are thus obtained from reduced ores and mill scale. Flow chart of carbon and gaseous reduction are illustrated in Fig. 3.5 and in Fig. 3.6. respectively.

Metal powders can be produced from aqueous solutions and fused salts by **Electrodeposition**. Electrodeposition is a reversed adaptation of electroplating. Thus, while in the case of electroplating, every effort is made to form continuous and tenacious sheet of metal on the cathode, in Electrodeposition the conditions favouring successful plating exactly reversed. As many as 30 metals can be prepared as powder by electrolysis of aqueous solutions accompanying simultaneous refining, but this technique is mainly employed for the commercial production of metal powders such as copper, beryllium, iron, zinc, tin, nickel, cadmium, antimony, silver and lead. There are three different types of Electrodeposition which are in practical use: (i) deposition as a hard, brittle mass, which is subsequently ground to powder.(ii) deposition as a soft, spongy substance; only loosely adherent with fluffy texture and easily pulverised by light rubbing, and (iii) direct deposition as powder from the electrolyte which drops to the bottom of the cell. The last two methods produce the largest quantities of electrolytic powders employed in the sintering process while the former method is unsuitable for molding purposes.

The conditions favouring the production on a cathode of powders easily removable and pulverisable, are (i) high current density, (ii) low metal-ion concentration,(iii) high acidity and addition of colloids, (iv) low temperature, (v) high viscosity, and (vi) circulation of electrolyte in such a way as to avoid and suppress convection¹⁵⁸. By regulating these conditions close control of the desired characteristics can be obtained.

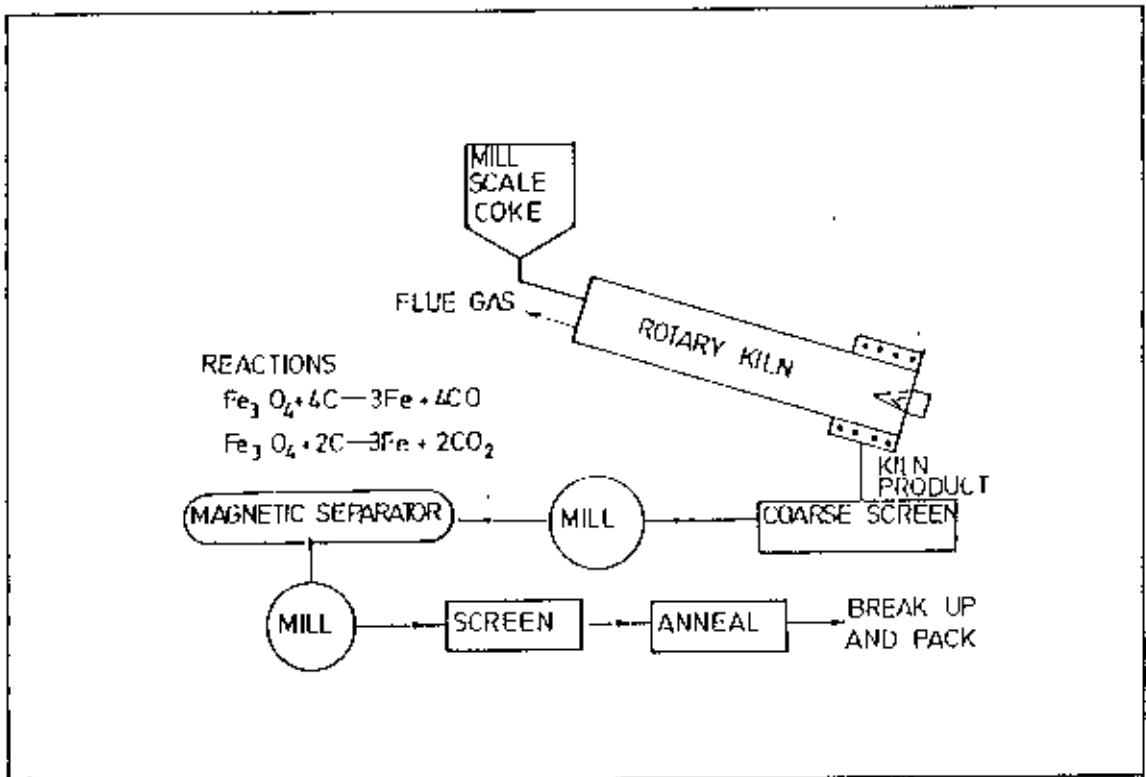


Figure 3.5 : Schematic outline of reduction process with carbon in rotary kiln.

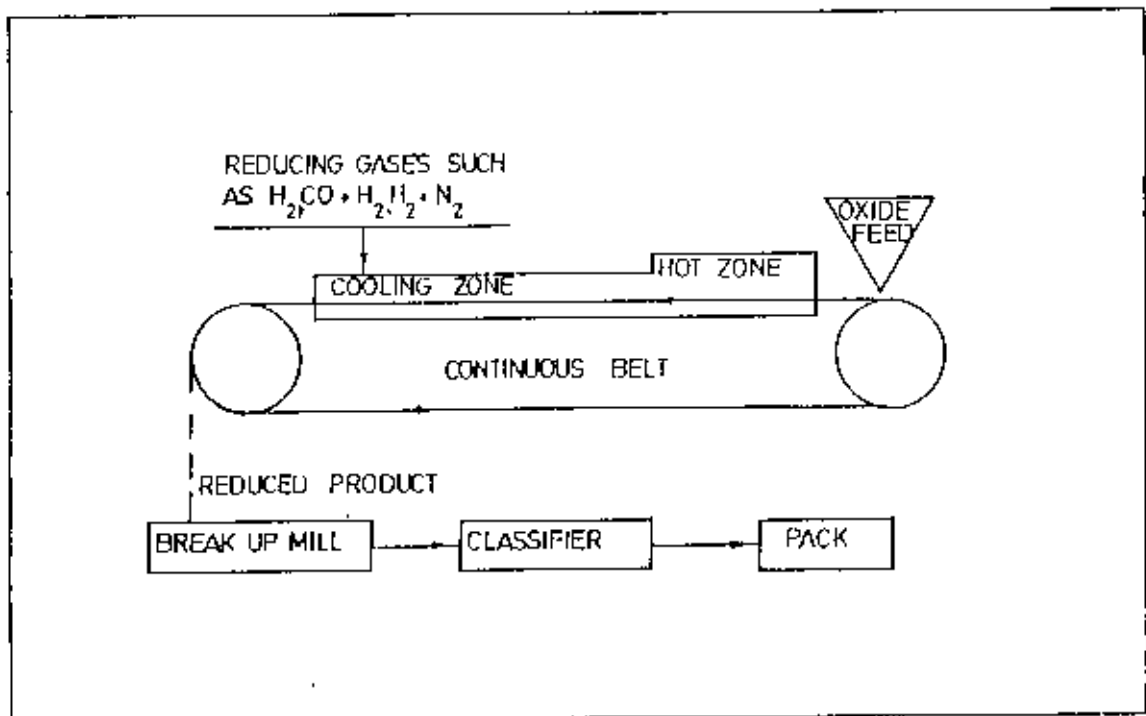


Figure 3.6 : Schematic outline of gaseous reduction process.

The selection of a suitable cathode material permitting the complete removal of the deposit is of great importance for continuous commercial production of metal powders. Highly polished and smooth surfaces are desirable and the deposit is stripped from the cathode by flexing or it can be recovered by using cathode as anodes in case of the formation of interfering films on cathode. The deposit is readily removed by scrapping it away from the cathode, or by use of other methods such as rotating cathodes, rapid circulation of the bath. The removal of powder from the cathode, either continuously or at frequent intervals is also essential.

The electrolytic powders deposited in the powder form, which are characteristically crystalline, are generally characterised by their dendritic or fern like shape of low apparent density and flow rate, favourable for pressing due to the tendency for individual particles to readily interlock. The particle size is largely dependent on the conditions obtained during deposition. Angular or needle-like shape is obtained in the case of powders produced from hard, brittle deposits, and the particle size is a function of mechanical methods employed for subsequent comminution. Electrodeposited powders are usually very reactive and brittle and hence special heat treatment may be given to them.

Electrodeposition of iron and copper powders is obtained most frequently by the electrolysis of sulphate solution but chlorides, cyanides and others can also be employed with success. Fig. 3.7. illustrates the principle of Electrodeposition. These electrolytic baths may contain one or more than one metal salt and organic reagent is occasionally added to promote powder formation. Iron powder is produced commercially by the electrolysis of sulphate or chloride bath. Addition of NH_4Cl increases the conductivity and reduces oxidation of the product. Chloride bath has been preferred to sulphate bath by Ljungberg et. al¹⁵⁸ because the latter results in the precipitation of sulphur in the deposit and tends to cause anode passivity. Copper powder is also produced commercially on a large scale by electrolysis. In this case the electrolyte employed is copper sulphate and sulphuric acid. This process has been thoroughly investigated by Modi et. al¹⁵⁹. The copper concentration has a considerable effect on cathode current efficiency, apparent density, and particle size of the powder. Crude copper is used as the anode material and formation of spongy deposit of copper takes place which adheres only loosely to the cathode. The oxygen content of electrolytic copper powder is high owing to the large surface area, but as in the case of iron powder, the characteristics of the powder can be precisely controlled.

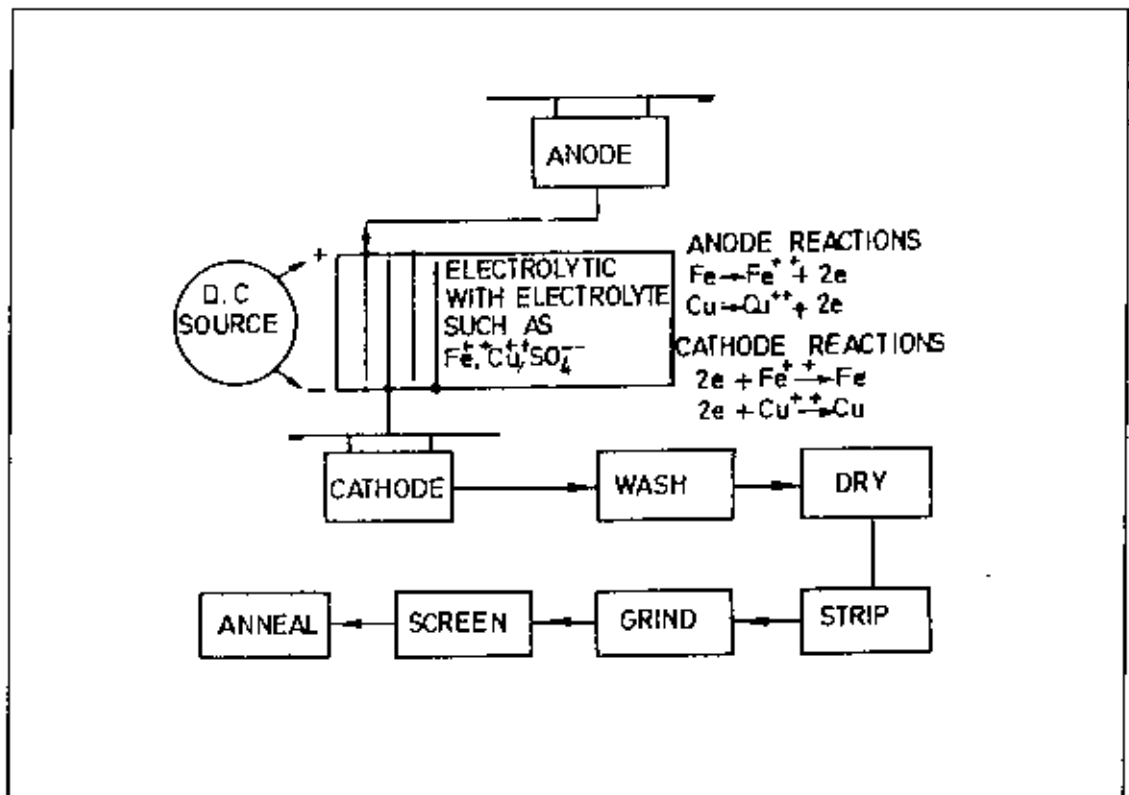


Figure 3.7 : Schematic representation of electrolytic process of making powders

The preparation of alloy powders is possible by the use of a mixture of electrolytes with two or more metal salts. In this way, electrolytic bronze and brass powders have been produced.

If fused salt electrolysis is performed at a temperature below the melting point of the metal, the deposition of metal will occur in the form of small crystals with dendritic shape. Among the metals prepared in the form of dendrites are iron, copper, nickel, silver, chromium, cobalt, tungsten, molybdenum, niobium, tantalum, thorium, uranium, beryllium, aluminium, zirconium and metals of platinum group. Ta powder is formed commercially by the electrolysis of tantalum oxide dissolved in a bath of K_2TaF_7 , KCl and KF. The addition of tantalum oxide is made continuous during the reaction and bath composition is maintained at the cathode. Leaching of tantalum removes trapped electrolyte, but the evolution of hydrogen at this stage causes embrittlement of the metal which is easily crushed to the required size and finally softened by heat treatment under vacuum.

Precipitation from aqueous solution. The principle of precipitating a metal from its aqueous solution by the addition of a less noble metal which is higher in the

electromotive series has been applied in numerous metallurgical processes. This process permits the production of very fine metal powders of low apparent density which are occasionally used for sintering purpose. Ag powder is produced in quantity from its nitrate solution by adding copper or iron; tin powder is precipitated by metallic zinc from stannous chloride; copper, iron, and nickel powders are obtained by adding aluminium to their sulphate solution containing HgCl_2 , HCl or alkaline salts which serve as activating agents. Gold powder is obtainable by precipitation with zinc and copper.

A very common method of producing copper powder is by precipitation from sulphate solutions with iron. In this case, carefully cleaned scrap iron or steel or sometimes even iron powder is usually employed to displace the copper. Moreover, the acidity of the solution and the rate of flow of solution over iron controlled to get a very fine powder having low apparent density. The raw material in this case may be a copper ore.

The precipitated metal powders are in general porous. A drawback of the precipitation method lies in the fact that the adherent or entrained salts are more difficult to remove than in electrolytic powder products. The precipitation of selenium and tellurium powders are possible by SO_2 from solutions obtained in the hydrometallurgical treatment of sludges from copper refineries.

Powders, particularly of reactive metals, are prepared by **Precipitation from fused salts**. For the production of zirconium powder the ZrCl_4 salt is mixed with an equal amount of KCl , and some magnesium. Magnesium replaces the zirconium when heated to 1380°F (749°C) and particles of latter settle at the base of the chamber. Another method uses the introduction of ZrCl_4 vapour to a salt bath of NaCl and MgCl_2 . Thus beryllium and thorium powders may be produced by following a similar technique. Several intermetallic compounds have been prepared in powder form by reacting two amalgams.

In recent years, metal powders particularly Ni, Co and Cu are precipitated on commercial scale by **Hydrometallurgical or gaseous reduction process**, by the reduction of aqueous solutions or slurries of salts of metals with hydrogen¹⁶⁰ when subjected to the correct combination of high pressure (between 400 and 900 psi.) and temperature (between 130°C and 210°C)¹⁶¹⁻⁶³ according to the represented type of reaction^{160,162}. $\text{M}^{++} + \text{H}_2 \rightarrow \text{M}^0 + 2\text{H}^+$.

In the process employed by Sherrit Gordon Mines Ltd., Canada for production of nickel metal powders, a sulphide concentrate is leached with ammonia and air under pressure¹⁶⁴. The sulphides are oxidised and non-ferrous metals react with ammonia to form ammine ions such as $[\text{Ni}(\text{NH}_3)]^{2+}$. The insoluble residue containing silica, iron hydroxide, etc. are separated out. Copper is then precipitated from the liquid so that the remaining solution containing only cobalt and nickel react with hydrogen to precipitate nickel metal in the pure state until the concentration of both in solution reach about the same value^{163,165}. Due to considerably higher thermodynamic activity and faster rate of reduction, reduction reaction of nickel is favoured in the mixed system. If pure cobalt is to be obtained (or nickel is to be recovered from the solution containing approximately equal amounts of each), a chemical process or reduction reaction in a solution containing cobalt but no nickel is followed. When precipitating nickel, nickel powder particles as seed materials (to act as nucleation sites for the precipitating metal) are introduced which are held in suspension in the solution by agitation. Soluble catalysts such as ferrous or palladium sulphate may also be used as nucleating agent. The precipitation of cobalt from cobalt-bearing solution with hydrogen is similar in most respects to the nickel precipitation method.

Copper powder is produced from ammoniacal solution in much the same way as nickel and cobalt and similarly the molar ratio of NH_3 to metal is kept at slightly greater than 2 :1.25. All these metals must be washed free from the last traces of salts and then dried in hydrogen and these steps are used to remove oxygen, carbon, and sulphur considerably from the metal. For copper the drying temperature is sufficiently high but for nickel and cobalt, moderate temperature is required¹⁶³.

The process may be developed to produce powders of zinc, lead, and molybdenum. It may also be used to produce composite powders in which a coating of copper, nickel or cobalt into an inner particle of, for example, tungsten carbide or diamond occurs in order to facilitate subsequent sintering as well as for coating the fibers (such as carbon or zirconia).

Recently a successful hydrometallurgical method, better known as the Peace River Process, has been developed for the production of iron powder with high purity, particularly low H_2 loss and acid insoluble content and good pressing properties and sinterability¹⁶⁶. A distinct virtue of the process is that it can be operated on the low grade ores. Apart from the high purity (usually about 99.8%) of the product this

technique is characterised by a very narrow range of particle size distribution, spherical shape, high apparent densities and flow rates of the powder.

Intergranular Corrosion process for producing metal powder is based on the fact that the grain boundaries of the heat treated alloys are more susceptible to chemical attack than the grains, thus freeing particles of bulk material. This method¹⁶⁷⁻⁶⁸, consists in carburising stainless steel scrap at a proper temperature (500-750°C) for a definite time in order to precipitate chromium carbide at the grain boundaries and corroding the boundary region of this sensitised material by corrosive solutions, for example, by a boiling aqueous solution of 11% copper sulphate and 10% sulphuric acid so as to cause disintegration of the stainless steel into powder. Rapid disintegration may be obtained using stainless steel as anode and solutions of a mixture of $\text{CuSO}_4\text{-H}_2\text{SO}_4$ acid as electrolyte in an electrolytic cell¹⁶⁹. The powder particles possess angular shape and the final particle size is determined by the grain size of the sensitised material.

Oxidation and decarburisation method has been developed for the production of pure reactive metal powders, particularly niobium, by reacting metal carbide with metal oxide in vacuum at elevated temperature so that both oxygen and carbon are removed as CO. Mannesmann process employed for the production of iron powders (where cast iron is atomised with compressed air) may also be regarded as the oxidation and decarburisation method, since it also involves the elimination of both carbon and oxygen.

Ultrafine powders can be produced by various methods such as milling, reduction and other methods, but the most versatile among these are based on precipitation from sols and gels. Ultra fine particles of high-melting point metals which do not react or dissolve in mercury to a considerable extent such as iron, nickel and beryllium have been prepared by electrolysis method employing a mercury cathode.

In recent years, the underlying methods have been employed to produce complex **alloy powder** : (i) atomisation process, (ii) combined precipitation in the thermal decomposition of carbonyls, (iii) combined precipitation of metals in electrolysis, and (iv) spray drying.

Atomisation process has already been discussed earlier chapter. Simultaneous thermal decomposition of several carbonylic metals, or unstable organic compounds

following combined recrystallization of powder particles result in the production of alloy powders such as iron-nickel powders with a nickel content in the range of 10 to 80% and iron-nickel-molybdenum powders with a molybdenum content up to 1.5% and with various nickel contents¹⁷⁰.

Complex alloy powders such as iron-nickel, iron-manganese, iron-molybdenum, iron-nickel-molybdenum, brass, bronze, etc. are produced by electrolytic deposition method by using (1) a mixture of electrolytes containing two or more salts, (2) cast alloy of required composition as the anodes, or (3) composite anodes of the appropriate metal and alloy component¹⁷⁰.

Spray drying, a technique originally developed by the chemical industry, consists of contacting a spray (of an aqueous mixture of salts such as cobalt oxalate, nickel oxalate, chromium acetate, molybdenum trioxide and thorium nitrate containing low solid content) with a blast of hot air, calcining the dried mass to convert all the metal compounds to the oxides at 800°C in air and reduction in hydrogen in order to produce a super alloy powder with dispersed thoria¹⁷¹.

Characterisation of powders

Introduction : The characterisation of powders is difficult because of the complex nature of a solid material in powder form and the many characteristics of an individual powder particles.

Characterisation of the powder particle shape : The behaviour of a metal powder in powder metallurgy processing depends on the characteristics of the respective powder. The factors which characterise an individual particle and a powder, and the effects of these factors on the powder behaviour are rather difficult to determine because several of these characteristic factors are even hard to define; and many of them are closely interconnected.

Characteristics of a powder particle :

A. Materials Characteristics :

1. Structure, 2. Theoretical density, 3. Melting point, 4. Plasticity, 5. Elasticity, 6. Purity.

B. Characteristics due to the process of fabrication :

1. Particle size (particle diameter), 2 Particle Shape, 3. Density (porosity), 4. Surface conditions, 5 Microstructure (crystal grain structure), 6. Type and amount of lattice defects, 7. Gas content within a particle, 8. Adsorbed gas layer, 9. Amount of surface oxide, 10. Reactivity.

Characteristics of a Mass of Powder.

1 Particle of aforesaid characteristics, 2. Average Particles Size, 3. Particle size distribution, 4. Specific surface (surface area per 1 gram), 5. Apparent density, 6. Tap density, 7. Flow of the powder, 8. Friction conditions between the particles, and 9. Compressibility (compactability).

Among the characteristic which are difficult to define the shape of a particle is probably the most difficult to determine A variety of particle shapes which differ in many ways are shown in Fig. 3.8

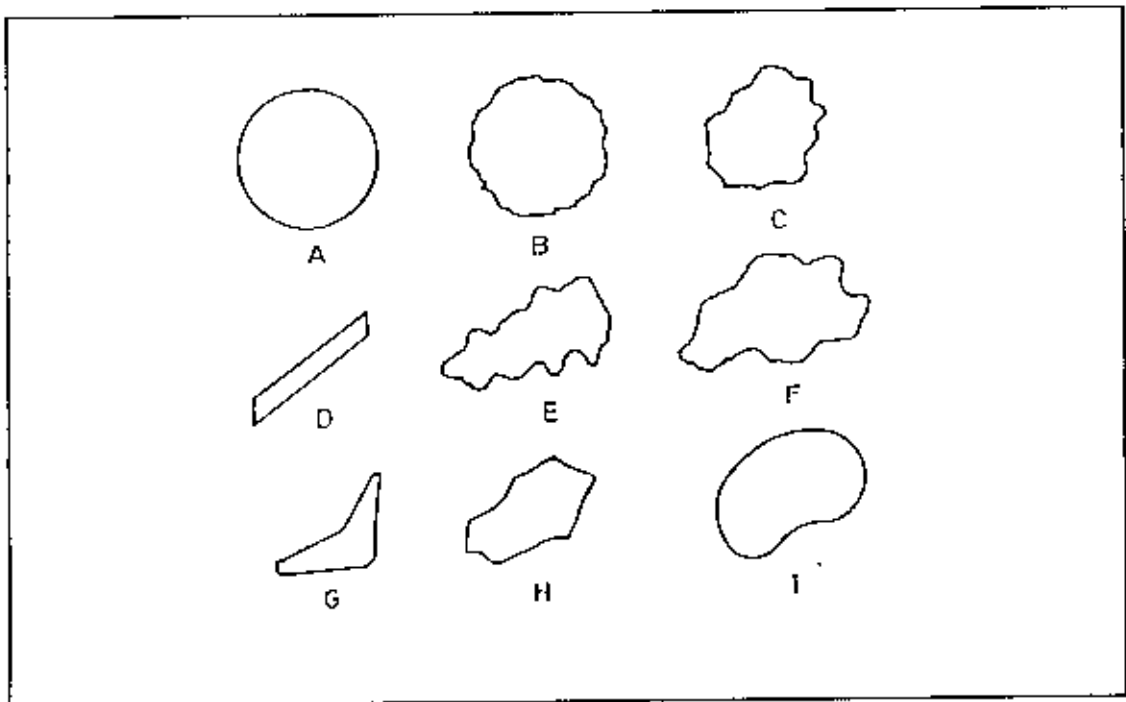


Figure 3.8 . Various shapes of Metal powder

a = Spherical smooth	f = elongated	b = Spherical rough
g = fragmented	c = Equiaxed irregular	h = angular
d = Acicular	i = rounded	e = dendritic

For each of these shapes the ratio $= \frac{\text{surface area}}{\text{volume}}$ is quite different. This ratio is also different for particles of precisely identical shape, if these particles just differ in size.

This ratio, therefore, can not be used for any characterisation of the shape. Herdan¹⁷², has extensively discussed shape factors, which however, did not refer to the shape of an individual particle, but rather to the average shape of all the particles in a mass of powder. This has the reliability because there is not only a variety or distribution of particle sizes in a mass of powder, but usually also a distribution of particle shapes.

Several assumptions and preliminary thoughts has to be taken into consideration for characterisation of the shape. These are: (a) Characterisation of the shape is an approximation, (b) A characterisation of the shape must consist of a series of factors or data, (i) to make an approximate sketch of the particle (ii) to predict the behaviour of this type of particle in processing, (c) The shape characteristics represents a three-dimension problem; for the sake of simplicity and better understanding it should be treated as a two-dimensional problem, (d) A two-dimensional treatment of the shape can be justified to a certain extent because most of the powder particles used in powder metallurgy are to a certain extent of rotational character, i.e., from the axis of the particle, usually two axes have practically similar dimensions. (e) A two-dimensional treatment of the shape excludes plate or flake-type particles, (f) For the characterisation of the shape, the diameter or any other figure concerning the actual size of the particle, is not useable.

One way to characterise an object consists of comparing this object with another well-known object which can easily be characterise. Such a comparison can be very valuable if some correlation between the object to be described and the well-known objects can be established. It has been proposed to compare a complicated shaped powder particle with a sphere of identical volume, and to characterise the complicated shape by its deviation from the sphere. It is therefor reasonable to compare the characteristics of a complicated shape as seen in the light of election microscope-actually the projection of the particle-with a rectangle drawn around the projection of the particle as shown in Fig. 3.9. Here assumed that the particle is placed on the stage in the most stable position, which however, already indicates that it is possible to draw a variety of rectangles around the projection of the particle rectangles of various side ratios and various areas. It is therefor proposed to select from the many rectangles the one which is characterised by a minimum area. This rectangle is perfectly characterised by its side lengths ,a and b, where a indicates the longer, and b is the shorter side of the rectangle. The projected particle area A and the circumference C of

this area together with the side lengths a and b of the rectangle, permit a useful characterisation of the particle shape (Fig. 3.10.).

The shape of a powder particle, whether it is approximately equiaxed or elongated and the extent to which it is elongated, can be given by the ratio $x=a/b$, where x the elongation factor. The minimum value of $x=1$ refers to equiaxed particles, the greater x is, the more pronounced is the elongation of the particle without giving information as to whether the elongated particle is needle-shaped or dendritic, or whether it is of some other shape. Even when $x=1$; one does not know whether this refers to a spherical or an irregular-shaped particle; in any case, it refers to a partially equiaxed particle. The value of x may vary between 5 to 10.

It is relatively easy to determine the projected area A of the particle, and to compare A with the area $a.b$ of the rectangle drawn around the particle projection. The ratio

$y=\frac{A}{a.b}$ refers in a certain way to the bulkiness of the particle. The factor y , the

bulkiness factor, is close to the value of 1 for a particle which fills the area of the rectangle, but will usually be considerably less than the value of 1. To certain extent a decrease in the value of y indicates a decrease in the bulkiness of the particle. The value of y may vary from 0.7 to 0.8.

For the characterisation of the particle shape, the surface configuration is to be taken into consideration. It is actually surface of a particle which contributes most of its activity. Whereas the first mentioned two factors, the elongation factor x and the bulkiness factor y , correlate the dimensions of the rectangle drawn around the particle cross section with the respective particle characteristics, these rectangle dimensions cannot be used to characterise the particle surface. The main reasons for this is the fact that the ratio $\frac{\text{surface area}}{\text{volume}}$ of the particle does not depend exclusively on the particle shape, but also, and to a large extent, on the actual particle size.

For a spherical particle where the cross section are $A=\frac{d^2 \pi}{4}$ and the circumference $C=d\pi$ the correlation exists. $C^2 = kA$, where $k=4\pi=12.6$. The spherical particle represents a special shape which is characterised by the minimum surface for a given volume.

For any particle a factor $z = \frac{C^2}{12.6A}$ exists. The factor z-the surface factor-will have the value of 1 for a spherical shaped particle with smooth surface, but will increase for a sphere with a rough or corrugated surface or for any other shape, the more the shape deviates from the smooth sphere, the surface factor z, therefore should be a valuable indicator of the particle shape with respect to its surface configuration, and without any reference to the actual particles size.

Fig. 3.11(A) to Fig. 3.11(L) show a variety of eleven different particles shape, the side lengths a and b of the rectangle, the projected particle area A, and the circumference of this area C. The following table shows the elongation factor x, the bulkiness factor y, and the surface factor z, calculated from a, b, A and C,

Table 3.1 :Relative dimensions and characteristic data of powder particles of various shapes

Shape No.	Relative dimensions				Particle characteristics		
	a	b	A	C	x	y	z
A	6.0	6.0	28.2	18.8	1.00	0.78	1.00
B	6.0	6.0	28.2	26.5	1.00	0.78	1.98
C	6.0	6.0	25.4	25.5	1.00	0.71	2.04
E	8.0	6.0	36.2	29.4	1.34	0.76	1.89
F	7.6	3.4	18.7	20.5	2.23	0.72	1.77
G	7.5	3.8	15.5	21.6	1.97	0.54	2.20
H	8.0	5.0	29.4	22.9	1.60	0.74	1.40
I	9.0	2.5	11.8	33.5	3.60	0.52	7.50
J	8.0	2.0	13.2	17.8	4.00	0.83	1.89
K	7.0	5.0	10.7	19.5	1.40	0.31	2.80
L	8.0	5.0	20.2	21.7	1.60	0.50	1.84

The surface factor z is minimum (z=1) for a smooth sphere, but increase considerably when the sphere surface is corrugated. The factor z may have any value between 1 and approximately 10. Dendritic shaped particles will have highest surface factors: rounded particles are usually characterised by small values for the surface factor.

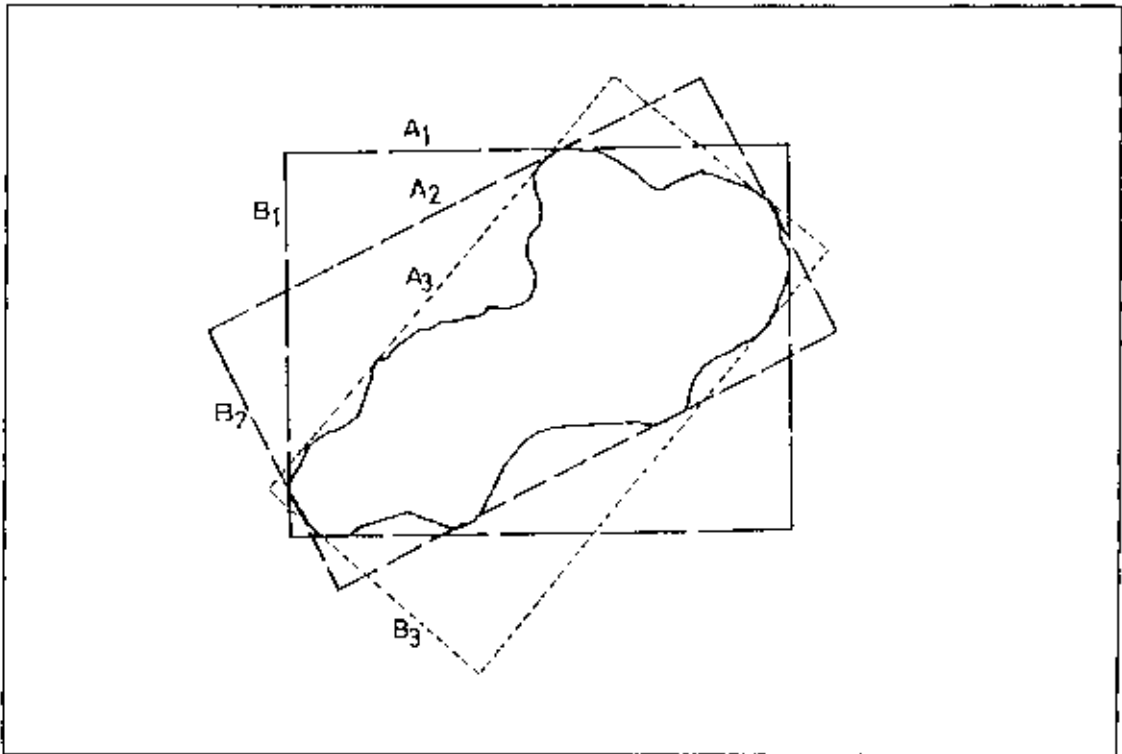


Figure 3.9 : Various rectangles drawn around the projected of a particle.

$a_1 = 10.9$	$a_2 = 12.2$	$a_3 = 11.7$
$b_1 = 8.3$	$b_2 = 6.3$	$b_3 = 6.0$
$a_1 b_1 = 90.5$	$a_2 b_2 = 76.9$	$a_3 b_3 = 70.2$

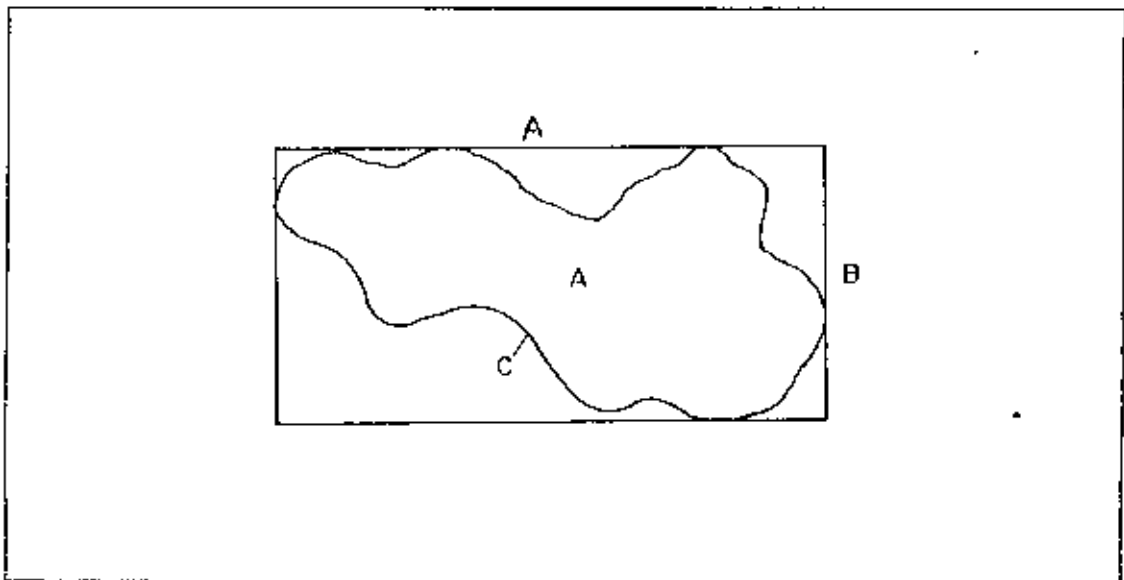


Figure 3.10 : Rectangle of minimum area drawn around the particle projection
 a, b = side length of the rectangle.
 A = area of the particle projection
 C = circumference of the projected particle

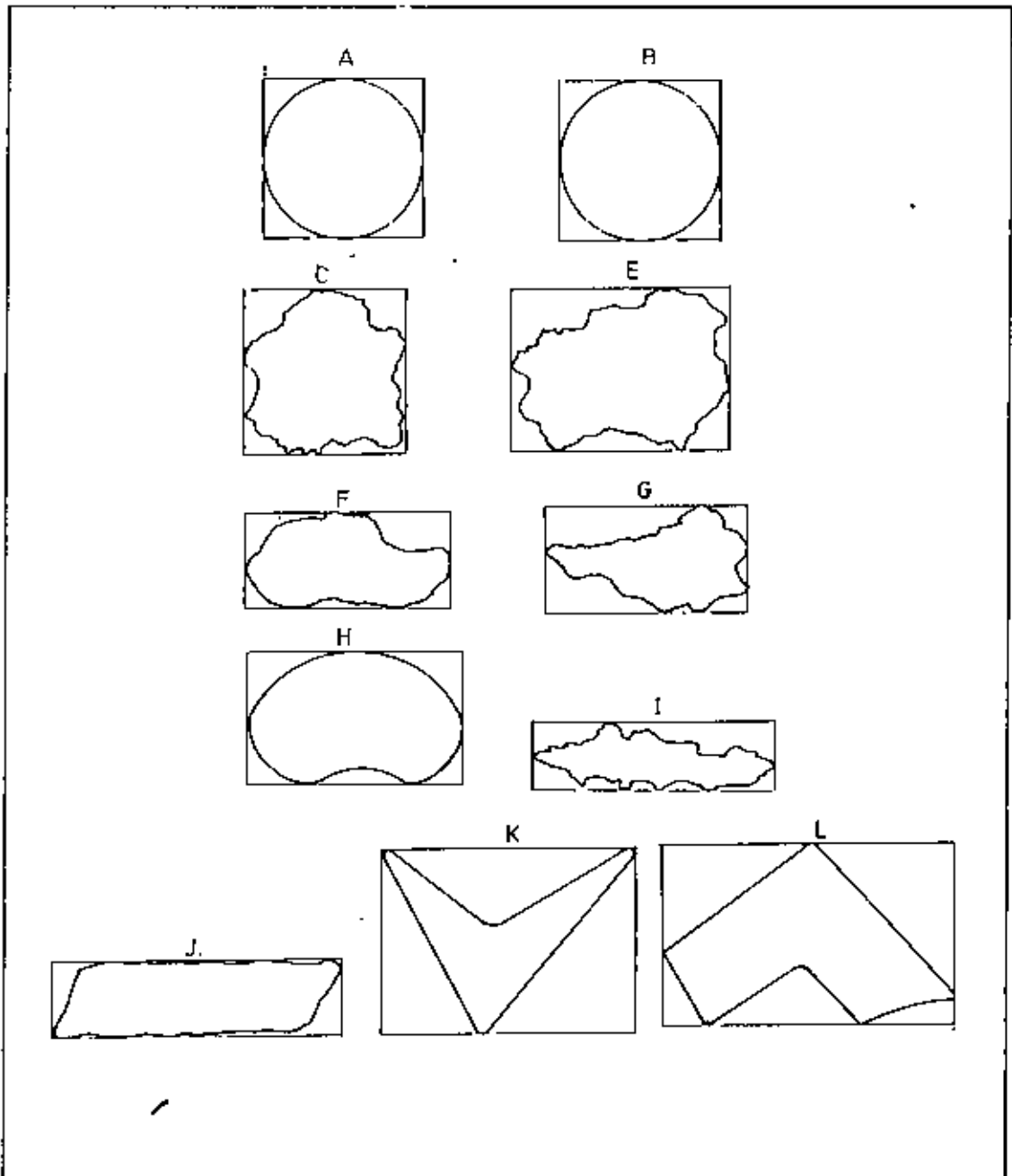


Figure 3.11 : Characterisation of the particle shape.

Figure A:

a = 6 A = 28.2
b = 6 C = 18.8

Figure E:

a = 8 A = 36.2
b = 6 C = 29.4

Figure H:

a = 8 A = 29.4
b = 5 C = 22.9

Figure K:

a = 7 A = 10.7
b = 5 C = 19.5

Figure B:

a = 6 A = 28.2
b = 6 C = 26.5

Figure F:

a = 7.6 A = 18.7
b = 3.4 C = 20.5

Figure I:

a = 9 A = 18.7
b = 2.5 C = 20.5

Figure L:

a = 8 A = 20.2
b = 5 C = 21.7

Figure C:

a = 6 A = 25.4
b = 6 C = 25.5

Figure G:

a = 7.5 A = 15.5
b = 3.8 C = 21.6

Figure J:

a = 8 A = 13.2
b = 2 C = 17.8

Design and Fabrication

Introduction :

Mechanical alloying originated from a long search for the means to add high temperature strength conferred by fine dispersion of ceramic particles to intermediate temperature strength developed by conventional alloying. From the initial laboratory success, the process has been developed into a well-controlled production operation: whole series of nickel, iron, aluminium and other alloys have been designed specifically to use the process and techniques have been developed to form and fabricate the alloys into useful components. But no work on mechanical alloying in Bangladesh had been reported till now. So considerable effort was decreed towards the design and construction of the mechanical alloying unit used in the present work.

Preliminary considerations :

Mechanical alloying offer the ability to process different starting materials with various characteristics, which can be converted into fully homogeneous alloys. This ability to apply the process to variety of systems is due to large number of complex and multifaceted variables involving the mechanics, mechanical behaviour, heat flow, thermodynamics and kinetics. In view of large number of variable, the investigations, if they are carried out on a large scale plant, will be time consuming and expensive. This is more important when one has to make e beginning in a field which is still alien to

Bangladesh. The use of a small scale unit ensures considerable economy in time, materials and expenses, thus permitting a variety and wider range of alloys and operating conditions to be examined. Modification in design or operation can also be easily incorporated in small units.

In small scale unit, trench's, which can be translated to full scale work, can be established. This also helps in gaining a better understanding of the process. This understanding together with fundamental data can give useful information. This is of particularly important since little is known about the process. Moreover in laboratory experiments, the treatment parameters can be closely controlled and hence the result can be fruitfully utilised in designing for large scale applications. From economical viewpoint a certain measure of risk is involved in going directly to an industrial or semi-industrial scale operation without preliminary experimentation, for total rejection may occur.

Theoretical considerations:

The original version of attritor used for mechanical alloying was designed by Szegvari¹⁷³. The invention related to fine grinding of solids. In the case of a fine grinding a liquid medium is used to prevent agglomeration of fine particles. In the study of mechanical alloying dry milling was adopted.

An attritor is essentially a high energy ball mill. It consists of a stationary vertical vessel and usually high chromium steel balls (preferably grinding balls should be of the same materials to be processed) as the grinding media. The agitation of these grinding media is affected by the rotation of a vertical shaft which is fitted with horizontally spaced impeller arms. Due to the rotating motion of the shaft, the arms of the impellers cut through grinding media imparting an activated relative motion. The activated condition of the grinding media is characterised by at least a partial random distribution of their momentum. There may be little or no movement of the grinding media around the edges and at bottom of the vessel. The movement of the grinding media is produced not only by contact with agitator but by the kinetic energy imparted by the other elements also. Each of the activated elements repeatedly and continuously bounces from contact with another element and with the agitator and remains in suspension in the system. There are two primary types of media interaction during mechanical alloying in an attritor. One, termed direct impacts, is high velocity collisions between grinding balls. These impacts are prevalent in the attritor core, where the impeller arms are located. However, little of the powder charge is located in

the core. Another type of impact, termed ball sliding, is found in regions outside the core. Sliding results from differential rotational velocities between adjacent rows or columns of the grinding balls. The predominance of this type of action is a result of the close-packed array by the grinding balls in the region outside of the attritor core. There exists a difference in velocities between adjacent rows (along the attritor walls) and columns (along the attritor bottom). The most efficient operation is that in which,

- (a) the number of **contacts** between the balls is maximum,
- (b) the higher the **rotational speed**,
- (c) the larger the number of **collision** between the balls.

The aforementioned (bolded) factors are described below :

The number of **contacts** and the number of **collisions** among the grinding media depend on the **type of agitation and nature of the movement of the agitator**. A very efficient type of agitator is one with an upright vessel with a central vertical shaft and horizontal agitating impeller arms with triangular cross section. For wet grinding this arrangement is enough but for dry grinding two such shafts may be used spaced further apart so that agitator arms overlap. The activated condition and hence the number of effective **contacts** between grinding media again depend on

- (a) the **depth** of the bed of grinding media,
- (b) **specific gravity** of grinding media,
- (c) the **viscosity** of the liquid (if any),
- (d) the **speed of agitation**,
- (e) the **size, shape and distribution** of grinding media.

The higher the speed of agitation, the higher the energy input and hence the more efficient of milling of powder particles. However, the higher speed of agitation the sets wearing action of the balls and the attritor wall. The wearing of the impeller or the agitator arms depend on the clearance between the agitator arms and the side walls of the vessel and this clearance has direct relation to the most practical agitator speed.

The smaller the size of the grinding media the more efficient of fine milling capacity of a given volume of elements. But this size decreases the attrition. While this can be counter balanced by an increase in the rpm, the condition is such that there is an optimum size which depends on the other conditions mentioned. As to the distribution of size of grinding media, it is significant that they should be uniform in size as far as possible. As to the shape of the grinding media, it is preferable to use spherical

elements. Other shapes are likely to jam the operation. However, Rydin et al.¹⁷⁴ suggested several ways for improving attritor efficiency. Among them is use of a mixture of differently sized balls in the mill which would result in a disruption of the close-packed array, thereby facilitating a greater incidence of direct impacts. Cook¹⁷⁵ has conducted a study of attritor behaviour when differently sized balls are used in the device. When differently sized balls are placed in the attritor, the smaller balls segregate to the tank bottom at low device rotational velocities. Increasing this velocity reduces ball segregation and, at a critical rotational velocity (which is ball size, ball size ratio and tank diameter dependent), complete ball mixing takes place. The close-packed array becomes defective when balls of different size are used. The defects are mainly substitutional or interstitial (depending on the radius ratio of the balls), although dislocations are sometimes recommended.

The size of the powder material to be mechanically alloyed has an influence on the most efficient speed to be used. If the size of this powder material is initially large, a certain amount of momentum is required to subdivide it and the energy is considerable. For an attritor of laboratory scale for milling very small size powder particles, $\frac{1}{4}$ " diameter grinding balls can be used. In commercial units $\frac{1}{2}$ " diameter grinding balls should be used.

Speed of rotation of an agitator depends on the length of the arms because the longer the arms, the faster the arms move and greater the agitation produced. Agitator should be maintained at such a distance above the bottom that there is no movement of grinding media at the bottom of the bed.

Although for the most efficient operation, a cylindrical vessel with dished bottom might be recommended, from an engineering standpoint it is most practical to construct a vessel with a flat bottom. The collisions, impacts and friction among the grinding media, the shaft and the inner surface of the vessel are to be preferably minimised to prolong the life of the attritor. To prevent excessive wear, it is better to coat the impeller arms and the inside wall surface of the attritor vessel with a very hard alloy.

Design and fabrication:

Based on the aforementioned preliminary and the theoretical investment, an attritor and all other accessory facilities for mechanical alloying, have been designed. The design was considered for four parts as mentioned below :

- (a) Design of an attritor,
- (b) Design of hot pressing unit,
- (c) Design of a powder production unit,
- (d) Design of accessory systems.

Design of an attritor:

The main parts :

The attritor designed and fabricated for this experiment was based on the model invented by Szegvari¹⁷³. The different part of this attritor are described below:

The vessel of the attritor was cylindrical with 6" in internal diameter and 12" in height. The vessel was made of mild steel with $\frac{1}{2}$ " wall thickness. A reaction chamber of 6" in diameter and $7\frac{1}{2}$ " in height has been machined within the vessel. The vessel has a flat bottom lid and a flat top lid. The bottom and top ends of the vessel were welded with flanges of 10" in diameter. Eight holes each of $\frac{5}{16}$ " diameter apart from each other by 30° have been arranged on a circle of 9" diameter on the flanges. The top and bottom of the vessel was covered with mild steel lid, matched with the flanges. The lids themselves have the provisions for O-rings to make the inside of the chamber completely isolated from the environment. The vessel rests on a firm foundation.

The grinding medium used in the attritor was $\frac{5}{16}$ " diameter high carbon; high chromium steel balls. The agitation of the grinding media was effected by a centrally located vertical shaft 1" in diameter and fitted with impellers by means of spacers. This portion of the shaft adjoined with impellers and spacers was of $\frac{2}{3}$ " diameter. The shaft was introduced into the vessel through air tight bearings. The bearings were fitted with the guilders spaced at a distance of 3". The shaft was made of stainless steel.

The impeller arms of uniform circular cross section of dimension of 2" length and $\frac{3}{8}$ " diameter were provided at the upper portion and that of $\frac{1}{2}$ " diameter at the lower portion of the vertical shaft. Three impellers of the same dimensions apart from each other by 120° were provided in the same plane. Six sets of such impeller plane were

provided within the vessel of the attritor. The distance between the impeller planes were adjusted using spaces. The impellers were made of stainless steel.

The spacers used were simple cylindrical with internal diameter of 6", outer diameter $1\frac{1}{2}$ " and were fitted to the shaft (with $\frac{7}{8}$ " in diameter portion). These spaces provided both the distance between the impeller arms planes as well as distribution of energy equally to the impellers. The spacers were made of stainless steel.

The dimensions and all others details of different parts and the layout of an attritor are represented from Fig. 4.1 to Fig. 4.9 C. and Fig p1.

The hot-pressing unit :

The hot pressing unit consists of the following parts as described below :

(a) **Pressing chamber** : It was a cylindrical chamber with 1" in internal diameter and $1\frac{7}{8}$ " in outer diameter and 4" in height. This chamber was made of stainless steel.

(b) Two die **plungers**, upper part $3\frac{1}{2}$ " in height and 1" in diameter and lower part 1" in height and 1" in diameter were made of stainless steel.

(c) The **furnace** was made by winding non-inductive nichrome wire on a heavy duty mullite tube. The constant temperature zone of the furnace was about 5 cm. and was maintained by means of an 'ON-OFF" controller. The combination of hot pressing chamber and die plungers were heated by means of this electrically heated furnace.

(d) The **press** adopted to consolidate the milled powder was based on the principal hydraulic pressing. The hydraulic press used was of the capacity of 20 Ton.

The dimensions and all other details of hot pressing unit are represented in Fig. 4.10. to Fig. 4.13. and Fig p 2 to Fig p 3.

The powder production cell :

The powder production cell, adopted in this experiment was designed and fabricated based on the principal of reversed electroplating . This unit consist, of an electrolytic tank, anode and cathode, and controlled electric power supply system.

The tank was made of plastic of dimension 20" x 7" x 9". It consisted six anodes of copper sheet each 2" x 7" and two cathodes of polished aluminium sheet of 5" x 7". Both the anodes and cathodes were arranged in series on an electric supplying rod of copper of 1" in diameter. A rectifier was provided to convert the a. c. supply to d. c. of required voltage and ampere.

The dimensions and all other details of the powder production unit are represented in Fig. 4.14. to Fig. 4.15 and Fig p4 to Fig p5.

The accessory systems :

The attritor adopted for mechanical alloying requires some accessory systems which were, (a) the power supply system.

(b) the cooling system

(c) the gas supply system

Power supply systems :

The power supply systems adopted in this experiment was two types.

(a) Alternating current supply for driving the motor (7.5 HP) which rotates the attritor shaft by means of pulley and belt system. The supply source was of 120 volts, 50 Hz, single phase a. c.

(b) Controlled direct current (d. c.) for powder production cell. The power supply for this purpose was adopted such that would be capable of providing the required voltage and current in the electrolytic cell to decompose copper and deposit it in the form of powder. A current density of 20 Ampere/square foot of cathode at a voltage of 10 volts adequate for the aforesaid purpose were required.

Since two aluminium sheet of each of area of 5"x7" were used as cathode and the effective portion to conduct ions was only 5"x4". The d. c. supply system was consisted of a variac, an step down transformer and a rectifying unit. The voltage can varied from 0 to 30 volts and the current from 0 to 200 amperes by regulating the input voltage. The power supply system itself was fed from 120 volts, 50 Hz, single phase a. c. source and necessary instruments for measuring output voltage and current were also provided.

The gas supply system:

In order to provide a reducing atmosphere in the attritor, it was devised to supply hydrogen gas. Gas was drawn from the cylinders containing commercial varieties of hydrogen gas supplied by the Bangladesh Oxygen Limited. This gas supply system consisted of a cylinder containing the treatment gas, fitted with regulators, flow meters, and piping system.

The cooling system :

During mechanical alloying tremendous heat was formed within the chamber either for solid state reactions among the powder particles and/or friction between the colliding balls, balls-impellers and balls -attritor vessel wall. Such high temperature inhibits the fracturing events of the powders. So a cooling system is needed to be adopted to minimise such a rise of temperature. This cooling system consisted of water supply, piping system and the copper tubing around the outer surface of the vessel of the attritor to circulate the cooling water.

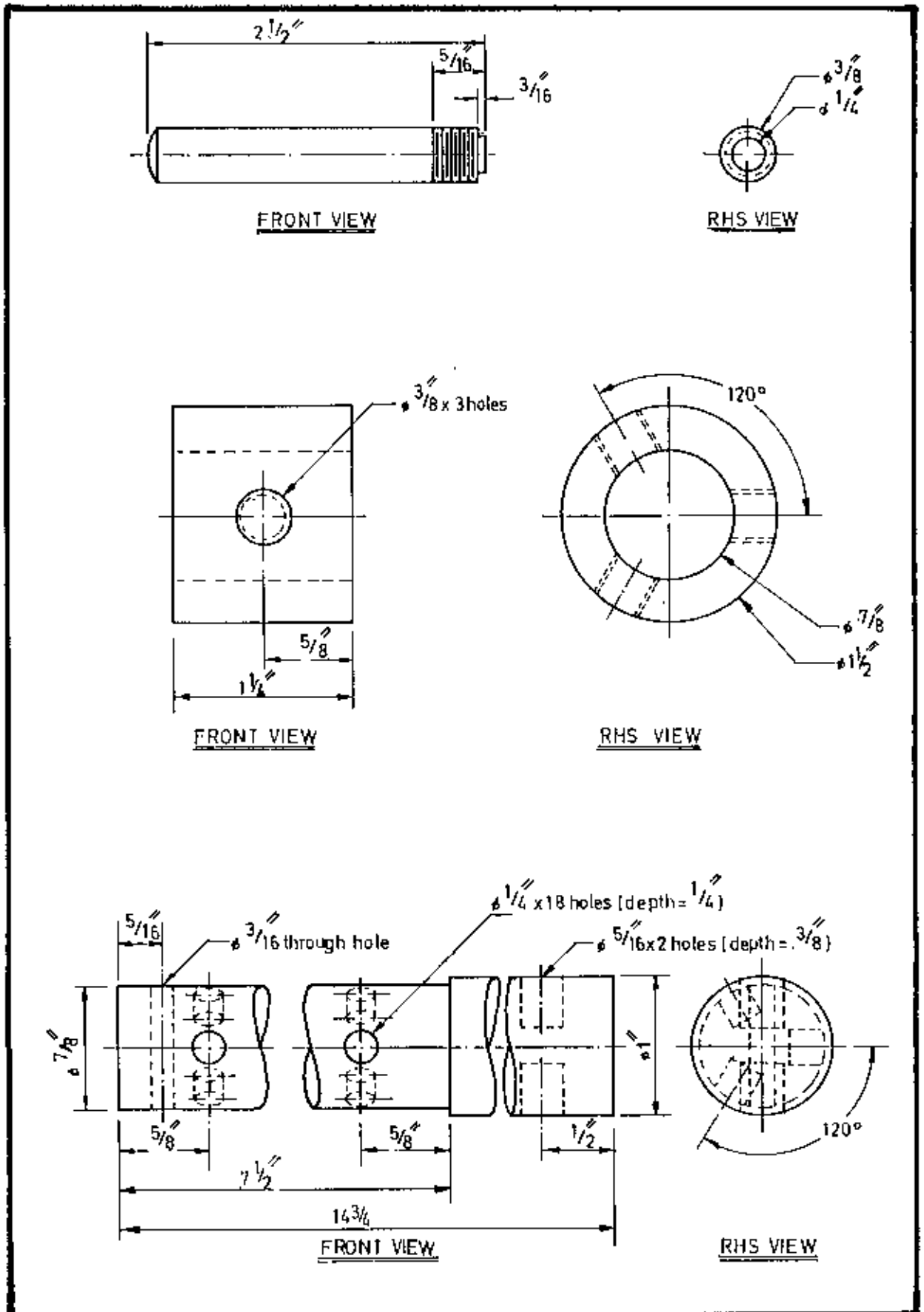


Fig. 4.1 :: IMPELLER

Fig. 4.2 :: IMPELLER HOLDER CUM SPACER

Fig. 4.3 :: DETAILS OF CENTRAL SHAFT

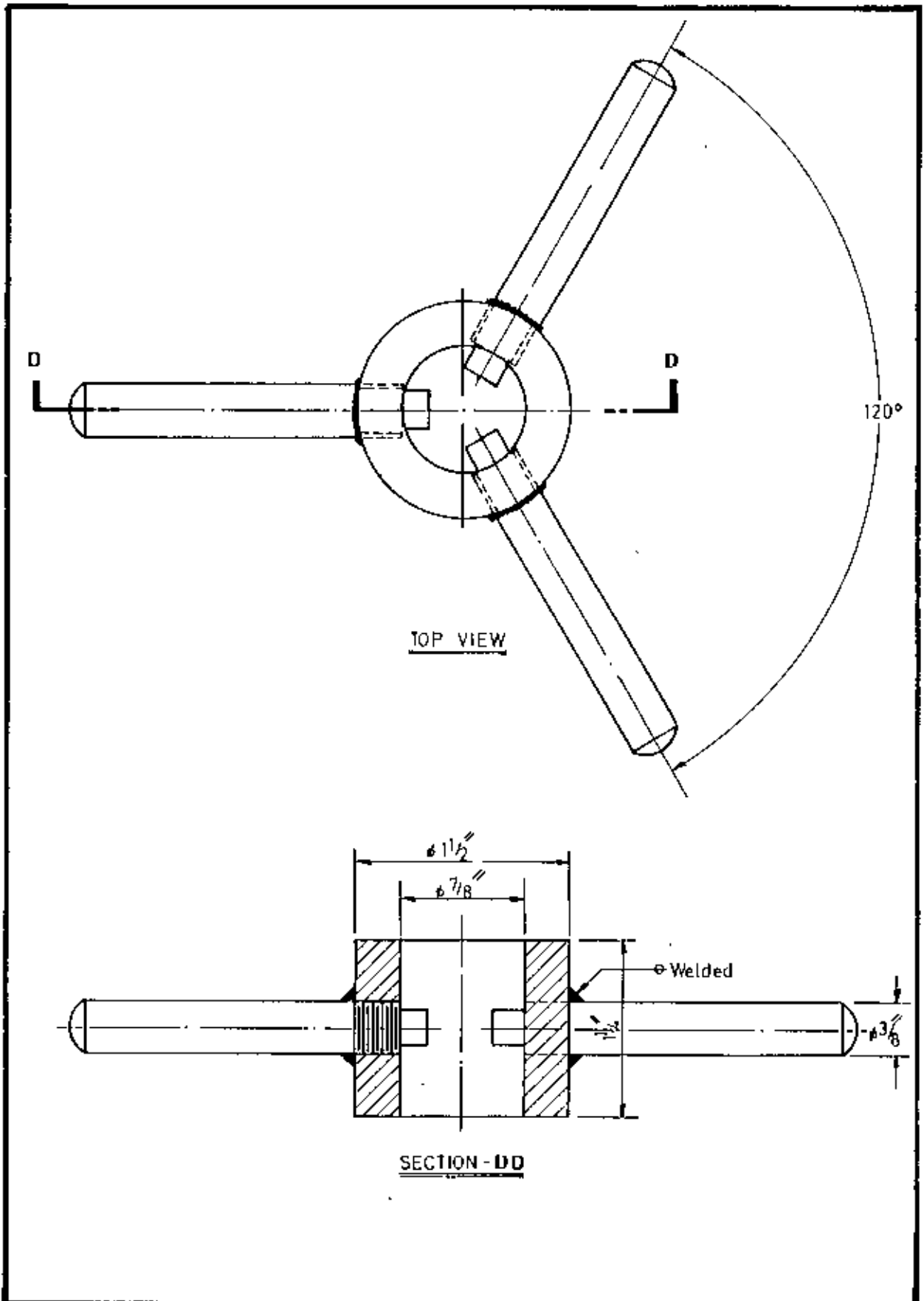


Fig. 4.4 : IMPELLERS WITH SPACERS SUB-ASSEMBLY

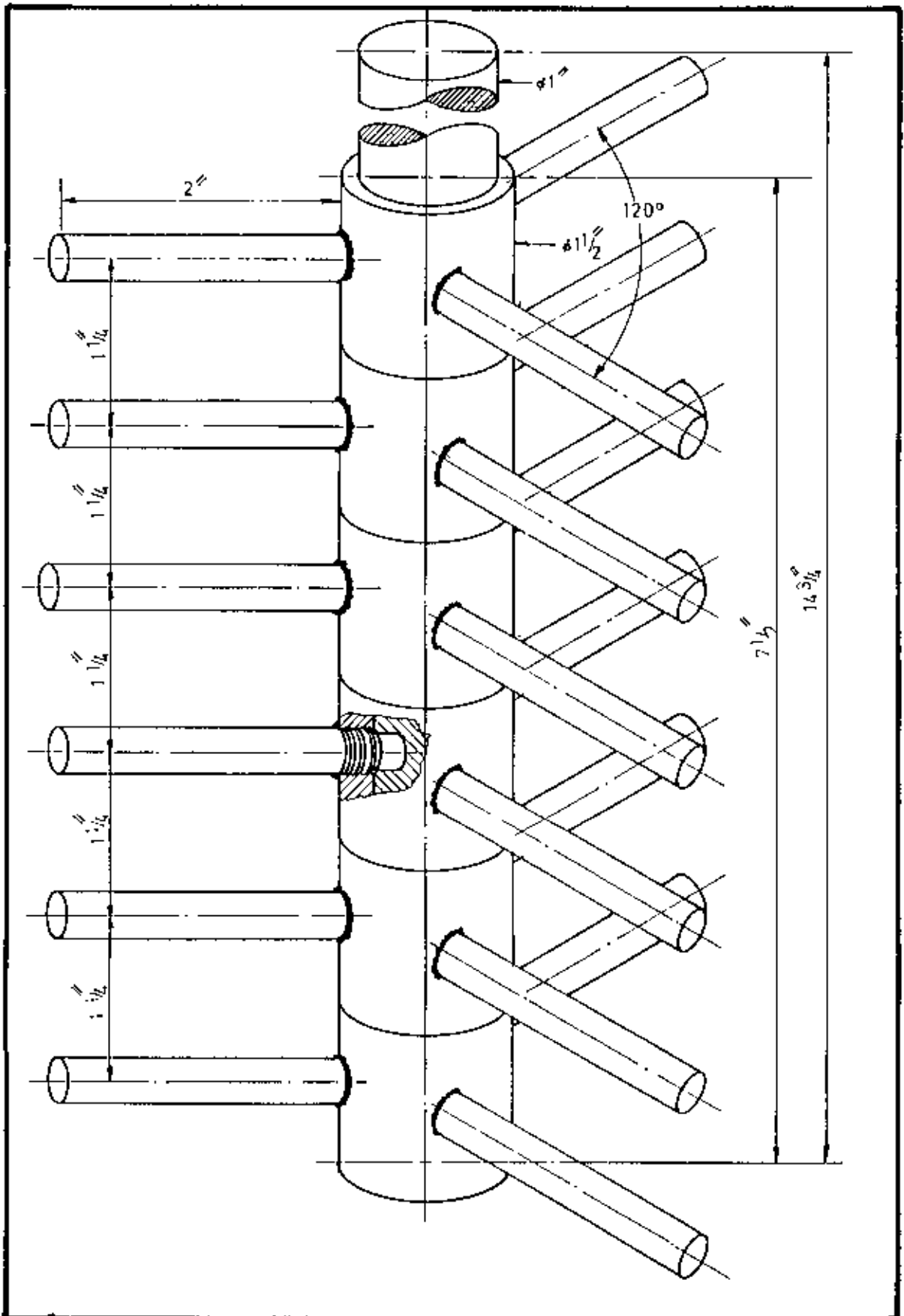


Fig.4.5 :- ISSOMETRIC DRAWING OF IMPELLER, SPACER & SHAFT COMBINATION

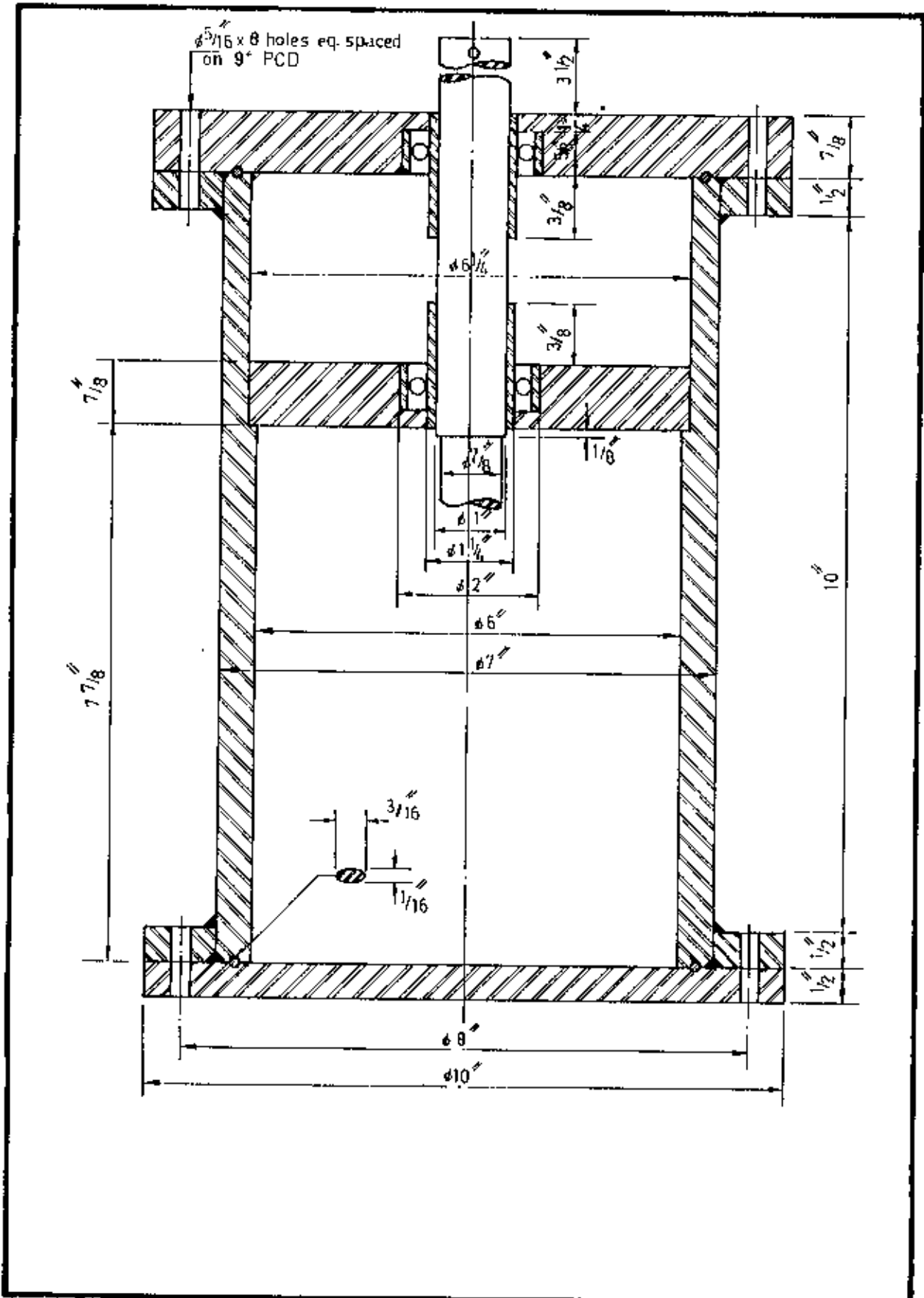


Fig. 4.6 - ATTRITOR CHAMBER ASSEMBLY AND DETAILS

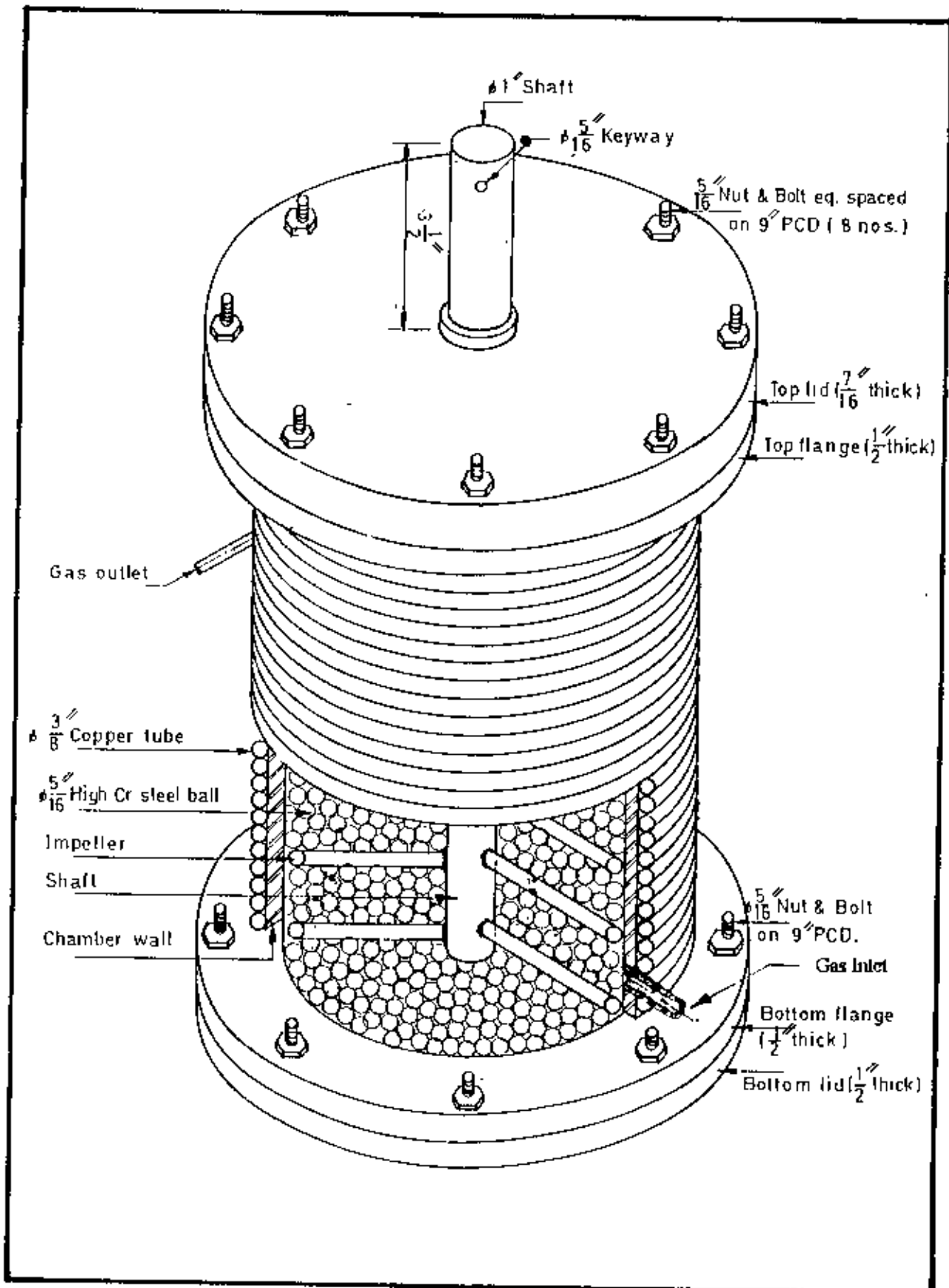


Fig.4.7: ATTRITOR

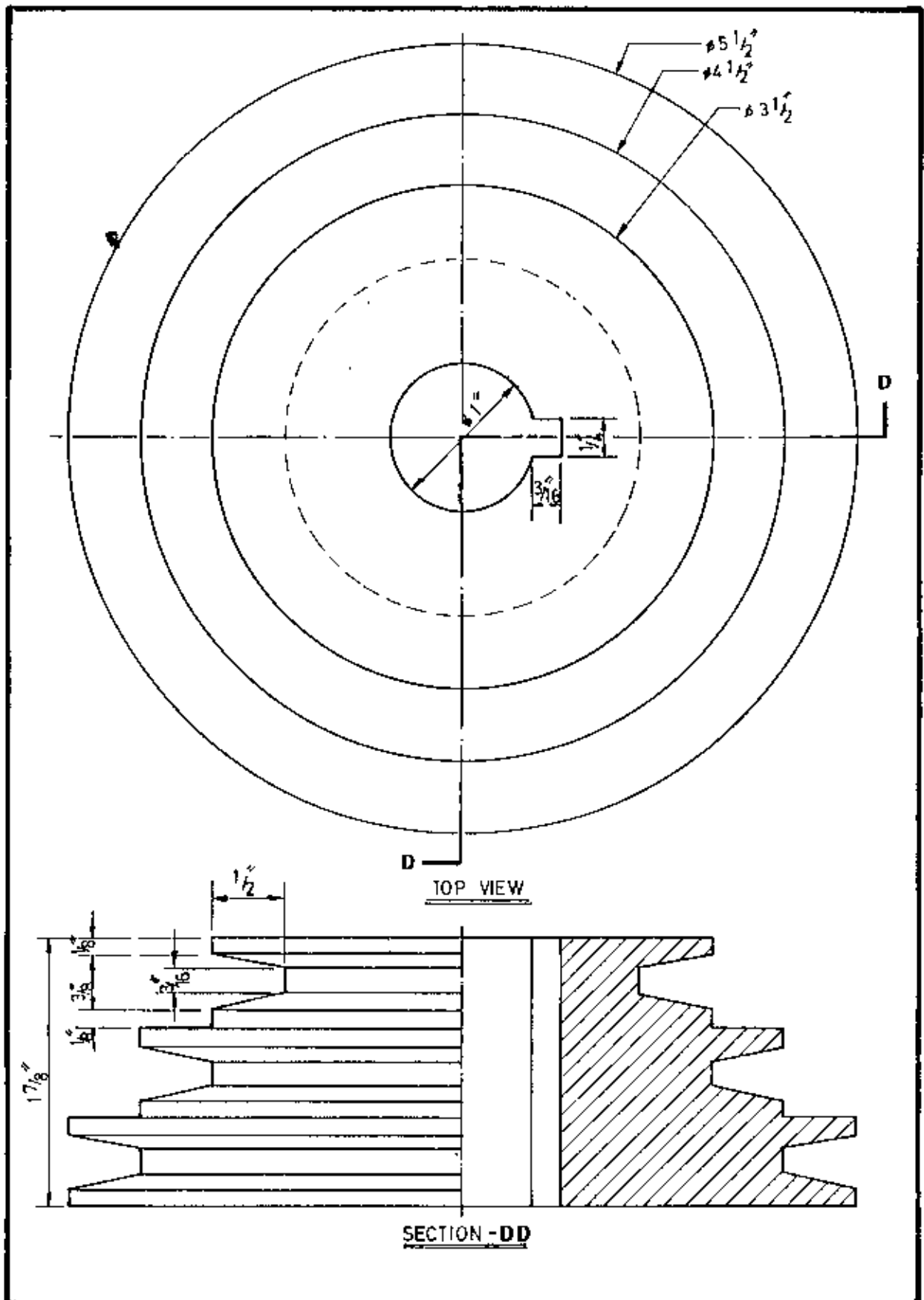
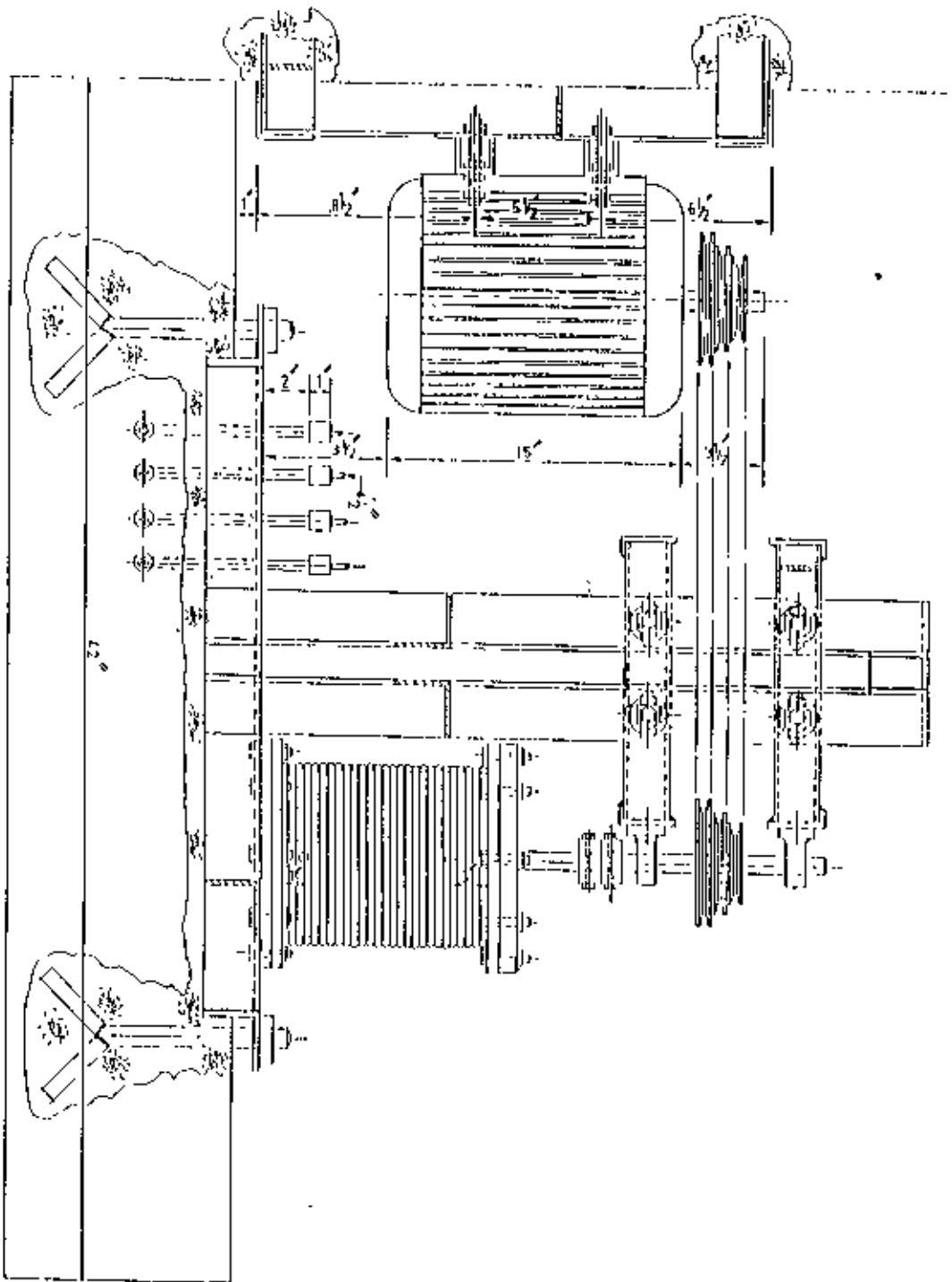


Fig.4.8-CAST ALLUMINIUM PULLEY



FRONT VIEW OF ASSEMBLY
FIG. 4 9A - ATRIPTOR LAYOUT

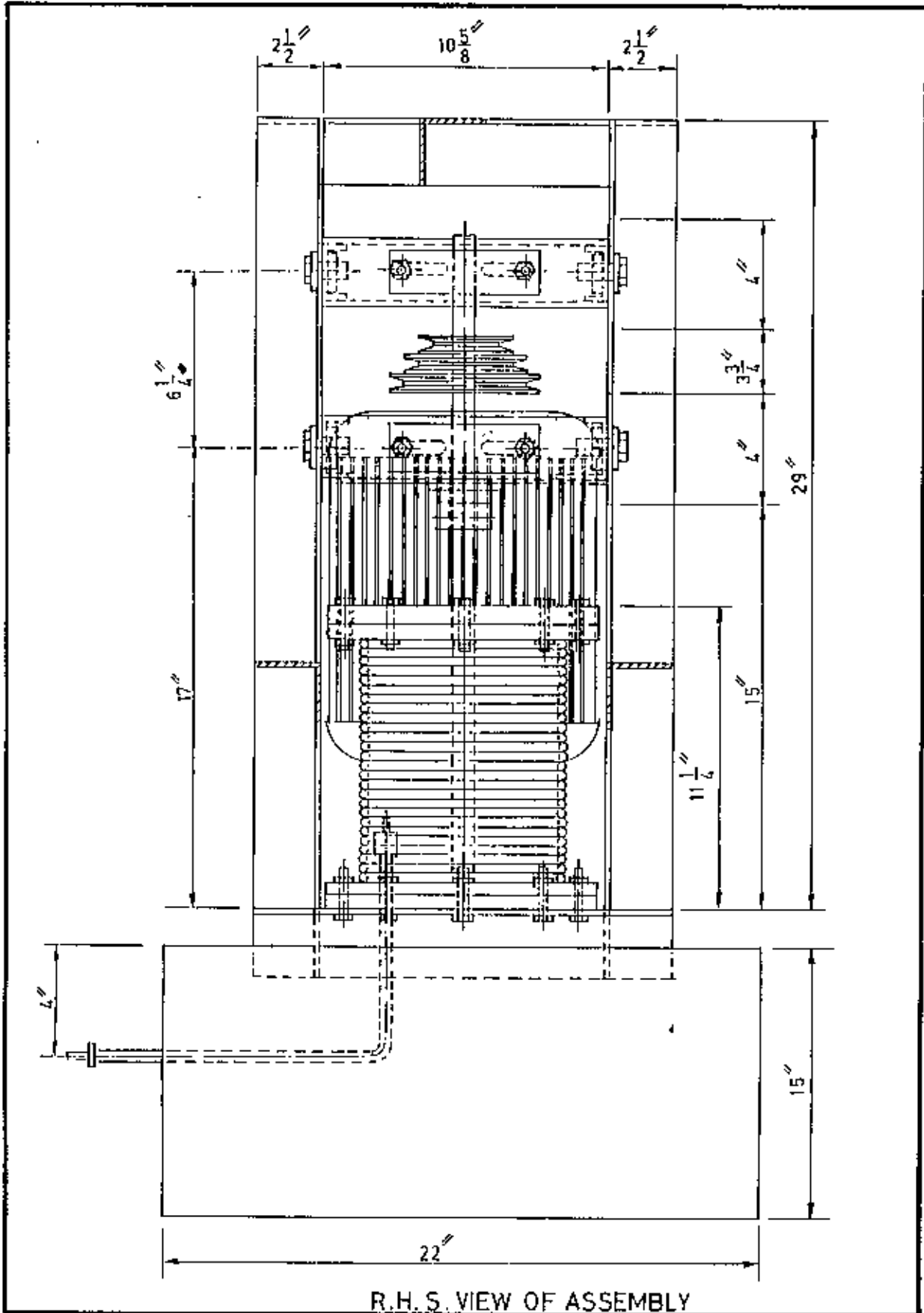


Fig. 4.9B:- ATTRITOR LAYOUT.

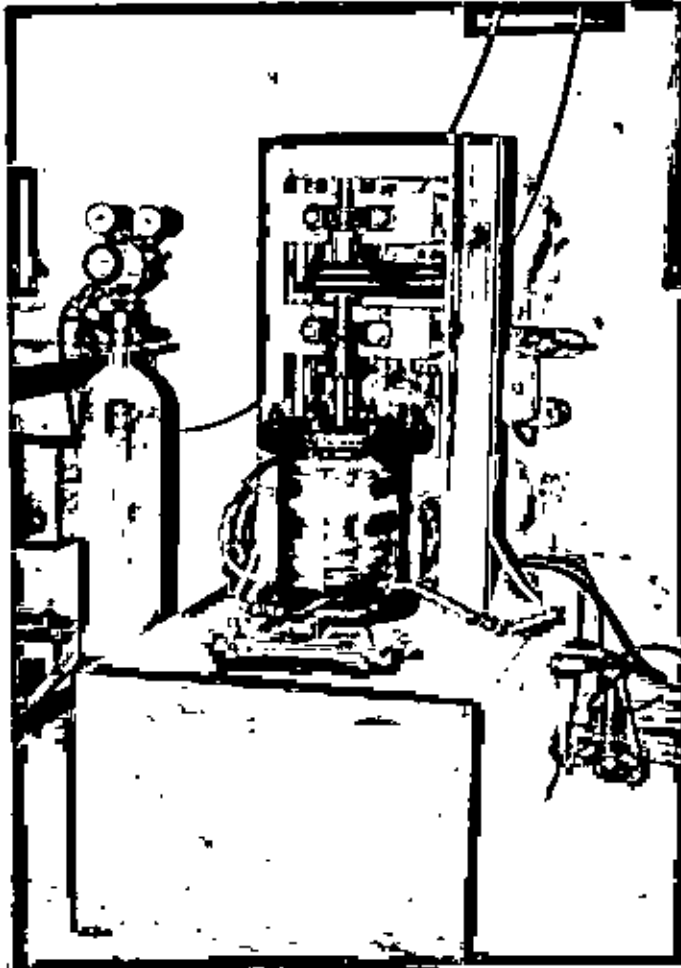


Figure P1 : PHOTOGRAPH OF AN ATTRITOR .

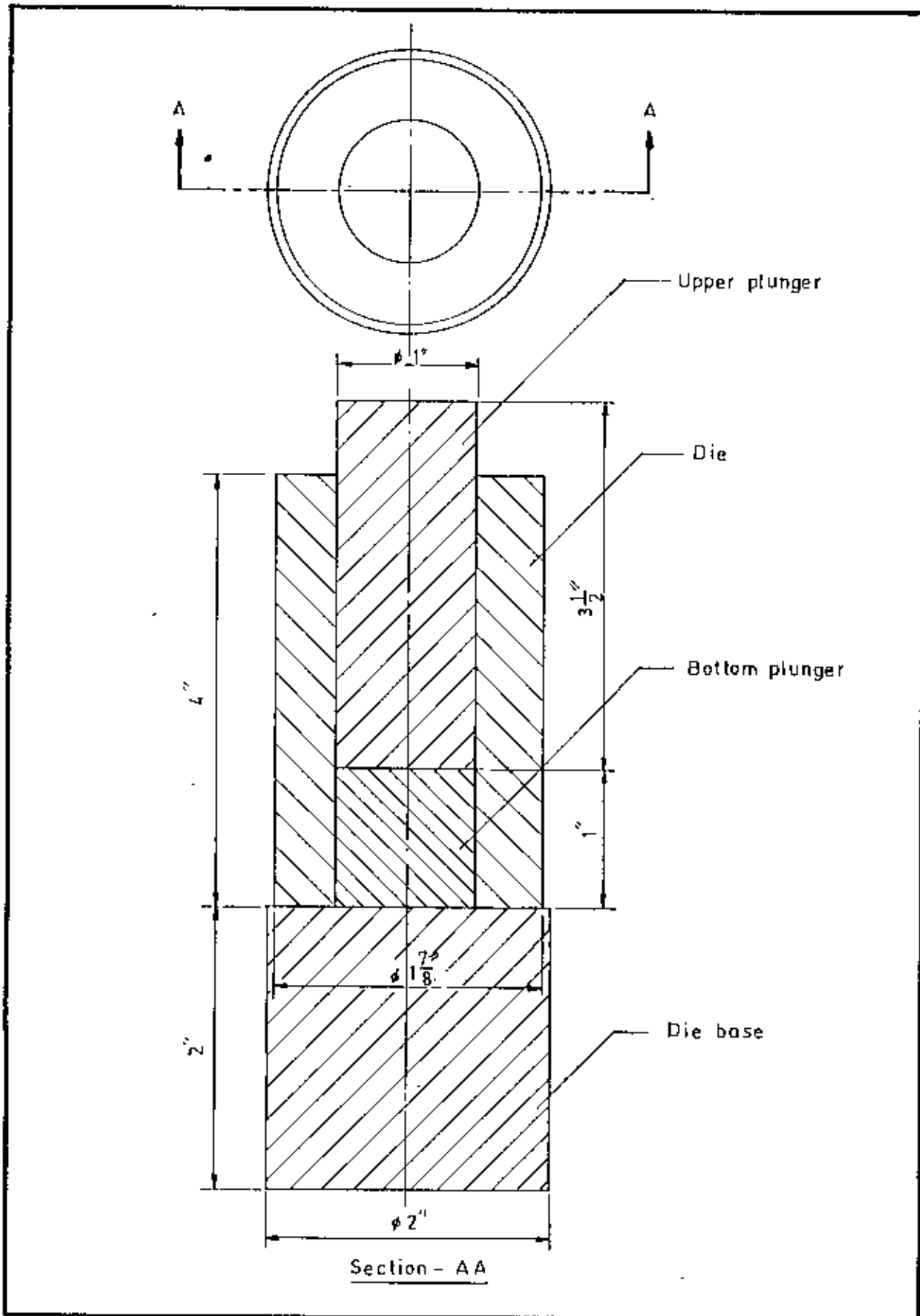


Fig. 10 - HOT PROCESSING DIE ASSEMBLY

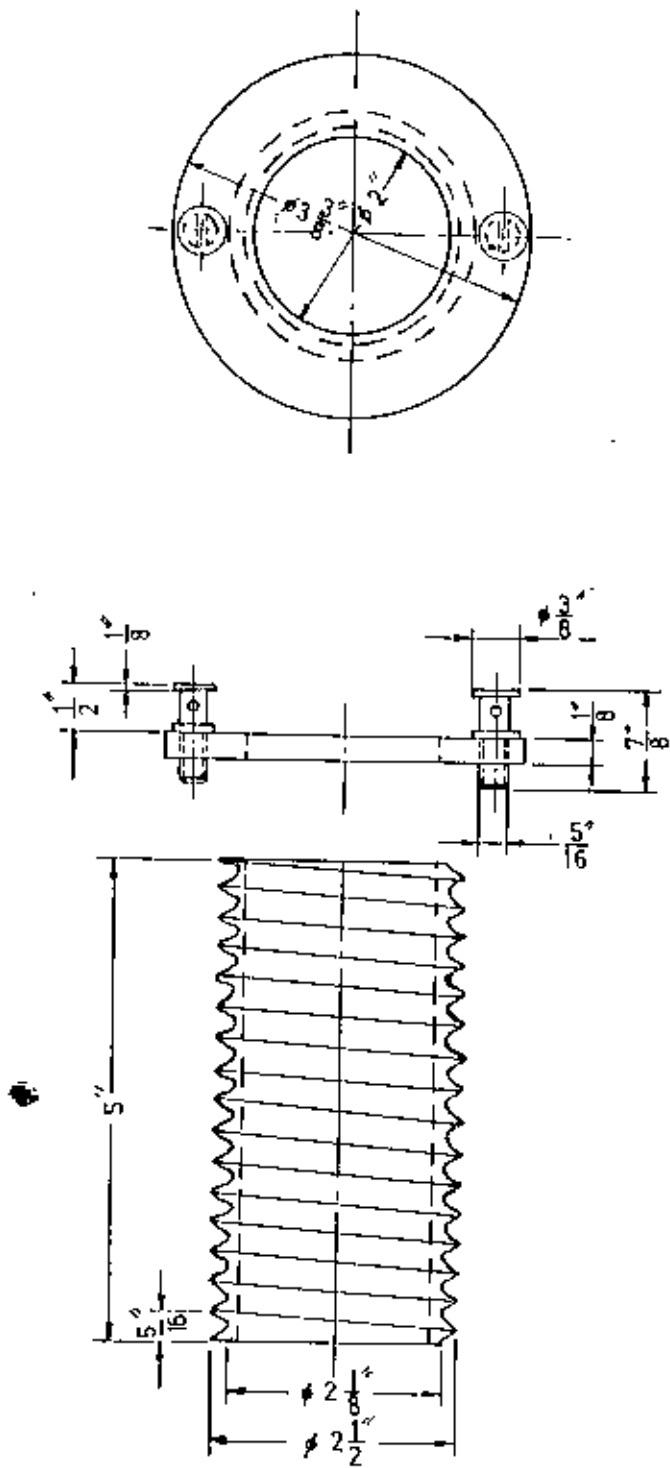


Fig 11 A : INNER REFRACTORY WALL AND ASBESTOS LID OF FURNACE

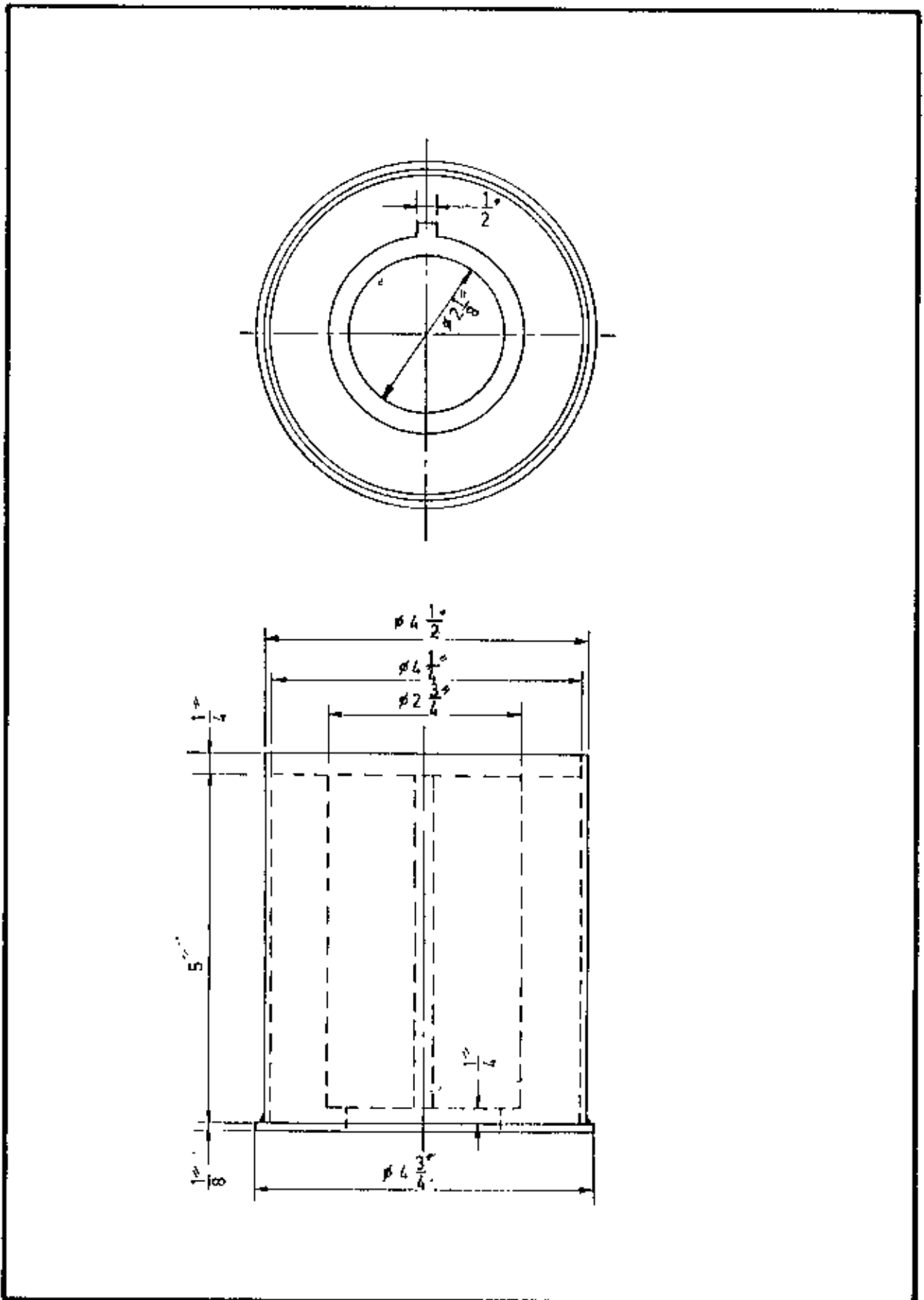


Fig. 11B : OUTER REFRACTORY WALL WITH STEEL SHELL OF FURNACE

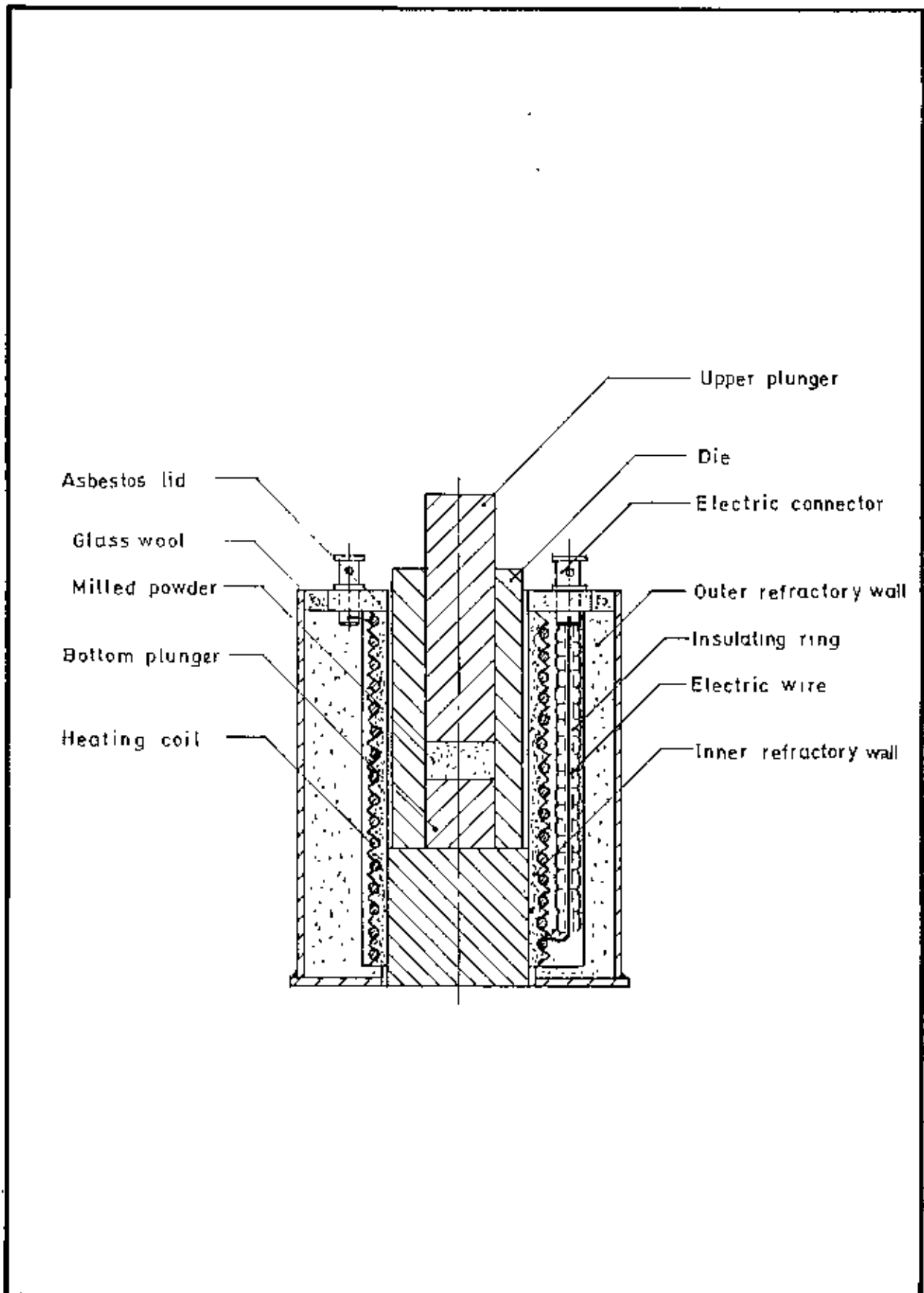


Fig. 4.12 : HOT PROCESSING DIE AND FURNACE ASSEMBLY

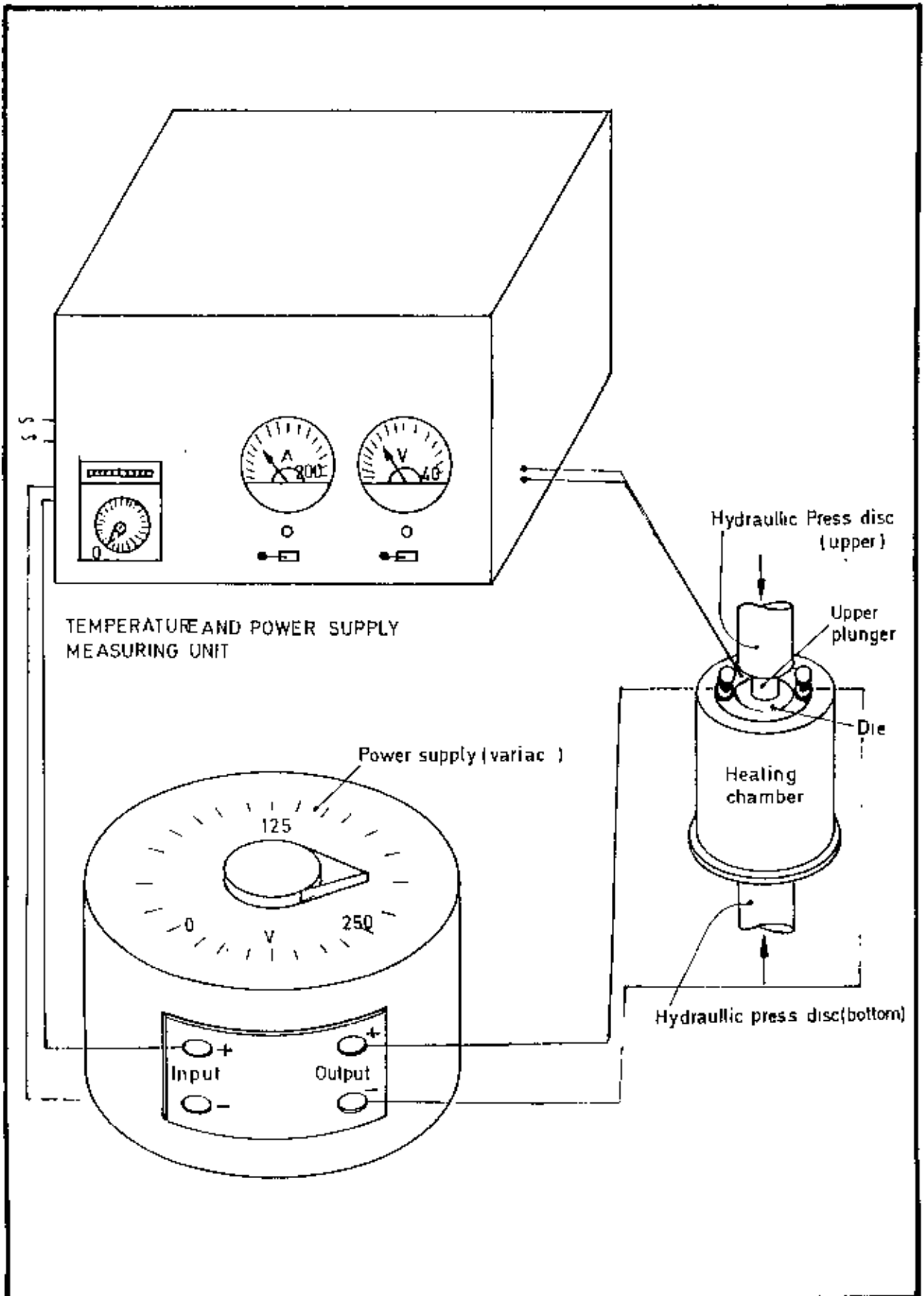


Fig.4.13 - HOT PRESSING UNIT

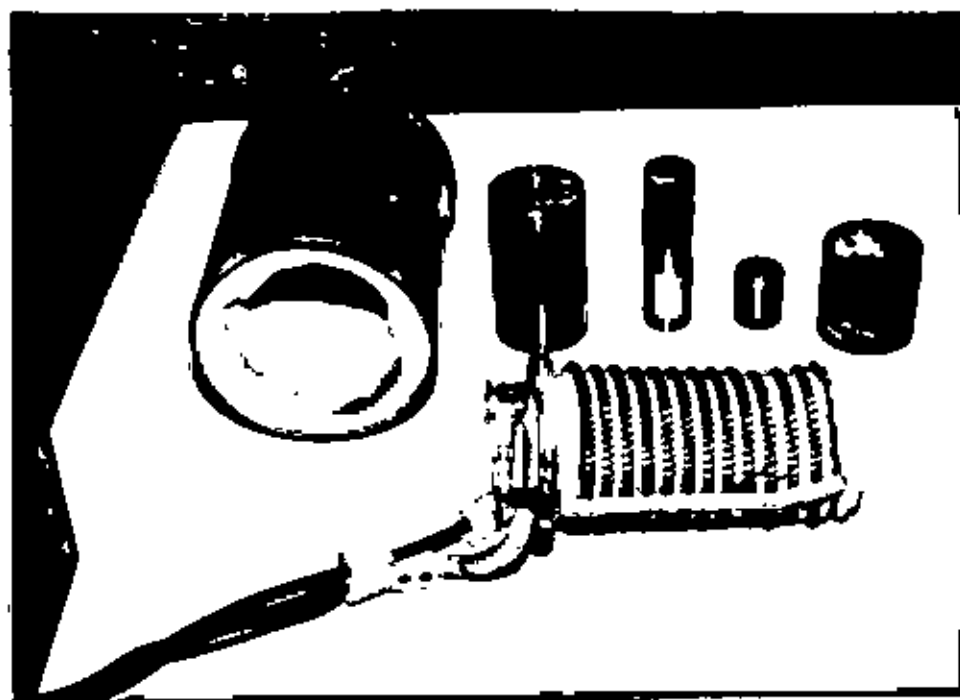


Figure P 2 : PHOTOGRAPH OF DIFFERENT PARTS OF A HOT PRESSING DIE.

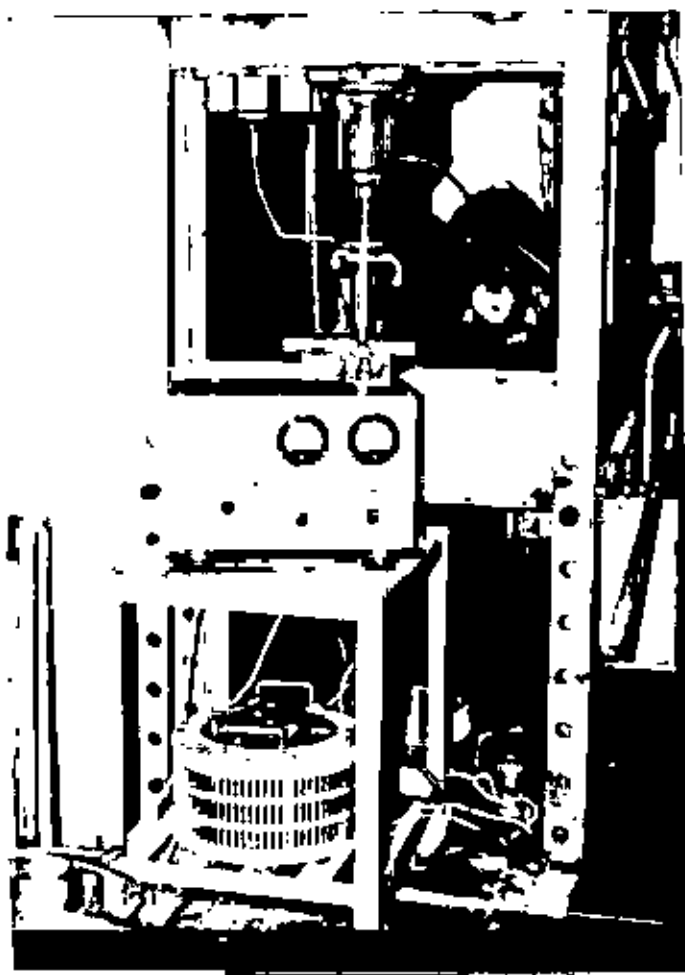


Figure P3 : PHOTOGRAPH OF A HOT PRESSING UNIT .

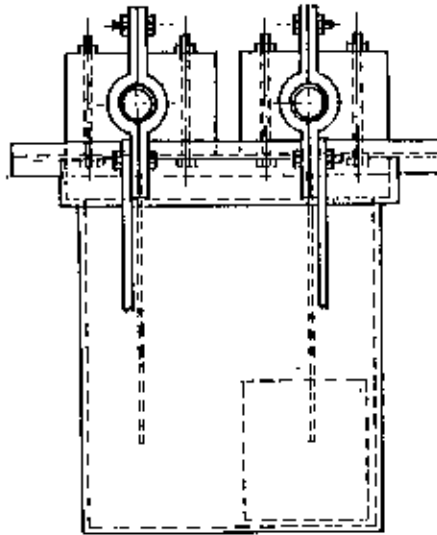


Fig. 4.14B:- L.H. SIDE VIEW OF POWDER PRODUCTION CELL

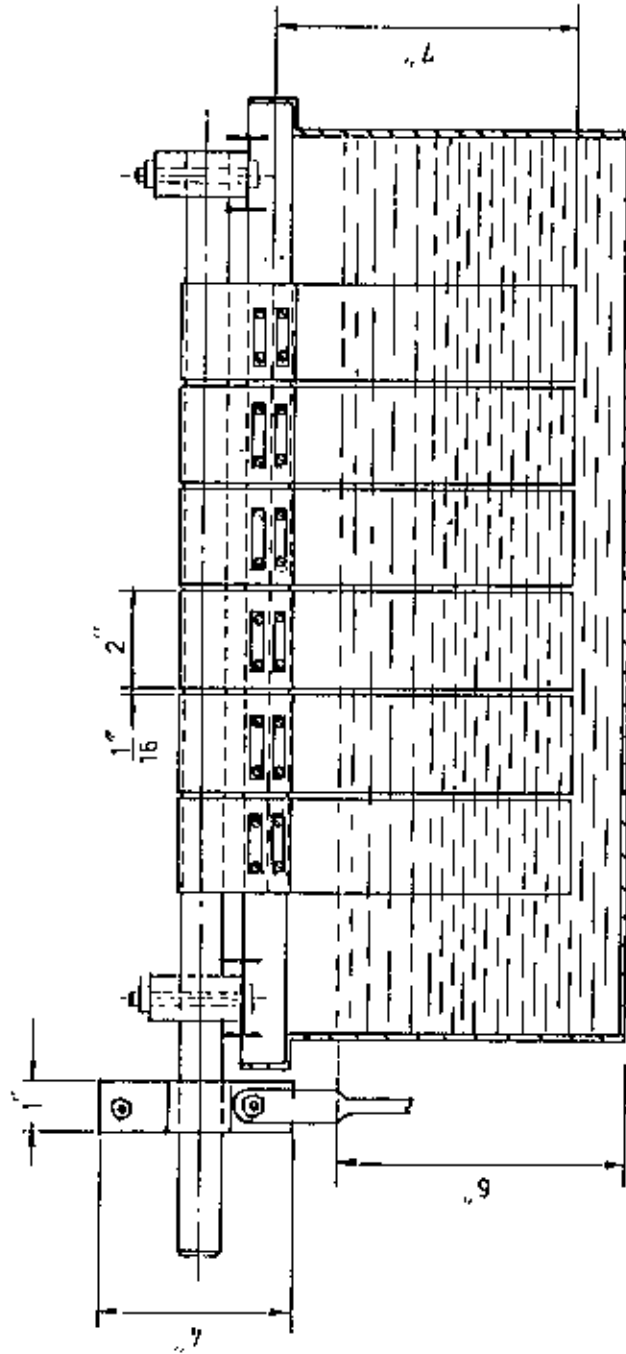


Fig. 4.14C : SECTION - A A POWDER PRODUCTION CELL

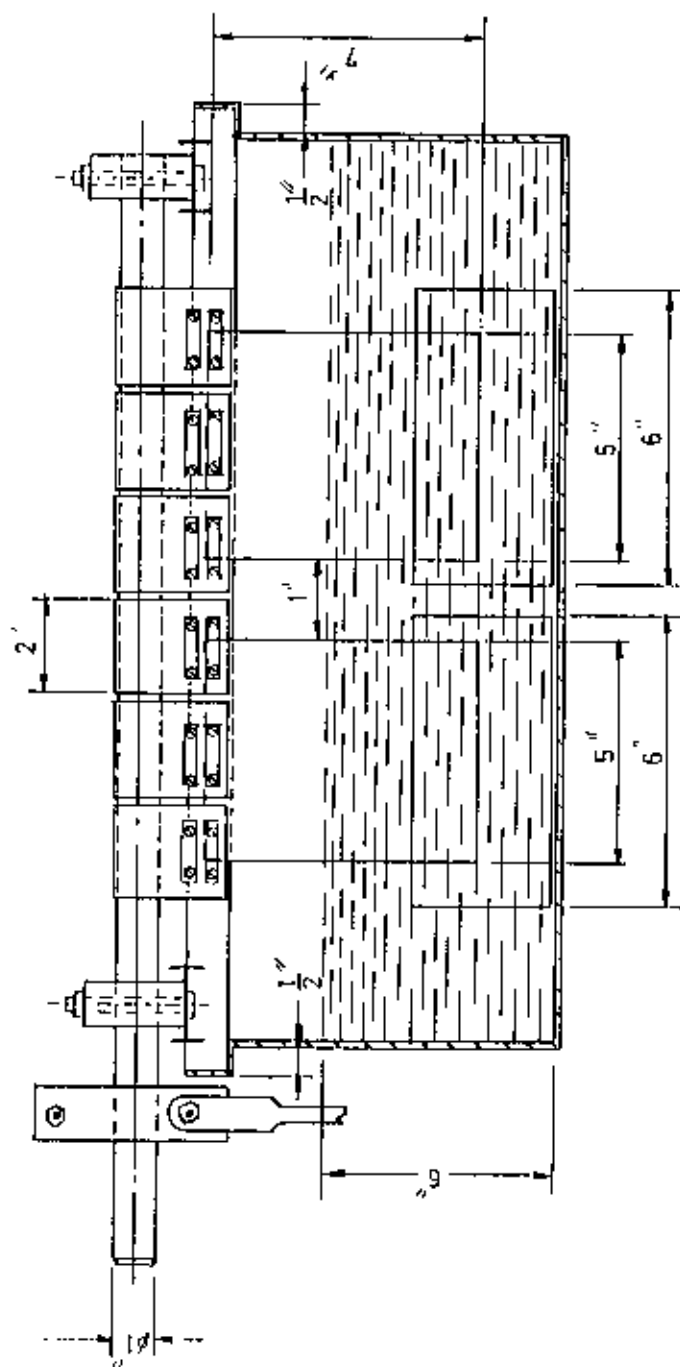


Fig. 4.14D : SECTION-BB POWDER PRODUCTION CELL

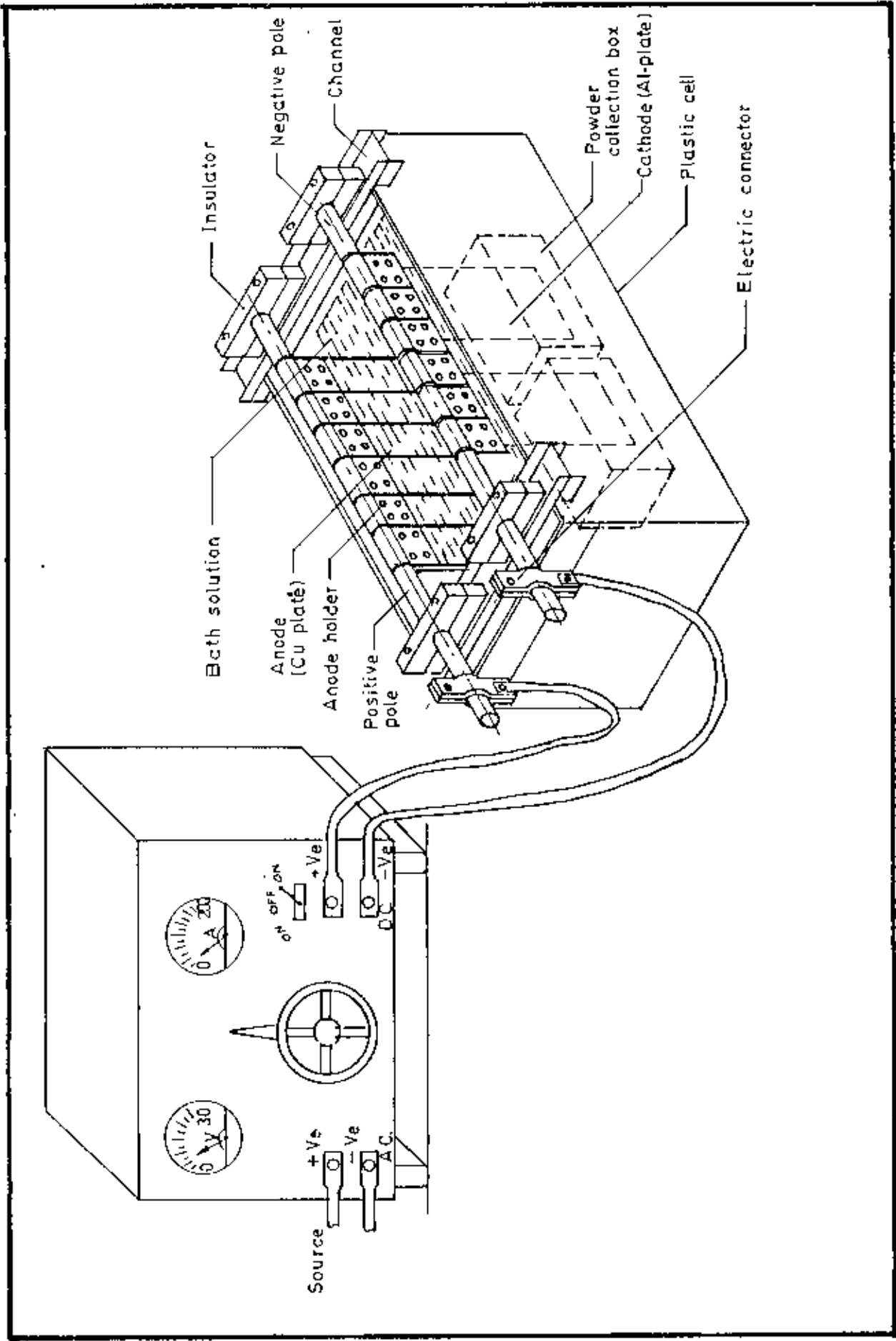


Fig. 4.15 : POWDER PRODUCTION UNIT LAYOUT

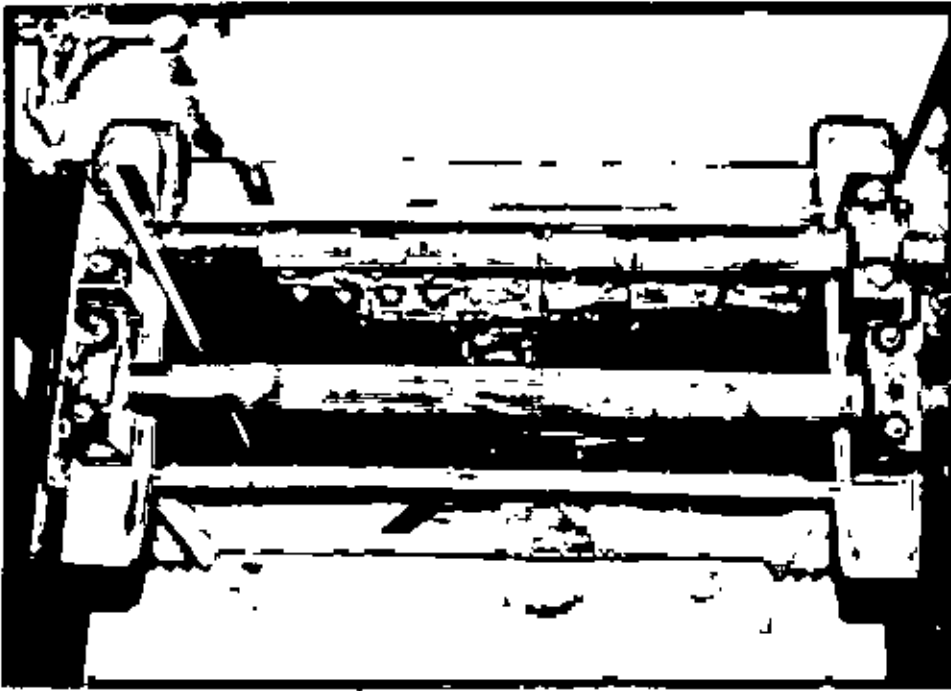


Figure P 4 : PHOTOGRAPH OF A POWDER PRODUCTION CELL (TOP VIEW).

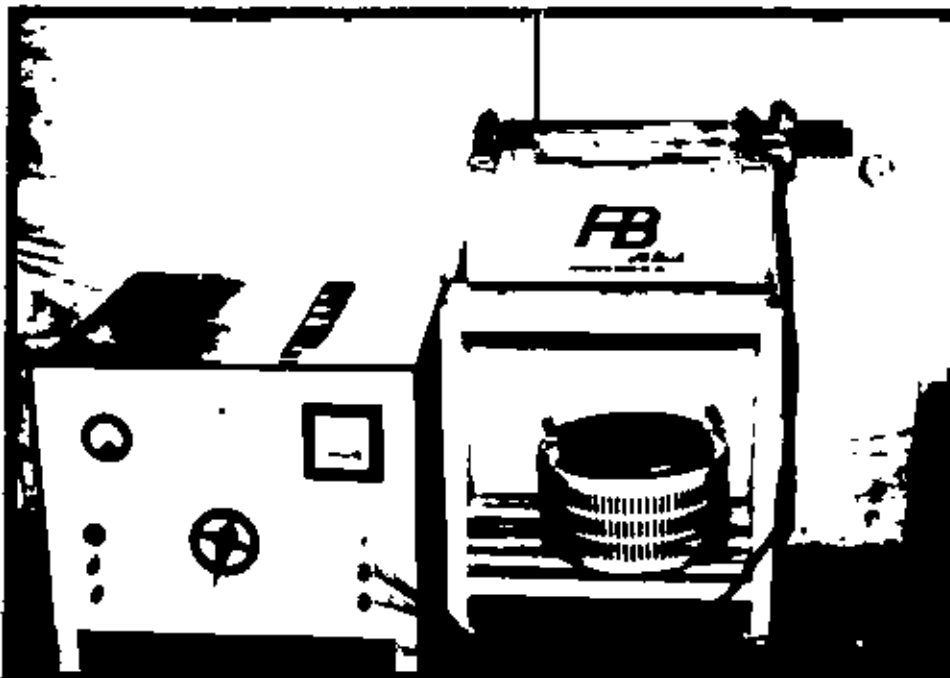


Figure P 5 : PHOTOGRAPH OF A POWDER PRODUCTION UNIT .

Experimental Methodology

Introduction :

The design, construction and operation of a mechanical alloying unit was one of the main goals at the start of this thesis. This was followed by experimentation on selected systems for study. A laboratory model mechanical alloying unit was designed and fabricated as already described. This was subsequently used to set process variables of mechanical alloying. A powder production cell was also designed and fabricated, so as to be able to produce metal powder (copper powder) locally, using commercial grade chemicals. In addition an existing pressing unit was modified to carry out sintering with simultaneous heating of milled powder.

A simple alloy system 70 wt.%copper-30 wt. % zinc was chosen to facilitate easy interpretation of the results obtained under different experimental condition. In this chapter the production of copper powder, characterisation of the powder particles, milling of the charge powder, X-ray diffraction of initial, milled (at different interval of processing time), hot-pressing of milled powder, study of microstructure of the initial, milled and consolidated powder have been described. In order to relate the mechanical property of the alloy with the micro structural refinement in the course of mechanical alloying micro hardness of consolidated specimen (hot pressed) was recorded.

Production of Powder :

The copper powder used in this experiment was produced by adopting the principle of reverse electroplating. The process involved the use of anodes made of commercial grade copper sheet and cathodes of highly polished aluminium sheet. As the d.c. current is supplied, copper anodes corroded i.e. copper atoms each releasing two electrons transform to positive copper ion which is attracted to the cathode. When the copper ion comes in contact with the cathode it consumes two electrons from the latter and is converted into copper atom. Huge number of such copper atoms when coalescence on the cathode, they form powder particles in the form of sponge. This spongy deposit was stripped from the cathode and was washed by stirring in distilled water by means of a magnetic stirrer to remove all the sulphate ions and last traces of sulphuric acid. This electrolysis process to produce copper powder is really electro-refining in nature and there is considerable purification as anode material is transferred to cathode. Reaction involved for copper powder production are :

Anode reaction: $\text{Cu} \rightarrow \text{Cu}^{2+} + 2\text{e}^-$, **Cathode reaction:** $2\text{e}^- + \text{Cu}^{2+} \rightarrow \text{Cu}$.

As already mentioned, the starting material was commercial grade copper sheet. The electrolytic cell consisted of six anodes of copper sheet, two cathodes of highly polished aluminium sheet and an electrolyte consisting of an aqueous solution of copper sulphate and sulphuric acid. Current passing through the cell caused copper to be deposited at the cathode. Depletion of metallic ions in the immediate area of the cathode caused a migration of ions by diffusion. The bath was intermittently supplied with metal ions from the anode materials and intermittent supply of sulphuric acid. Other particulars of the conditions of this experiment are given below:

Voltage (D.C) : 6-7 Volts.

Current : 5 Amp / inch.² (Total 200 Amp.).

Temperature : 60°C.

Composition of the Bath (Electrolyte):

10% CuSO_4 (weight)

16% Free H_2SO_4 (Weight)

74% H_2O (Volume)

Characterisation of Powder:

Characterisation of powder samples both initial copper and zinc powder and milled 70 wt. %-30wt. % powder mixture were studied by means of sieve analysis and optical metallography.

X-ray diffraction:

The aim of the X-ray diffraction study was to identify the presence of copper and zinc species at different intervals of milling time. The progress of mechanical alloying was evaluated by the determination of lattice parameters and by evaluation of integral peak intensities.

$$\text{Lattice parameter, } a = \frac{\sqrt{h^2 + k^2 + l^2}}{2 \sin \theta}$$

Here, hkl = Miller indices,

λ = Wave length.

θ = Diffraction angle.

The particulars of X-ray diffraction pattern recording are given below.

Target :	Copper,	Voltage :	30 K.V.,
Filter :	Nickel,	Current :	20 m A.,
Scanning Speed :	2°.,	Chart Speed :	10.,
Full Scale :	2x10 ³ C.P.S.,	Range :	30°-100°.

Hot pressing of milled powder :

The aim of hot pressing and to identify the micro structure of the alloy in a solid state. The same was carried out using fabricated hot pressing unit. The milled powder was put in the die and compaction was performed by means of a hydraulic pressure. The bottom plunger remained dead while the upper plunger moved under pressure. During pressing, heating by means of electrically heated furnace set rounding the die and plunger (both made of stainless steel). The constant temperature was recorded by means of thermocouple and the temperature as controlled by means of a variac and 'ON-OFF' control system. The all other particulars of hot pressing are given below:

Pressure : 12 tsi

Temperature : 280°C.

Time : 6 hrs.

Powder supply input : 230 Volts, 50 Hz, Single Phase a. c.

Powder supply output : (Input of furnace). 140 volts, 2 Amp single phase a. c.

Optical metallography :

The consolidated initial powder, milled powder at different time of processing and specimen after hot pressing were investigated to reveal structural refinement with the

progress of the mechanical alloying. Standard methods were used in specimen preparation for optical metallography. H_2O_2 and 25% NH_4OH in the ratio 1:1 mixture was used as etching reagent. The microstructures were observed and recorded by optical metallography.

Powder milling:

A binary system consisting 70wt. % copper and 30wt. % zinc was milled for different time interval in a locally designed and fabricated attritor. The all other particulars of milling are given below.

The high-chromium steel ball :	5/16" (in diameter)
The steel ball hardness:	56-57.6 C (Rockwell Hardness).
The size of powder :	Copper-AFS No.244.867 and AFS No 261.292., Zinc-AFS No. 292.439.
Weight of powder mixture :	100 gm.
Process controlling agent :	Methanol (95%), 3% Mass of powder mixture.
Ball to Powder weight ratio :	20 : 1
Speed of attrition :	900-2100 rpm.

Attrition was carried out in dry hydrogen (reducing) atmosphere (Inert atmosphere is preferable) and the attritor chamber was cooled externally by circulating water through a copper tubing system.

Measurement of micro-hardness :

Micro-hardness of different powder species and phases in the consolidated specimen were measured by means of a micro-hardness tester of 'Shimadzu 341-64278 Model' based on the following principle,

$$HV = 1854.4 P/d^2.$$

Where

HV is the Vickers Hardness,

P is the Load (gm),

d is the mean diagonal of indentation (μm).

The load applied in this experiment was of 100gm.for a duration of 10 sec.

Results and Discussions.

A laboratory model high energy ball mill (attritor), a powder production unit based on the principle of reversed electroplating and a hot pressing unit have been designed and fabricated locally. The satisfactory operation of the aforesaid units have been established.

The laboratory model attritor has been used for mechanical alloying of 70 wt % copper-30 wt. % zinc system. The progress of mechanical alloying of the alloy system have been investigated by means of X-ray diffraction, sieve analysis and optical metallography. To evaluate the mechanical properties micro-hardness of the phases present in consolidated samples were also determined.

Simultaneous considerations of the aforesaid investigations offer an explanation of structural refinements occurring during mechanical alloying. A comparative picture of the effect of initial particle size on the progress of mechanical alloying and the effectiveness of different zones of an attritor for alloying a particular alloy system have also emerged from this study.

Calculation of lattice parameters from x-ray diffraction patterns obtained for different processing time of the alloy system, show that the lattice parameter of copper increases while that of the zinc remain constant which indicates the fact that during mechanical alloying zinc atoms preferentially enter into the copper lattice; not the copper atom into the zinc lattice. Values of the diffraction angles, lattice parameters of

copper, copper-zinc alloy and zinc respectively and mean powder particles sizes obtained for different time ranges during the progress of mechanical alloying are given in table 6.1.

After a short period of milling (100 sec.) an increased profile widths of copper and zinc diffraction intensity peaks have been observed as represented by curve B in Fig. 6.1. Optical metallographs also revealed the well known fine layered lamellar structure. As the diffraction angles of copper and zinc are not changed to a considerable amount, no alloying has occurred. Profile widening is caused only by lattice defects which in turn is caused by severe deformation due to impact as well as frictional force between ball-powder-ball collision, ball-powder-attritor wall, ball-powder-impeller arms. Small mean powder particle sizes as well as subgrain refinement and increasing dislocation density due to severe deformation is the characteristics for partition (continuous deformation, welding, fracturing and rewelding) period of mechanical alloying. Particles with decreased average particle size AFS 299.338 (table 6.1) and the metallographs (as represented in Fig. 6.12) after 100 sec. milling supports this period of mechanical alloying. However, if line profiles were not widened there were no partition period during the course of mechanical alloying process.

X-ray diffraction pattern as curve C in Fig. 6.1 of sample milled for 1000 sec. milled samples revealed the asymmetric line profiles indicating that the alloying period has already been started. This asymmetry can be explained by local differences of copper lattice parameters due to the diffusion of zinc into copper followed by solid solution of zinc in copper. Solid solution of zinc in copper causes changes of copper lattice parameter. Continued milling yielded noticeable progress of alloying, caused by zinc concentration gradients in the copper-zinc alloy phase, increasing profile width of the alloy patterns as represented by curve C in Fig. 6.1.

As shown in Fig. 6.4 the lattice parameter of zinc remains constant where as the intensity of zinc-peaks decreases (Fig. 6.5), with increasing of milling time. This decrease of intensity is caused by the diffusion of zinc into copper to perform mechanical alloying, which results in a reduction of the amount of not-alloyed zinc. As zinc lattice parameter is constant there is no solid solution of copper in zinc (otherwise the zinc diffraction angle must change according to Vegard's Law). Mechanical alloying of copper and zinc is achieved only by diffusion of zinc into copper and solid solution of zinc atoms in the copper matrix form the copper-zinc

Table 6.1 Copper, zinc diffraction angles, lattice parameter of copper and zinc and mean particle size of mechanical alloyed copper 70% wt.- 30%wt. zinc powder blend.

Elements (hkl) Time	Diffraction Angle ($2\theta^\circ$)						Lattice Parameter (\AA)						Particle size
	Copper			Zinc			Copper			Zinc			AFS No.
	(111)	(200)	(220)	(002)	(101)	(104)	a_{111}	a_{200}	a_{220}	c_{002} a_{002} c/a	c_{101} a_{101} c/a	c_{104} a_{104} c/a	
0 (Sec)	43.20	50.30	74.00	36.18	43.10	89.60	3.6276	3.6283	3.6235	4.9660	4.9660 2.6744 1.8569	2.6741 4.9660 1.8571	Cu:244.867 Zn:292.439
100 (Sec)	43.10	50.20	73.80	36.00	43.10	89.60	3.6356	3.6351	3.6320	4.9660	4.9660 2.6744 1.8569	2.6741 4.9660 1.8571	299.338
1000 (Sec)	43.00	50.00	74.00	36.00	43.00	89.60	3.6437	3.6487	3.6235	4.9660	4.9660 2.6744 1.8569	2.6741 4.9660 1.8571	283.066
1500 (Sec)	42.40	49.60	73.80	36.20	43.20	89.60	3.6928	3.6762	3.6320	4.9660	4.9660 2.6675 1.8608	4.9660 2.6789 1.8527	-
1750 (Sec)	42.00	49.60	72.80	-	43.20	-	3.7260	3.6748	3.6748	4.9660	4.9660 2.6675 1.8608	-	276.140
Ideal Condition							$a_{Cu} = 3.6150$			$c_{2n} = 4.9-470$ $a_{2n} = 2.6650$ c/a = 1.8560			

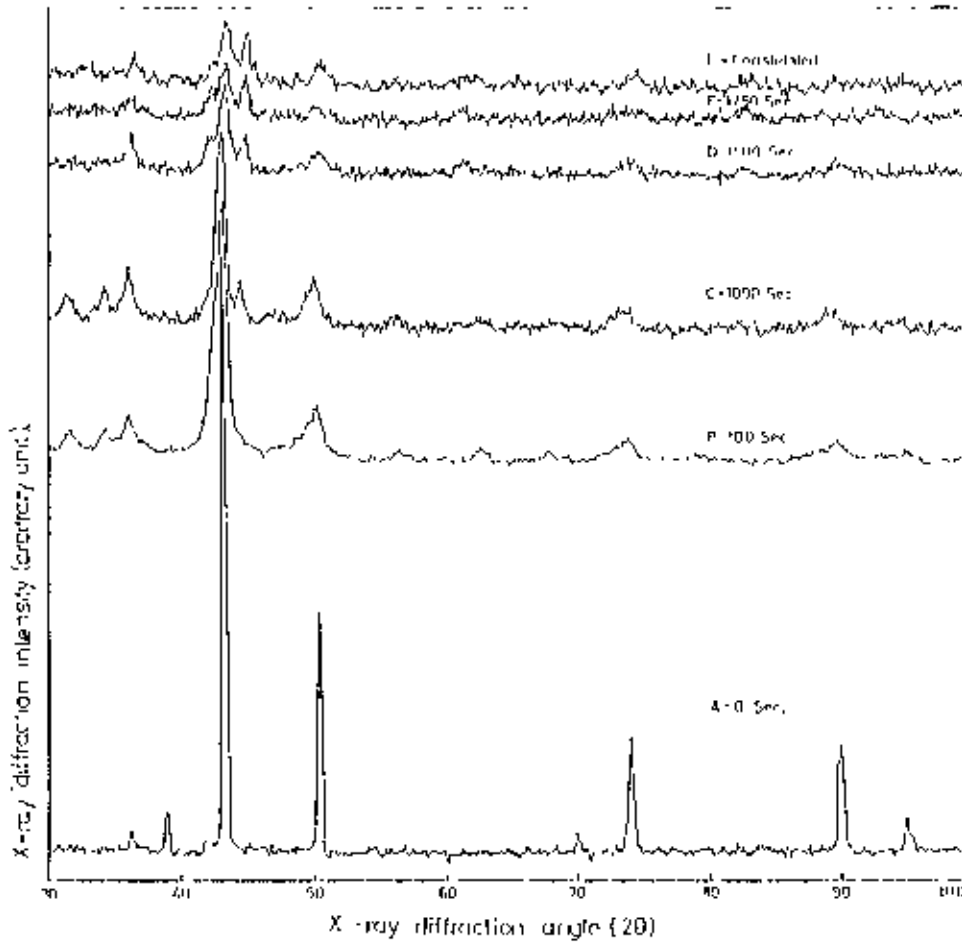


Figure 6.1: X-ray diffraction pattern for mechanical alloyed copper 70% wt. (AFS No. 244.867)-zinc 30% wt. (AFS No. 292 439) powders processed in attritor for different time interval.

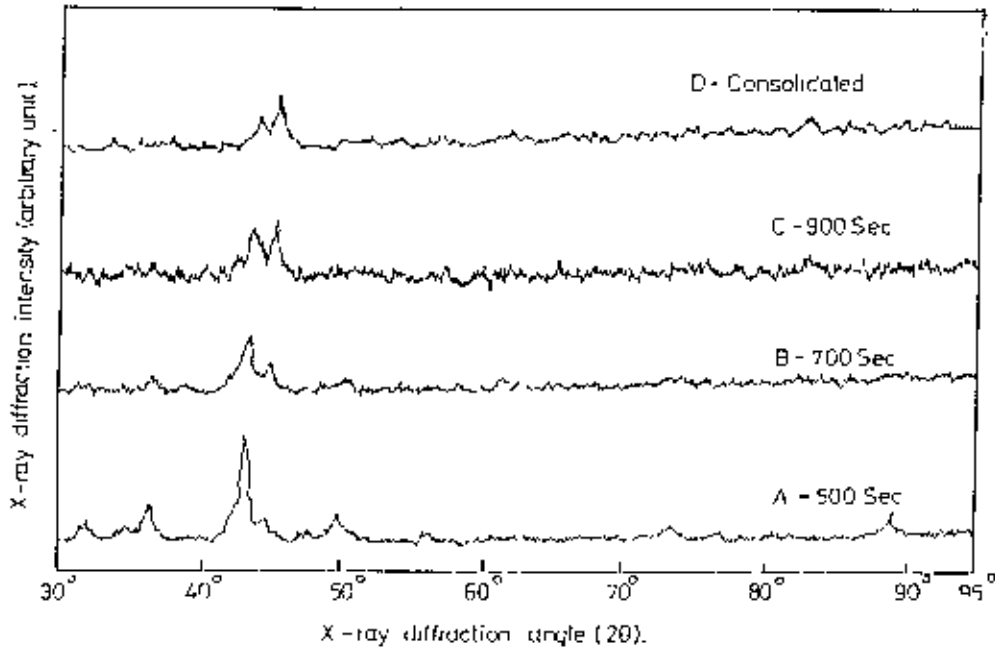


Figure 6.2 X-ray diffraction pattern for mechanical alloyed copper 70% wt. (AFS No. 261 292)-zinc 30% wt. (AFS No. 292 439) powders processed in attritor for different time interval

alloy. Giving attention to the lattice parameter, it has been observed (Fig. 6.3) that there is a sharp increase of the lattice parameter of copper after milling for 1000 sec. whereas at the initial stage there is a slow change in lattice parameter indicating a slow rate of alloying.

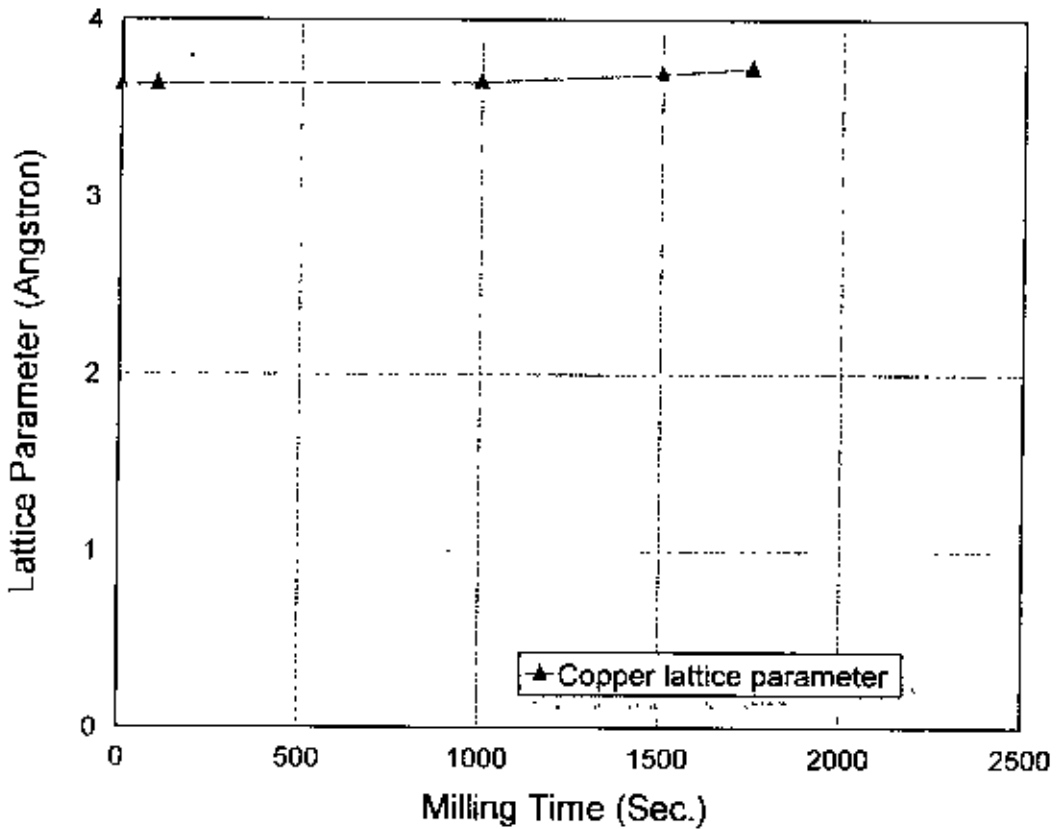


Fig. 6.3 : Change of lattice parameters of copper with the progress of mechanical alloying of 70%wt.copper- 30%wt.zinc system. Lattice parameter of copper increases with the increase of milling time.

After milling for 1750 sec. the zinc peaks have disappeared as represented by curve E in Fig. 6.1. At this stage X-ray patterns of milled samples indicate only interference of copper-zinc alloy as amorphous phase.

During the first short period (100 sec.) it has been observed that there is an increase of lattice defects due to deformation (Fig. 6.1. Curve B) The powder particle size firstly increases and then decreases with the progress of milling, so the structural refinement is mainly caused by repetitive particle deformation, flattening, welding and fracturing. It is reasonable therefore to observe an increase and then a decrease in powder particle size (table 6.1). On the other hand alloying which starts by diffusing of zinc into copper

is a thermally activated process. Therefore mechanical alloying of copper and zinc has concerned as a consequence of the creation of thin layered composite structure to achieve an interfacial area followed by diffusion, which is aided by temperature rises due to dissipation of kinetic ball energy (impact and collision).

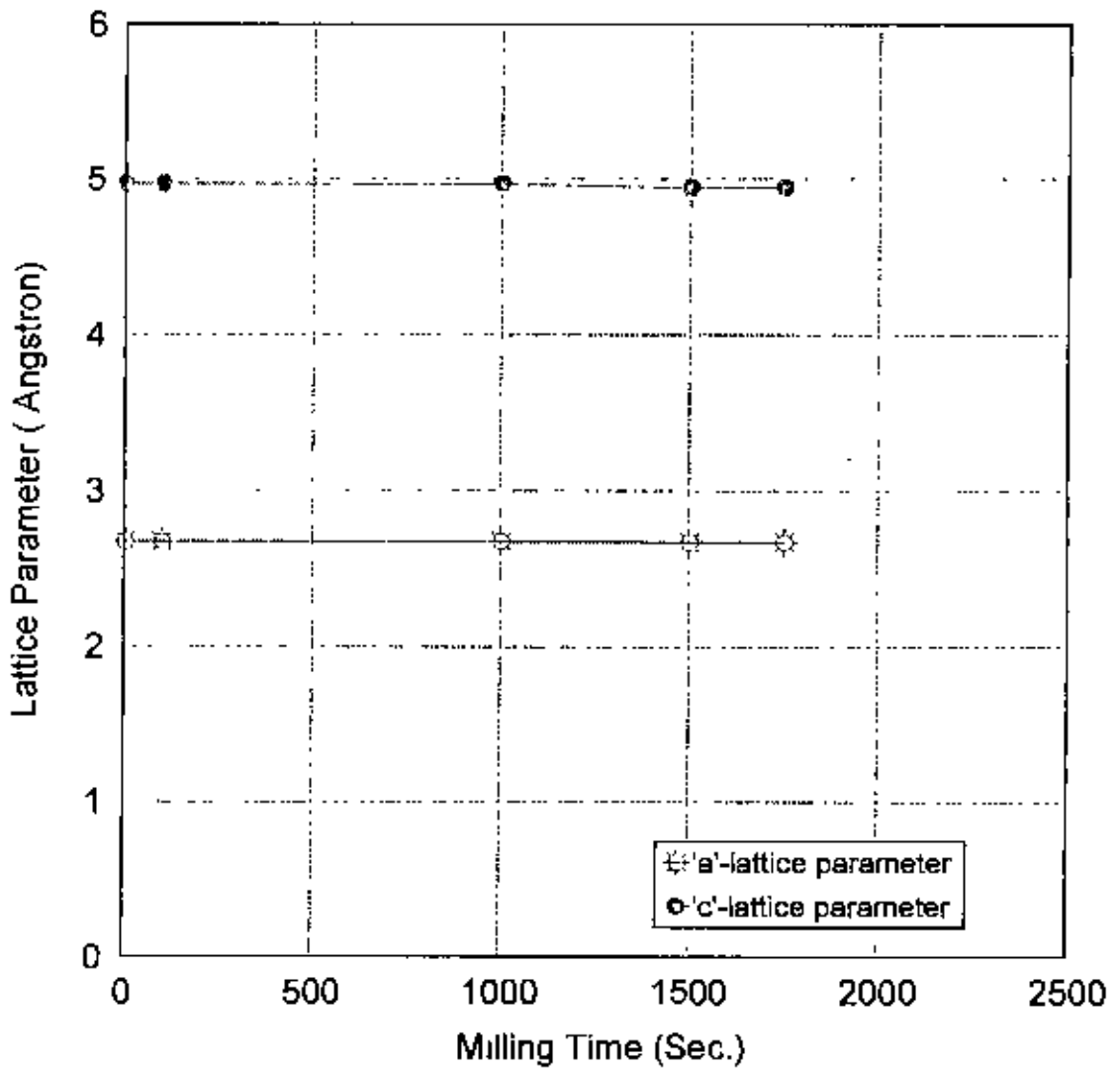


Fig. 6.4 : Change of lattice parameters of zinc with the progress of mechanical alloying of 70%wt.copper- 30%wt. zinc system. The lattice parameter of zinc remains constant with the increase of milling time.

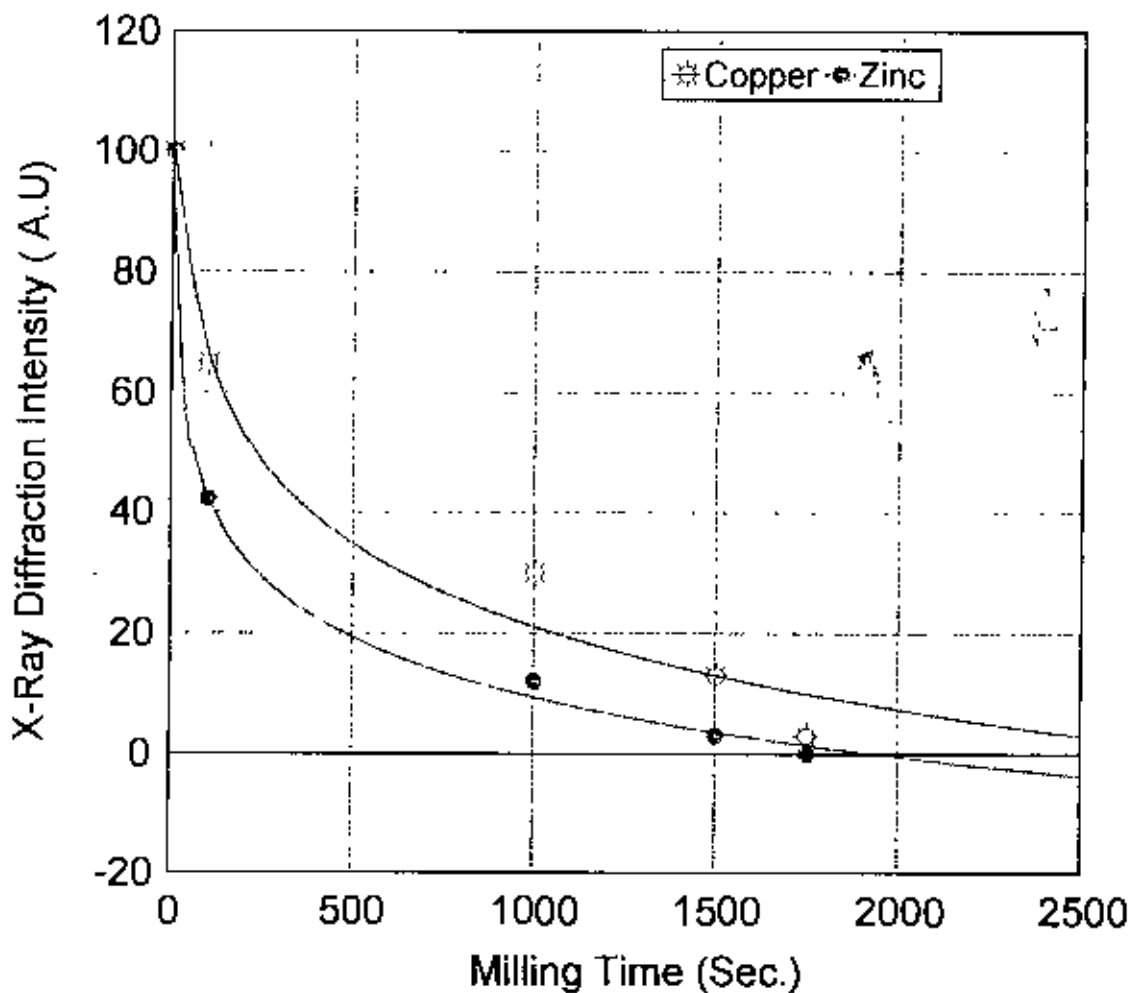


Fig. 6.5: Change of X-ray diffraction intensity (arbitrary unit) with respect to milling time of copper and zinc with the progress of mechanical alloying of 70%wt.copper- 30%wt. zinc system.

Investigation of particle shape characterisation, the initial powder particles of all fineness number were irregular and more or less were spherical or circular. With the progress of mechanical alloying particles of a specific fineness number tend to be more regular in shape as is clearly revealed in Fig. 6.6a, Fig. 6.7a, Fig. 6.8a., Fig. 6.9a Here noticeable that the initial irregularly shaped particles tend to be more circular and spherical. From the macro-structures of powder particles milled at specific time indicate that powder particles of finer grain size are more irregular shaped as compared of coarser powder particles.

Investigation of structural refinement during mechanical alloying of 70 wt. % copper-30 wt. % zinc by means of optical metallography showed that the initial coarser ductile copper powder (AFS No. 244.867, VH 94.71) and relatively fines brittle zinc



Figure 6.6(a) : Macro-structure (x120) of 0 sec. milled powder particles of grain fineness No.100. Here bright particles are of zinc and off dark particles are of copper.

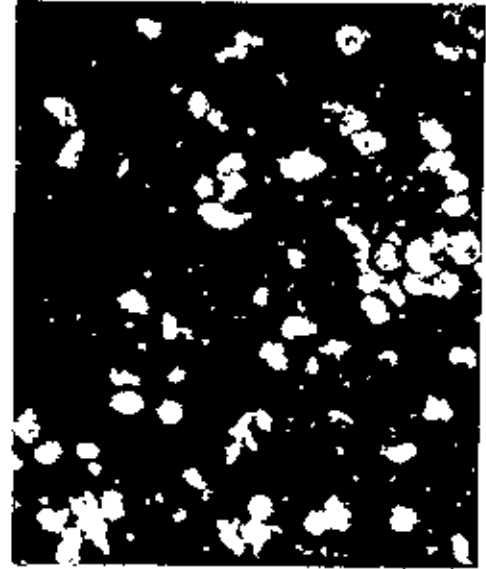


Figure 6.6(b): Macro-structure(x120) of 0 sec. milled powder particles of grain fineness No.140. Here bright particles are of zinc and off dark particles are of copper.

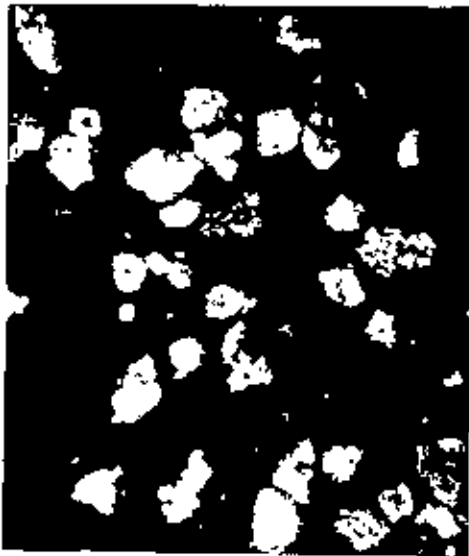


Figure6.6(c): Macro-structure(x120) of 0 sec. milled powder particles of grain fineness No.200. Here bright particles are of zinc and off dark particles are of copper.



Figure 6.6(d): Macro-structure(x120) of 0 sec. milled powder particles of grain fineness No.270. Here bright particles are of zinc and off dark particles are of copper.

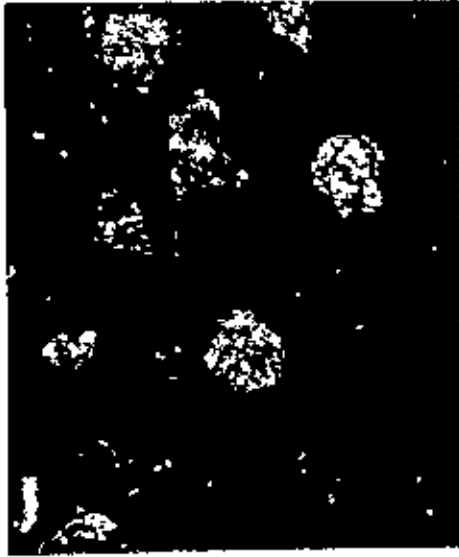


Figure 6.7(a) :Macro-structure(x120) of 100 sec. milled powder particles of grain fineness No.100.



Figure 6.7 (b) :Macro-structure(x120) of 100 sec. milled powder particles of grain fineness No.140.

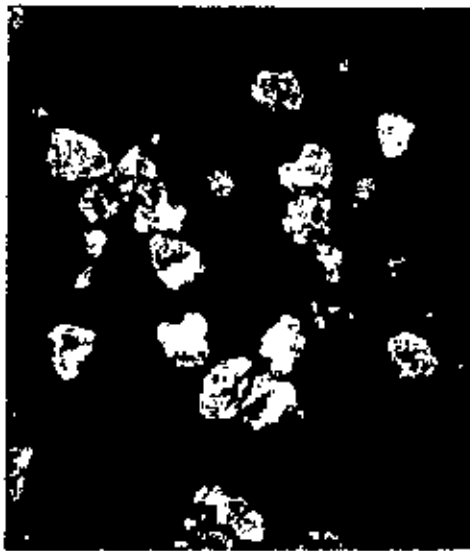


Figure 6.7(c): Macro-structure(x120) of 100 sec. milled powder particles of grain fineness No. 200.

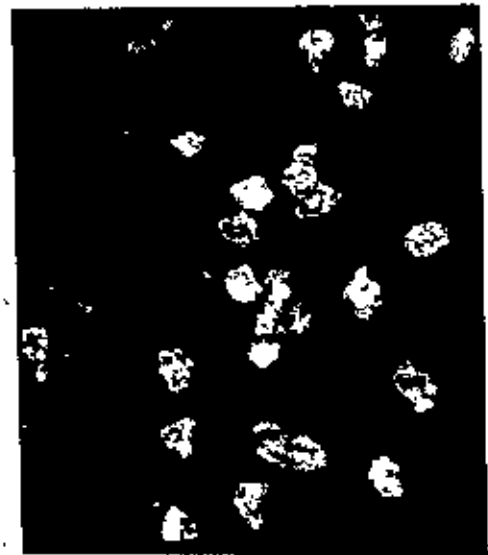


Figure 6.7 (d): Macro-structure(x120) of 100 sec. milled powder particles of grain fineness No. 270.



Figure 6.8 (a): Macro-structure(x120) of 1000 sec. milled powder particles of grain fineness No.100.

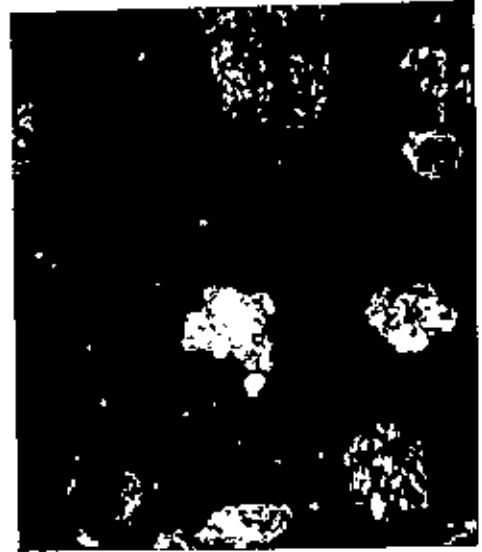


Figure 6.8 (b): Macro-structure(x120) of 1000 sec. milled powder particles of grain fineness No.140.

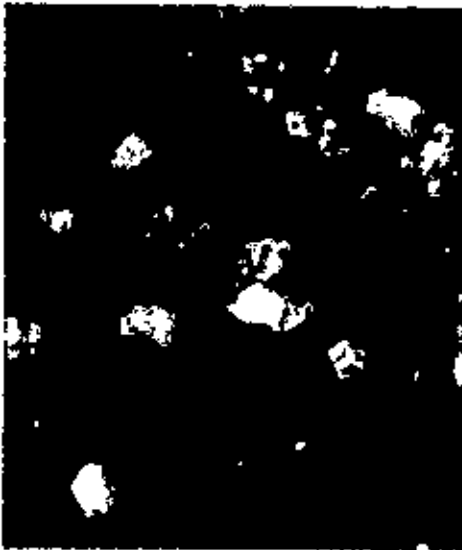


Figure 6.8 (c): Macro-structure(x120) of 1000 sec. milled powder particles of grain fineness No. 200.



Figure 6.8 (d): Macro-structure(x120) of 1000 sec. milled powder particles of grain fineness No. 270.



Figure 6.9 (a): Macro-structure(x120) of 1750 sec. milled powder particles of grain fineness No. 100.



Figure 6.9 (b): Macro-structure(x120) of 1750 sec. milled powder particles of grain fineness No. 140.



Figure 6.9 (c): Macro-structure(x120) of 1750 sec. milled powder particles of grain fineness No. 200.



Figure 6.9 (d): Macro-structure(x120) of 1750 sec. milled powder particles of grain fineness No. 270.

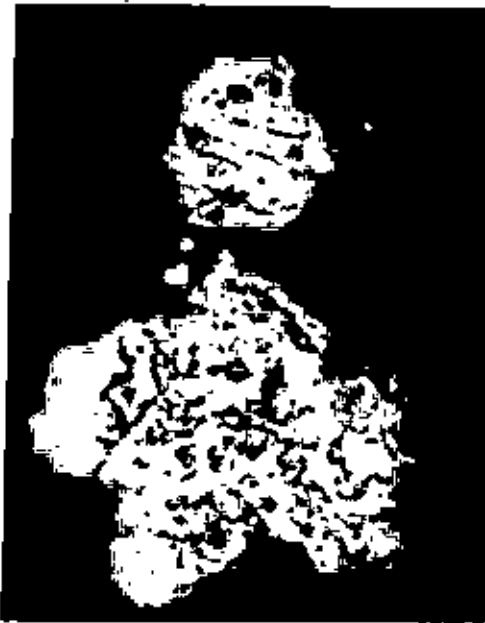


Figure 6.10: Microstructure(x1200) of copper powder particles.

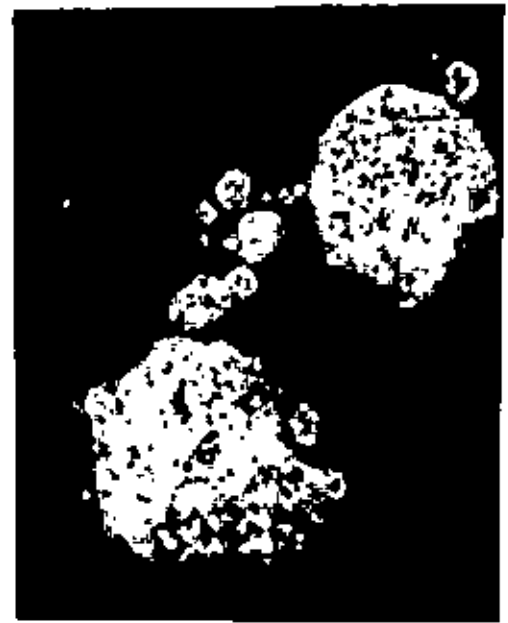


Figure 6.11: Microstructure(x1200) of zinc powder particles

powder (AFS No. 292.439, VH 350.5), were irregular and more or less spherical (circular in two dimensional view) shaped as represented in the above Fig. 6.10 and Fig. 6.11.

After the first short period of milling (100sec.), the initial finer zinc powder particles are embedded and welded in the matrix of coarser copper powder particles and a large fraction of them fractured into finer particles. The individual ingredients of the composite particles are visible. The copper powders are visible as off bright and the zinc powders are visible as bright particles as are represented in Fig. 6.12. The average size is finer as compared with that of the initial powder. The sieve analysis data also supports this argument.

After 1000 sec of milling the repetitive deformation, flattening, welding and fracturing of the particles build up a characteristic layered structure due to trapping of opposite species. Trapping was somewhat like as represented in Fig. 6.13 which results in the final optical homogenised particles. Some of the composite particles are in the form a layered plate like the structure as represented in Fig. 6.12 and most of them are no more finer. The sieve analysis data shows that the average particle size is increased which may be due to coalescence of the individual particles.

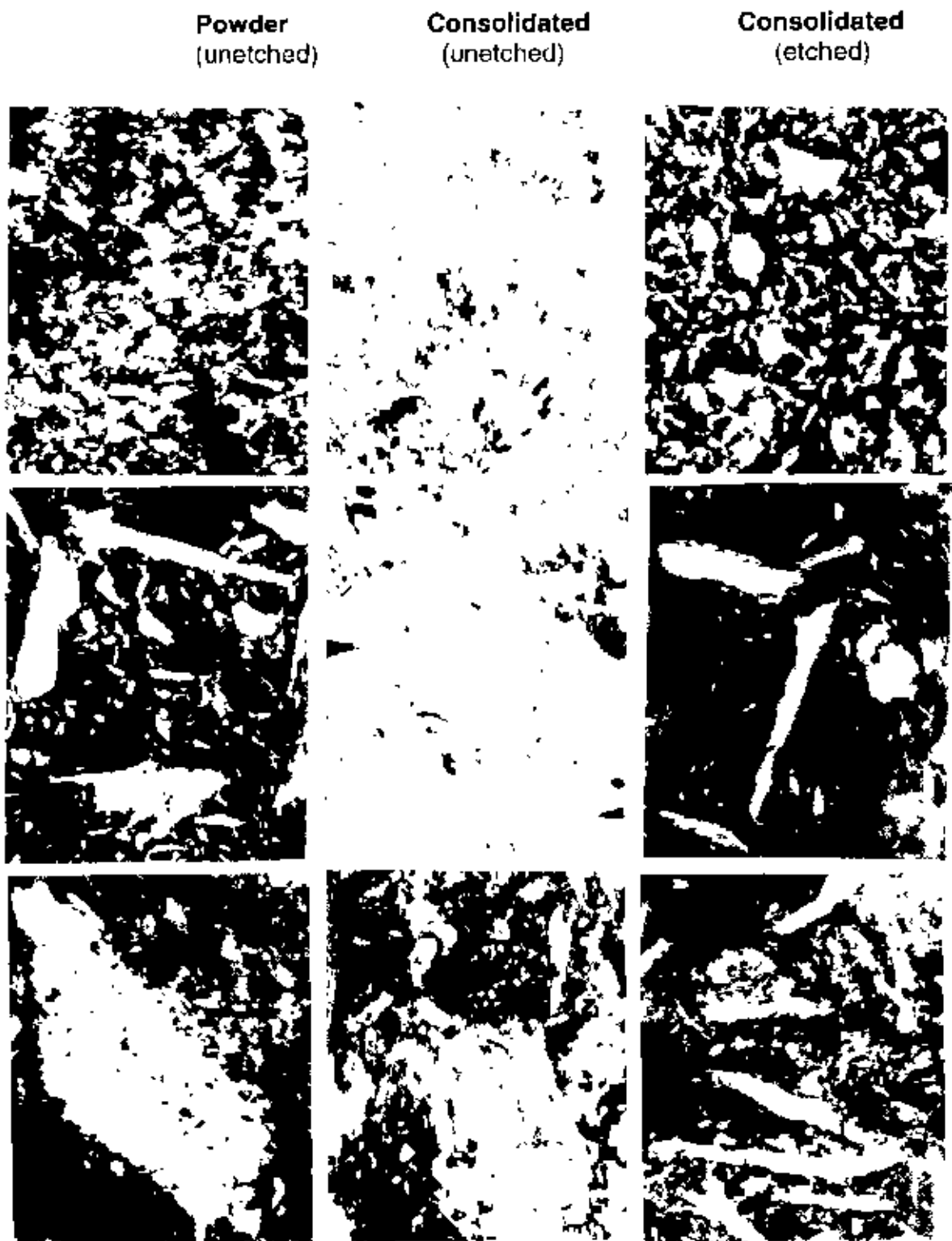


Figure 6.12 : Microstructure (x1200) of the products of mechanical alloying of 70% wt. copper-30% wt. zinc system at different stages of milling. The zinc particles are trapped in the copper particles and are welded. After 100 sec. of milling the welded powder particles are fragmented into finer particles. After 1000 sec. of milling composites and the welded deformed powder particles are moved together and the spacing among them has decreased to a noticeable amount. Finally after 1750 sec. of milling they are optically homogenised and no more resolvable by means of light microscope.

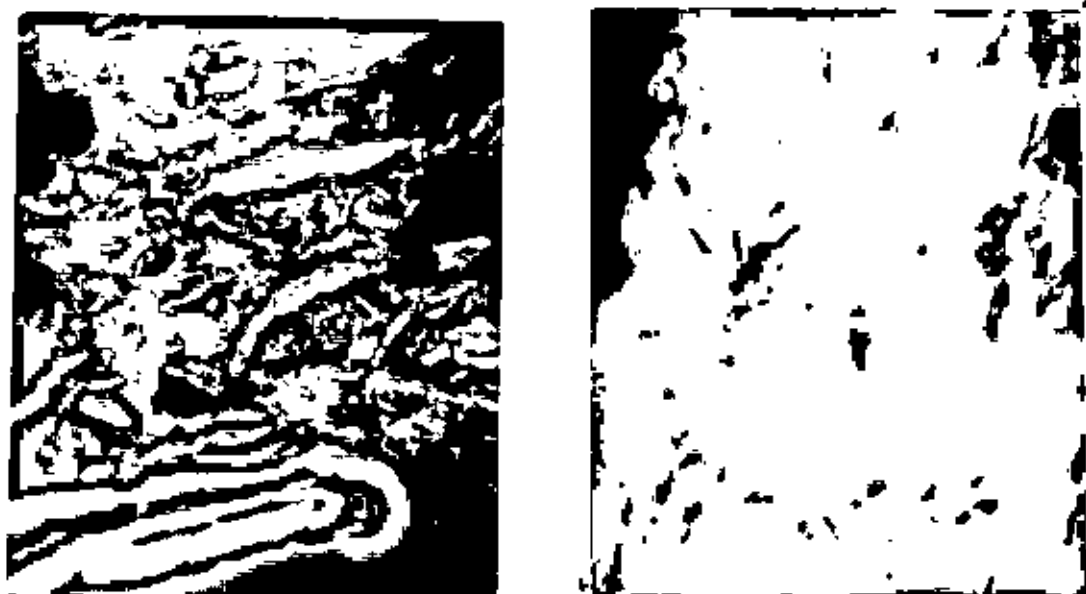


Figure 6.13: Microstructure representing the trapping mode of different species of powder particles (X1200) which finally results in optically homogenised (X3000) structure after consolidation. Here bright particles are zinc and off white particles are copper and the dark particles are metal oxides.

After 1750 sec. of milling the powder particles continue to appear plate like, but the layered structure are no longer resolvable. The optical metallographs revealed a microstructure of about uniform colour as is represented in Fig. 6.12. This uniformity in colour is the indication of the visual homogeneity which in turn is the indication of alloying.

The uniformity in the structure is more prominent in the in the consolidated samples. Consolidation was carried out in a locally designed and fabricated hot pressing die. The milled powder particles was consolidated at 280°C under a pressure of 12 tsi (tons per square inch) for 6 hours. Consolidation facilitated the homogenisation of both species at the large inter surface area of very fine layered composites leading to the formation of matrix of uniform visual homogeneity as represented in Fig. 6.12.

The effect of initial powder particle size has a noticeable effect on the progress of mechanical alloying and on its final homogenised structure. A mixture of initial copper powder of AFS No. 261.295 and zinc powder of AFS No. 292.439, resulted to the same degree of mechanical alloying as compared to the mixture of initial copper powders of AFS No. 244.857 and zinc powder of AFS No. 292.439 has taken around half milling. This is due to the larger interfacial areas available in the finer particle size

powder facilitating the diffusion between the species. The effect of particle size on mechanical alloying time has been compared in Fig. 6.1 and Fig. 6.2. The resulting final optical homogenised structure has been compared in Fig. 6.14.

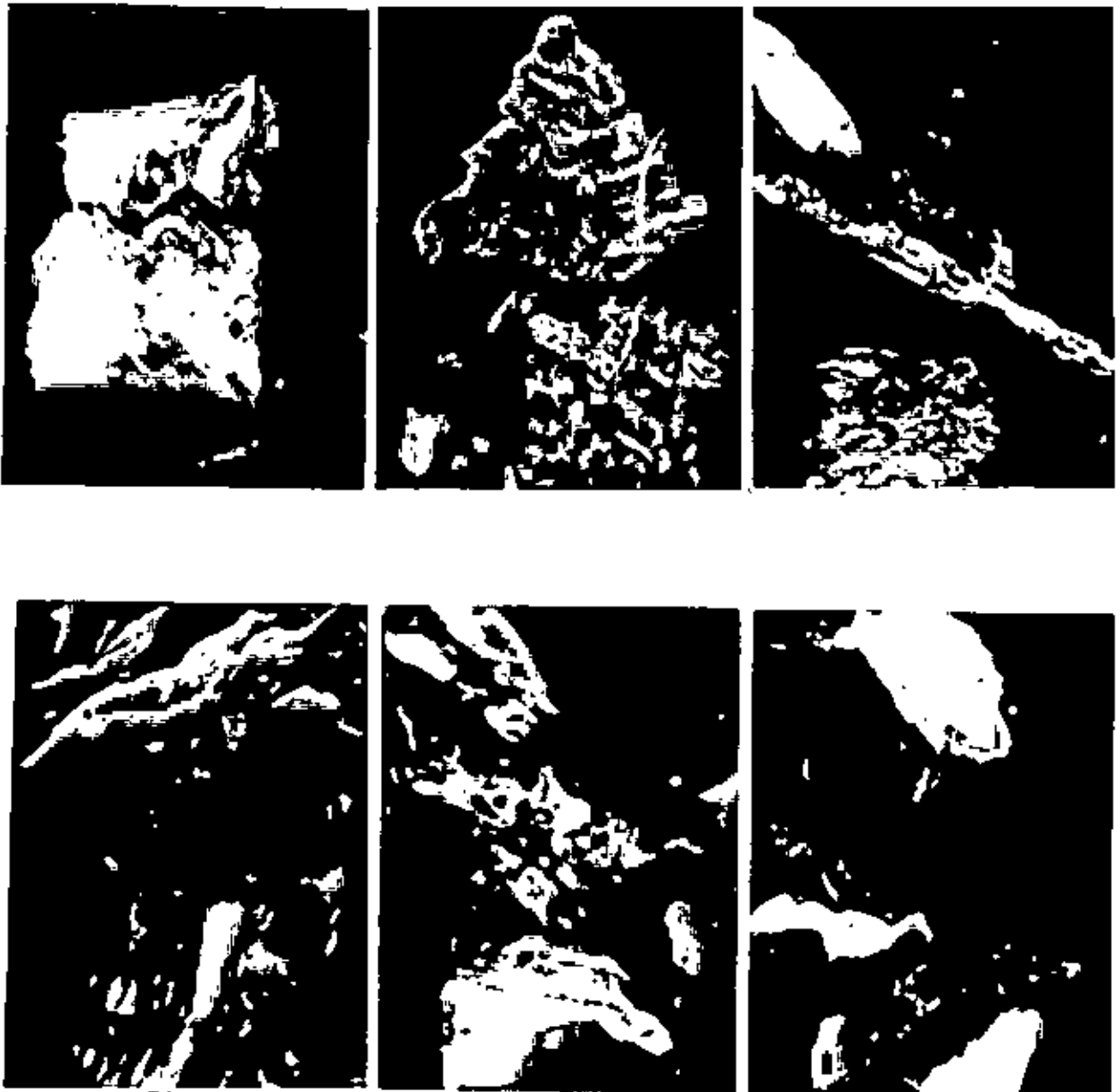


Figure 6.14: Microstructure representing the comparative optical homogenisation of the mechanical alloyed products from initial particles of different grain size. The upper three microstructures (X1200) are of mechanical alloyed copper 70% wt., AFS No.244.867-zinc 30% wt., AFS No. 262.439 powders processed in attritor for 1750 seconds. The lower three microstructures (X1200) are of mechanical alloyed copper 70% wt., AFS No. 261.292-zinc 30% wt., AFS No. 292.439 powders processed in attritor for 900 seconds.

The study of effectiveness of different zones of an attritor, termed media interaction zone (where powder particles are trapped between grinding balls), out side of media

interaction zone (where powder particles are trapped between grinding balls and the attritor wall) and the bottom edge dead zone (where powder particles are segregated) by have been investigated. The resulting comparative progress of mechanical alloying has illustrated by X-ray diffraction patterns (Fig. 6.15, Fig. 6.16 and Fig. 6.17.). Among the aforesaid three attrition zone, the dead zone shows the lower, the media interaction shows the medium and the outside of the media interaction zone shows the higher degree of mechanical alloying. The higher degree of mechanical alloying at the outer media interaction zone is probably due to the higher centrifugal impacts together with friction between grinding ball and the attritor wall. The medium degree of mechanical alloying at the media interaction zone is due to the high collision impacts and the sliding impacts between the grinding balls, where sliding results from differential rotational velocities between adjacent rows or columns of the grinding balls and due to the closed packed array by the grinding balls. There exists a difference in velocities between adjacent rows along the attritor wall and columns along the attritor bottom.

Powder added to the attritor, with the progress of milling process segregated to the bottom edge of the attritor. This is due to the lack of grinding ball motion there. However, the ineffectiveness of the dead zone was decreased by providing a ring-pad, adjacent to the dead zone, which assists the powder particles to segregate into the dead zone.

Micro-hardness of different species and phases in the conventional powder metallurgy route product and that of in the consolidated mechanically alloyed product were evaluated. A very large difference of hardness from VH 95.76 to VH 350.5 were observed in the conventional powder metallurgy product . This is due to the structural inhomogeneity which inturn is resulted from insufficient diffusion. Microstructural inhomogeneity, in other words, the presence of mother species (zinc and copper) was also detected from optical metallography (Fig. 6.18) and X-ray diffraction pattern (Fig. 6.19). Although the mechanically alloyed powder were consolidated at the same conditions as applied in the former case more or less uniform micro hardness ranging from VH 681.1 to VH 771.9 were observed. This improved and uniform micro-hardness in the mechanically alloyed consolidated specimen is due to the very fine plate-like composites which provide short circuit diffusion path leading to production the homogenised microstructure.

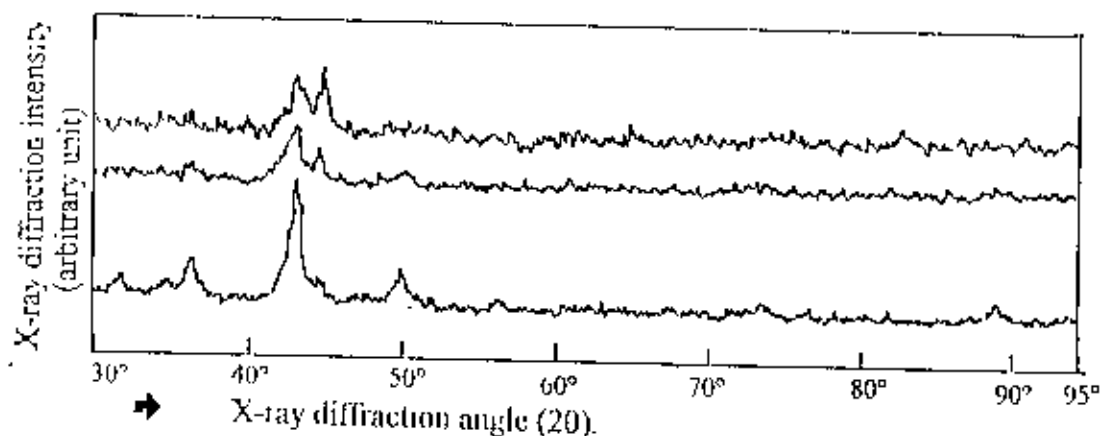


Figure 6.15: X-ray diffraction pattern for mechanical alloyed copper 70% wt.-zinc 30% wt. powders processed in attritor for different time intervals (sample trapped between grinding balls).

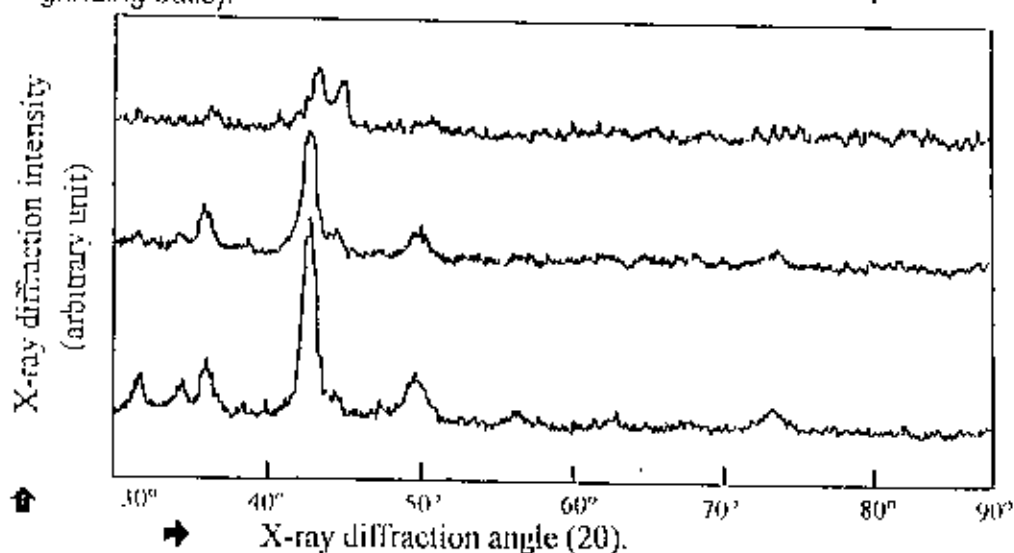


Figure 6.16: X-ray diffraction pattern for mechanical alloyed copper 70% wt.-zinc 30% wt. powders processed in attritor for different time intervals (sample trapped between grinding ball and attritor wall).

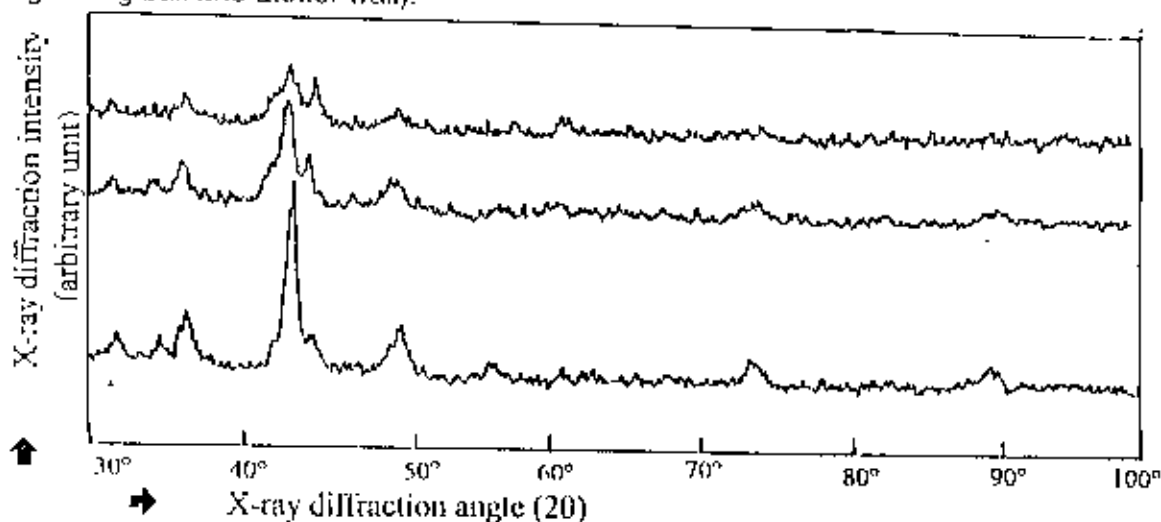


Figure 6.17: X-ray diffraction pattern for mechanical alloyed copper 70% wt.-zinc 30% wt. powders processed in attritor for different time intervals (sample the dead zone).

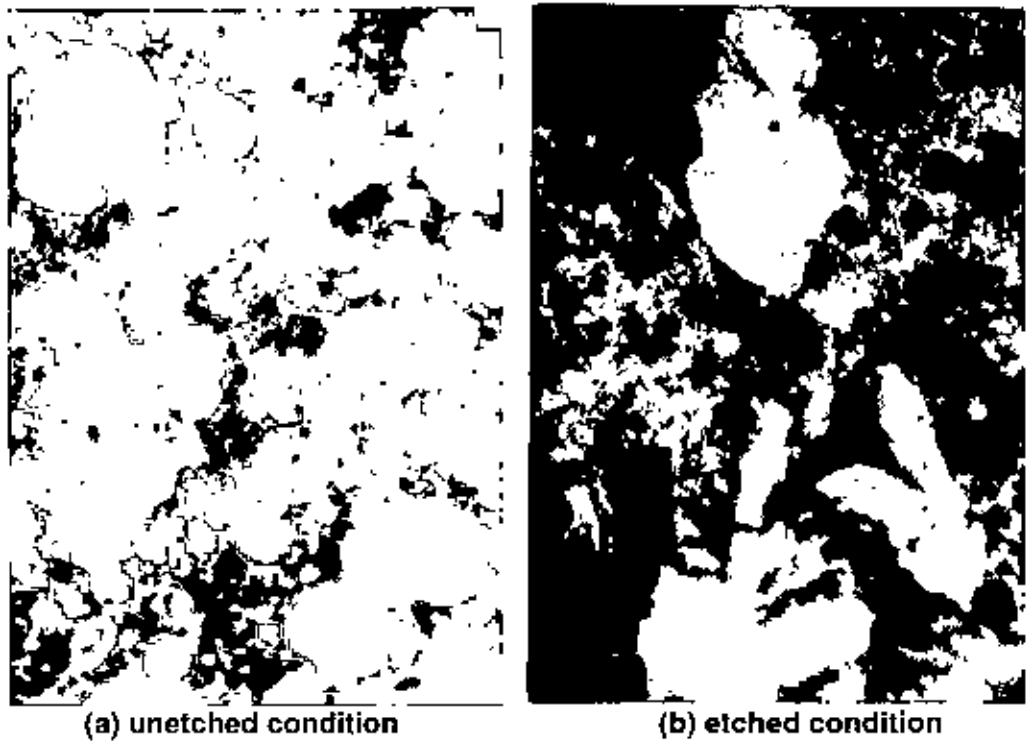


Figure 6.18: Microstructure (x1200) of conventional powder metallurgy product (copper 70% wt., AFS No. 261.292 and zinc 30% wt., AFS No. 292.439) powders consolidated under the same conditions of hot pressing, indicates the microstructural inhomogeneity,

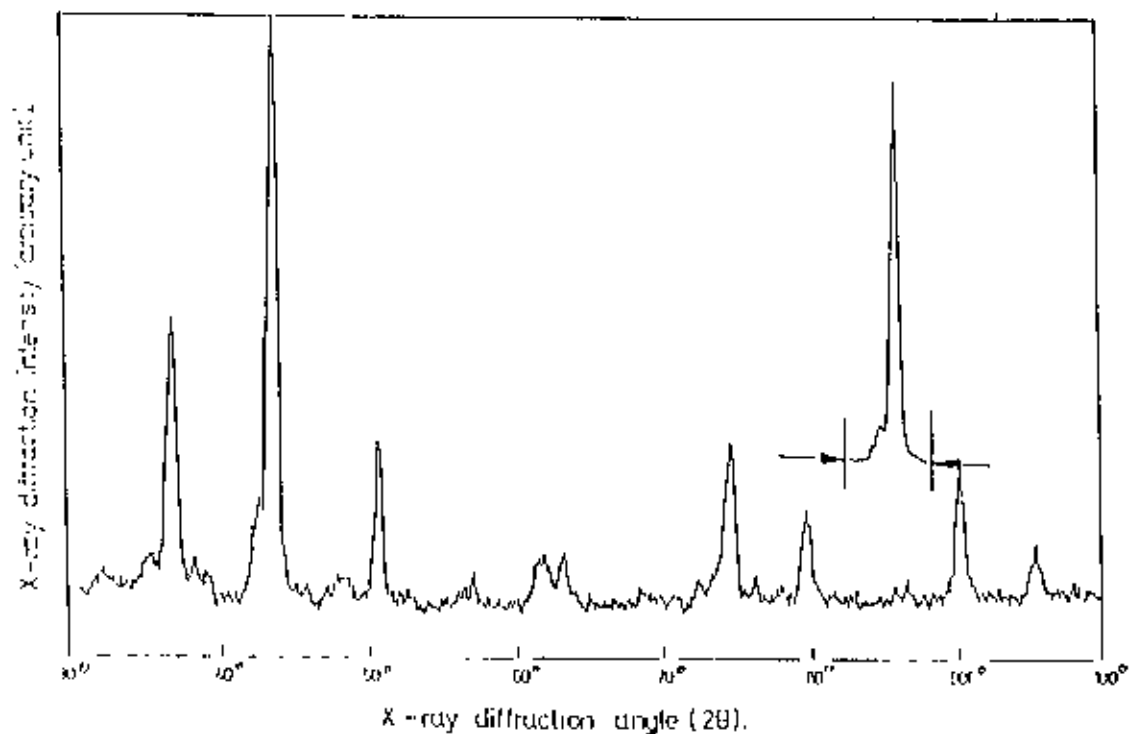


Figure 6.19: X-ray diffraction pattern for conventional powder metallurgy product (copper 70% wt., AFS No. 261.292 and zinc 30% wt., AFS No. 292.439) powders consolidated under the same conditions of hot pressing, indicates the structural non homogeneity i.e. the presence of mother species (zinc and copper).

Conclusions

The following conclusions concerning the mechanical alloying of 70% copper-30% zinc system can be drawn based on the results obtained in this study.

1. During mechanical alloying, zinc atom preferentially enters into the copper lattice leading to the formation of a copper-zinc alloy and finally reaches to the amorphous state .
2. Formation of composite particles and structure refinement in the course of mechanical alloying appears to occur predominantly due to the severe deformation, cold welding and fracturing of free powder particles.
3. After consolidation the micro-hardness of visually homogenised phase of mechanical alloying product is much higher and uniform than the non-homogenised individually visible powder particles and phases appearing in the conventional powder metallurgy product under the same condition of processing.
4. The rate at which mechanical alloying towards a given structure occurs is dependent on the size of initial powder particle and finer particle size leads to the faster rate of mechanical alloying of a given system.
5. The different degrees of mechanical alloying for a given time occurs at different zone within the attritor vessel. At the interaction zone large amount

of moderate degree, at the outer interaction zone small amount of high degree and at the dead zone small amount of low degree of mechanical alloying occurs.

6. Unless perfect inert atmosphere is provided, the process is amenable to the severe oxidation of metal powder particles due to the large available surface area.

Recommendation for future work.

Mechanical alloying is completely and distinctly a different direction of production technology for normally incompatible systems with great flexibility. So many facts about this technique are still in embryonic state and warrant more in-depth exploration. From the fundamental stand point of locally developed mechanical alloying facilities and all other available facilities at this university, the following work can be recommended for further study.

- (1). Alloying of incompatible alloy systems e.g. immisble systems, metastable phases, incongruent intermetallic etc. through mechanical alloying and studies of their microstructural and mechanical properties.
- (2). Development of metal matrix composites of light alloys through mechanical alloying and study of their microstructural and mechanical properties. Al-Cu, Al-Ni and Al-Co systems can be considered as candidate materials. Micro-scale fine layered composites are expected to form with improved mechanical properties.
- (3). Development of aluminium-alumina dispersion strengthened alloys through mechanical alloying and study of their mechanical properties both at low and at high temperature. Al-Mn system can be studied. Stabilised structure dispersed with inert particles of Al_2O_3 by mechanical alloying is expected to form. Ultimate tensile strength more than 500 MPa. at room-temperature and

more than 200 MPa. at 400°C are expected promising applications in the automotive sector.

- (4) Assessment of the stability of mechanically alloyed aluminium based alloys. Al-Mn, Al-Fe-Mn alloy systems can be studied. Fine grained aluminium matrix stabilised by oxides and carbide dispersions and by the intermetallics $Al_6(Fe\ Mn)$ and $Al_{13}Fe_4$ are expected to form. Improved tensile strength, Young's modulus and wear properties at higher temperatures are expected.
- (5). Development of ceramics metal composites through mechanical alloying and study of their thermal and mechanical performance.
- (6). Study on mechanical nitriding Fe-Cr alloy system. Elemental Fe and Cr can be milled in nitrogen gas at ambient temperature. Stabilised metal nitrides or high nitrogen alloys are expected to form.
- (7). Development of amorphous alloys e.g. Cu-Ta, Fe-Ni, Ni-Zr etc. locally by mechanical alloying route.
- (8). Production of metals and alloys from their oxides directly by mechanical alloying. ZnO with Ca, CuO with Ca and equal quantities of ZnO ,CuO and Ca can be milled. Metallic Zn, Cu and β' -Brass are respectively expected to form. The process thus can be used to produce metals and alloys directly from their oxides, thereby potentially decreasing overall production costs.

Expressions and Equations.

□ The Hertz radius and collision duration

$$r_h = g_r v^{0.4} \left(\frac{P}{E} \right)^{0.2} R \quad [\text{Eqn. A-1.}]$$

$$2\tau = g_r v^{-0.2} \left(\frac{P}{E} \right)^{0.4} R \quad [\text{Eqn. A-2.}]$$

where g_r , are constants of order unity, v is the media collision velocity and R , ρ and E are the media radius, density and tensile modulus, respectively.

□ The alloying time:

$$\text{The alloying time } t_p = \frac{\Sigma h_o}{v \tau r_n^2 h_o} \quad [\text{Eqn. A-3.}]$$

Where Σ is critical amount of deformation, v is the media collision velocity, τ is collision time, r_n is Hertz radius, h_o is the height of powder cylinder (the powder volume affected is treated as a cylinder of radius r_n and height h_o .)

□ Deformation:

$$\alpha(r) = Rv \left(\frac{\rho_b h_o}{H_v} \right)^{1/2} - \frac{r^2}{R} \quad [\text{Eqn.A-4}]$$

Where r is the distance from the center of contact, R the radius of the balls, v the relative velocity of the balls at impact, ρ_b the density of the grinding balls, and H_v the powder hardness. This expression ignores factors of order unity and the effect of impact angle of the colliding balls.

□ **Flow Stress:**

$$\sigma_y = \sigma_{y0} + K\epsilon^n \quad [\text{Eqn. A-5}]$$

Where K is the strength coefficient, n the work-hardening exponent, σ_y the flow stress at the accumulated plastic strain ϵ , and σ_{y0} the initial flow stress. On using $H_v = \sigma_y$,

$$H_v = H_{v0} + K\epsilon^n \quad [\text{Eqn. A-6}]$$

□ **Strain :**

$$\text{The strain is determined from } \epsilon = -\ln \left\{ \frac{h_0 - \alpha(r)}{h_0} \right\} \quad [\text{Eqn. A-7}]$$

Where $\alpha(r)$ is the approach of the balls which is a function of distance, r, from the contact area (cf. Eqn. A-4) and h_0 the powder coating thickness.

□ **Area of metal to metal contact :**

$$A_w = \pi r_p^2 \left[J \left(\frac{\Delta S}{S_f} \right)^2 - n_d \left(\frac{r_d^2}{r_p^2} \right) \right] \quad [\text{Eqn. A-8}]$$

Where J is a constant =0.7-0.8, $\Delta S = S_i - S_f$, S_i is the pre-deformation metal-surface area and S_f is the post deformation metal-surface area, n_d is the number of dispersoids trapped in the potential weld region of radius r_p , and r_d is the radius of the dispersoids.

□ **The force require to separate the weld :**

$$F_w = A_w \sigma_u \quad [\text{Eqn. A-9}]$$

Where σ_u is the tensile strength of the weld, F_w and A_w have there usual meanings. For two adhering particles of the same material, this strength is equal to the tensile strength of the bulk material. For two welded particles of different materials, the weld strength is assumed to be the lesser of the tensile strengths of the different materials. When a cold weld is made between two lamellar particles (i. e. composite particles containing two species), weld strength is taken as a rule of mixtures strength on the basis that the weld is a mixture of similar and dissimilar metal bonds.

□ **Total elastic recovery force :**

$$N_e = \pi r_p^2 H_v \left[\frac{n_d r_d^2}{r_p^2} + \frac{\pi^4}{6(1+1.33 \tan^2 \theta)^{0.5}} \left(\frac{R_p^2}{r_p^2} \right) \delta^2 H_v^2 \right] \quad [\text{Eqn. A-10}]$$

Where $\delta = (1 - \nu^2) / E$, and R_p is the particle's volume effective radius, θ the relative impact angle, ν the particle's Poisson's ratio, and E its elastic modulus. The second

term in parentheses represents the elastic response of the annulus around the plastic zone.

□ **The average shear force acting over the weld surface:**

$$T_b = \pi r_p^2 H_v \left(\frac{0.44 \tan^2 \theta}{1 + 1.33 \tan^2 \theta} \right)^{0.5} \quad [\text{Eqn. A-11}]$$

Where the symbols have there usual meanings.

□ **Reduction is represented in the second term in the following equation:**

$$Z_i = \left(\frac{\Delta S}{S_f} \right)_i - \zeta \frac{Z_{i-1}}{(\Delta S/S_f)_i} \quad [\text{Eqn. A-12}]$$

Where $(\Delta S/S_f)_i$ is the fraction of surface exposed through cumulative deformation through impact i , and ζ is the fraction coated during the interval between relevant impacts

□ **J intregal :**

$$J = \beta \sigma_0 \epsilon_0 \alpha \pi \sqrt{m} \left(\frac{\sqrt{3} \sigma}{2 \sigma_0} \right)^{m+1} \quad [\text{Eqn. A-13}]$$

where $\beta = (1/\epsilon_0) (\sigma_0/K)^m$, with K being the strength coefficient and $m = 1/n$ (n is the work-hardening coefficient). The critical J value (J_{lc}) is related to the critical stress-intensity factor, K_{Ic} , through $J_{lc} = K_{Ic}^2/E$. The critical crack length (a_c) is obtained for $J = J_{lc}$ or

□ **Critical Crack Length:**

$$a_c = J_{lc} \frac{K^m}{\pi \sqrt{m}} \left(\frac{2}{\sqrt{3} \sigma_u} \right)^{m+1} \quad [\text{Eqn. A-14}]$$

Where J_{lc} , a_c , K_{Ic} , E , K , σ_u , and m have there usual meaning.

□ **Condition for forging fracture:**

$$\frac{\alpha(r)}{h_0} = 1 - \left(1 - \frac{a_c^2 f_s^{2/3}}{4R_p^2} \right)^{0.5} \exp(-\epsilon_c) \quad [\text{Eqn. A-15}]$$

where ϵ_c is the critical strain to fracture. The factor of 4 in the denominator of the last term on the right-hand side of this equation stems from the radial symmetry of the particles,

□ **Volume of an oblate spheroid:**

The major semi axis is c ; the minor semi axis, which also defines the axis of revolution, is b . The shape factor is defined as $f_s = b/c$. The volume of an oblate spheroid is $V_c = \frac{4\pi}{3} c^2 b$ [Eqn. A-16]

A volume equivalent radius of the spheroid can be defined as $R_p = (c^2 b)^{1/3}$, and both semi axes may be expressed in terms of this radius and the shape factor.

$$b = R_p f_s^{2/3}, c = R_p f_s^{-1/3} \quad \text{[Eqn. A-17]}$$

□ **Shape Factor:**

$$f_{sl} = \left(\frac{b_f}{b_i} \right)^{1.5} f_{sl} \quad \text{[Eqn. A-18]}$$

where the subscripts i and f denote the pre-and post-deformation shape factors, respectively. The change in the minor axis dimension can be related to powder deformation:

$$\frac{b_f}{b_i} = 1 - \frac{\alpha(r)}{h_0} \quad \text{[Eqn. A-19]}$$

Thus, the shape factor can be expressed in terms of bulk deformation:

$$f_{sl} = \left(1 - \frac{\alpha(r)}{h_0} \right)^{1.5} f_{sl} \quad \text{[Eqn. A-20]}$$

□ **Reaction kinetics:**

$$k = A \exp(-Q/RT), \quad \text{[Eqn. A-21]}$$

where k is the reaction rate at temperature T , A is the pre-exponential factor (collision frequency), Q is the activation energy of the rate-controlling step, and R is the universal gas constant.

□ **Rate of diffusion:**

$$D = D_0 \exp(-Q/RT), \quad \text{[Eqn. A-22]}$$

where D is the diffusivity, D_0 is a constant, Q is the activation energy, and R and T have the usual meanings.

Appendix - B

Mechanics of collision and particle deformation.**Article One: Collision mechanics :**

Considering two balls colliding at some relative velocity and impact angle, as depicted in Figure B-1. To a first approximation it can be written

$$N = F \cos \theta_i \quad [\text{Eqn. B-1}]$$

where F is the force developed during the collision as a result of the resistance of the composite bell to deformation, N is the normal component of that force, and θ_i is the initial angle of impact. The tangential component of the force is

$$T = \left[\frac{2(1-\nu)}{2-\nu} \right] F \sin \theta_i \quad [\text{Eqn. B-2}]$$

where the term in brackets arises from the ratio of normal to tangential compliance¹⁷⁶. Designating this term as C , we have

$$T = CN \tan \theta_i \quad [\text{Eqn. B-3}]$$

Eqn. B-1 and through Eqn. B-3 apply for collision angles below which gross slip between the colliding balls occurs. For such slip, the entire contact area of one ball slides on that of the other ball. In these circumstances, $\tan \theta_i$ in the equations must be replaced by μ , the coefficient of friction. In this Appendix, it has been considered that the collision has been taken place under "sticking" conditions, i.e., without gross sliding.

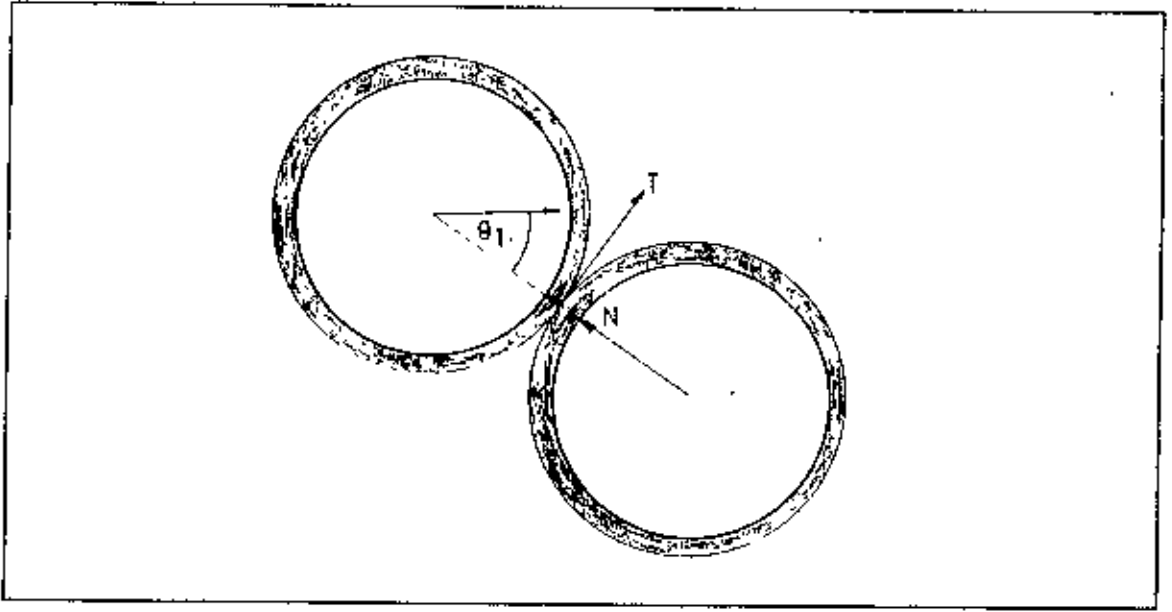


Figure B-1: Two composite balls colliding at an initial impact angle of θ_i produce both normal (N) and tangential (T) components of stress arising from the balls resistance to deformation.

The stress distributions corresponding to these forces can be approximated as¹⁷⁷

$$\sigma_n = \left(\frac{3N}{2\pi a^3} \right) (a^2 - r^2)^{1/2} \quad [\text{Eqn. B-4}]$$

$$\text{and } \sigma_t = \left(\frac{3CN \tan \theta_i}{2\pi a^3} \right) (a^2 - r^2)^{1/2} \quad [\text{Eqn. B-5}]$$

where the subscripts n and t denote normal and tangential stresses, respectively; a is radius of the circle of contact, and r is the radial position within the contact area. The effective stress at any point in the contact area is given by

$$\sigma_e = (\sigma_n^2 + 3\sigma_t^2)^{1/2} \quad [\text{Eqn. B-6}]$$

$$\text{Using the results of goldsmith}^{177}, \quad a^3 = \left(\frac{3\pi}{4} \right) (RN\delta) \quad [\text{Eqn. B-7}]$$

where $\delta = (1-\nu^2)/\pi E$, then the effective stress can be written as a function of radius in the contact zone:

$$\sigma_e = \left(\frac{2}{\pi^2 R \delta} \right) (a^2 - r^2)^{1/2} (1 + C^2 \tan^2 \theta_i)^{1/2} \quad [\text{Eqn. B-8}]$$

The development until now holds as long as the composite ball experiences only elastic deformation. However, the powder coating clearly experiences plastic

deformation during mechanical alloying. The onset of this deformation occurs when the effective stress approximately equals the powder hardness (H_v). This occurs first at the center of the contact zone ($r=0$). The contact radius and the normal approach of the balls at this elastic to elastic-plastic transition are then given by

$$a_{ep} = \left(\frac{\pi^2 R \delta H_v}{2} \right) (1 + 3C^2 \tan^2 \theta_i)^{-1/2} \quad [\text{Eqn. B-9}]$$

and
$$\alpha_{op} = \left(\frac{\pi^4 R \delta^2 H_v^2}{2} \right) (1 + 3C^2 \tan^2 \theta_i)^{-1} \quad [\text{Eqn. B-10}]$$

This transition approximately takes place for a value of α on the order of $2 \mu\text{m}$. During the elastic deformation stage, the composite balls have been obeying the equation of

motion¹⁹²
$$\frac{1}{2} (\alpha^2 - v^2) = -\frac{2}{5} k_1 k_2 \alpha^{5/2} \quad [\text{Eqn. B-11}]$$
 where α

is the instantaneous relative velocity of the balls; v is the pre-impact velocity; $k_1 = 2/M$, where M is the mass of one ball; and $k_2 = 2R^{1/2} / 3\pi\delta$. Substituting the value for α_{ep} given by Eqn. B-9 into Eqn. B-10, α will be approximately equal to v at the transition. Therefore, the greatest part of the collision duration involves plastic deformation of the powder.

The transpires after the transition from elastic to plastic deformation of the powder is as follows (neglecting any work-hardening of the powder that may take place during the course of the collision). The plastic zone of the powder grows radially, as a circle, with uniform hardness. The corresponding stress distribution has been illustrated in figure 2.11. The equations of motion for the composite balls undergoing elastic-plastic deformation can be developed. There are two components of the normal force resisting the approach of the balls: the plastic circle surrounding the contact center and the elastic annulus around the plastic zone

The normal force acting in the plastic zone is given by $N_p = \pi r_p^2 H_v$ [Eqn. B-12]

where r_p is the radius of the plastic zone. The normal force in the elastic annulus is

$$N_e = \int_{r_p}^a \sigma_n 2\pi r dr \quad [\text{Eqn. B-13}]$$

If we assume that outside the plastic zone the stresses given by Eqn. B-4 and Eqn. B-5 remain valid, the equation of motion of the composite ball is given by

$$\ddot{\beta} + Q\beta = 0 \quad [\text{Eqn. B-14}]$$

$$\text{where } \beta = \alpha \left(\frac{\pi^4 R \delta^2 H_v^2}{6(1+3C^2 \tan^2 \theta_i)} \right) \quad [\text{Eqn. B-15}]$$

$$\text{and } Q = \frac{\pi R H_v}{M(1+3C^2 \tan^2 \theta_i)^{1/2}} \quad [\text{Eqn. B-16}]$$

The solutions to Eqn. B-14 are

$$\beta = C_1 \sin (kt + C_2) \quad [\text{Eqn. B-17(a)}]$$

$$\dot{\beta} = C_1 k \cos (kt + C_2) \quad [\text{Eqn. B-17(b)}]$$

$$\ddot{\beta} = -C_1 k^2 \sin (kt + C_2) \quad [\text{Eqn. B-17(c)}]$$

$$\text{where } k = \frac{1}{2R} \left[\frac{3H_v}{\rho(1+3C^2 \tan^2 \theta_i)^{1/2}} \right]^{1/2} \quad [\text{Eqn. B-18}] \quad \text{with}$$

ρ being the powder density. For a typical impact in an mechanical alloying device k is on the order of $60,000 \text{ s}^{-1}$. The values of C_1 and C_2 can be determined by use of the initial conditions that at $t = 0$, $\alpha = 0$ and v is the relative impact velocity. Over the vast duration of the contact, $kt \gg C_2$, so C_2 can be neglected. On this basis, $C_1 = v \cos \theta_i/k$. The duration of the compression phase of the collision is

$$\tau = \pi/(2k) \quad [\text{Eqn. B-19}]$$

which is approximately 2.5×10^{-5} seconds, or about twice that determined through elastic analysis. Knowing the duration of the compression phase allows to calculate the final approach of the two composite balls (and hence the deformation of the

$$\text{powder coating them) as } \alpha_f = 2Rv \cos \theta_i \left[\frac{\rho(1+3C^2 \tan^2 \theta_i)^{1/2}}{3H_v} \right]^{1/2} \quad [\text{Eqn. B-20}]$$

Here the effects of tangential force on the collision is neglected. As a result of the tangential force, the balls rotate during the collision, effectively reducing the angle of incidence¹⁷⁸⁻⁷⁹. Nevertheless, the collision time and the maximum approach are dependent on k , and it has been found that a change in the angle of incidence from 45 to 0 degree results in only a 25 pct change in the value of k .

Article Two - Particle deformation as a function of position :

The deformation of individual particles significantly influences their coalescence and fragmentation proclivities. Considering two oblate spheroids in contact, as depicted in (Fig. B-2) are pressed together, the greatest displacement occurs at the center of contact, and the amount of displacement decreases away from the center. It is

necessary to determine this variation in displacement in order to subsequently determine strain as a function of position.

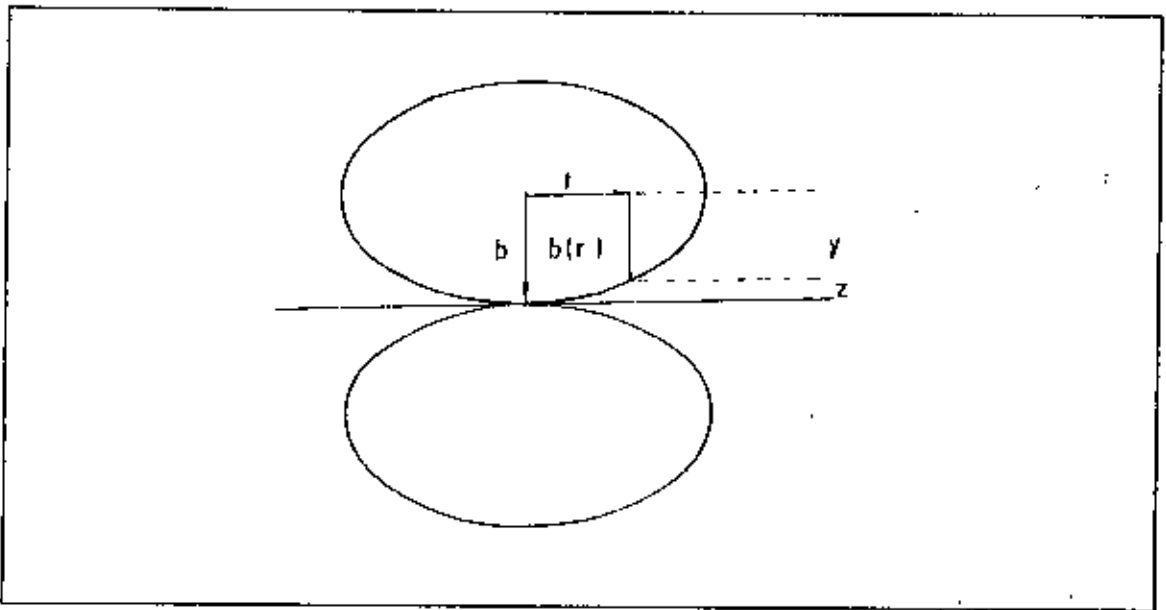


Figure B-2 : Deformation of particles along the contact radius between them

In a vertical section (Fig. B-2.), the spheroids are ellipses and the plane defining their contact area is a line. It is a simple matter to find the distance from any point on the perimeter of this ellipse to this line, and hence to determine the difference in displacement as a function of radial position in the oblate spheroid. The equation for

an ellipse is $\frac{x^2}{c^2} + \frac{y^2}{b^2} = 1$ [Eqn. B-21] Rearrangement of Eqn. B-21 provides an

expression for y , the vertical distance of Fig. B-2. The difference in displacement (distance of a point on the surface from the plane) is $z = b - y$, which is obtained as $z = b$

$\left[1 - \left(1 - \frac{x^2}{c^2} \right)^{0.5} \right]$ [Eqn. B-22] Thus the strain at any point can be defined

$$\text{by } \epsilon = -\ln \left[\frac{b(r) - \left[\left(\frac{\alpha_p(r)}{2} \right) - z(r) \right]}{b(r)} \right] \quad \text{[Eqn. B-23]}$$

where $\alpha_p(r)$ is the approach between homologous points on two particles being

pressed together. Since $b(r) = b(o) - z(r)$, and recognizing that $\frac{\alpha_p(o)}{2b(o)} = \frac{\alpha}{h_o}$ [Eqn B-24]

the strain becomes
$$\epsilon_z(r) = -\ln \left[\frac{\left(1 - \frac{\alpha}{h_o} \right)}{\left(1 - \frac{z(r)}{b_o} \right)} \right] \quad \text{[Eqn. B-25]}$$

Article Three - Welding and fracturing probabilities :

Welding and fracturing probabilities can be determined based on kinetic principles¹⁶⁰⁻⁸² and some critical assumptions, the most important being that the particle fracture and welding frequencies, while species dependent, do not depend on particle size or on milling time. This can be schematised in Fig.B-3 indicating the populations of elemental starting powders (A and B) and alloy (C) particles change as a result of particle fracturing and welding.

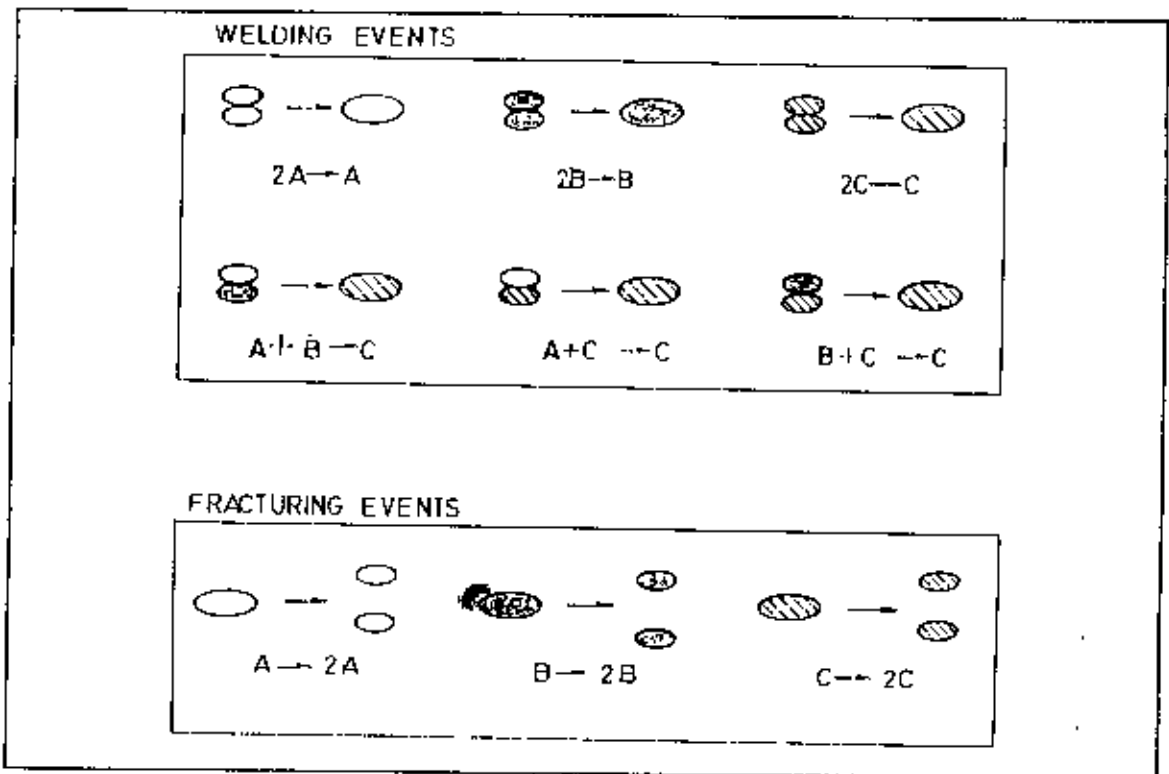


Figure. B-3 : Powder particles' numbers change as a result of fracture and weld events. A and B particles are alloyed to form composites C. When an AB particles weld to any other particle, the number of AB is reduced by one and the number of C particle is increased by one. When two C particles weld the number of C particle is reduced by one.

A welding probability is assigned to each possible coalescence event; e.g., α_{AA} represents the probability per unit process time of two particles of A welding to each other, α_{AC} represents this probability for particles of A and C welding to each other, etc. Similarly, α_i represents the probability per unit time of a particle of species I (=A, B or C) fracturing. Using first order reaction kinetics the number of A particles (N_A) is shown to vary with milling time as $\frac{1}{N} \left(\frac{dN_A}{dt} \right) = \frac{f_A}{\tau_c} \{ \alpha_A - f_A \alpha_{AA} - 2f_B \alpha_{AB} - f_C \alpha_{AC} \}$,

where N is the total number of powder particles (of all species), τ_c the time between powder particle collisions and f_i the (particle number) fraction of species I. An equation similar in form to the aforesaid applies for B particles. The analogous equation for C particles is $\frac{1}{N} \left(\frac{dN_C}{dt} \right) = \frac{1}{\tau_c} \{ f_C \alpha_C - f_C^2 \alpha_{CC} + 2f_A f_B \alpha_{AB} \}$, Taking into account that both N ,

and N vary with time, the time variation of f_A is expressed as $\left(\frac{\tau_c}{f_A} \right) \left(\frac{df_A}{dt} \right) = (1-f_A) \alpha_A - f_B \alpha_{AB} - f_C \alpha_{AC} - f_A (1-f_A) \alpha_{AA} + f_B^2 \alpha_{BB} + f_C^2 \alpha_{CC} - 2(1-f_A) f_B \alpha_{AB} - 2(1-f_A) f_C \alpha_{AC} + 2f_A f_C \alpha_{BC}$

A similar expression pertains for f_B , and the comparable expression for f_C is

$$\tau_c \left(\frac{df_C}{dt} \right) = -f_A f_C \alpha_A - f_B f_C \alpha_B + f_C (1-f_C) \alpha_C + f_A^2 f_C \alpha_{AA} + f_B^2 f_C \alpha_{BB} - f_C^2 (1-f_C) \alpha_{CC} + 2f_A f_B (1+f_C) \alpha_{AB} + 2f_C^2 (f_A \alpha_{AC} + f_B \alpha_{BC}).$$

Here should be noted that for milling of an elemental species (e.g., A) the number of powder particles varies with time as $\frac{N}{N_0} = \exp \left[\frac{(\alpha_{AA})t}{\tau_c} \right]$ where N_0 is the initial number

of such particles. Therefore measurement of the time variation of N allows the differences between the welding and fracture probabilities of the elemental species to be determined. On the assumptions that the fracturing and rewelding probabilities are size independent, the temporal variation of particle size distribution during milling of an elemental species powders is represented by

$$\tau_c \left[\frac{dn(v)}{dt} \right] = -\alpha_A n(v) - \alpha_{AA} n(v) \int_0^{\infty} f(v') dv' + 2\alpha_A \int_v^{\infty} \frac{n(v')}{v'} dv' + \frac{\alpha_{AA}}{2} \int_0^v n(v') v f(v-v') dv'$$

where $n(v) dv$ is the number of particles having volume between v and $v + dv$ and $f(v)$ is the corresponding particle fraction.

Appendix - C

References.

1. L. Schultz, K. Schnitzke and J. Wecker, *J. Magn. Magn. Mater.*,80(1989)115.
2. E. Ivanov et al., *J. Less-Com Met.*, 131(1987) 25.
3. M. L. Green, et.al , *Mater. Sci. Eng.*, 62 (1984) 231.
4. F. H. Froes, *J. Met.*, 41 (1989) 25.
5. P. S. Gilmen and J. S. Benjamin , *Ann. Rev. Mater*, 1983, Vol. 13 pp. 279-300.
6. Curwick, L. R 1983. *Frontiers of High Temp.Mats. Conf Proc. New York* , Inco Alloy Products Co. 176 p.
7. Rothman, M. F Tawancy, H. M. 1980 *Superalloys 1980*, Proc. 4th. Intl. Symp. on Superalloys, pp. 179. Metals Park, Ohio : Am. Soc. Metall. 708 p.
8. Traccy, V. A. Worn, D. K. 1962. *Powder Metall.* 10 : 34-48.
9. Benjamin, *Scientific American* 234 (1976) 40.
10. Benjamin J. S. Volin, T. E., Weber, J. H. 1974, *High Temp. High Pres.* 6:443-46.
11. Raghavan, M., Keln C., Pelkovicc Iuton, R. 1981, Proc. 39th Ann. Mat. Electron. Microsc. Soc. Am. p142. Baton Rouge: Claitors.
12. Ubhi. H. S. Hughes, T. A. Nutting. J. 1983, *Sec Ref.* 3.
13. Howson, T. E., Stulga, J. E. Tien, J. K. 1980, *Metall. Trans*, 11A: 1599-1607.
14. Morsc, J. P., Benjamin, J. S., 1976, *New Trends in Mats. Processing*, pp 165-99, Metals Park. Ohio, Am-Soc. Metall.

15. Weber, J. H. 1980. The 1980's pay off Decade for advanced Materials 25:752-64. San Diego. SAMPE.
16. K. Himmel. L 1981, US Army tank-Automotive Com. Research and Development Centre Laboratory Technical Report 12571 Warren Mich: US Army Tacom. 82pp.
17. Hotzler, R. K., Glasgow, T. K. 1980. See Ref.5 p.563.
18. R. W. Rydin et. al, Metall. Trans. A. 1993, Vol. 24A, pp 3-19.
19. D. Maurice et. al, Metall and Mats. Trans A. Vol. 25A. Jan 1994 p. 148.
20. D. Maurice et. al, Metall and Mats. Trans A. Vol. 25A. Jan 1994 p. 147-158.
21. T. H. Courtney et al. Solid State Powder Processing, (Ed. by A. H. Clauer and J. J. deBarbadillo), TMS, Warrendale, Pa., (1989), p. 3.
22. C. W. Thruston and H. J. Deresiewicz. J. Appl. Mech., 1959, Vol. 26, pp, 251-58
23. D. Maurice et. al, Metall and Mats. Trans a. Vol. 25a. Jan 1994 p. 150.
24. J. Gil Sevillano, et al. Prog. Mater. Sci, 1980-81, Vol. 25 pp, 69-412.
25. N. Bay, Met., Constr. 1986, Vol. 18, pp. 369-74
26. N. Bay; Weld. J., 1983, Vol. 62, pp. 137S-42S.
27. H. A. Mohamed and J. Washburn, Weld, J. 1975, Vol. 54, pp. 302S-10S.
28. L. Nybourg: Met. Powder Rep., 1989, Vol.4(1), pp. 32-34.
29. V. P. Antipin, V. A. et. al. : Poroshk. Metall., 1984, Vol.8(206),pp.4-9.
30. D. Maurice, Ph. D. Thesis, University of Virginia, Charlottesville, V. A. 1992.
31. V. Avitzur : Metal Forming: Processes and Analysis, R. E. Kreiger Co., Huntinton, N. Y. 1979, pp. 77-150.
32. P. W. Lee and H. A. Kuhn : Metall. Trans., 1973, Vol. 4, pp. 969-74.
33. Y. Bai and B. Dodd: Res Mech., 1985, Vo. 13, pp. 227-41.
34. J. W. Hutchinson : J. Appl. Mech., 1983, Vol. 50, pp. 1042-51.
35. B. J. M. Aikin et. al. Mats. Sci. Engg. A147(1991) 229-237.
36. T. H. Courtney. Mats. Trans. JIM, Vol 36. No.2, Feb. 1995, p 118.
37. Kramer, K. H. 1977. Powder Metall. Ins. 9:105-12.
38. Buzzanell, J. D., Lherbir, L. W. 1980 Sec Ref 4, p.149.
39. Pardoc, J. A. 1979, Powder Metall 22: 22-28.

40. W. D. Jones, *Fundamental-Principles of P/M*, Arnold, London, 1960.
41. M. Yu Balshin, *Vestnik Metalloprom*, 18, No. 2, and Vol. 124, 1938.
42. C. G. Goetzal, *Treatise on P/M*, Interscience, New York, 1949.
43. R. P. Seeling and J. Wulff, *Trans. Am. Inst. Mining Met. Engrs.*, 66, Vol 492, 1946.
44. Anil Kumar Sinha, *Powder Metallurgy*, Delhi, 1982, pp. 81-83.
45. R. L. Hewitt, et. al., *Powder Metallurgy*, Vol.17, No. 33, Spring 1974, pp. 1-2.
46. Anil Kumar Sinha, *Powder Metallurgy*, Delhi, 1982, p 83.
47. Bahrani and B. Crossland, *Metals and Mats and Met. Rev.*, March 1968, pp.68-80.
48. G. Geltmann, *Progress in Powder Metallurgy*, Vol. 18,1962.
49. R. A. Cooley, *Powder Metallurgy* (Ed. W. Leszynski, Interscience Publisher), N. Y. London, 1961, pp. 16-17
50. Anil Kumar Sinha, *Powder Metallurgy*, Delhi, 1982, pp. 122-122.
51. P. E. Evans, C. Smith, *Powder Metallurgy*, No. 3,1959, p. 36.
52. *Trans. A.I.M.E.*, Vol. 166,1946, p.492.
53. *Trans ASM*, Vol 58, 1963, p.863
54. Anil Kumar Sinha, *Powder Metallurgy*, Delhi, 1982, p 125.
55. *Engineer*, 1955, 199, 215
56. D. K. Worn, *Powder Met.*, No. (1/2), 1958, pp. 85-93.
57. P. E. Evans. *Perspective in P/ Met.*, Vo.1, Plenum Press, N. Y., 1967, 99-118.
58. Anil Kumar Sinha, *Powder Metallurgy*, Delhi, 1982, p 130
59. J. Williams, "Symp. on P/M;(I.S.I), London, 1956, p.112.
60. P. Murray, et al., *Trans. Brit. Cerams, Sec. Vol. 53, No. 8,1954, pp. 474-510.*
61. J. S. Jackson, *Powder Met.*, No. 8, 1961, pp 73-100.
62. M. Nilsson, *Particulate Matter*, *Spacial Powtech*, 73 issue, 1973, pp. 23-30.
63. Benjamin., J. S., Bomford, M. J. 1977. *Metal Trans.* 8 A;1301-5.
64. Gilman, P. S., Nix, N. D. 1981, *Metall. Trans.* 12A:813-823.
65. White. R. L. 1979. Ph. D. Thesis, Stanford Uni. 145 pp.,
66. Rainden. J. R. Habesch. E. B. 1981, *Thin Solid films*, 83:353-60.
67. P. H. Shingu et. al. *Metal Trans. JIM*, Vol.19 (1988), 3-10.

68. M. Umemoto, S. Shiga and K. Fuzimoto, Proceedings of the 12th Intr. Conf. on Thermo Electric. Materials, 1993 Nov. 9-11, Yokohoma.Japan.
69. M. Umemoto, Mats. Trans. JIM, Vol.36 No. 2, Feb. 1995. Metal and Mats Tech, Sept'83, 443.
70. E. S Bhagiradha Rao, Mechanical Alloying, Defence Metall. Lab. Hyderabad.
71. F. Yuasa, et. al., Powder Metallurgy, 1992, Vo.35, No. 2.
72. Otsuka et al., Proc. ASM Intl. Conf. Myrth Beach. S. Carolina, 27-29 March. 1990.
73. S. Sumimoto., J.J. Sunol and M. D. Baro Mats. Sci. Engg. A181/A182 (1994)
74. Nabuo Ashahi et al. Mats. Sci. Engg. 181/A 182 (1994) 819-822.
75. G. B. Schaffer et al.,. Appl. Phys. Lett. 55 (1) 3, July 1989, pp 45-46.
76. A. J. Heron and G. B. Schaffer J. of Mat. Syn and Proc, Vol. 2, No. 5, 1994.
77. G. B. Schaffer and P .G. McCormick, 1992, Metall Trans, 23 A, pp 1285-1290.
78. G. B. Schaffer et al., Metall Trans. Vol. 22A. Dec. 1991 pp.3019-3024.
79. J. S. Forrester et al. , Metall Trans. Vol. 26 A March 1995, pp 725-730.
80. M. Miki, T.Y. and Y. Ogino, Mat. Trans, JIM, Vol. 34 No.10,(1993) pp. 952-959.
81. K. J. Kim, K. S., H. O., K. Suzuki, J. Alloy and Compd., 203 (1994) 169-176.
82. C. H. Lee et al., J. Phase equi. Vol.14 No.2(1993) pp. 167-171.
83. W. P. Gomes and W. Dekeysø. In Treatise on Solid State Chemistry, N. B. Hannag, eds., Plenum Press, New York, NY, 1976, Vol.4. pp.61-113.
84. C. H. Bomford and C.F.H. Tipper Compressive Chemical Kinetics.,(eds. Elsvier Scientific) Amsterdam, 1980, Vol. 232. pp247-82.
85. V. V. Boldyrev: in Reactivity of Solids, K Dysek, J. Haber and Nowotry, eds. Elsvier Scientific, Amsterdam, 1982, Vol.2, pp519-50.
86. G. B. Schaffer and P. G. McCormick: Metall Trans.A.1990 Vol.21A, pp2789-94.
87. R. A. Rapp, A. Ezisand. G. J. Yurck: Metall. Trans. 1973, Vol.4. pp.1283-92.
88. G. B. Schaffer and P. G. McCormick: Metall Trans.A.1991, Vol. 22A, pp. 3019-24.
89. K. B Gerasimov et. al , J. Mater. Sci , 1991, Vol. 26, pp 2495-2500.
90. N. Burgio, A. et. al, 11 Nuovo Cimento, 1991, Vol. 13d, pp. 459-76.
91. K. Raviprasad, et al., J. Powder and Powder Metallurgy,411315 (1994).

92. P. H. Shingu, et. al., in *Solid State Powder Proc*, (ed., A. H. Clauser and J.J deBarbadillo), TMS, 21 (1990).
93. Dermott and C.C. Koch, *S. Metall.*, 1986, 20, 669.
94. Kang and R. C. Benn, *Metall. Trans. A*, 1987, 18A, 747.
95. J. S. Benjamin, *New Materials by Mechanical Alloying Techniques* (eds E. Arzi and L. Schultz), DGM, Germany, 1989, P.3.
96. Y. Ogino et al, *Proc. Int. Symp. Mechanical Alloying, Kyoto, Japan, 1991, Mater. Sci. Forum*, 1992, 88-90,795
97. A. Calka, *Proc. Int. Symp. Mechanical Alloying, Kyoto, Japan, 1991, Mater. Sci. Forum*, 1992, 88-90, 787.
98. C. Baker, University of Western Australia, unpublished research, 1989.
99. H. G. Chakurov et. al , *Bulguruska Akad, Nauk-Soffia-Dokl.*, 1979,32,47.
100. R. M. Davis and C. C Koch, *S. Metall.*, 1987, 21, 305.
101. E. Ivanov, *Int. Symp. Mechanical Alloying, Kyoto, Japan, 1991.*
102. E. Ivanov, I.G. et. al., *Dokl. Akad, Nauk. SSSR*, 1986,286,385.
103. L. Schultz, J. Wecker and E.J. Hellstern, *J. Appl. phys.*, 1987,61,3583.
104. L. Schnitze, L. Schultz, J. Wecker M. Katter, *Appl. Phys. Lett.*, 1990,57,2853.
105. J. Wecker, M. Katter and L. Schultz, *J. Appl. Phys.*, 1991,69,6058.
106. J. Ding, R. Street and P. G. McCormick, *J. Magn. Magn. Mater.*, inpress, 1992.
107. J. K. Gregory, J. C. Gibeling and W. D. Nix, *Metall. Trans. A*, 1985, 16A,777.
108. C. C. Koch and M. S. King, *J. Phys.*, 1985, 46,C8-583.
109. M. L. Trudeau, J.Y. Haot and R. Schultz,1991,58,2764.
110. S. S. Sergev, S. A. Black and J. F. Jenkins, *U. S. Patent 4264362,1981.*
111. C. Politis, *Physica*, 1985, 135B,286.
112. M. Stubicar, et. al., *Int. Symp. Mechanical Alloying, Kyoto, Japan, 1991.*
113. U. Mizutani, et. al., *Proc. Int. Symp. Mechanical Alloying, Kyoto, Japan, 1991, Mater., Sci. Forum*, 1992, 88-90, 415.
114. L. Schultz et al., *J. Magn. and Magn. Mater.*, 1989, 80, 115.
115. T. Alonso et al., *Appl. Phys. Lett.*, 60, Feb.1992.
116. P. A. I. Smith and P. G. McCormick, *S. Metall, Mater.*,1992, 26, 485.

117. K. B. Gerasimov, et. al., *J. Mater. Sci.*, 1991, 26, 2495.
118. N. Burgio, A. et al., *11 Nuovo Cimento*, 1991, 13D. 459.
119. G. A. J. Hack, *Metallurgia*, 1985, 49, 256.
120. Benn, R. C., Curwick, L. R., Hack, G. A. J. 1981, *Powder Metall.* 4: 191-95.
121. Block, E. A. 1961. *Metall. Rev.* 6: 193-239.
122. Erich, D. L., Donachie, S.J. 1982 *Met. Prog.* 121: 22-25.
123. R. H. Kane, et al., *Proc. Conf. Corrosion '84, New Orleans, La. U. S. A. April 1984, National Association of Corrosion Enggs.* paper 12.
124. E. Grundy, C. J. Precious and D. Pinder: in *Proc. Conf. 'PM aerospace materials '84', Berne, Switzerland, Nov. 1984. Metal Powder Report, Paper 12.* .
125. Rairden, J. R. Habesch, E. M. 1981. *Thin Solid Films* 83: 353-60.
126. Gedwill, M. A. et. al., 1982. *Metall Coatings 1982, Vol.1. N Y: Elsevier Sequoia.* 382 pp.
127. Black, S. A. 1979, *Development of Super Corroding Alloys for Ocean Engg. Applications, Civil Engg. Lab.(NAVY), Port Huene, California, 40p.*
128. Sargev, S. S., Black, S. A , Jenkins, J. F. 1981, *US patents No. 4, 264, 362.*
129. White R. L., Nix, W. D. 1978, *New Developments and Applications in Composites*, p.78, Warrendale, Penn: AIME.
130. C. C. Koch et al., *Appl. Phys, Lett.*, 1983, 43, 1017.
131. A. W. Weebar and H. Bakker, *Physica B*, 1988, 153, 93. 51.
132. C. C. Koch , *ANN. REV. Ma. Sci.* 1989,19,121.
133. R. B. Schwarz, R. R. Petrich and C. K. Saw, *J. Non-cryst. Sol.*, 1987, 76, 281.
134. E. Hellstern and L. Schultz, *J. Appl. Phys.*, 1988, 63, 1408.
135. C. C. Koch and M. S. Kim, *J. Phys.*, 1985, 46, C8-573.
136. C. C. Koch and M. S. Kim, *J. Appl. phys.*, 1987, 62, 3450.
137. E. Hellstern, H. J. Frecht, Z. Fu. and W. L. Johnson, *J. Mater, Res.*, 4, 1292.
138. P. G. McCormick, et al., *Microcomposites and Nanophase Materials*, (eds D. C. Van Aken et al.), T. M S, Warrendale, Pennsylvania, 1991, p. 65.
139. D. G. Morris and M. A. Morris, *Mater. Sci. Eng.*, 1991, A134, 1418.
140. M. L. Trudeau and R. Schultz, *Mater. Sci. Eng.*, 1991, A134,1361.

141. H. J. Fecht et al., *Advances in Powder Metall.* Vol. 1, (eds T. G. Gasbarre and W. F. Jandeska), MPIF/APMI, Princeton, N. J. 1989, p.III.
142. F. S. Badger et al., Jr. *Symposium on Materials for ASTM*, p. 99 (1946).
143. J. S. Hirschhorn, *Intr. to P/M (book)*, Am. Powd. Met. Inst., N. Y., (1969).
144. R. F. Smart, *Developments in P/M.*, Mills and Boon Ltd., London, 1973, p. 24.
145. G.H. Gessinger, *Metal Science*, Vol. 8, No. 11. Nov. 1974, pp. 394-396.
146. Don O. Noel in *P/ Metallurgy* (Ed. John Wulff), A. S. M., 1942, pp. 112-123.
147. H. E. Carlton and W. H. Goldberger, *J. of Metals*, June, 1965, pp. 611-618.
148. R. M. Lewis, et. al., *J. of Metals*, Vol. 10, No. 6, June 1958, pp. 419-424.
149. G. V. Samsonov et al., *Proizvodstvo Zheleznogo Poroshka*, Moscow, 1957.
150. L. B. Pfeil, *Iron Steel Inst.*, Special Report No. 38, (1947), pp. 48-51.
151. Alan Arias, *Powder Metallurgy*, Vol. 11, No. 22, (1968), pp. 411-429.
152. G. Meiter, *Metal Progress* 53, (4) 1948, pp. 515-520.
153. B. P. 675933.
154. U. S. P. 2446062.
155. G. A. Meyerson, *Progress in Nuclear Energy*, Series IV, Vol.1, 1956, pp131-132.
156. P. U. Gummesson, *Powder Metallurgy*, Vol.15, No. 29, 1972, pp. 67-94.
157. S. A. Gregory et al., *P/Metallurgy*, 1968, Vol. 11, No. 22, 1968, pp. 233-260.
158. L. Ljungberg, *Stahl u. Eisen*, 1950, 24 (5), pp. 279-285.
159. H. J. Modi and G. S. Tendolkar, *F. Sci. Res.*, 1953, 128, 9, pp. 431-438.
160. T. P. Forbath, *Chem. Engg. Jan.*, 1957, pp. 194-197.
161. *Symposium on Development in the production and quality of metal powders held on 4 Dec., 1957.*
162. F. D. Richardson, *J. Iron and Steel Inst.*, Vol. 203, 1965, pp. 217-226.
163. A. R. Burkin, *Powder Metallurgy*, 1969, Vol. 12, No. 23 pp. 243-250.
164. V. N. Mackiw et al., *Journal of Metals*, June, 1957, pp. 786-793.
165. A. R. Burkin et al., *Powder Metallurgy*, 1967, Vol. 10, No. 19 pp. 33-57.
166. P. C. Finlayson et al., *Powder Metallurgy*, 1968, Vol. 11, No. 22 pp. 224-232.
167. J. Wulff in *Powder Metallurgy*, (J. Wulff Ed.), A. S. M., Cleveland, p. 137 (1942).

168. J. Wulff, U. S. P. - 2407862 (1946).
169. P. R. Marshall, Symp. on P/Met. (1954) , Report No. 58 , I S I., London, 1956.
170. N. F. Vyaznikov et al., P/Met Mats and Products, Foreign Trade Tech. Div., Ohio, May, 1970.
171. H. W. Blakeslee, P/M. in Aerospace Research, NASA, Washington, 1971.
172. G. Herdan, 'Small Particles Statics' (eds. Elsevier Publishing Co.) 1953.
173. A. Szegvari, US Patent No. 2764359 issued 25 Sept. 1956.
174. Rydin, D. Maurice and T. H. Courtney: Metall. Trans. A, 24A (1993), 175.
175. T. M. Cook: M. S. Thesis, Michigan Technological University, (1994).
176. R. D. Mindlin: J. Appl., Mech., 1949, Vol. 71, pp. A259-68.
177. W. Goldsmith: Impact, E. Arnold, London, 1960, pp. 82-98.
178. I. V. Maw: Wear, 1976, Vol. 38, pp. 101-14.
179. D. Halliday et al. Fundls of phy, John Willy and Sons, N. Y, 1966, pp. 190-93.
180. B. J. M. Aikin et al. Mater. Sc. And Engg., A147(1991), 229.
181. B. J. M. Aikin et al. , Metal. Trans.A, 24A(1993)647.
182. B. J. M. Aikin et al., Metal. Trans.A, 24A(1993)2465.

